NASA TECHNICAL TRANSLATION

NASA TT F-303

NASA TT F-303

SURVEY OF JAPANESE SPACE PROGRAM WITH EMPHASIS ON KAPPA AND LAMBDA TYPE OBSERVATION ROCKETS

by Hideo Itogawa, et al.

From *Seisan Kenkyu,* Vol. 15, No. 7, 1963

NATIONAL AERONAUTICS AND SPACE ADMINISTRATION • WASHINGTON, D. C. • FEBRUARY 1965

NASA TT F-303

SURVEY OF JAPANESE SPACE PROGRAM WITH EMPHASIS ON KAPPA AND LAMBDA TYPE OBSERVATION ROCKETS

By Hideo Itogawa, et al.

Scripta-Technica, Inc. translated and prepared the reproducible copy for this publication and is responsible for the accuracy and fidelity of the translation and editorial quality of the contents.

From Seisan Kenkyu, Vol. 15, No. 7, 1963

NATIONAL AERONAUTICS AND SPACE ADMINISTRATION

For sale by the Office of Technical Services, Department of Commerce, Washington, D.C. 20230 -- Price $7.00

TABLE OF CONTENTS

Kappa-8L-1 type space rocket: the first two-stage space rocket which was launched at Kagoshima Space Center in August, 1962.

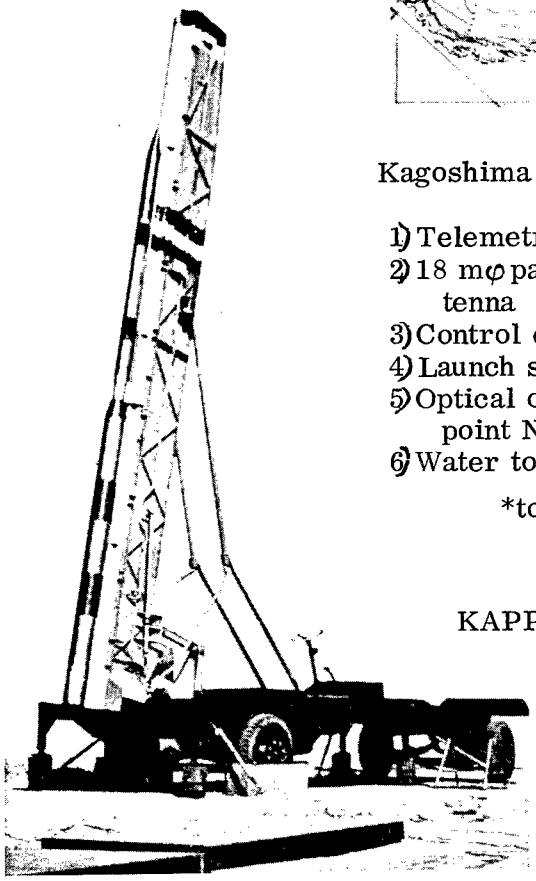

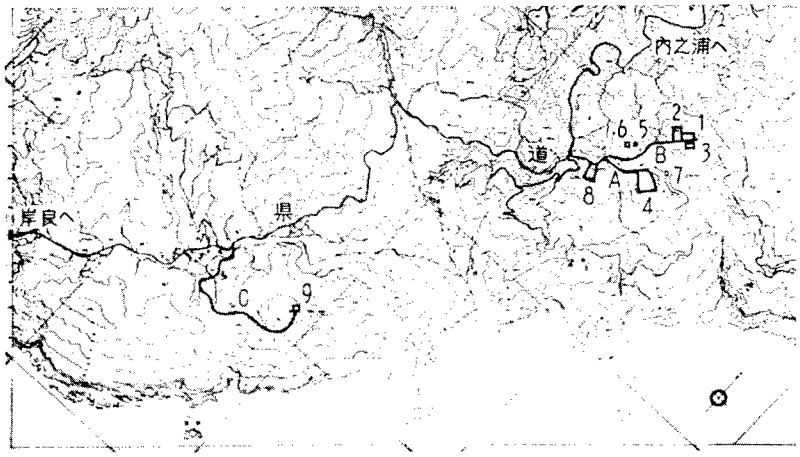

Kagoshima Space Center, Tokyo University

1) Telemetry center
2) 18 mφ parabolic antenna
3) Control center
4) Launch stand
5) Optical observation point No. 1
6) Water tower
7) Reservoir
8) Computing center
9) Radar center; optical observation point No. 2

A. Road construction area No. 1
B. Road const. area No. 2
C. Road const. area No. 3

*to Kishyo **Province highway ***to Uchinoura

KAPPA-8L, -9L, AND -9M

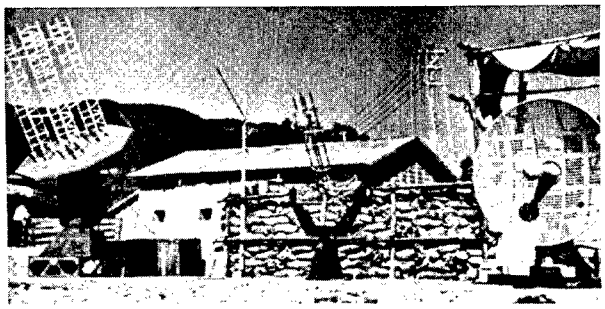

Telemetry and radar: optical observation team worked in a temporary facility.

Launch stand viewed from the rear hill: Kappa series launching point is at left and Lambda series launching point is at right.

Launch stand viewed from telemetry center: launch point for Lambda series, under construction, is shown at right.

Photographed by Yashina Yaster (Pages 1 - 21).

A view at the test center: tropical plants were set by the residents of Uchino-ura town.

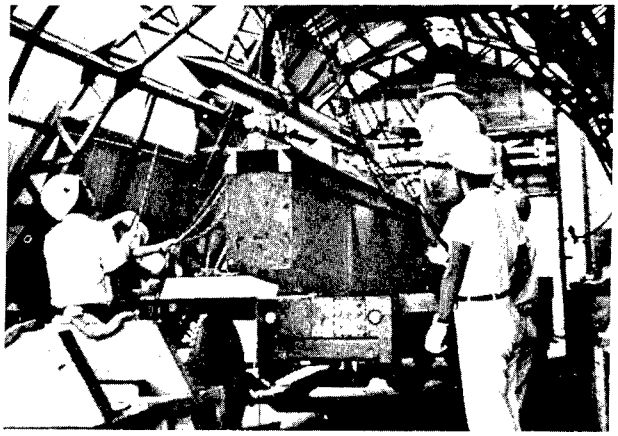

Kappa-8L type space rocket assembly (August, 1962).

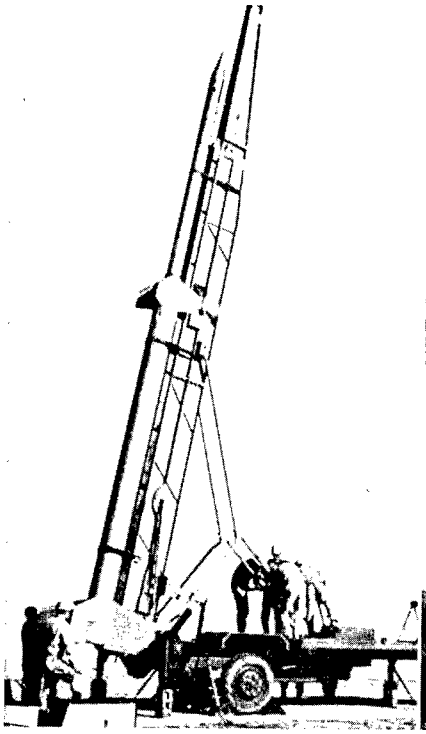

K-8-11 type space rocket with geomagnetic aspect meter, noise wave and cosmic-ray detectors (December 1962).

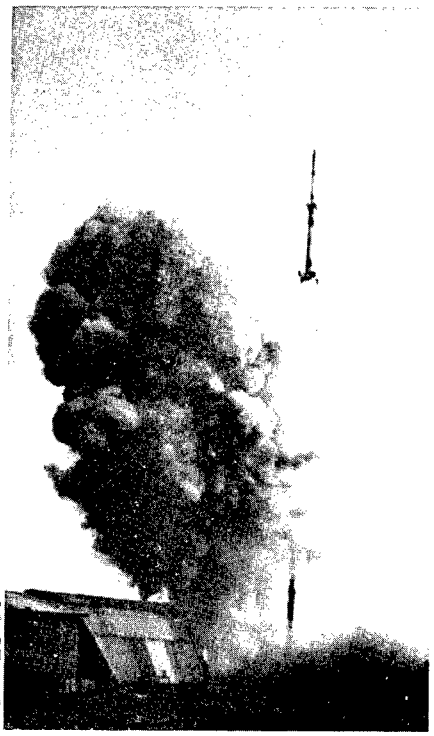

K-9M-1 type rocket: developed from K-8 type and reached the maximum altitude 350 km (November 1962).

Kappa-8L, -8, -9L, and -9M type rocket: Along with the improvement of the rockets, the construction of Kagoshima Space Center of Tokyo (Cont'd. p. 4)

University, as a new Pacific test site, was begun in February, 1962. Hills were cut, valleys were filled; thus, flat grounds and roads were made, and various facilities constructed. However, the first launches were performed before the site construction was completed. A temporary facility was used in August, 1962. And three large space rockets, 8L, 9M, and 8-11 type, and seven small model rockets were launched before the end of the year.

Flat land for the computer center: arrow shows Miyahara plateau where the radar center is located.

The view of the launch site from air: the radar center is located upper right end. The curve of the road makes the ground more beautiful.

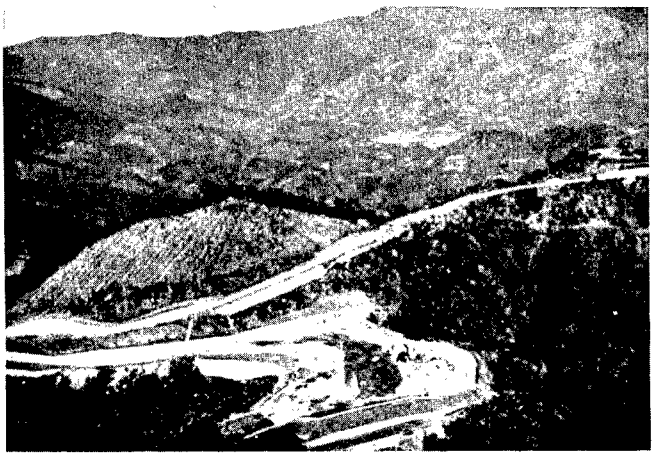

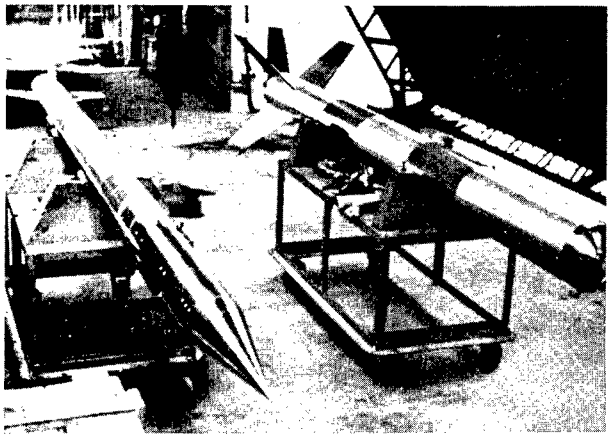

The main rocket and booster of K-8-L type.

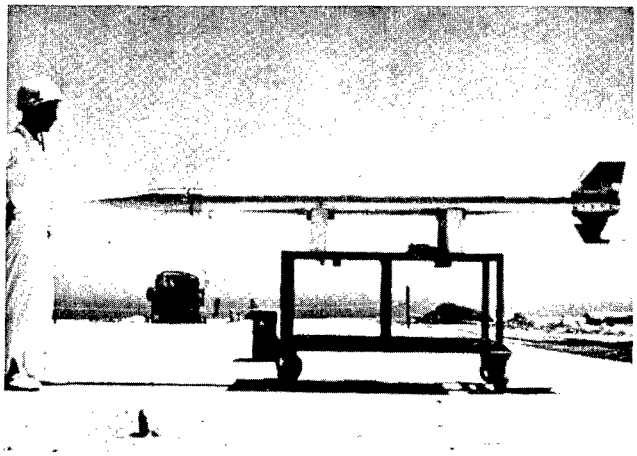

AT-150 type model rocket for antenna test (August 1962).

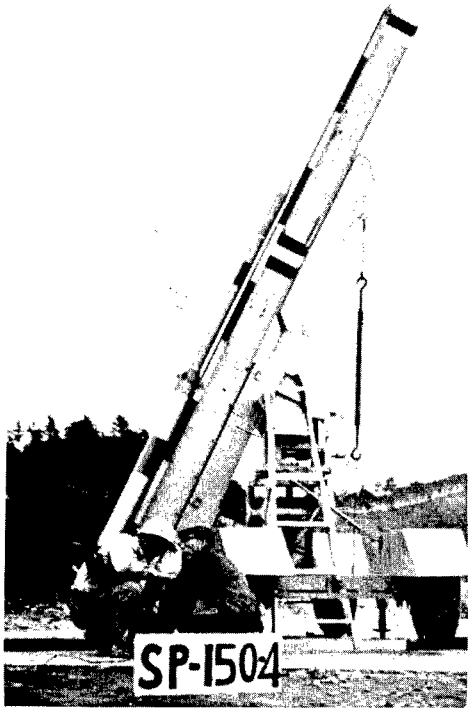

SP-150-4 type model rocket for spin test (December 1962).

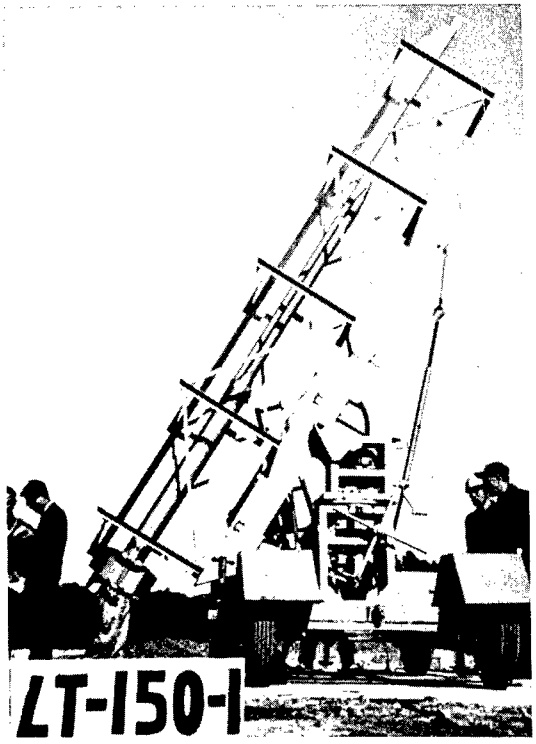

AT-150 type model rocket for "suspended" launch test (November 1962).

The launch site, past and present (refer to the preface)

Survey by Maruyasu laboratory team (June 1961).

Ground is levelled (February 1962).

Ground test at Noshiro Test Center

Noshiro Test Center was ready in September 1962 for a ground test site for the large engines of the Lambda series. The ground test of 735 3/3 engine was performed in October 1962.

View of the wide test site: the test stand is near the seashore at left, and the computer room and control room are at right foreground.

Computer room is at right and control room is at left.

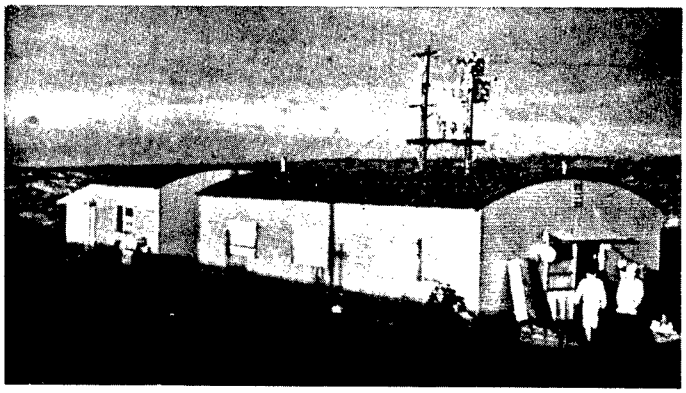

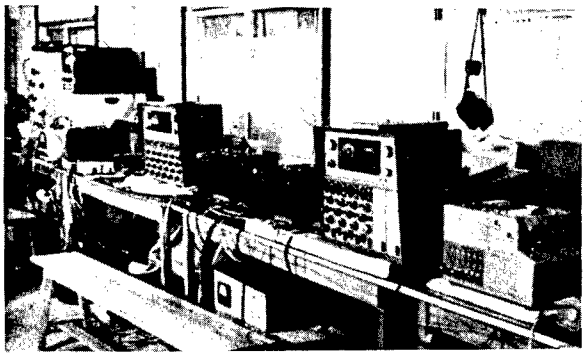

Thrust, stress, and vibration meters in the computer room.

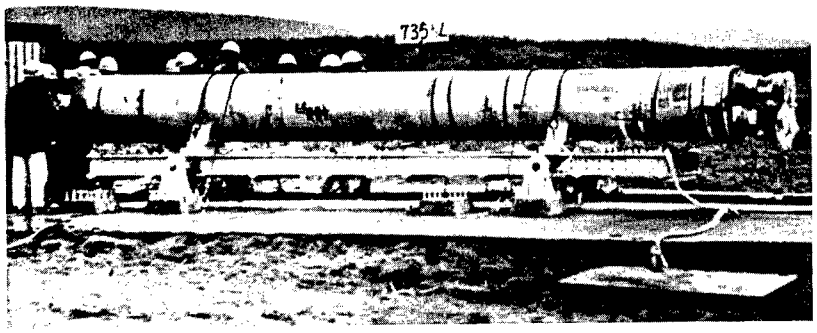

735 3/3 engine, total length 8 m, is set on the test stand.

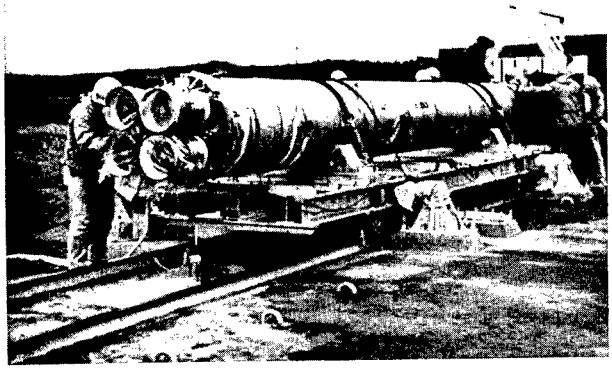

735 3/3 engine has four nozzles.

Thrust meter.

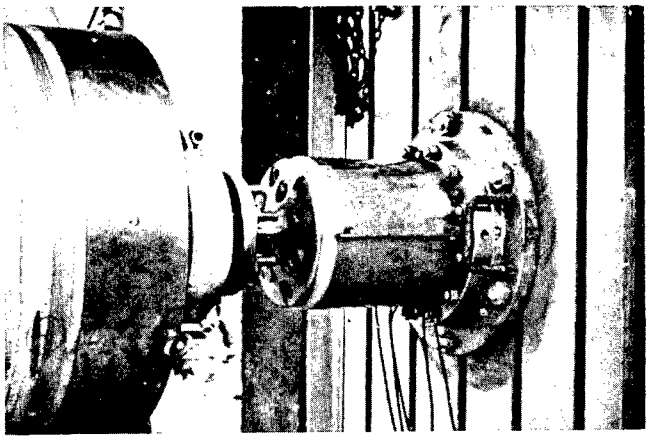

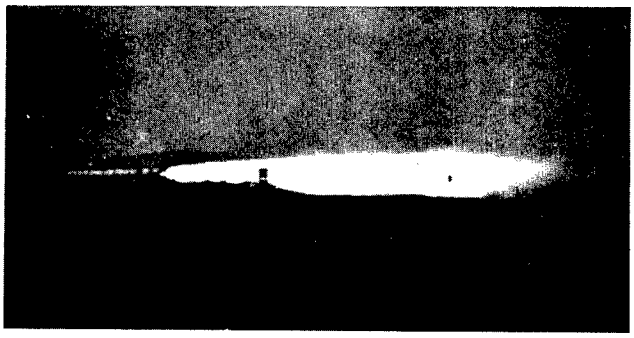

Combustion of 735 3/3 engine (at Noshiro Test Center): the length of flame was about 25 m (October 1962).

TESTS AT AKITA TEST CENTER

Space observations by K-8-8, -9, and 92-2 type space rockets, ground tests of 735 1/3 and 735 2/3 engine, and launching tests of small rockets were continuously performed at the center.

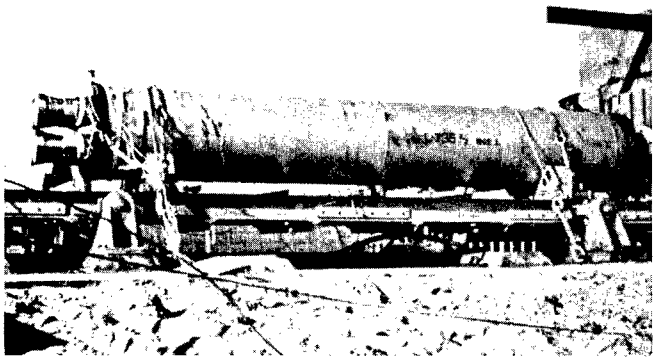

735 2/3 engine; as a previous model of 735 3/3 engine, it was tested at Akita Test Center in April 1962.

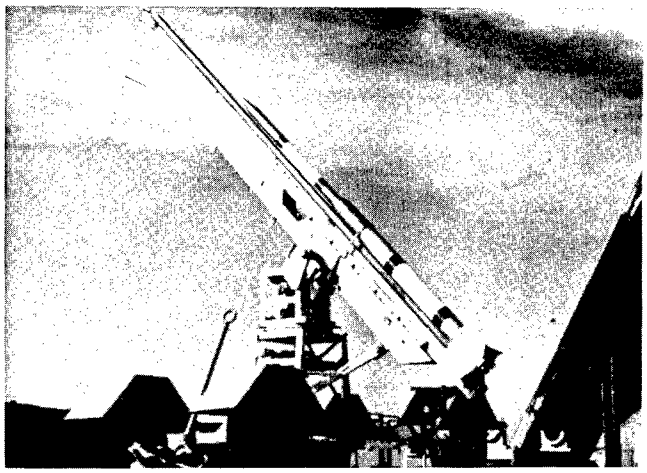

FN-150 type model rocket which was tested to find the characteristics of four-nozzle system (October 1961).

K-8-9 type space rocket: it performed the night observations of the ionosphere and air-glow (October 1961).

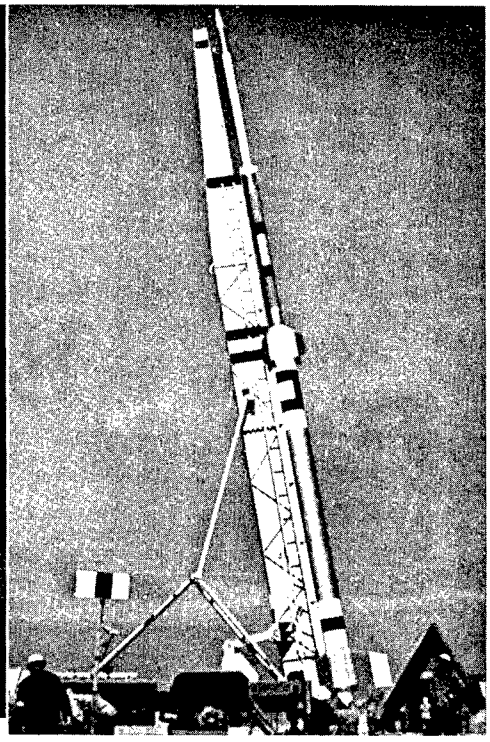

K-9L-2 type space rocket: a three-stage space rocket which performed ionosphere observations (December 1961).

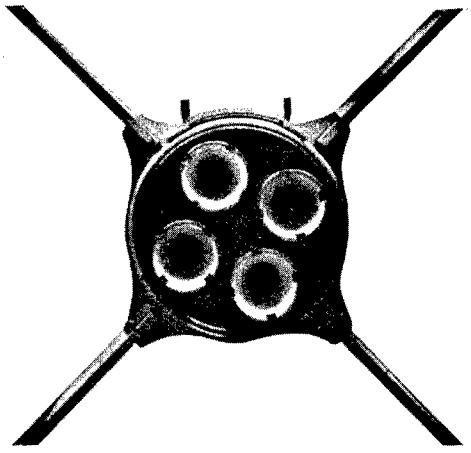

Four nozzles of FN-150 type model rocket.

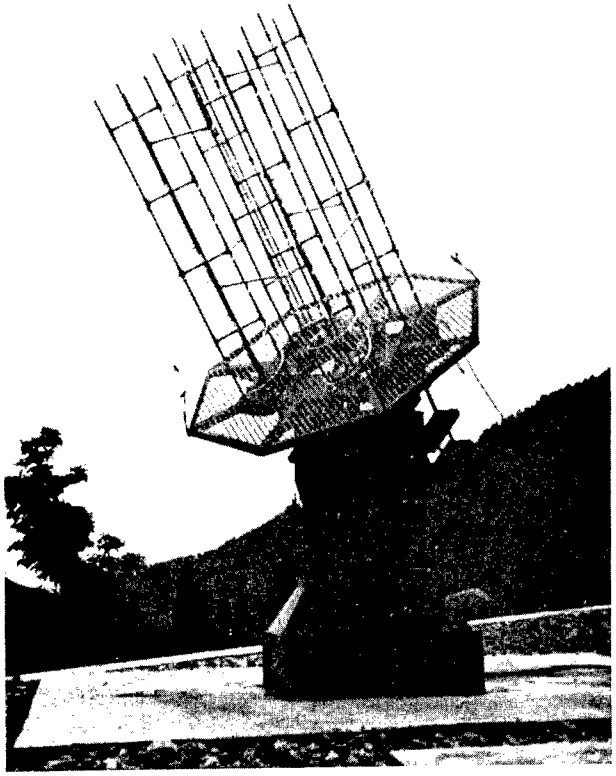

Telemetry antenna (K.S.C.).

TELEMETRY SYSTEM

With larger space rocket, observation items were increased and the telemetry incorporated ten channels. Secondary transmitting wave oscillator of the transmitter was transistorized.

Electronics devices of K-9M-1 type space rocket; from right, radar transponder, telemetry, thermometer, strain gage and accelerometer.

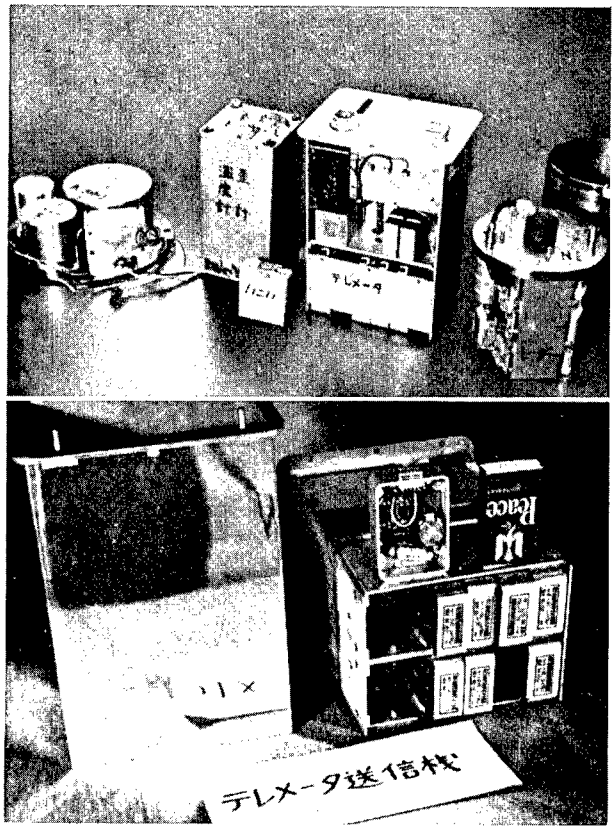

Telemetry transmitting unit: secondary transmitting wave oscillator was transistorized.

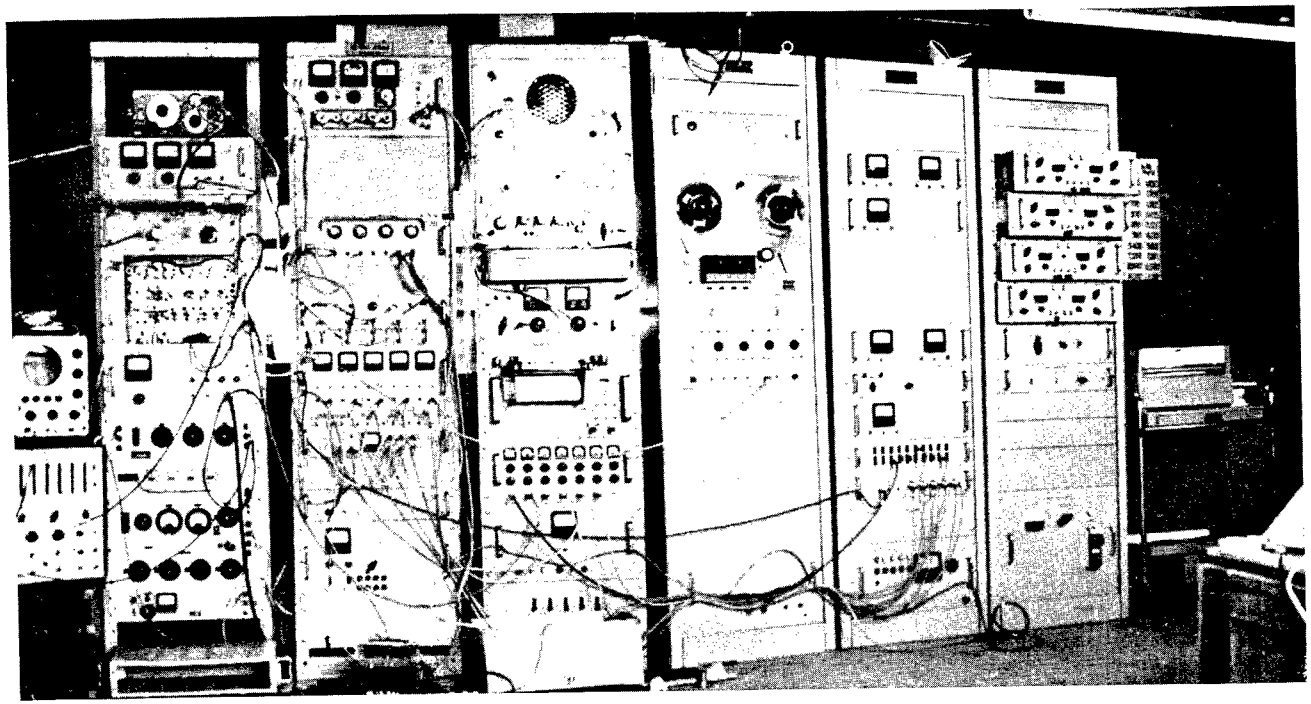

Telemetry receiving and recording system: 225 Mc/s FM-FM type which can receive and record from ten channels (K.S.C.).

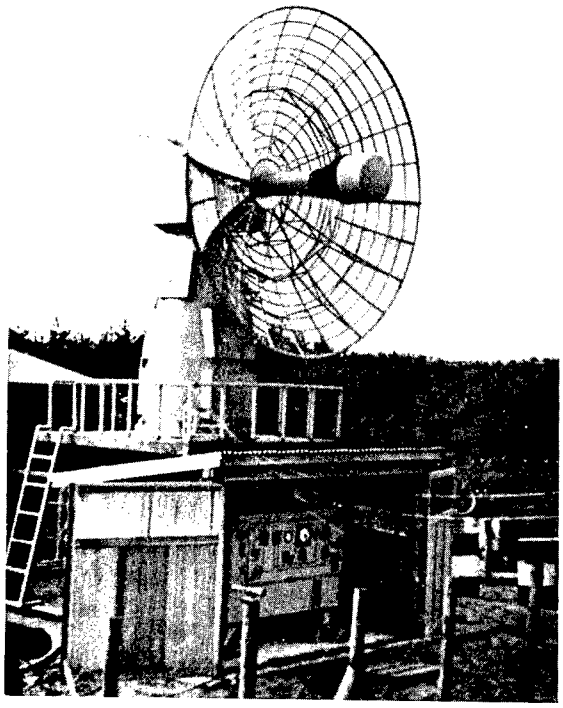

Antenna unit of the radar system: 4 m — diameter parabolic antenna. Oil pressure system is shown under the radar.

Transmitting and receiving units of the radar system. It has 500 kw of transmitting and receiving power. In the receiving unit, parametric amplifiers were used.

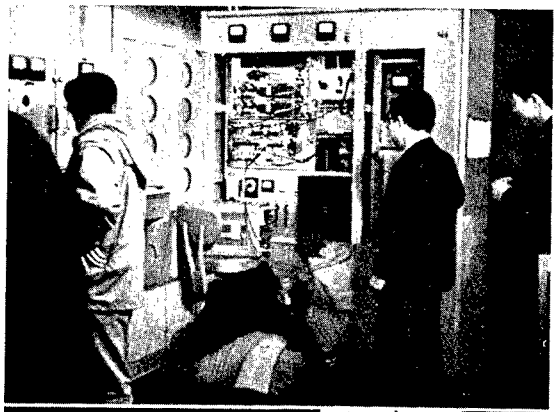

Indicating and control system of the radar system; indicates and controls the operation of the radar system.

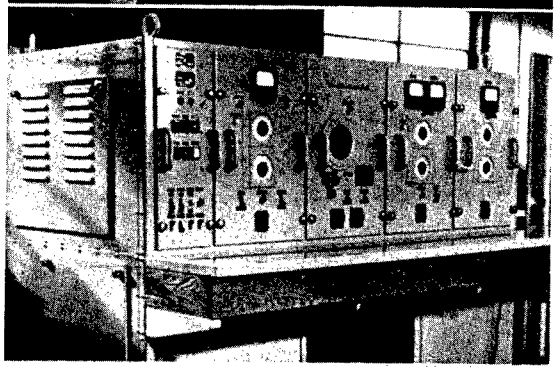

MODERN AUTOMATIC TRACKING RADAR SYSTEM

(4 m radar system)

With larger space rockets a new automatic tracking radar system was installed in order to extend the tracking range of a rocket flight. It is driven by oil pressure and has the capacity of tracking a rocket up to 1,500 km distance.

Recording system of the radar system: range and coordinate angles with respective time are filmed by a 16 mm movie camera.

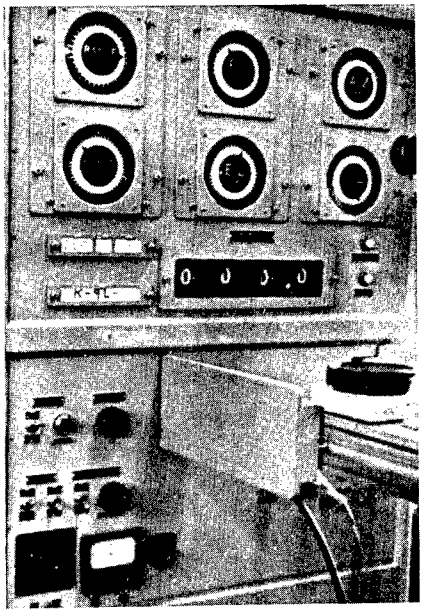

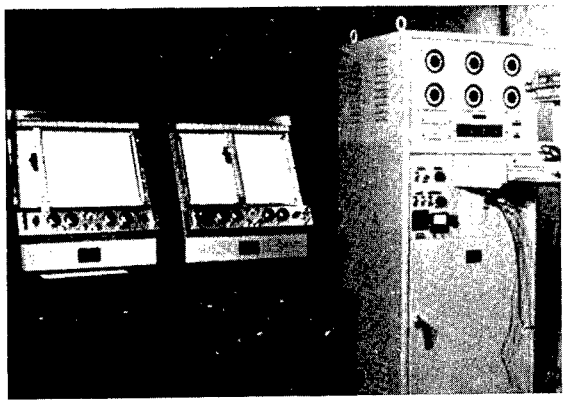

Data recording system and trajectory plotter: trajectories are automatically computed and plotted.

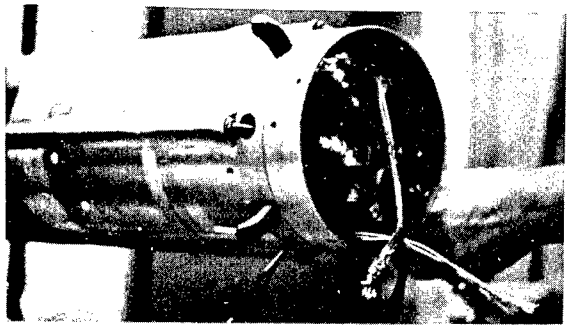

Radar antenna (K-8L type).

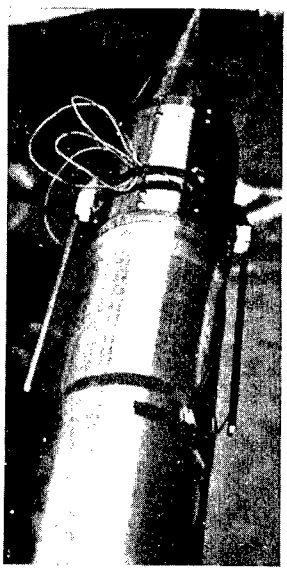

New telemetry antenna (AT-150 type).

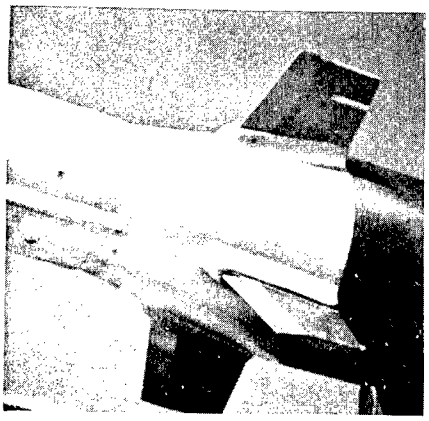

Radar and telemetry antenna (K-9L type).

INSTRUMENTS FOR OBSERVATION (P. I.)

With new requirements for observations, various measuring instruments have to be carried.

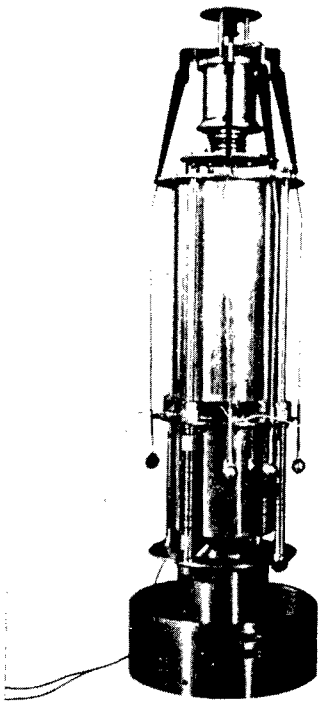

Ionosphere direct observation device: probes are kept in fold until the nosecone is opened (for K-8-10).

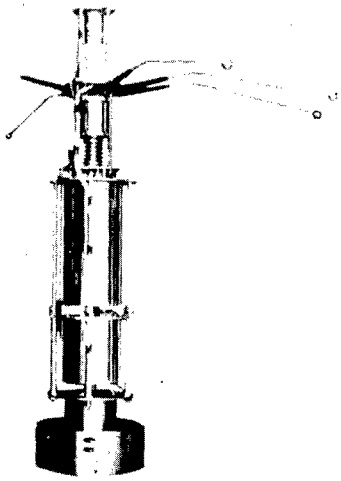

Ionosphere direct observation device: with the nosecone open, five probes strech out like umbrella spokes. Geomagnetic aspect meter is mounted on top of the device (for K-8-10 type).

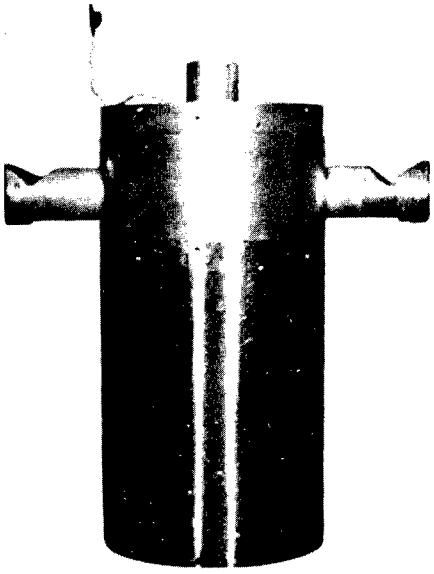

Airglow observation device: two periscopes are stretched out on both sides to take in light (for K-8-9 type).

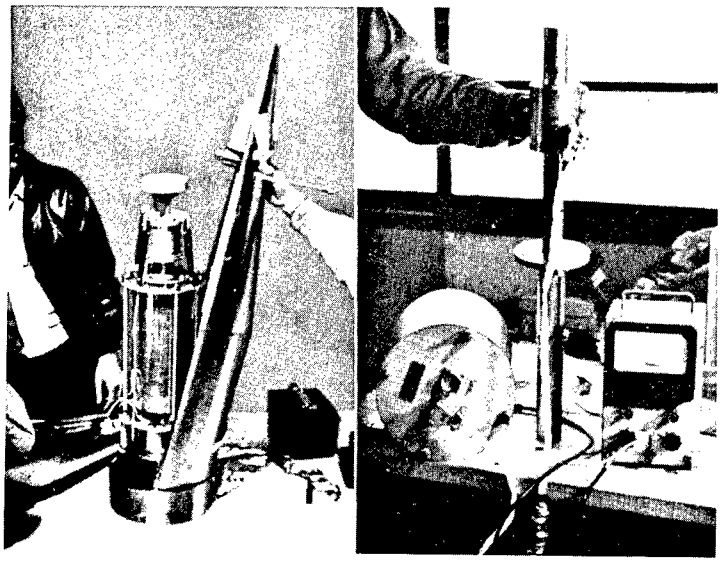

Geomagnetic aspect meter (right): detector is stretched out when the cone is opened in order to escape from the influence of the rocket body.

Nosecone opening and ionosphere direct observation devices (left): nosecone opening timer and "pusher" are set at the top of the rocket (for K-9M-1 type).

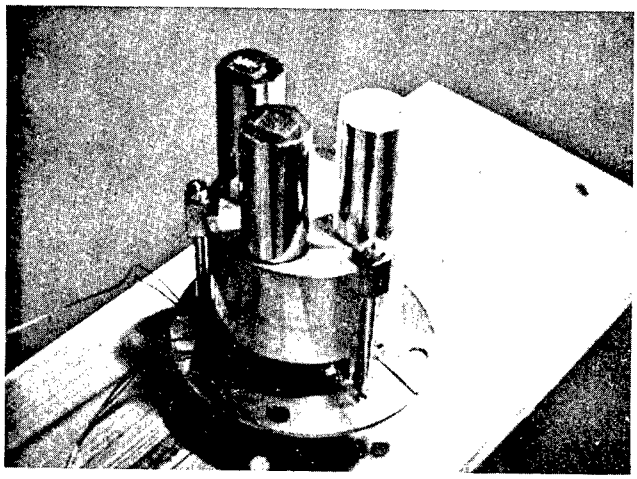

Cosmic-ray detector: three Geiger counters, enclosed in different materials and thicknesses, are used (for K-8-11 type).

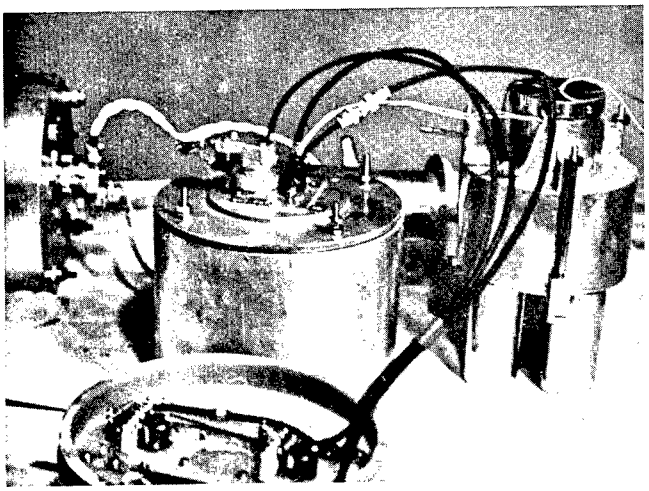

Noise wave observation system: cosmic-ray detector is shown at night (for K-8-11 type).

BASIC TESTS:

Various basic tests must be performed in order to launch safely a space rocket and observe the super high region of the atmosphere.

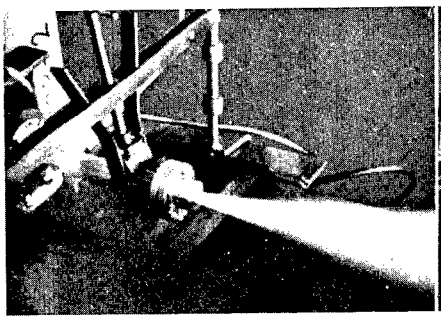

Basic test for controlling a rocket.

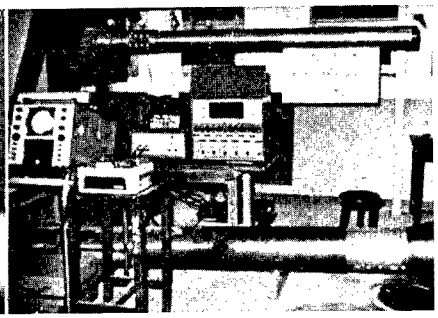

Strength test on connecting portion (for K-8L type).

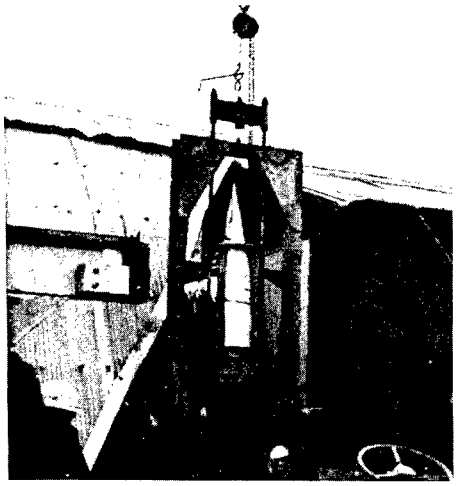

Impact test on measuring devices in nosecone.

Nosecone opening function test: from top are geomagnetic aspect meter, RN loop antenna, and cosmic-ray counter.

PR and RN antenna: they are stretched out 3m by compressed gas.

Environmental test device for vacuum and heat.

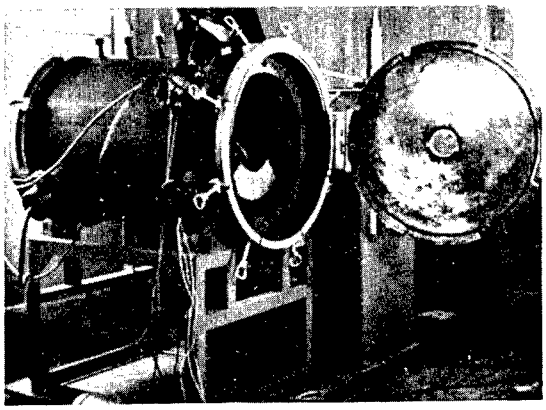

RECOVERED ROCKETS

Launched rockets sank under the sea, but some of them were recovered with the help of the residents of the shore area.

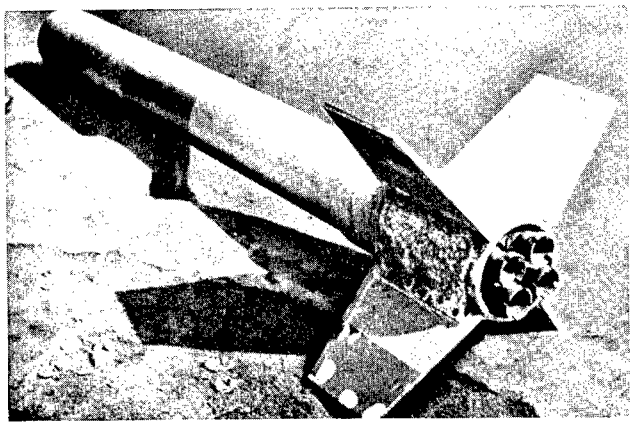

SP-150-4 type model rocket was recovered from the sea as it was caught in a fishing net.

Booster of K-8L-1 type space rocket was floating on the sea and recovered.

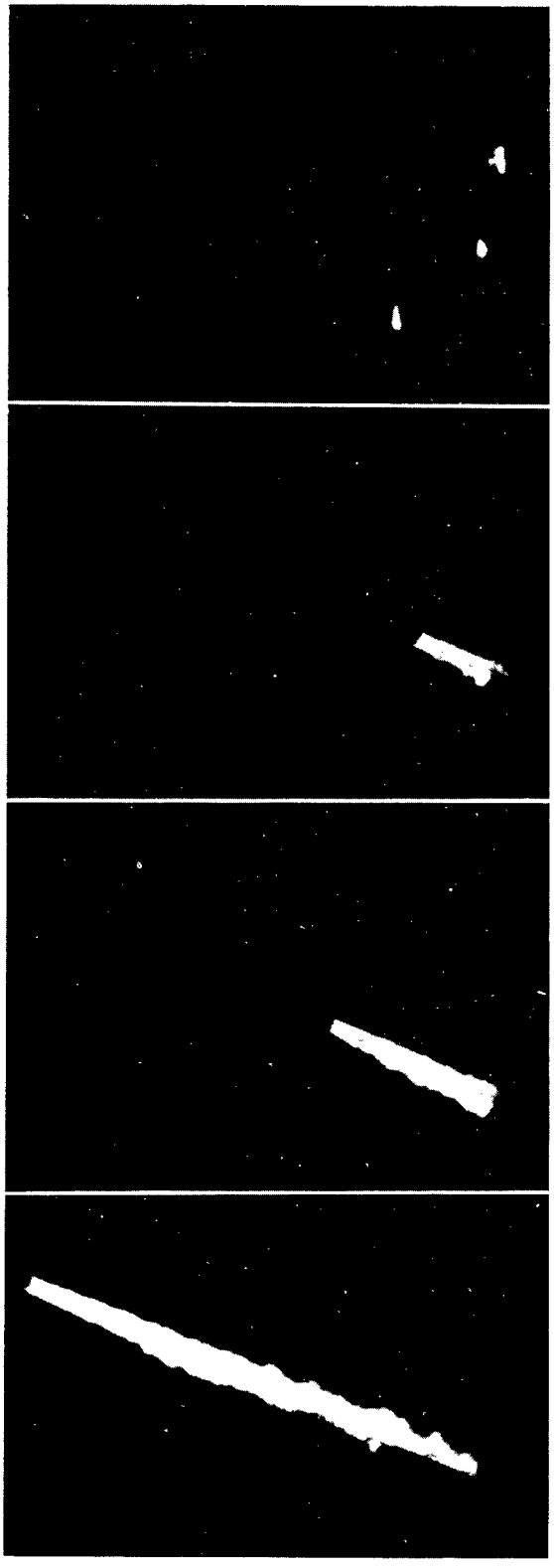

Flight of K-8-9 type space rocket (night test): filmed by a high speed 16 mm movie camera (from high-speed-camera observation point).

1) The moment of ignition

2) 0.38 sec after ignition

3) 0.47 sec after ignition

4) 0.65 sec after ignition

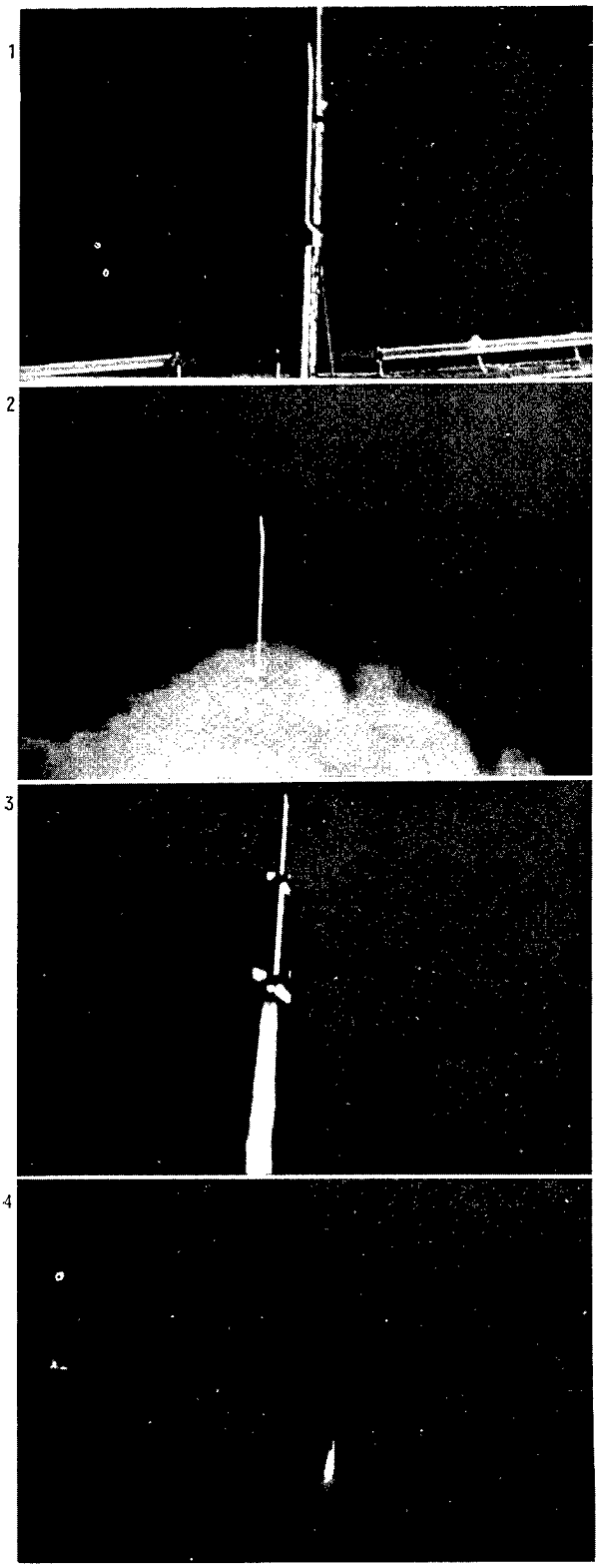

Flight of K-8-11 type space rocket: filmed by 35 mm modified Mitchell camera (from optical-observation-point No. 1):

1) The moment of ignition

2) 1.7 sec after ignition

3) 5.5 sec after ignition

4) 12.0 sec after ignition

Observation by optical tracking device. Photographs on pages 22 and 23 were taken by Shikimura laboratory team.

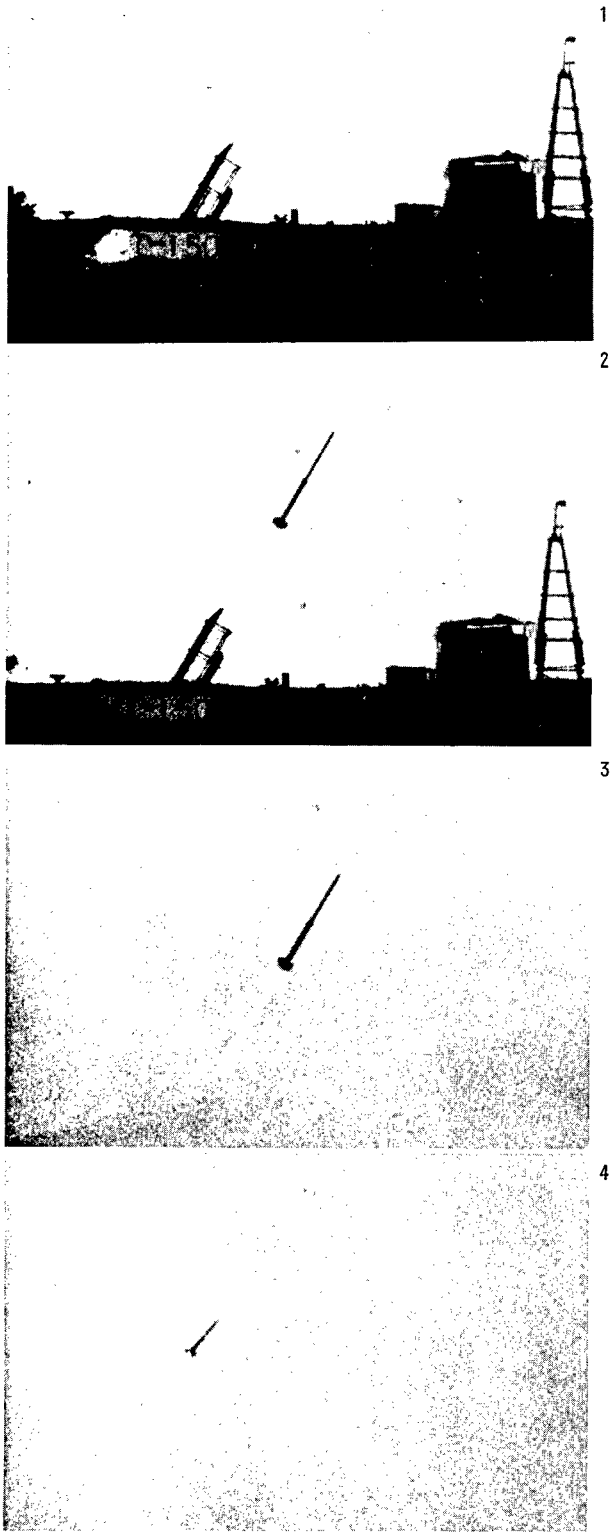

Flight of LT-150-1 type model rocket: filmed by a 35 mm Bell & Howell camera (from optical-observation-point No. 2).

1) The moment of ignition

2) 0.3 sec after ignition

3) 0.5 sec after ignition

4) 2.1 sec after ignition

Flight of K-9M-1 type space rocket: filmed by a 35 mm Bell & Howell camera (from the optical-observation-point No. 2).

1) The moment of ignition
2) 0.5 sec after ignition
3) 2.1 sec after ignition
4) 3.6 sec after ignition

Observation by optical tracking device. Photographs on pages 24 and 25 were taken by Shikimura laboratory team.

1

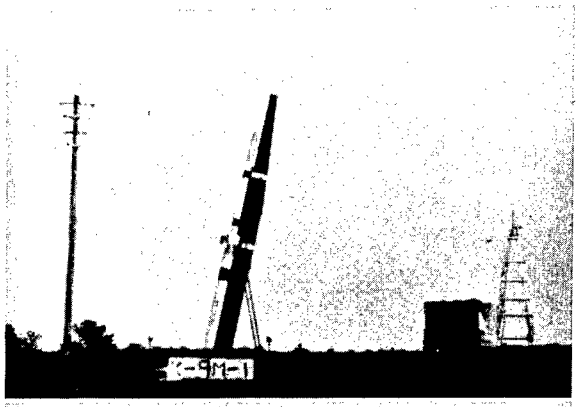

2

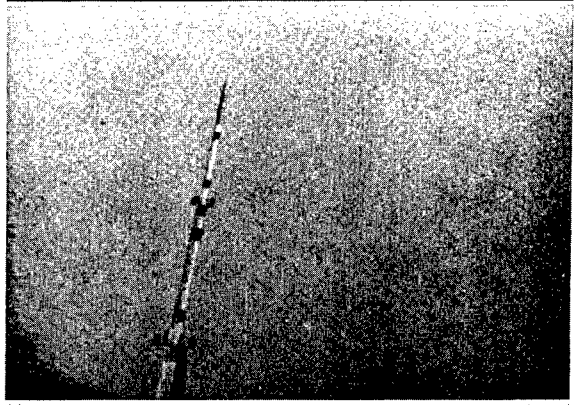

3

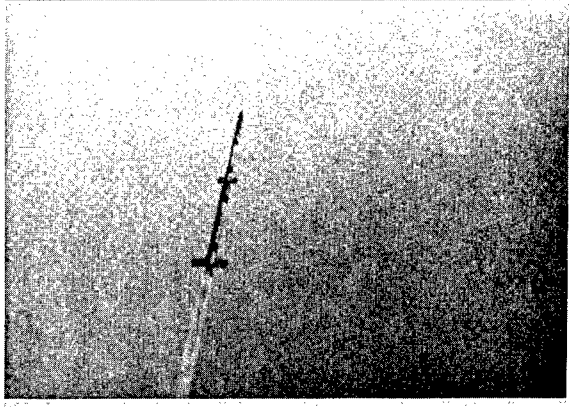

4

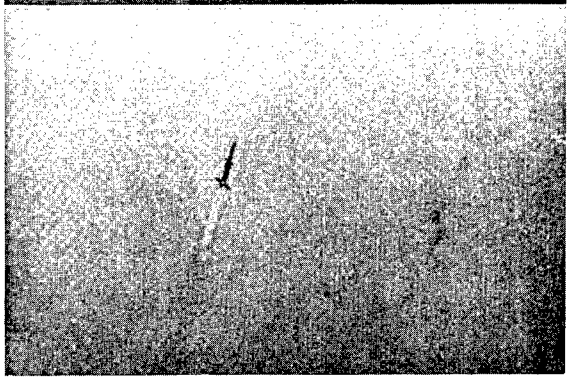

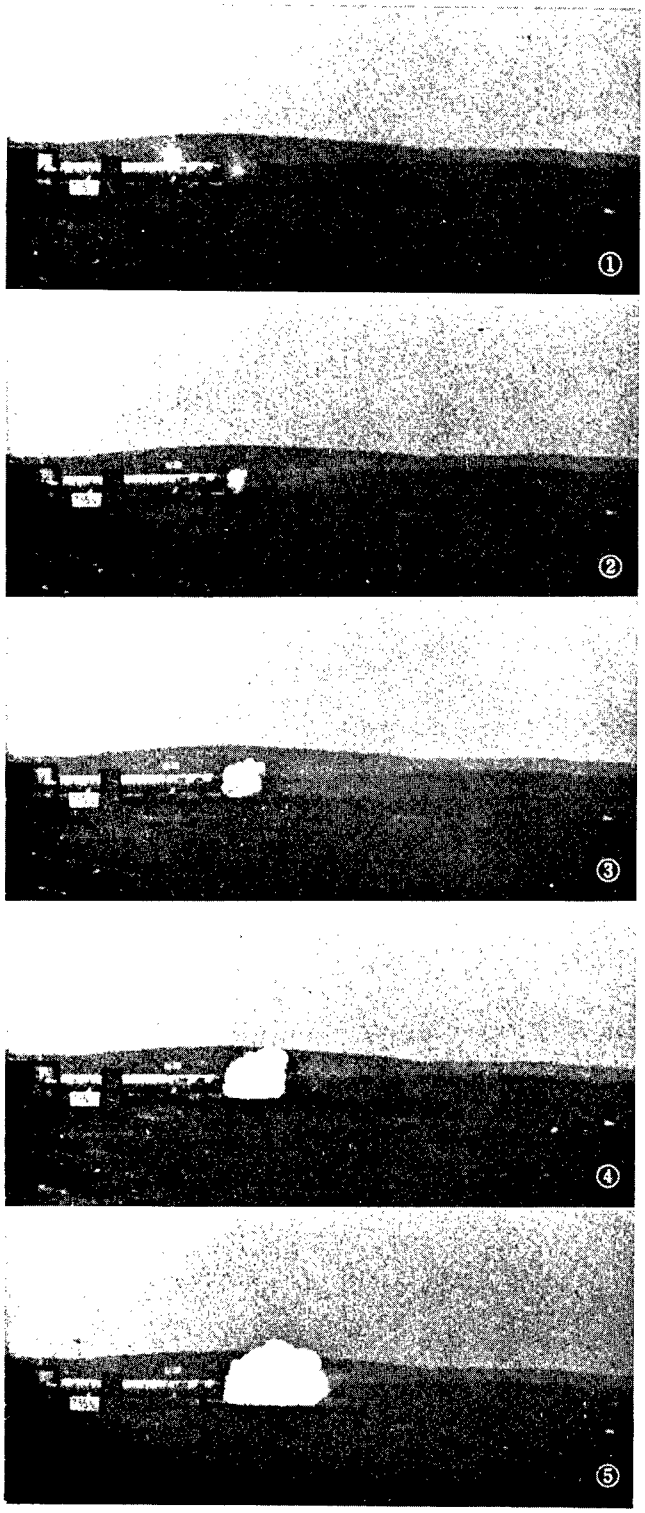

Ground combustion test of 735 3/3 engine for Lambda type space rocket: filmed by a 35 mm Bell & Howell camera.

1) The moment of ignition
2) 0.1 sec after ignition
3) 0.2 sec after ignition
4) 0.3 sec after ignition
5) 0.4 sec after ignition

Observation by optical tracking device. Photographs on pages 26 and 27 were taken by Shikimura laboratory team.

6) 0.5 sec after ignition
7) 0.6 sec after ignition
8) 1.0 sec after ignition
9) 20.0 sec after ignition
10) 24.0 sec after ignition

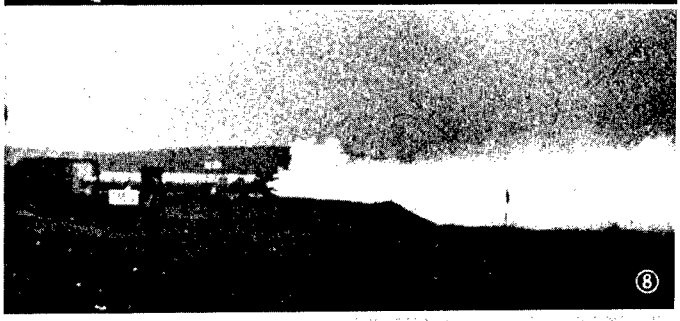

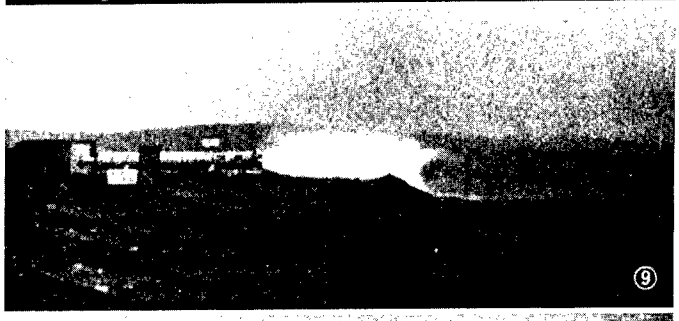

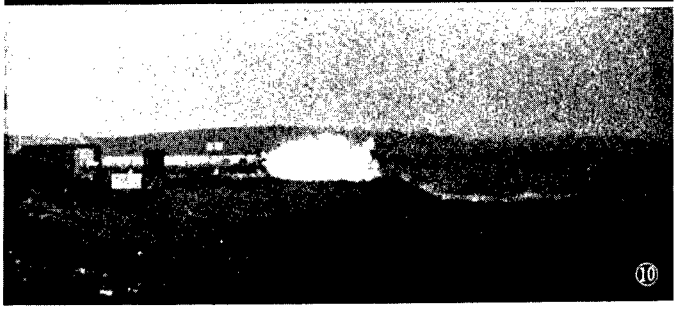

A SCHEDULE FOR OBSERVATION ROCKETS IN 1963

By Hideo Itogawa

The Kappa-Series Rockets Launched for Space Observation

As of March 1963, the Japanese observation rocket research groups had successfully launched five types of observation rockets. All of these rockets had been constructed by the group consisting of the SE group of the Industrial Production Research Institute of Tokyo University, which worked with the help of other observation rocket research groups. The specifications of the five types of rocket are shown in Table 1.

Table 1

Types of rocket	Alt(80°)km	PAYLOAD(kg)	No. of Stages
K-6	60	12	2
K-6 H	85	12	2
K-8 L(K-6 S)	200	12~15	2
K-8	202	40~50	2
K-9 L	350/110	12/25	3
K-9 M(K-8 H)	400	40~50	2

The relative sizes of these rockets are shown in Fig. 1. In Table 1, the row: rocket-type K-9L, altitude 350/110, payload 12/25, and number of stages 3, means that this rocket is a multi-stage rocket having a maximum altitude with the second-stage booster and 25 kg of payload, of 110 km; and with the last-stage booster and 12 kg of payload, of 350 km. In other words, the K-9L rocket is equivalent to a combination of two rockets, one of which has a maximum altitude of 110 km with 25 kg of payload, and the other, 350 km with 12 kg of payload. It is obvious, however, that the facilities on the ground for this rocket such as a telemetry system, a radar system, and an optical observation system, etc., have double capacities compared to the other rockets.

As of May 1963, the number of rockets launched are as follows:

K-6 series (including K-6H, K-8L)	20
K-8 series (including K-9H)	13
K-9L	2
Total	35

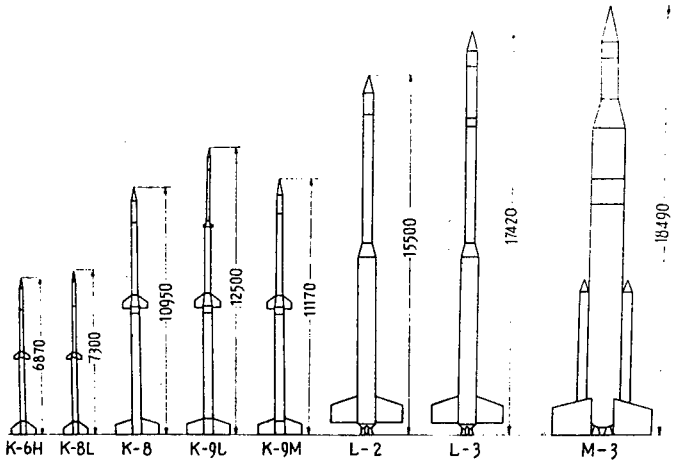

Fig. 1

These rockets were launched during the past five years, from June 1958 (IGY) to May 1963. The average payloads carried by these rockets were 12, 45, and 3 kg for K-6, K-8, and K-9L series rockets, respectively. The total payloads carried by those rockets for the past five years were as follows:

K-6 series		252 kg
K-8 series		585 kg
K-9L		74 kg
	Total	911 kg

The flight data for these rockets are listed in Tables 2, 3, and 4.

Table 2: K-6 firing records
Table 3: K-8 firing records
Table 4: K-9 firing records

The sizes and number of rockets fired each year during the five-year period are shown in Fig. 2. The data obtained from these Kappa series rockets are listed in Table 5.

Schedule for the Future

Through the test launches of the Kappa series rockets, it has become clear that the basic specifications of a rocket are 1) payload, 2) altitude, 3)

economic factor, 4) safety, 5) reliability, and 6) acceleration. We shall consider these specifications in detail.

1. The Payload

During the IGY, it was generally believed that a single-purpose, small-sized rocket was better than a multi-purpose big rocket. Dr. Newell, now with NASA but formerly with the Naval Research Laboratory, was one of the well-known scientists believing in this idea.

Table 2. Firing Records of Kappa-6

	Date of Firing	Name of Rocket	Launching Time	Angle of Launcher	Altitude (Km)	Flight Duration (sec)	Instruments
1	16 Jun. 1958	K-VI-1	11: 36	75°			Flight Test
2	20 Jun. 1958	K-VI-2	15: 15	78°	40-50	200″	Flight Test
3	24 Jun. 1958	K-VI-TW-1	10: 51	78°	25	21″	Temperature and Wind
4	30 Jun. 1958	K-VI-TW-2	16: 52	75°	45	75″	Temperature and Wind
5	12 Sept. 1958	K-VI-3	10: 31	78°	40	208″	Flight Test
6	14 Sept. 1958	K-VI-4	11: 40	78°	40	207″	Flight Test
7	25 Sept. 1958	K-VI-RS-1	14: 50	78°	40-50	140″	Solar Radiation
8	25 Sept. 1958	K-VI-TW-3	11: 55	78°	50	100″	Temperature and Wind
9	26 Sept. 1958	K-VI-TW-4	12: 50	78°	60	100″	Temperature and Wind
10	28 Sept. 1958	K-VI-CP-1	12: 05	78°	36	205″	Pressure and Cosmic Rays
11	29 Nov. 1958	K-VI-RS-2	12: 05	78°	40	130″	Solar Radiation
12	30 Nov. 1958	K-VI-CP-2	13: 00	78°	49	230″	Pressure and Cosmic Rays
13	23 Dec. 1958	K-VI-TW-5	12: 03	80°	60	120″	Temperatue and Wind
14	17 Mar. 1959	K-VI-RS-3	10: 35	80°	56	240″	Solar Radiation
15	18 Mar. 1959	K-VI-TW-6	11: 45	80°	50	104″	Temperature and Wind
16	19 Mar. 1959	K-VI-RS-4	10: 15	78°	50	215″	Solar Radiation
17	20 Mar. 1959	K-VI-TW-7	11: 50	80°	50	104″	Temperature and Wind
18	17 Sept. 1960	K-6-TW-8	11: 47	80°	47	228″	Grenades Temperatue and Wind Experiments
19	29 Sept. 1960	K-6H-1-TW-9	11: 46	78°	70	270″	Grenades Temperature and Wind Experiments
20	23 Aug. 1962	K-6S-1(K-8L-1)	16: 15	80°	173	424″	Flight Test (KSC)

Table 3. Firing Records of K-8

No.	Date	Time	Launching Angle (deg)	Peak Alt. (km)	Flight Time	Pay-load (kg)	Items of Observations
K-8-1	11 July. 1960	13: 24 JST	73°	150	380	35	Flight Test, Acceleration Deceleration Temperature Strains
K-8-2	17 July. 1960	3: 11 JST	78°	182	413	35	Flight Test Preliminary Test of Ion Probe
K-8-3	22 Sept. 1960 (COSPAR)	15: 32 JST	80°	200	440	35	Positive Ion Density and Cosmic Ray Intensity
K-8-4	26 Sept. 1960	20: 25 JST (night)	78°	185	433	35	Positive Ion Density and Cosmic Ray Intensity
K-8-5	27 March. 1961	13: 08 JST	79°	173	419	45	Ion and Electron Density Electron Temperature and Air Glow
K-8-6	18 April. 1961 (COSPAR)	21: 27 JST (night)	80°	150	376	45	Ion and Electron Density Electron Temperature and Air Glow
K-8-7	21 July. 1961 (COSPAR)	12: 42 JST	80°	100	410	54	Ion and Electron Density Electron Temperature and Air Glow
K-8-8	24 Oct. 1961 (COSPAR)	12: 58 JST	81°	200	440	31	Two Ion Probes, Electron Probe Plasma Probes
K-8-9	30 Oct. 1961	20: 13 JST	81°	175	407	45	Two Ion Probes, Plasma Probe Electron Probe, & Two Air Glow Meters
K-8-10	24 May, 1962	19: 50 JST	81°	failure		40	Two Ion Probes, Resonance Probe, Electron Probes Electron Density Probe, Plane Probe, Geomagnetic Aspect-meter
K-9M-1	25 Nov. 1962	11: 01 JST	78°	Second stage ignition failed		40	Two Resonance Probes, one plane Probe, one Mesh Probe, Acceleration, Deceleration, Vibration, Strain, Temperature Gauges
K-8-11	18 Dec. 1962	14: 03 JST	79°	202	443	40	Cosmic Ray Counters, Geomagnetic Aspectmeter, Radio Noise Propagation
K-9M-2	20 May 1963	11: 09 JST	79°	345	620	50	Geomagnetic Aspectmeter VLF and MF wave in ionosphere

Table 4. Flight Records of K-9

	date	time	launching angle	range
K-9L-1	1 April 1961	12: 25 JST	80°	Akita
K-9L-2	26 Dec. 1961	14: 05 JST	80°	Akita

	payload	altitude	time	item of observation
K-9L-1	11.3 kg	350 km	630 sec	acceleration, deceleration, temperature, telemetering system
K-9L-2	25 kg	350 km	630 sec	resonance probe for electron density, acceleration, temperature

After the IGY, however, people became more favorably disposed toward the multi-purpose rocket because of the accumulation of a number of multi-purpose rocket launches and data obtained from these rockets. This new tendency to use a multi-purpose rocket was due mainly to the need to derive the correlation among the various measured physical quantities. For example, we have to simultaneously observe the following quantities in order to study the ionosphere: the ion and electron densities, the temperature, and the electric and magnetic fields.

Even for the single-purpose observation, a large payload rocket still might be best, especially for uses such as tracing solar X-rays by the sun-follower method. As seen in Table 1, the K-9L and K-8 rockets have maximum altitudes of 350 km and 200 km, and payloads of 12 kg and 40-50 kg, respectively. And during the five-year period, two of the K-9L's and 13 of the K-8's were launched. This statistic obviously indicates the fact that the drawback in altitude was not significant compared to the advantage in payload of the K-8 rocket over the K-9L rocket. In other words, the most important factor for a rocket of today is not high altitude but large payload. This fact will lead to designing new observation rockets with large diameters, large total weights, and large payloads. Consequently, a giant-sized observation rocket will inevitably be developed in Japan.

2. Economic Factor

Since space research is always very expensive, the economic factor is one of the most important aspects, particularly in light of the present economic capacity of Japan. From the viewpoint of cost, we have to maximize the following quantity which corresponds to the efficiency of over-all research on rockets:

(payload) x (altitude) x (number of firings) x (percentage of success)

In other words, to get maximum efficiency within a certain budget, we have to minimize the following quantity:

$$\frac{\text{Total cost}}{\text{(payload) x (altitude) x (number of effective firings)}}$$

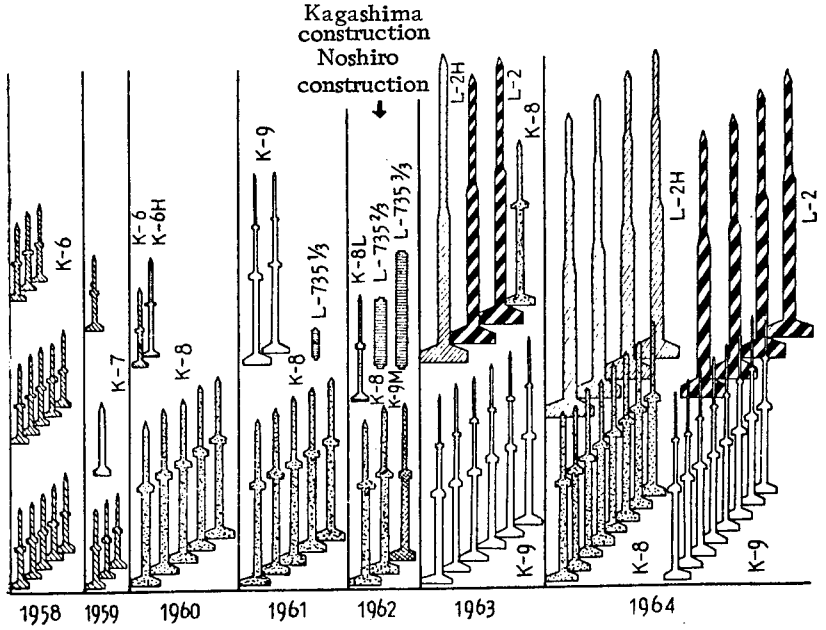

Fig. 2. Observation rockets which have been launched and are in the launching schedule

Table 5. Basic Data of Kappa-Series Sounding Rockets

Name	K-6	K-6 H	K-8 L(K-6 S)	K-8	K-9 M (K-8 H)	K-9 L
First Flight	Jun. 1958	Sep. 1960	Aug. 1962	July. 1961	Nov. 1962	Apr. 1961
Total Length (m)	5.6	6.9	7.3	11	11	11
Max, Diameter (mm)	250	250	250	425	425	425
Total Weight (kg)	260	330	337	1,500	1,400	1,600
Second Stage Rocket Length (m)	3.5	3.3	3.8	4.7	5.4	third stage rocket 3.4
Weight (kg)	83	89	92	320	330	98
Diameter	155	155	160	245	250	150
Velocity at second stage b•o	1370 m/s	1460 m/s	2210 m/s	2040 m/s	2800 m/s	2750 m/s
Max. Acceleration	29 g	27 g	43 g	25 g	46 g	32 g
Flight Time(sec)	84	95	440	440	600	630 sec

Table 6. Specific Cost per 1 kg Payload to 100 km Altitude

by K-6: $\frac{¥\,76\times10^6}{156\times0.5}=11\times10^6=\$\,30,000$

by K-8: $\frac{¥\,68.4\times10^6}{360\times1.75}=100,000=\$\,300$

by L-2: $\frac{¥\,60\times10^6}{400\times5.5}=¥27,000=\$\,75$

(Payload) × (Altitude) × (Number of Effective Firings) $\rightarrow$ Minimum Total Cost

Yen (a unit of Japenese currency, 360¥ = U.S. $1)

The specific cost needed to lift 1 kg of payload to 100 km altitude by K-6, K-8, and L-2 type rockets is listed in Table 6. From Table 6 we can see that as the diameter of a rocket increases, the specific cost decreases significantly. For example, we need $30,000, $300, and $75 to lift 1 kg of payload to 100 km altitude by K-6, K-8 and L-2 type rockets, respectively. Consequently, through economic necessity, rocket diameters will inevitably increase for a while in the future.

3. Safety and Reliability

Safety in launching a rocket is extremely important in a country having a very high population density such as Japan. We can easily understand this by recalling the disaster caused by unexpected trouble in the K-10 rocket flight. In this connection, we have to be aware of the fact that the nearest houses are only 250 m and 1 km from the launching pads of the Akita and Kagoshima testing sites. Even if we consider the longer distance, the 1-km safety factor in Japan is too small when compared with testing sites in America such as White Sands and Cape Kennedy with 100 km x 100 km and 200 km x 300 km areas of launching sites. Therefore, to overcome this geographic disadvantage, we have to have extremely reliable rockets so that launches can be made very safe.

The rate of failure in rocket launchings is related to the diameter of the rocket as shown in Eq. 1:

$$\frac{\int C_D \frac{1}{2}\rho V^2 S \times dZ}{\text{mass of rocket}} \propto \frac{D^2}{D^3} \propto \frac{1}{D} \cdots\cdots \tag{1}$$

$$\text{failure percentage} \propto \frac{1}{D}$$

As indicated in Eq. 1, the friction heat generated by the friction between a rocket and air, which is the most important factor accounting for failure of rocket firings, is proportional to the air drag. And the pressure on the tail and body of a rocket in dense air is proportional to the air drag. On the other hand, the mass of a rocket which can resist the two effects is proportional to the cube of the diameter (D^3) of the rocket. Therefore, considering safety, the diameter of a rocket should increase to obtain a higher success rate. In other words, the failure percentage is proportional to 1/D. Consequently, to develop a safer and more reliable rocket, its diameter should increase.

4. Acceleration

Connected with the acceleration of a rocket are the operational conditions of counter and measuring devices carried by the rocket. It was found that the lower the G, the more favorable the condition for operation of the counter and measuring devices. Actually, the acceleration of the Kappa series rocket is at most about 10-30 G, and this is a very low G factor compared with the accelerations of many American rockets. Thus, the low acceleration gives good conditions for operation of various devices in a rocket. And in considering aerodynamic heating of a rocket during its passage through dense air layers, the low G is a much more favorable acceleration for a successful rocket launching. A higher G is, however, required to prevent a rocket, in the presence of strong winds at launch, from missing its intended orbit.

If a rocket is small, such as a small weather rocket, and easily affected by wind, the deviation of the rocket from its intended trajectory is not controllable and presents a very difficult problem. Therefore, for such a rocket, the high G is much preferred. Thus, both low and high accelerations have their own advantages and disadvantages, and the most suitable accelerations must be fixed on a case by case basis. The various accelerations of the Kappa series rockets are listed in Table 5.

Based on these factors, the future plan for development of rocket research is as follows: by improving the Kappa series rocket, the K-6 is planned to be developed up to the K-6H, and this should also be developed up to the 8L type rocket. And the K-8 rocket is planned to be developed up to the K-9M type rocket. Simultaneous with these developments, two kinds of booster developments are planned to be developed to meet the requirements for large motors.

The first plan for the booster development is called the Lambda plan in which a 735-mm diameter engine would be constructed; and employing the engine as a booster, a Lambda observation rocket would be constructed. For more details about the Lambda engine, readers may find a detailed discussion in the chapter on "Development of Lambda-735-Type Rocket Engine."

In order to fix the diameter of the Lambda rocket at 735 mm, we went through an optimization study covering a wide range of diameters, from 400 mm to 1 m in diameter. From the result of this survey, the diameter of 735 mm was chosen as the most suitable diameter for the booster. The ground tests for the 735 mm diameter booster, which was called the L-735 project, were completed by 1962. A special research group, which was called the LD group, was organized in 1963 to develop a rocket having a much larger diameter. For the past two years, the LD group has concentrated its study on a booster size which will follow the 735 mm diameter Lambda series booster. As the result of the studies, the LD group finally decided that the diameter for the next booster would be in a range from 1.3 m to 1.5 m, based on an optimization system engineering approach, and at last fixed it at 1.4 m. And this was to be the engine.

In 1963, the group received a budget sufficient for two smaller sized Mu engines, 1/3 and 2/3 the length of the actually designed booster. The group is working within a schedule designed to go through all the ground tests in 1963. Under the assumption that the Lambda booster will be successfully developed, construction of L-2 and L-3 types of two- and three-stage rockets are scheduled. If the ground test of the Mu booster is successful, multistage rockets such as M-1, M-2, M-3, and M-4 rockets will be added to the schedule. The L-2 is a 2-stage type rocket employing a Kappa series booster as a second-stage rocket. The diameters of the first and second stage boosters are 735 mm and 420 mm, respectively. This L-2 rocket is expected to carry about 200 kg and 100 kg up to 500 km and 600-700 km altitudes, respectively. The L-3 is a 3-stage type rocket employing one L-735 as the first-stage booster and two 420 mm diameter boosters as the second- and third-stage boosters. The maximum altitude of the L-3 booster is not exactly known for the time being, but it is generally believed that it can lift a 20 or 40 kg payload up to 1000-2000 km altitude. At least, 1000 km altitude is expected for the L-3 booster.

The ground tests of the full size M-type booster are in the schedule for 1964. Under the assumption that these tests will turn out to be successful, launches of multistage rockets employing M-type boosters are also in the schedule for the 1964-1965 period. Specifically, the M-3 rocket is planned to employ an M-type booster and a Lambda booster for the second and third stages; and by adding one more spherical rocket to an M-3 rocket, a four-stage M-4 rocket is also in the schedule. By a rough calculation, the M-4 rocket is expected to reach 18,000 km with 40 kg payload. Since the altitude of the M-4 rocket is much larger than the radius of earth, 6,700 km, it has enough power to put a satellite into orbit.

Table 7 shows the outline of our plan for rocket research in the future.

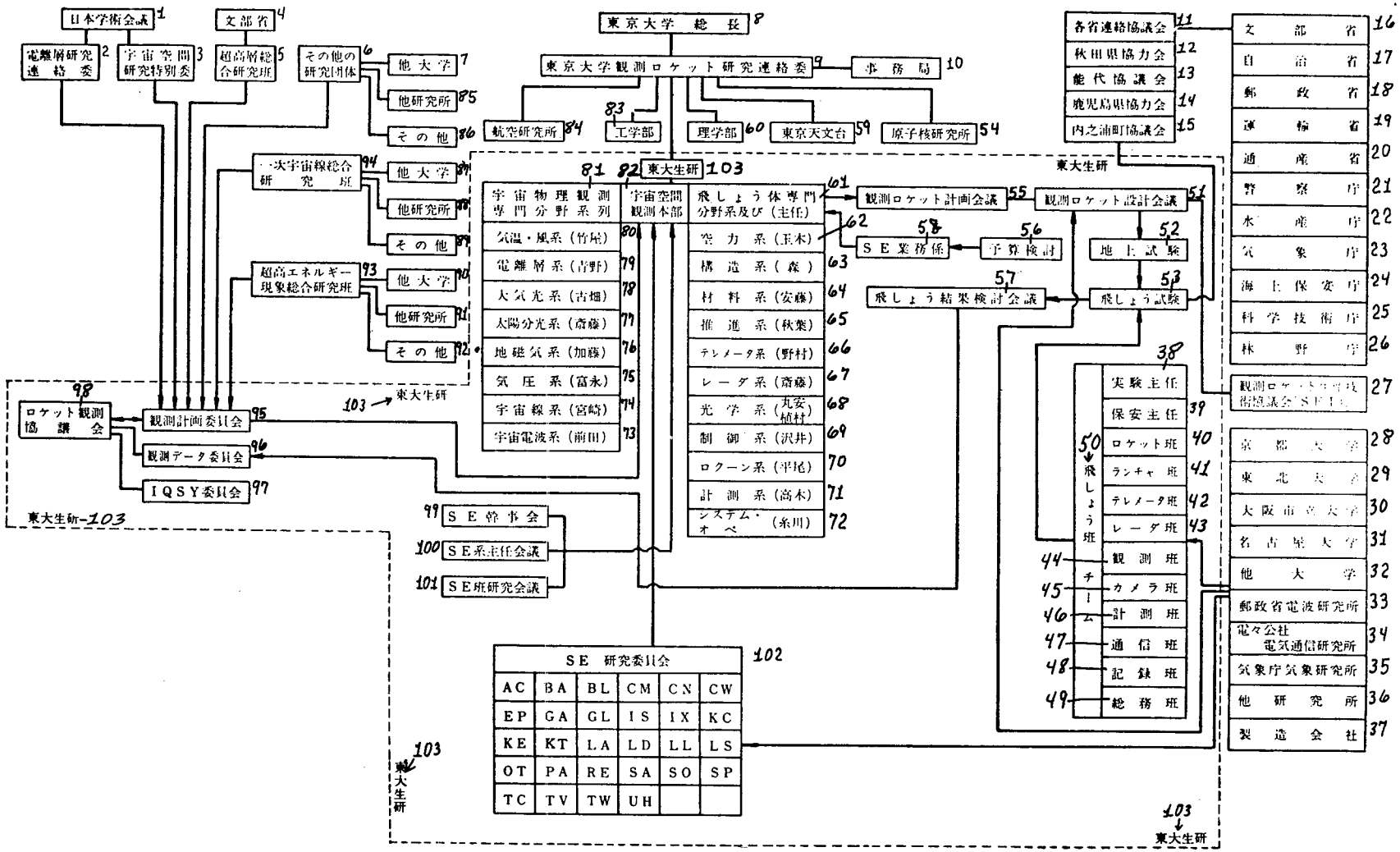

Fig. 3. Organization diagram of space observation rocket research

Fig. 3.

1. Japanese Academy of Science
2. Liaison Committee for ionosphere research
3. Special Committee on space research
4. Ministry of Education
5. Combined superhigh altitude layers research section
6. Other research sections
7. Other universities
8. President of Tokyo University
9. Liaison office of Tokyo University rocket research committee
10. Administrative office
11. Interministries Committee for Cooperation
12. Akita Province Cooperation Committee
13. Noshiro Province Cooperation Committee
14. Kagoshima Province Cooperation Committee
15. Uchinoura City Committee
16. Ministry of Education
17. Ministry of Autonomy
18. Ministry of Postal Service
19. Ministry of Transportation
20. Ministry of International Trade and Industry
21. The Policy Agency
22. The Fishery Agency
23. The Weather Agency
24. The Maritime Safety Agency
25. The Science and Technology Agency
26. The Forestry Agency
27. The Rocket Construction Technology Committee (SEIC)
28. The Kyto University
29. The Dohokoo University
30. The Ohoshaka City University
31. The Nagoya University
32. The other universities
33. The Radio Research Institute of Ministry of Postal Service
34. Electronics Communication Research Institute of Dendeng Company
35. The Weather Research Institute of the Weather Agency
36. The other institutes
37. Industrial companies
38. The chief of testing team
39. The head of security team
40. The Rocket team
41. The Launcher team
42. The Telemetry team
43. The Radar team
44. The Observation team
45. The Camera team
46. The Counting team
47. The Communications team
48. The Recording team
49. The Administration Office
50. The teams of flight sections
51. The Observation Rocket Design Committee
52. Ground test
53. Flight test
54. The Nuclear Physics Research Institute
55. The Rocket Planning Committee
56. Budget study
57. The Flight Result Subcommittee
58. The S.E. Business Office
59. The Tokyo Observatory
60. Departments of Science (a system which includes all science departments)
61. The specified groups in the rocket research and (chief of group)
62. The aeronautics group (damaki)
63. The structure group (Hayashi)
64. The material group (Anto)
65. The propulsion group (Akiba)
66. The telemetry group (Namura)
67. The radar group (Shaida)
68. The optics group (Maruyasu, Shikimura)
69. The control group (Zawai)
70. The rocking group (Hirao)

Fig. 3 (cont'd)

71. The counting group (Takagi)
72. The systems operation group (Idakawa)
73. The cosmic radiation group (Maeda)
74. The cosmic-ray group (Miyashaki)
75. The atmospheric pressure group (Tomanaga)
76. The geomagnetic group (Kato)
77. The solar-spectrum group (Shaida)
78. The airglow group (Hurutake)
79. The ionosphere group (Aona)
80. The atmospheric temperature and wind group (Takeya)
81. The space physics observation groups
82. The headquarters of space observation
83. College of Engineering
84. The Aeronautics Research Institute
85. The other research institutes
86. Others
87. Other universities
88. Other research institutes
89. Others
90. Other universities
91. Other research institutes
92. Others
93. The combined research sections for super-high energy phenomena
94. The combined research sections for the primary cosmic rays
95. Subcommittee of planning of observations
96. Data subcommittee
97. IQSY subcommittee
98. Rocket Observation Committee
99. Subcommittee of S.E. secretaries
100. Subcommittee of heads of S.E. groups
101. Research subcommittee of S.E. research sections
102. S.E. Research Committee
103. The Tokyo University Production Research Institute

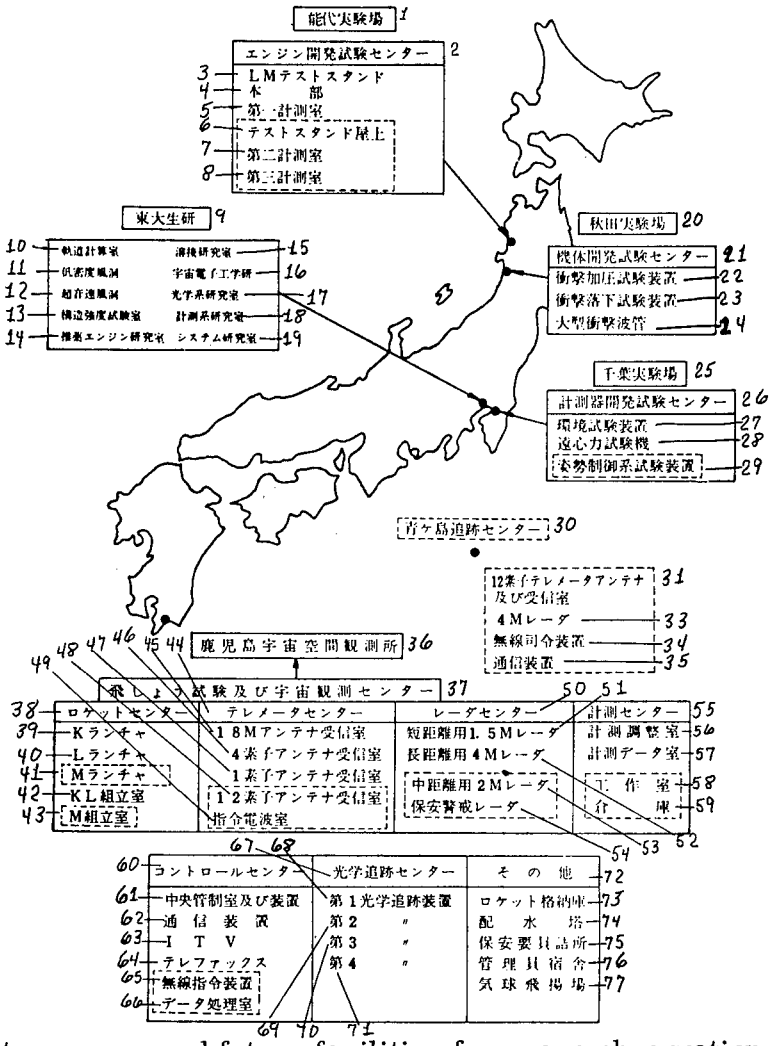

Fig. 4. Contemporary and future facilities for space observation rockets in Japan

1. The Noshiro testing ground
2. The engine testing center
3. The LM testing stand
4. The headquarters
5. The first counting and measuring section
6. Roof of the test stand
7. The second counting and measuring section
8. The third counting and measuring section
9. The Tokyo University production research center
10. The orbit computing laboratory
11. The low density wind tunnel
12. The supersonic wind tunnel
13. The structural strength test laboratory
14. The engine fuel research laboratory
15. The welding research laboratory

Fig. 4 (cont'd)

16. The space electronics laboratory
17. The optics research laboratory
18. The counting measuring devices research laboratory
19. The rocket system research laboratory
20. The Akita Test Center
21. The rocket body development and test center
22. The pressure impact (impact due to externally applied pressure) test device
23. The dropping impact test device
24. The giant shock wave tube
25. The Chiba Test Center
26. The counting and measuring device development and test center
27. The environmental test device
28. The centrifugal force tester
29. A control device for rocket attitude
30. The Akeshima Tracking Center
31. The 12-element telemetry antenna and receiving device
33. The 4-m radar
34. The radiowave control device
35. The communications device
36. The Kagoshima Space Center
37. The flight and space observation center
38. The rocket center
39. The K-launcher.
40. The L-launcher
41. An M-launcher
42. The KL assembly line
43. An M assembly line
44. The telemetry center
45. The radio signal receiving room with an 18-m antenna
46. The radio signal receiving room with a 4-element antenna
47. The radio signal receiving room with a one-element antenna
48. A radio signal receiving room with a 12-element antenna
49. A command radio wave transmission room
50. The radar center
51. The short range 1.5-m radar
52. The long range 4-m radar.
53. A middle range 2-m radar
54. A safety guard radar
55. The measuring center
56. The measurement control room
57. The data measuring room
58. A workshop
59. Warehouses
60. The control center
61. The central control room and devices
62. The communications devices
63. ITV
64. The Telefax
65. A remote control device
66. A data processing room
67. The optic tracing center
68. The first optic tracing device
69. The 2nd optic tracing device
70. The 3rd optic tracing device
71. The 4th optic tracing device
72. Others
73. The rocket hangers
74. The water tower
75. The quarters for safety guard
76. The residence for employees
77. The balloon launching ground

Table 7.

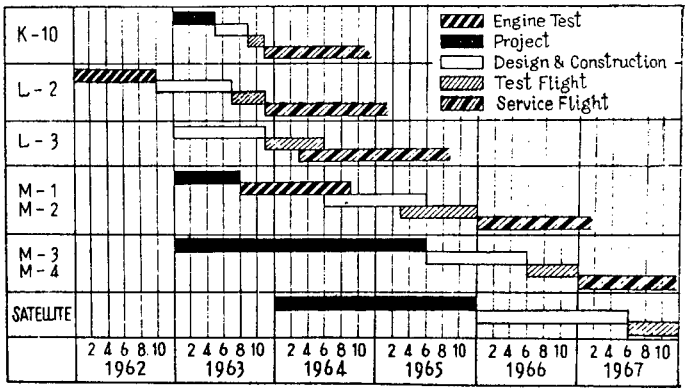

5. The Facilities

Fig. 4 shows details of the facilities for space rocket research centers, for those already completed and those scheduled to be constructed in Japan.

In Fig. 4, those facilities in the solid line blocks are already completed and in the dashed line blocks are either under construction since 1963 or in the schedule. If all these facilities are constructed, it may be possible to launch M-4 rocket and M-4 type satellites, if necessary.

The Noshiro test ground is an engine development and test site. The Akita test site was formerly used to launch small rockets; however, it is planned to rebuild it as a rocket-body research center for large rockets such as the Lambda and Mu rockets. The Chiba test site is under construction to become a counting device and measuring center for satellites of the future. And, as of this writing, the environmental and centrifugal force test devices are completed and installed in the Chiba test ground. And a small test stand is under construction and a rocket attitude control device is scheduled to be installed in 1963. The Kagoshima Space Center has six centers. This testing site already has almost the full equipment needed to launch the Lambda series rocket; however, if all the planned facilities, which are shown in the dashed line blocks in Fig. 4, are added to the original facilities, this testing site might have all the necessary facilities to launch up to the M-type rocket. A new observation center planned to be constructed in Akeshima will be equipped with telemetry, radio signal receivers, and radar to track the Lambda and Mu series rockets.

These are the fundamental timetable lines for Japanese rocket research until 1967. As we have heard in previous discussions, if there arise many demands to launch a satellite in Japan, the launch will start around 1967. The manpower plan, construction plan, and rocket plan are well on the way now.

6. The Organization

In order to put this extremely complicated work in good order, a nationwide organization is set up as shown in Fig. 3, in which the S.E. group of Tokyo University is the most important central organization and they co-operate well with other universities and industries all over the country.

(Received on May 20, 1963)

MEASURING DEVICES AND OBSERVATIONS

By Noboru Takaki

1. Introduction

The devices installed in a space rocket can be divided into three classes: 1) an observing device used to observe physical phenomena in a high-altitude atmosphere and a counting device used to detect the operational condition of a rocket, 2) a teletransmitter used to send observed data to the ground stations, and 3) a radar transmitter to give instantaneous information about the trajectory of a space rocket. Of course, a rocket has equipment in addition to these three fundamental devices in order to ensure all devices and the flight operating efficiently and effectively.

Some special techniques are needed to obtain an effective flight for a space rocket having all those measuring and counting and communication devices on board. And some other techniques are needed to get effective operation of the measuring and communication devices. For example, we have to open a window on the nose of the rocket to expose a measuring device to the outside atmosphere, or stretch out an antenna to send radio waves to ground stations. All techniques described here will be under the general heading of device-operation techniques.

In the following sections, we shall see the achievements of device-operation techniques; and the author's personal opinion on the future trend of development in the technical field will be briefly described.

2. The Measuring and Counting Devices

Formerly, the following quantities were being measured during space observations: atmospheric temperature and wind, cosmic rays, airglow, ionosphere, noise of cosmic radio waves, and geomagnetism; and the following quantities were being measured to learn the efficiency of a rocket: acceleration, deceleration, vibration, and temperature rise of the rocket.

A sound-bomb method is used to measure the temperature and wind in the atmosphere. Since for this kind of observation, eight sound-bombs should be fired one by one at exactly predetermined altitudes, the space rocket should be equipped with a precise timer to fire the sound-bomb at exactly predetermined times; and each sound-bomb should also have its own timer to explode the sound-bomb after it reaches a safe distance from the space rocket, so that the explosion will not damage the space rocket. The space rocket has to be equipped with telemetry to send radio signals giving the exact time of ejection of a sound-bomb to the ground station, and also to detect whether the sound-bomb had exploded or not. Thus, many difficult problems are involved in the measuring devices and techniques supporting this method. The sound-bomb method, however, has been used more than ten times for actual observations in Japan, and many valuable data were obtained for the temperature and wind of the atmosphere above the Japanese territory. These data contributed very valuable information for world weather map research. Since this method could not be used in the atmosphere higher than 100 km above the ground, a sodium-ejection method was discovered to replace the sound-bomb method in the high-altitude atmosphere. An experimental test proved that the sodium-ejection method could be used in actual observations of temperature and wind in the atmosphere higher than 100 km above the ground. Encouraged by the experimental test, the actual observation using the sodium-ejection method had been scheduled and was well prepared by May 1963. However, the weather conditions were so bad that the observation was postponed until now.

Cosmic rays were measured several times and the data are now being analyzed. However, the observations were limited to measure the total intensity of the cosmic rays and the intensities of a few particular energy ranges. The cosmic-ray counter was installed at the best position to receive the maximum cosmic-ray flux and the window in the nose of a space rocket was opened during the counting. By using an altitude instrument, a new kind of cosmic-ray intensity counter is now under construction for practical use.

In order to measure the airglow, a space rocket should have a device by which a light-collecting cylinder stretches out from the nose of the space rocket when the space rocket reaches more than 10 km above the ground, so that the light-collecting cylinder can supply enough light to a photoelectric cell, and a counting device which can analyze the airglow after separation into various wavelengths.

A resonance probe is used successfully to measure the ionosphere. In the ionosphere measurement, there is no particular technical difficulty because the only thing that has to be done for this observation is to expose the probe to the outside atmosphere at the proper altitude.

A coil method is used to measure the geomagnetic components along three axes. The only operational technique needed for this observation is to open the small window at the nose of a space rocket. The geomagnetic measurement was used successfully to detect the attitude of a space rocket at every instant

during the flight of the space rocket. A geomagnetic attitude detector will be used in the future as well as at the present time, even though another attitude detector which uses the sun instead of the geomagnetic field as a reference, is now well in progress. To detect the geomagnetic field, two other detectors are now under construction, the proton flux meter and a rubidium flux meter.

The noise of cosmic radio waves in the high-altitude atmosphere was also studied successfully by stretching an antenna out through the open window in the nose of a space rocket.

As we have previously seen in this report, in order to obtain satisfactory results in the observation of atmospheric physical phenomena by space rockets, we have to have both very effective measuring devices and device operation techniques to make those devices work effectively.

Of course, the single-purpose measurement using a small space rocket, which was formerly used many times in the U.S., has its own advantages; but simultaneous measurement of many physical phenomena is more important because the accumulation of various single-purpose observation data has significance only when the correlation between different physical quantities is made clear. Therefore, the multipurpose observation is very important and its progress is well along in Japan.

The most painful problem for multipurpose observations is the unavoidable increase in volume and weight of the measuring devices. The increase in weight is not hard to overcome, but the increase in volume is not an easy problem. The increase in volume, in turn, increases the size of a space rocket and thus it reflects very badly on the efficiency of the space rocket. Hence, because of the urgent need for multipurpose measurements in space observation, the need for smallness of measuring devices is inevitable. Therefore, it is important to develop miniature observation devices for future space research. Entirely the same argument can be raised about the counting devices, too.

3. The Teletransmitter

Formerly, subminiature tubes were used for the teletransmitter, but except for the very high frequency region a partly transistorized teletransmitter is now used for practical observations. The number of channels of the teletransmitter was increased by five to ten channels. The number of channels is planned to be increased to 12-15 channels. Even with 15 channels, it will not be enough to carry out the newly demanded multipurpose measurements. The present telemetry employs the FM-FM method, and so it is impossible to increase the number of channels to more than 15, because with 15 or more than 15 channels, each channel cannot operate separately and decreasing of observation efficiency is unavoidable. Faced with this difficulty, it is generally agreed to install two teletransmitters to increase the number of channels of the

teletransmitter, and for the Lambda series space rocket two teletransmitters are planned to be installed.

In such a case, the twin teletransmitter also gives a continuing problem with the efficiency of a space rocket flight. First of all, a completely transistorized twin teletransmitter is to be made as small as possible. The complete transistorization is therefore necessarily accompanied by a decrease in its efficiency. However, this disadvantage can be well covered by decreasing the noise and increasing the sensitivity of the radar receiver on the ground.

In the Kappa series space rocket, the devices such as the measuring devices, the telemeter, and radar, etc., are installed only in the main space rocket. However, in the Lambda series space rocket, those devices are planned to be installed in the second and third booster rockets as well as in the main rocket. This might be possible because the second and third booster rockets are expected to reach altitudes of the order of tens of kilometers and about 100 km maximum altitude; and so these booster rockets can be regarded as space rockets themselves. To use this new approach in space rocketry, we have to construct an effective but small body for the main rocket and booster rockets, and also particularly designed measuring devices.

A giant parabolic antenna having an 18-m diameter is under construction to track the Lambda series space rocket, which is expected to have several thousand km of flight range.

For some particular observation methods, such as sending information to the ground station through a television picture transmitter or pulse type signals, a wide frequency range for a teletransmitter is required. And in order to process many observed data with minimum error, a PCM type teletransmitter is evident.

4. The Radar

By much work on the radar-transponder used in a space rocket, an almost 100% reliable unit was built. Because of the difficult problems involving the volume of a device in a space rocket, the radar volume should also be minimized. To track the Lambda series rocket, we need as many radars as the number of rocket stages. And we have to determine the methods needed to prevent interference between radar signals.

At present, a 4-m diameter parabolic antenna is in operation, and it can track a space rocket as far out as 15 km. This antenna will be used to track a main space rocket; and a 2-m diameter parabolic antenna is planned to track booster rockets.

5. Future Problems

Thus far we have the present devices used in space rockets. For the past eight years, we launched more than 70 Kappa series rockets, but there were almost no two measuring devices alike because after launching one rocket, we would carefully study its results; and whatever defect showed up in the devices was immediately improved for the very next launch. Therefore, the measuring devices have been improved day by day, and every combination of various devices was different in every case. And the best of operating techniques was determined for each case.

Even though for technicians the standardization of the devices is very desirable, it is almost impossible at present because every device is nearly hand-made. Even the teletransmitter and radar transponder, which in a certain sense are already standardized, are facing a big change due to the volume problem in space rockets.

Considering the purpose of the space observation rocket, it is hoped to improve the conventional methods and at the same time develop our own observation methods. The attitude of a rocket has been detected by a geomagnetic attitude meter. As of now, though, there is no way to control the attitude of a space rocket and thus a certain kind of attitude control device is hopefully expected in the future.

According to our flight records, the Kappa 8 held more measuring devices than the Kappa 6 and the former cost more than the latter. And it turned out that the Kappa 8 cost less than the Kappa 6 in over-all average cost per each data bit. From this fact, we can see if a large space rocket can operate successfully, a large space rocket is better than a small one.

Since the Lambda series space rocket can hold many measuring devices and the booster rockets can also be used as observation rockets with properly designed measuring devices, the author believes it is very important to utilize successfully the Lambda series space rocket for observation rockets in the future.

(Received on June 26, 1963)

THE SELECTION AND CONSTRUCTION OF NEW TEST GROUNDS

By Hideo Itogawa

Dr. von Braun, the designer of V-2 rocket, wrote the following words in his recollections: "Rocket research begins with walking." A history of Dr. von Braun tells us that he traveled every corner of Germany to select a site for ground-testing the combustion of a rocket engine at the beginning of V-2 rocket research. The famous words of Dr. von Braun are fully applicable to every experimenter engaged in rocket research. We in the SE group had also surveyed many places and obtained much information before we finally chose Akita for the Kappa series rocket-launching ground. With the improvement of the Kappa series rocket, however, the Akita launching ground turned out to be unsuitable because it did not have enough ground area; and the Japan Sea, which was formerly used as the landing area, was not wide enough for the improved rocket. Therefore, once again we were faced with the first step of rocket research, namely, finding a proper launching ground.

Actually, we first noticed that the Akita launching site was inadequate in the period January to February of 1959, when the Kappa 9 rocket construction was started. It was predicted that the maximum altitude of the Kappa 9 rocket would be 300 km. It reached a maximum altitude of 350 km in an experimental test later. It was generally agreed that with some more improvements it would reach 400 as a maximum. Therefore, from the beginning, it was almost impossible to launch Kappa 9 rockets in the Akita launching site, which had the relatively narrow Japan Sea as its landing area. These situations were reported in the Production Research, vol. 13, No. 10, p. 30 (Oct. 1961). It was, however, not easy to find a new launching site to replace the Akita launching site. Since the main difficulty of the Akita launching site -- as well as any other new launching site -- was the available clear area, and since the Japan Sea was not wide enough for the Kappa series rocket, we had to find a new launching site along the coastline of the Pacific ocean. At last, we decided to use the Ohsumi Peninsula as the new launching site; and, as many people know, a new launching site was constructed there.

The construction of a new launching site at Ohsumi was accompanied with problems of additional facilities. Thus, the Noshiro test site was established for a new test stand for rocket engines; and we had to install entirely new rocket research facilities in the Chiba test site because when the Production Research group moved from Chiba to Asanuno, they took all their facilities with them. In other words, three new test grounds, Kagoshima, Noshiro, and Chiba, had to be established as the result of the unsuitability of the Akita launching site.

The Kagoshima test site is now known as Kagoshima Space Center and abbreviated KSC. Its full name is the Tokyo University Kagoshima Space Observation Center. The Noshiro test ground and the Chiba test grounds are known as Noshiro Test Center and Chiba Test Center, and abbreviated NTC and CTC, respectively. These three centers and Asanuno Headquarters will be the foundation of the space observation rocket research in Japan for the future.

1. On the Selection of the Kagoshima Space Center

As mentioned before, it was early in 1959 when the selection of a new launching site along the coastline of the Pacific Ocean was discussed in detail. However, the actual survey was made in 1960 and the final decision was made in late 1960. It was formally announced in the newspapers on April 11, 1961, that Kagoshima was selected as a test site. Then the ground-breaking ceremony followed. In January 1962, the first small-size rocket was launched at the Kagoshima launching site. Thus, the launching-site survey took two years. Many places were considered as possible launching sites and careful surveys were carried out during the two years. The chief candidates considered as possible launching sites are as follows: Hokkai Island and Aomori, Iboragi, Wokayama, Miyosaki, and Kagoshima Provinces. Among these provinces, only those places located along the Pacific coastline were actually surveyed. The fundamental factors considered in choosing a launching site included considerations of the area surrounding the site, the nearby sea, and sky above. With respect to the surrounding area, a site is more favorable if it has as small amount of residential area, farmland, and factories as possible in order to eliminate unexpected and unnecessary damage to people and property. In other words, the more open land, the better the place is as a launching site. It is desirable to have a place with many roads already existing in order to eliminate expensive road construction works. These two conditions are the basic factors for the area surrounding the site. In short, the conditions of the surrounding area are adequate transportation and good security. With respect to the nearby sea, we have to consider the regular shipping lanes and average number of fishing boats in the sea. For the ideal launching site, it is desirable to have as small a number of regular shipping lanes and fishing boats as possible on the nearby sea.

In selecting a new launching site along the Pacific coastline, the fishing-boat problem was the most important and difficult: we had had many experiences through space-rocket launches in the Akita launching site that indicated the most difficult thing in a rocket launching was to get agreements from the fishery union. As for the conditions of the sky above, it should be possible at a particular launching site that a rocket launching would be possible at almost any time without disturbing the international and domestic airlines. And the weather of the particular place was also one of the important factors. It was desirable to have considerably clear and stable weather for the launching site. With these conditions as the fundamental qualifications for the new launching site, actual surveys were made at the following places:

A. Monahitohama (at Kinshio-misaki, Hokkai Island)

As a beach, Monahitohama is a wide flat land surrounded by hills about 2 km from the coastline. During July and August, there are some foggy days, but there is almost no snowfall in the winter. The place is famous within Hokkai Island for the fine weather. In recent years, Kinshio-misaki became known as a tourist land. Since many tourists visit the place during the summer, bus lines are fairly convenient and road conditions are satisfactory for our needs. Since the off-shore area of Kinshio-misaki is one of the best fishing areas in Japan and, what is more, the continental shelf stretches far off into the sea, a great many fishing boats ply the nearby sea. Thus, the condition of the sea is not satisfactory from our viewpoint. We can find feasible remote areas at Uroka, but it takes one and one-half hours to drive from Uroka to Monahitohama.

B. Obuchi Beach (at Simokami Peninsula, Aomori Province)

This beach is flat and quite a wide area having hills on three sides and the Pacific Ocean on the east side. We at first decided on a possible launching site about 1 km south of the test site of the Tokyo University Production Research Center. This place has the big advantage of being completely isolated from a residential area. However, this land belongs to a private estate and costs about 20,000 Yen per 300 Hyo (Yen is the unit of Japanese currency, and Hyo is one of the Japanese area measurements and 36 square feet correspond approximately to one Hyo). To make things worse, strong northeast winds blow through this area and it is very cold and has very heavy snows during the winter. Thus, it poses very difficult problems for winter operation. This place is also believed to be very good farming land so that many farmers nearby come to this area to cultivate the land. This also gives us an uneasy feeling.

C. Sikashima-dai (at Kamisu-Mura Iboragi Province)

Restricted by the airline routes, it was generally agreed to find a new launching site between the north latitude 36° to 36°30'. For this reason, the beaches of Sikashima, Ono, Toiyo, and Hokoda towns were considered as possible launching sites. We actually surveyed Otoko Beach of Hokoda town, Kumiage Beach of Toiyo town, Simazu Beach of Sikashima town, and Okunotani Beach of Kamisu town. As the result of several survey reports made by one of the survey team, one of these places was believed to meet all the qualifications as a launching site. More specifically, this particular beach is wide and confined by hills, and there are only a few houses within the beach area and almost all the remaining area is occupied by farmlands. In re-examining the place, however, it was found that there were about ten houses in the woods close to the spot we had chosen as a launching site. The other problem was to construct a new and long road to connect this area to the nearest highway. On the other hand, this place had the desirable advantages of being located near Tokyo and having good weather for a rocket launch the year round. The province also had its own weather observatory for high altitude work. In spite of all these advantages, the sea condition did not allow this place to be used as a launching

site. After discussing the problem with responsible representatives of the shipping lines and fishing boats, we discarded this place as not being proper for a rocket launching site.

D. Kazitori-saki (at Taichicho, Wokayama Province)

There are two possible places in Wokayama Province: Totsutansihano-Misaki and Kazitori-Misaki, which is on the north of Totsutansihano-Misaki. The former place has wide empty ground at Kankenhana opposite a lighthouse. A sightseeing bus route goes very close to this place. The latter place also has wide flat land and a lighthouse at seaside; and the flat land is just wide enough for a launching site; and a highway passes close by. There is no home within the minimum safety distance. The weather makes it possible to use this place all through the year. We can find remote areas at either Kushino or Nimia. However, there are many fishing boats working and many regular shipping lanes on the nearby sea, and many regular airline routes in the sky above. These problems forced us to discard this place from the list of new launching sites.

E. Toisaki (at Kushima, Miasaki Province)

Since only a few airline routes pass through this area, we believed it to be a desirable place as a launching site. However, we could not find enough wide empty land even after several surveys. Several roads are well developed in this area and a good road reaches to flat land at Toi-Misaki. The city planners were planning to develop the area as a sightseeing place and were not enthusiastic about our space rocket research. The place was occupied partly by pastures for wild horses and partly by living areas for wild monkeys.

F. Ohosumi Peninsula (Uchinoura, Kagoshima Province)

As the result of the surveys on Toi-Misaki and other places located at the southern coastline of Kyushu Island, it was impossible to find a launching site along the southern coast of Kyushu. There is almost no flat land available and the coastline itself is made up of steep mountains. However, Ohosumi Peninsula has a fairly good beach, the weather is mild, and a bus line runs between Uchinomura and Kishino. There is only one small village — with about ten houses — which is called Nagohiro, between Uchinomura and Kishino. Nagohiro stretches from the province highway to the coastline in a gentle slope having several small hills. In case we decided to develop a new launching site at Nagohiro, we would have to smooth the hills and construct new roads with the soil from these hills. In other words, we would have to change the face of the natural geographic terrain. Unless such huge construction work were done, this place would not be suitable as a launching site. Among the possible places considered as a launching site, Ohosumi Peninsula has been regarded as the worst place, and until the final decision was made, it was generally believed impossible to establish a new launching site here.

An electric power line has to be extended 7 km from Uchinomura to Nagohiro. It takes about 20 minutes by bus from Uchinomura. Northwest and southeast winds with year-round average speeds of 1 3 km/hour blow in this area. This particular area is the most frost-free land in this province. There are some empty lands wide enough for a rocket launching site. We can use Shikaoku, Uchinomura, and Kagoshima cities as the remote areas. The following transportation routes are available: one can reach this place from Kagoshima via Suisu or one can reach it by transferring to the Sihuzi line from the Nichiko line at Toshiro and again to the Hurakawa line. It takes 31 hours by train from Tokyo to Shikaoku. As we see, this possible site is located far from Tokyo and there is no direct train line available. Therefore, another difficult problem was the transportation expense. Except for some cultivated land, all the lands were owned by the Forestry Agency, and we thought it might not be hard to purchase the land.

G. Tane Island (at Kumage, Kagoshima Province)

Tane Island running north to south is less than 10 km wide. There are one city and two small towns on the island. Its east coast is steeper than the west coast. The weather is mild, and seasonal winds do not affect the island too much. With these characteristics, it is possible to use this area as a year-round launching ground. Anno Beach of Nishinomode City, Kamikada Beach and Kumanoura Beach of Nakodane town, and Hiroda Beach and Simonoka Beach of Minamidane town were originally selected as the possible launching sites. All beaches except Anno beach are sandy hill. The biggest beach is Simonoka Beach, but it is located at the south end of the island. In view of all the factors, Kamikada Beach was believed the most desirable place for a new launching site. Kamikada Beach is 2.5 km away from Nakodane town and an automobile can be driven near this place. There is only one road, which runs perpendicular to the coastline; and there is no home within the safety limit. The beach is flat at the seaside and rises gradually to a hill surrounded by pines at its inland boundary. The beach stretches out into two highlands, one to the south, the other to the north, and both of them are about 2 km long. Noma and Nishinomura can be used as the remote areas. It takes 1.5 hours by bus from Nishinomura to this place. This island is 120 km away from Kagoshima harbor and it takes 6 hours by ship or 30 minutes by air. A ferry is in operation every day except every fourth day, and the airline operates two round trips every day between Kagoshima and this island.

Summary of the Surveys on the Possible Sites

Place of Survey

	Kinsho-Misaki	Simokita Peninsula	Sikashima-Dai	Kise Peninsula	Ohosumi Peninsula	Tane Island
1 Width	O	O	O	Δ	Δ	O
2 Obstacle	O	O	Δ	O	Δ	O
3 Land owner			O		O	
4 Air route	O	Δ°	O	Δ	Δ	Δ
5 Sea route	Δ	Δ	Δ	Δ°	Δ	Δ°
6 Fishery	×	×	×	×	Δ	Δ
7 Weather	O	Δ	O	O	O	O
8 Seasonal wind	Δ	Δ	O	O	O	O
9 Possibility of year-round use	Δ	Δ	O	O	O	O
10 Distance	Δ	Δ	O	Δ	×	×
11 Highway	O	O	O	O	O	O
12 Existing road	O	Δ	Δ	Δ	×	O
13 Elec. power	×	Δ	Δ	Δ	×	Δ
14 Living qtrs.	Δ	Δ	Δ	O	Δ	Δ
15 Storm observation	×	×	×	Δ	O	O
16 Space communications	O	Δ	×	Δ	O	O
17 Space observations	Δ^{x}	Δ^{x}	Δ°	Δ°	O	O
18 Latitude change	Δ	×	Δ	Δ°	O	O
19 Centrifugal force due to Earth's spin	Δ^{x}	Δ^{x}	Δ	Δ°	O	O
20 Radio wave observation	Δ	Δ	Δ	Δ^{x}	O	O

O—Excellent; Δ°—Good; Δ—Average; Δ^{x}—Fair; x—Poor.

Summary of the Survey of Possible Sites

The last difficult problem was to select one launching site which would enable us to launch a space rocket without bothering the fishing boats on the nearby sea which would be in the rocket landing area. The Marine Safety Agency and the Fisheries Agency arranged several discussion sessions for us at the Marine Casualty Prevention Association and the Codfish Association. We explained our situation with fish brokers there and heard their opinions. In the meantime, the Marine Casualty Prevention Association carefully examined statistical data on the sailing frequency of the regular ships and the situation of the fishing fleet. This information was obtained from reports of all member companies. We finally reached the following conclusion. The north, middle, and south parts of the Pacific Ocean could be graded into categories: the busiest, busy, and fairly inactive areas. In other words, we had to be able to launch a space rocket almost without considering the situation of the nearby sea. By this finding, we had to discard Iboragi Province from our list of possible launching sites, even if it had been regarded as the best place within a relatively short distance from Tokyo. In connection with the activity on the nearby sea, the south part of Kagoshima Province did not pose many problems as a space-rocket launching site. Beyond that, Kagoshima had another advantage which we happened to learn later on: Japan is located at a relatively low geomagnetic latitude and so the country is a very favorable place for doing research in low-altitude geomagnetism; and, as a matter of fact, this research is becoming one of the major fields of space research in Japan. For this purpose, the southernmost location is better than any other place and Kagoshima is the southernmost location in our list of possible sites. And, when a space rocket is to be used for weather research, Kagoshima is the best place to catch a typhoon by a space rocket because almost all typhoons passing over Japan move from south to north. The province government was very much interested in our plan, too. The weather of this place is far better than that of Akita and so there would hardly be any delays due to weather. From the viewpoint of financial economy, the large number of days the location would be useful would cover the high cost of transportation. Based on these reasons, we finally decided on Uchinoura of Kagoshima Province as the new launching site. The formal announcement to newspapers of the final decision was made on April 11, 1961. The announcement was as follows:

"Tokyo University Production Research Institute had been launching low-altitude atmospheric research rockets at Michigawa Beach of Akita Province. It has become unable to use the Akita test site to launch a new series of space research rockets because of the high-altitude and long horizontal landing distance of the new series of space research rockets. For this reason, the Institute asked government agencies to cooperate in finding a new test site along the Pacific coastline to replace the Akita test site. In the meantime, the Institute performed surveys on possible places and reached the conclusion that Uchinoura town of Kimotsuki county, Kagoshima Province, is the most favorably situated in many ways. With the agreement of all the concerned governmental agencies, province

authorities, and town authorities, the Institute decided to establish a test site at the above place. The construction work was scheduled to start in 1961.

"Unless unforeseen problems arise, the Akita test site, in addition, will be used to launch a small space research rocket whose maximum altitude will not exceed 300 km."

In May 1962, K8, K9 and K10 rockets were launched at the Akita launching site and caused the first big accident at the Akita test site. The accident upset the residents so badly that we had to re-examine more thoroughly the safe distance required for a space rocket launching. To study this particular problem, a special group was organized and from their research it was found that it was very expensive to safely continue the space rocket launches at the presently operating Michigawa test site. It was also economically and technically unsound to operate both the Kagoshima Space Center and the Akita test site. Thus, we arrived at our conclusion of operating one launching site at Kagoshima Space Center. As we shall see later in this paper, Akita test center was planned to be turned into a space rocket development center.

2. Noshiro Test Center (NTC)

In a space rocket engine performance ground test, we set a rocket engine on a test stand, which is called an engine bed, and then igniting the engine we test the power and its performance. In short, it is a sort of engine operation test on the ground. There are several test stands used in Japan for observation, research, and development. For example, Tokyo University used the test stand of the Chiba test site and the test stand of Akita test site; and the Prince Automobile Co. used the test stand at the Kawakosh test site. Among these stands, the Chiba test stand was used for a small engine and Kawakosh test stand was and will be used for a medium-size engine. As the result of the development of a large rocket engine, the Akita test stand became too small to test the large engine. We decided to find a new site having enough space and environmental conditions to establish a large-engine test site. When we made two experimental ground tests for L-735 1/2 and L-735 2/3 rocket engines at the Akita test site, we found the following difficulties:

1) Moving an engine larger than L-735 2/3 would be extremely dangerous because the road leading to the test site has a narrow and sharp curve on a steep hill at the junction where the road meets the Haori train line.

2) The geographic features and structure of the launching facilities put the test stand 1 m above the adjoining road from which a rocket engine should be unloaded to be put on the stand. It would be extremely dangerous to set an engine larger than L-735 2/3 on the stand without having a specially designed crane for this purpose.

3) When an engine larger than the L-735 2/3 rocket engine is involved in a test, it is estimated that the explosion fragments from an accidental

combustion would reach as far as 1 km. However, there are many residences within 250 m of the test stand, and it is too expensive to provide shell protection facilities for those houses.

4) According to what was scheduled by the province government planning group, the province highway running parallel to the national railway's Haori line will change to a national highway, and it will change its route to one approaching the Michigawa test site. When the highway plan is carried out, the highway will run within 250 m of the test stand. Even under the present situation, we have to schedule our combustion tests in such a way that they do not fall within the time period trains are running on the nearby railroad. When the highway plan is completed, the road situation will be so bad that we will not be able to have a safe combustion test unless a road block is made on the national highway.

In considering the above difficulties existing in Michigawa test site, we reached the conclusion that we should establish a new test site by taking the test stand of the Michigawa test site and adding minor facilities rather than by improving the old test site. In this way, we are able to secure safety and convenience and consequently to speed up our space research with less expenditures.

Having reached this conclusion, we decided to select a new test site based on the following conditions:

1) There should not exist combustible things, particularly woods, around the test stand since flame and flakes reach quite a far distance for several minutes during the time a rocket engine is being tested. In other words, there should not exist any possibility of a forest fire.

2) There should be no residence within 1 km of the test stand, and no people or animal should be allowed to come any closer than 1 km. Therefore, a test site should have safe and unoccupied surrounding areas.

3) If possible, it is desirable that the test site be isolated from residential areas by mountains or hills and to have a sea or lake at one side.

4) To make transportation of an engine easy, land must be flat and there must exist convenient roads.

5) Electric power transmission must be easy.

6) It should be possible to get wholehearted cooperation from the province government and town office.

Considering all these conditions, we selected the Hamaasauchi area of Noshiro city of Akita Province as the most suitable place among other possible places such as Sizuoka, Aichi, Aomori, Tochigi, Kagoshima, Akita, Iboragi, and Saitama Provinces and several other places near Tokyo. Among those

possible places, we surveyed Ohama Beach of Sizuoka Province. As the result of our survey, it was found that the land was undergoing reclamation and there were factories and also the selected place was very close to a residential area. The town was growing rapidly. Consequently, we concluded that the place was not suitable as a new test site.

We surveyed Iyokomisaki of Aichi Province in June 1962, and found that the area was under rapid development and had a very crowded population throughout the area. One vacant lot which we selected as a possible test site would be filled in the near future. Therefore, this place also was not favorably considered for the new test site.

In Aomori Province, the already existing flight-test site was considered a fairly good engine-test site, and it remained as the best choice for a while. However, we finally found that it was not suitable as a test site because the weather was bad, particularly in the winter, and transportation was very inconvenient.

For Tochigi Province, we considered establishing a test site in a mountainous area by building tunnels, if necessary. However, this area was also excluded from the list of possible sites because it was covered with woods.

Many people including the SE group members saw the advantage of establishing the new test site in Kagoshima Province, where the Space Test Center had been established. Therefore, an extensive survey was performed for this province, particularly in the vicinity of Uchinoura and the coastline from Sihuzi Bay to Satsubora Peninsula. However, we could not find even a single place for a test site. The Pacific Ocean side of the island was covered with woods and had the high possibility of catching fire. The Satsubora Peninsula area was a popular sightseeing area; and some other possible places that we found needed excessive road construction funds. Therefore, we had to turn our faces from the province in spite of our strong feelings.

We had one more choice in Iboragi Province. We considered converting the already existing launching site into an engine-test site. For many reasons, though, this also turned out to be impossible.

Thus, almost all possible places were eliminated from the list of possible locations and we were stymied until Mr. Kenzo Saido told us that Hamaasauch Beach had been investigated as a possible site for a future nuclear powerplant, but the plan was canceled for some reason, and he believed the same place might be used as a rocket research site. As a result of this advice, we surveyed the place and found that it met all conditions to a quite satisfactory degree. We decided to establish a new test site at the place and named it Noshiro Test Center.

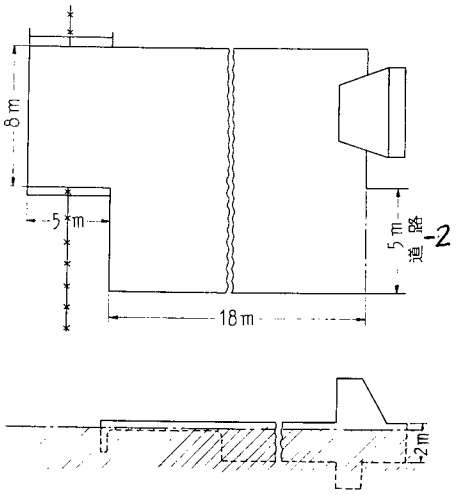

1-(a) 能代テスト・スタンド平面および側面図

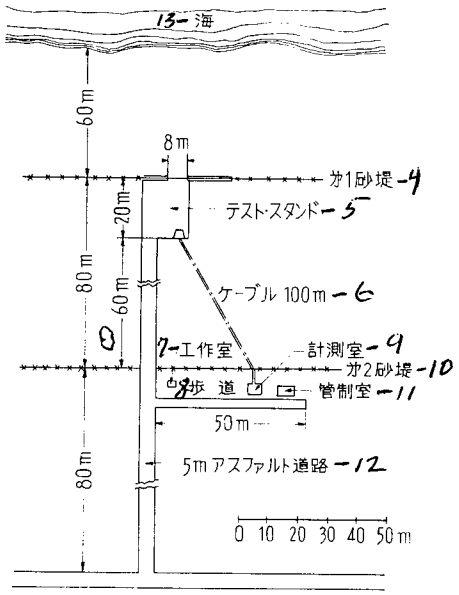

3-(b) 能代テスト・センター（おもな施設）

1 - (a) Plan and side views of Noshiro Test Center; 2 - Road; 3 - (b) Main facilities at Noshiro Test Center; 4 - First sand bank; 5 - Test stand; 6 - Cable; 7 - Workshop; 8 - Sidewalk; 9 - Counting room; 10 - Second sand bank; 11 - Control tower; 12 - Paved road; 13 - Sea

As the first step of the Noshiro Test Center construction project, an LM test stand was constructed; and then the base of the test stand of the Michigawa test site was taken here to put on the LM test stand. A thrust power meter is to be installed on the test stand, which will be able to measure up to a maximum of 100 tons of thrust. With all this equipment, the Lambda and Mu

series space rocket engine will be tested. Two counting rooms, one control tower, and other research facilities are in the schedule. The plan and diagram are shown in the figure. This place is located at longitude 139°59'27" East, and latitude, 40°8'32" North. The first test in this place was done for the L-735 2/3 space rocket engine in February 1962.

3. Chiba Test Center (CTC)

Chiba Test Center is scheduled to be used for the vibration test, shock test, and vacuum test of counting devices, which will be installed in a space rocket and tested in a large environment test device. We also have a plan to construct several small test stands to research the basic problems of propellants and to test small space-rocket engines.

4. Akita Test Center (ATC)

Finally, Akita Test Center at Michigawa is considered being used as a body development center for testing rocket bodies by dropping, shock-wave studies and other means. However, there is no actual plan for this work.

(Received on May 18, 1963)

THE IQSY AND THE SPACE ROCKET

--OBSERVATIONS DURING THE IQSY--

By Kengich Maeda

The Meaning of IQSY

The present paper is a report on the International Quiet Sun Year (IQSY) conference, held in Rome for five days from March 18 to 22, 1963. The author attended this conference and returned to Japan on March 26, 1963.

The IQSY is a period during which the sun is least active -- from 1964 to 1965. Several years ago, it was proposed that the international scientific community cooperate in observing the many physical phenomena that would occur during this unusual period of a quiet sun. Previously, during the International Geophysical Year (IGY) -- 1957-1958 -- many physical phenomena of space were successfully observed while the sun was very active. The IQSY project has the same objectives: to make scientific observations as was done during the IGY project; however, due to the activity of the sun, the IQSY project is expected to yield significant but different results. Encouraged by what was obtained by the IGY project, many countries all over the world are willingly cooperating for the IQSY project. During the Rome IQSY conference, general agreement was obtained on the basic phenomena to be observed. The first IQSY conference was held in Paris, France, in February 1962, and the Rome conference was the second IQSY meeting. Since it was only nine months before the IQSY was to begin, many people from all over the world attended the conference; and the participants put their efforts into drawing up the basic plan for the IQSY project. During the conference, it was agreed to cover many scientific fields in observing space and terrestrial phenomena; and it turned out that ground observations were considered most important and dominant. The satellite and space rocket observations were planned as parts of the project; however, the significance of these observations was also emphasized.

The international activities for satellite and space rocket observation are managed by COSPAR (Committee on Space Research). COSPAR organized a working group to discuss and plan the research for IQSY, and the author attended the Rome conference as a member of the working group.

The International Trend in Space Rocket Observations

Since the first satellite was launched, the non-specialists as well as the specialists in space research have been completely surprised by the success of the satellite and applauded its value in space research. The very significance of a space rocket in space research seemed about to disappear. It goes without saying that a satellite has very significant advantages over a space rocket: for example, by virtue of its long duration of flight, a satellite can collect enough data to be used in a statistical analysis for various phenomena; can catch instantaneously many unexpected phenomena of the sun; and can dwell a long time in space for the occurrence of any particular instantaneous event; and its observation can be made deep in space, etc. On the other hand, a satellite also has some disadvantages over a space rocket in certain aspects: for example, a satellite cannot make observations in the low-altitude atmosphere, lower than about 200-300 km (formerly said to be the ionosphere); and a satellite's cost is very high. By several recent events, space observations using small space rockets became more important than ever before; as a result, many specialists in space research recently recognized the advantages of space rockets. Many countries are competitively working on the space rocket for their own space research; and the IQSY is fast approaching. The small rocket (this terminology stands for a space rocket and the term "small" means small compared to the rocket used to put a satellite into orbit) able to reach about 200-km altitude would be used during IQSY.

Formerly many small rockets were used for space research in the U.S., Soviet Union, Great Britain, and Japan. Canada worked together with the U.S.; Australia cooperated with Great Britain for space-rocket research and launches. With the help of the U.S., Italy, Argentina, Norway, and Pakistan have already successfully worked out their space-rocket observations. Sweden and India are hurrying with their space-rocket observation program. Canada is working hard on its own space rocket (Black Brant) and trying to have its own space-research program independent of the U.S. The European Space Research Organization (ESRO) was established by several European countries, and each member country is going to use its own space rockets for space research within ESRO. Many German scientists have actively joined in the organization. The author heard that Holland would launch space rockets in Africa, and Pakistan would adopt Japanese space rocket techniques; and Brazil would join in space-rocket observations. Considering all these ambitious movements in space-rocket research, even though Japan is one of the senior countries in the field, we have to mobilize our whole national effort to speed up our space research.

Space Observations During the IQSY

Several working groups were organized since COSPAR was founded. The second working group (WG2) was mainly concerned with the determination

of items of observation by a satellite and a space rocket. During the IQSY sessions of the Washington COSPAR conference in May 1962, the WG2 was reorganized to take over all the research plans. Dr. Friedman of the U.S. was elected leader of the group. Within WG2, a group named the Joint Space Rocket Observation Panel was formed; and during the COSPAR conference, the panel selected the following five important items as the principal observations for the IQSY project: 1) Weather, 2) atmospheric temperature and wind (using a sodium cloud method), 3) atmospheric temperature and wind (using a sound-bomb method), 4) atmospheric density, and 5) oxygen molecule. The author was elected the leader of the atmospheric electron density group. This election might have been influenced by the author's past research with a resonance probe for making atmospheric electron density measurements. The author had prepared recommendations for his own specific field and also had outlined his own theories before leaving for the Rome conference. In the Rome conference, four more items (the ion composition, the geomagnetic field, the low-altitude ionosphere, and the atmospheric density) were added and so a feeling of accomplishment pervaded.

1. The Weather Group

Mr. Johnson of the U.S. Weather Bureau was elected the leader. The group would observe the atmospheric temperature and wind in the low-altitude atmosphere within the band between 60-70 km and up to a maximum altitude of 80 km. The group would use the following methods for their observations: the drop method, the metallic parachute method, and a method which uses a Mylar sphere containing a radar target; and in the U.S., an active method was adopted in which a transmitter and a radar-transponder would be loaded in a space rocket. The U.S., Soviet Union, Great Britain, France, Italy, Pakistan, Germany, and India participated in this group. The U.S. and Soviet Union would launch the majority of space rockets. The Japanese Weather Agency is going to launch experimentally its own space rocket independently of the group research. One of the interesting things is that Great Britain will not use Woomera of Australia, but one of the Japanese islands for its weather rocket launching ground. France will launch her weather rocket at Hammoguir.

2. The Atmospheric Temperature and Wind Groups

There are two groups for the atmospheric and wind research. One would use the sodium cloud method and the other would use the sound-bomb method for the research. Mr. Blamont of France is the leader of the group using the sodium cloud method. The first joint observation of this group was successfully carried out from November to December 1962. The U.S. offered two of her space rocket launching grounds; and each country: Great Britain, Italy, France, and Argentina, offered one of its space rocket launching grounds, and consequently, a total of six space rocket launching grounds were used for the first joint observation. The next joint observation was scheduled to be held from May 13 to 18, 1963. And the U.S. offered 12 space rockets and four launching grounds. Great Britain offered one launching ground (Woomera in Australia); France offered three space rockets; Algeria offered six space rockets and two

launching grounds; Pakistan offered two space rockets; Argentina offered three space rockets, and Japan offered one space rocket. And three space rockets from Italy are expected. The third joint observation was scheduled to be held either in June or December 1964 without waiting until the IQSY. The participators agreed to make all other schedules after the COSPAR general meeting in Warsaw in June 1963. A research team of the U.S. Air Force is developing a luminous material for sightings even in the night. The team is experimentally testing NO, $CSNO_3$, and Al in the Air Force research laboratory. If its research turns out to be successful, it will provide significant progress in space research because the sodium-cloud method can be used only in the daytime and about 30 minutes before sunrise and after sunset. The author asked for more detailed information at the Rome conference, which will be available shortly.

The other group, led by Mr. Nordberg of the U.S., will study the movement of wind in the atmosphere all over the world within the altitude band of 50-90 km above the ground. To cover the northern hemisphere, the U.S. offered four weather research stations; and Italy, Japan, and Sweden each offered one weather research station. Argentina offered one and Great Britain offered Woomera of Australia to cover the southern hemisphere.. The Soviet Union is expected to join this program and Pakistan may possibly join, too. Italy is going to construct a movable launching stand to carry to the launching site. The members decided to select appropriate and mutually convenient days for their joint observations; however, no further details were discussed at the Rome conference. Since we have much experience in this field, we may possibly achieve good rapport and results with this group.

3. The Atmospheric Density Group

Under the direction of Mr. Jones of the U.S., this group will use the sphere dropping method to measure the atmospheric density. By measuring the downward velocity of a sphere, experimenters will determine the atmospheric density. The group planned to send a 37-Mc radio wave from the ground control station to the sphere; and the sphere would be designed in such a way that it would return a 74-Mc radio wave by means of a transponder installed in the sphere; and thus a radar on the ground station would be able to track the sphere to determine its velocity. In Japan, a similar experiment was planned by the Weather Research Institute and the author hopes we can join the group for the joint observation.

4. The Oxygen Molecule Group

It is generally known that an oxygen molecule starts to decompose to oxygen atoms about 100 km above the ground. The main object of this group is to measure the vertical component of density distribution of the oxygen molecule. Dr. Friedman of the U.S. proposed to measure the amount of oxygen molecule by measuring absorption of the solar radiation using three kinds of optical filters: saline (1480 Å) , sulfur (1425 Å) , and BaF_2 (1350 Å) , through

a detecting circuit employing a secondary electron amplifying tube which is, for the time being, not available in the commercial market. This method was invented in France, and is based on the fact that the oxygen molecule absorbs the 5-mm radio wave.

5. The Ion Composition Group

Mr. Jones, who was mentioned above, was elected leader of the group. This group is engaged in measuring the percentages of O_2, O, NO and N_2 ions in the atmosphere, using a mass analyzer. There are many kinds of mass analyzers available now. Mr. Jones proposed to use a 4-pole mass analyzer. The Japan Radio Wave Research Institute constructed its own 4-pole mass analyzer, and it will be tested experimentally in the near future.

6. The Atmospheric Electron Density and Temperature Group

As mentioned before, the author was elected leader of this group, and was asked to organize an observation network. This field is believed to have very important academic significance in the joint observations of the IQSY project. The author proposed to measure atmospheric electron density and to find out the structures of the sporadic E layer and D layer. One other important objective is to measure the distribution of electron temperature. We wish to check the theories on the formation of the sporadic E layer and the structure of the D layer by combining our observations on the electron density with the observations on the movement of wind. These observations were very difficult problems by the radio wave measurement method. By simultaneous measuring both atmospheric and electron temperatures, it may be possible to check the linear relation between the altitude and the distribution of electron temperatures. We wish to have a somewhat clearer picture of electron temperature distribution all over the world. There are several kinds of measuring methods at hand: for example, a resonance probe method; a method using the impedance of an antenna; and a method using the propagation characteristics of a radio wave, etc. We agreed that each country may use whatever method it likes best. It was already determined before the Rome conference that the resonance probe method or some other probe methods would be used in Japan for the IQSY project by the Radio Wave Research Institute. Kydo University designed space observation devices using the impedance of an antenna and the propagation characteristics of radio wave for the observation of the atmospheric electron temperature and density in the IQSY. We wish to measure the ion density and airglow at night when we measure the atmospheric electron density and temperature.

7. The Geomagnetic Group

The main purpose of this group is to measure the geomagnetic field in the E layer and sketch rough maps of the electric current flow in the E layer. For this task, Mr. Cahill of the U.S. was elected leader. The geomagnetic observation is also a very important field in the IQSY project. There are many

kinds of available magnetic flux meters; however, a useful meter for this observation should enable observers to measure with accuracies within the range of 10-100 gamma in measuring 30,000-40,000 gamma of permanent magnet. This group planned to measure the geomagnetic fields in the E layer at the three typical geographic regions: near the aurora, middle latitude, and magnetic equator, regions. Mr. Cahill proposed to measure the geomagnetic field at these three regions by the U.S. space rocket and he appealed for international cooperation. Answering his appeal, the Tohoku University agreed to take charge of one of the observation stations for the middle latitude region and Uchinceura was selected as its observation center.

8. The Low-Altitude Ionosphere Group

All the research of the IQSY project is directly related to the physical phenomena in the D and E layers, but they are all separate phenomena and no correlation of them is included so far. To cover this point, Mr. Bowhill of the U.S. presented D and E layer packages to study D and E layers as a whole. The D package consists of a radiation absorption detector, direct current probe (electron and ion counters), a density meter (using the Lyman line of an X-ray), and a magnetic flux meter. And the E package consists of an ion analyzer, a magnetic flux meter, a density meter (using a(1450 Å)optical filter), and an atmospheric electron density meter. Each package would be loaded in a space rocket to measure the combined properties of the D and E layers.

9. Miscellaneous

Experimenters hope to measure the solar radiation in the daytime and the airglow at night. This would be done at the same time the atmospheric electron density and temperature are being measured. Nevertheless, the two former measurements are important by themselves and would possibly be scheduled as independent measurements for the IQSY project. A combined multipurpose observation for those above-mentioned fields was already proposed. It was believed that the noise and propagation of a radio wave and the particle rays having various energy levels (including the cosmic ray) would be measured in the IQSY. However, nothing was discussed about the international joint observations for these fields at the Rome conference. It will perhaps be discussed at the Warsaw conference in June 1963. No matter whether this work will be part of the IQSY project taken up during the Warsaw conference, one thing is clear: those observations should be anticipated for the IQSY project because they are extremely important scientifically.

The Participators and Their Facilities

The delegates from Italy, Canada, and Australia did not present enough information about their future plans. Delegates from the Soviet Union agreed to present their reports on research and plans at the Warsaw conference in

detail. Therefore, for the time being, it is impossible to know exactly about the participants and their facilities for the IQSY project. The author, however, is giving this report based on the information obtained at the Rome conference.

The Goddard Flight Center of NASA, NRL (Naval Research Laboratory), AFCRL (Air Forces Cambridge Research Laboratory), the Weather Bureau, and NBS (National Bureau of Standards), the University of Illinois, the University of Michigan, and Pennsylvania University will participate in the project for the U.S. London University, Buckingham University, and the Imperial College will join under the direction of the Royal Society. The Superhigh Altitude Research Institute and the Communication Research Institute of France, the Communication Research Laboratory of the Defense Department of Canada, the National Ordnance Research Laboratory of Australia, the Roma Institute of Technology of Italy, the Space Research Committee of India, the Space Research Committee of Atomic Energy Commission of Pakistan, the Space Research Committee of Norway and Sweden, and the Denmark Institute of Technology all join in the IQSY project. ESRO directed by Dr. Rower of Germany also joined with other participants.

	Launching grounds	Countries	Geographic latitudes	a	Regions
1	Trivandrum	India	8.5°N 77°E	− 1°	b
2	Hawaii	U. S. A.		(+21°)	Low latitude
3	Sonmiani	Pakistan	(26°N 67°E)	(+20°)	
4	Eglin, Florida	U. S. A.	30°N 87°W	+40°	c
5	Chamical	Argentina	30.5°S 66°W	−20°	
6	Hammaguir	Algeria	31°N 3°W	+34°	
7	Woomera	Australia	31°S 137°E	−41°	
8	Uchinoura	Japan	31°N 131°E	+21°	
9	White Sands	U. S. A.	32.5°N 106°W	+41°	
10	Wallops Id.	U. S. A.	38°N 75.5°W	+48°	Middle latitude
11	Saldinia	Italy	39.6°N 9.5°E	+40°	
12	Ile du Levant	France	43°N 6°E	+44°	
13	Ft. Churchill	Canada	59°N 94°W	+69°	Either high latitude or the aurora
14	Andöya	Norway	69.3°N 16°E	+67°	
15	Franz-Josef Land	U. S. S. R.	80.5°N 58°E	+72°	

a—geomagnetic latitudes; b—geomagnetic equator; c—almost same latitude.

According to the author's findings, the actual space rocket launching ground for those participants are listed in the above table. The table contains all the launching grounds that are related with the observation of the physical phenomena in the ionosphere, such as the atmospheric temperature and wind, and the atmospheric electron density and temperature, etc. However, the launching grounds related to the weather research of the U.S. are not included in the table.

The International Joint Observation Dates

As mentioned before, ground observations are the most important and will constitute the majority of observation activities for the IQSY project. Thus, a sched ıle for international joint ground observations was fixed in detail, and we call it the International Geophysical Calendar. Those people who are engaged in space rocket observations must recognize the following dates: 1) every Wednesday, 2) Regular World Day (RWD three middle days of every month), 3) the days when 1) and 2) days would overlap (middle day of every month), and 4) the world day which exists four times in every year. It was proposed that as far as possible all space rockets should be launched on the world days. For the time being, world days for 1964 would be fixed in January, April, July, and October. The sodium-cloud method observation is scheduled to be held in January and December 1964. Other groups had not announced exact dates for their observations. In the author's opinion, when our group observes the atmospheric electron density, it is better to measure at the same time the ionosphere by the ground radar.

Conclusion

As we have seen in this report, the international joint observation for the IQSY project is raising international interest and receiving worldwide support. As a senior country in this field, we have to hurry to do our share and subsequently be justly recognized in the field. More specifically, we have to have enough space rockets and various counting and measuring devices and methods of combination of these devices according to the needs of every particular case. To obtain effective and rapid progress, these problems should be extensively discussed by those people familiar with them. The Government, related industries, the Tokyo University Production Research Institute, and electronic technicians particularly engaged in space rocket field should give their wholehearted support and willing cooperation for the great opportunity, namely IQSY.

(Received on April 25, 1963)

COSPAR AND JAPANESE SPACE ROCKET RESEARCH

By T. Tanaka

1. COSPAR

COSPAR is the abbreviation of the "Committee for Space Research." There is no formal Japanese translation of it and it is translated as the International Committee on Space Research in this paper. The author put the word "international" before COSPAR for many countries have their own organizations as members of COSPAR and there is a possibility of misunderstanding. For instance, Japan has the Special Committee in Space Research in the Science Council of Japan, and this is also the country's committee to COSPAR.

COSPAR is a subordinate organization of ICSU. ICSU is the abbreviation of the International Council of Scientific Unions. ICSU has academies and councils of many countries as its members. The Science Council of Japan joined ICSU.

There are many unions and committees in ICSU such as COSPAR. The unions are organizations such as the International Astronomical Union (IAU) or the International Union of Theoretical and Applied Mechanics (IUTAM). COSPAR is, however, not similar to these unions although it is an organization directly under ICSU to which many unions and academies of the member countries join.

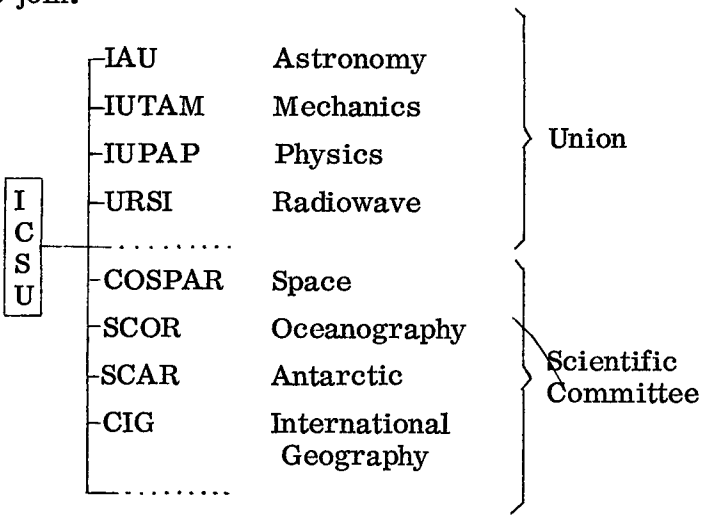

SCOR, SCAR and CIG are on the same level of organization as COSPAR and these organizations are sometimes called scientific committees.

COSPAR consists of the following ten unions:

IAU	Astronomy
IUGG	Geodesy and Geographical Physics
IUPAP	Pure and Applied Physics
IUPAC	Pure and Applied Chemistry
URSI	Radiowave Science
IUBS	Biological Science
IUTAM	Theoretical and Applied Mechanics
IUB	Biochemistry
IUPS	Physiological Science
IUM	Mathematics

Besides the unions, academies of many countries attend COSPAR as members.

COSPAR has a president and two vice presidents. The president is selected from among the heads of the constituent unions not from the representatives of the member countries because the work the president performs may be sensitive to some of the member nations. The first president was Van de Hulst, a Dutchman, from the Internation Astronomy Union; and the second and present president is Roy, a Frenchman, from the Internation Union of Theoretical and Applied Mechanics. Members of the executive committee include one chairman, two vice chairmen, and four executive committee members. The two vice chairmen from the United States and Soviet Union are to be the candidates for the chairmanship. And the chairman is to be selected from those two candidates by voting. This is quite a complicated structure. Present members of the executive committee are Bucher from Czechoslovakia, Zonn from Poland, Hassey from England, and Van de Hulst from Holland. Among them, Van de Hulst is not the representative of his nation but the head of the International Astronomy Union and after his resignation from the COSPAR presidency, Roy took the position.

COSPAR holds a general meeting and symposium annually. A meeting was held at Washington, D. C., U.S.A., in 1962 and will be held at Warsaw, Poland in 1963.

CIG, the Committee on International Geophysics, is the successor of the organization which performed the International Geophysical Year Project between 1957 and 1958. Under CIG, there are the International Quiet Sun Year (IQSY), Upper Mantle Project (UMP), and World Magnetic Survey (WMS) subcommittees. IQSY is a project to perform worldwide geophysical research

during 1964 to 1965 when the activity of the sun will be minimum; observations by space rockets will have great importance for this project.

2. Japanese Space Rocket Research and its Bearings on International Activities

Space rocket research in Japan has its origin in IGY, during 1957 to 1958. The entire Japanese plan for IGY, then, was made by the Committee on the International Geophysical Year (CIGY, chairman Mr. Maukichi Hasegawa) in the Science Council of Japan. And the observations by space rockets and manned satellite observations were originally developed by Mr. Ken-ichi Maeta (on space rockets) and Seishi Miazi (on satellites), who were the members of a subcommittee to CIGY. In addition, there was also the Observation Rocket Special Committee (chairman Kaeomo Kaukuro) in the Science Council of Japan because development of the space rocket itself was another aspect and posed other organizational problems.

After the IGY project, COSPAR was organized internationally and the Space Research Special Committee (SRSC, chairman Mr. Kaukuro Kauemo) was born in Japan. Since COSPAR consists of ten unions and representatives of seventeen member countries which are performing space research, SRSC in the Science Council of Japan consists of ten representatives from the other research liaison committees of the Science Council of Japan, the representatives from the other related organizations, professors, and the representatives from the special committees such as the Ionosphere Research Special Committee and the Nuclear Energy Special Committee. SRSC maintains close contact with COSPAR and, at the same time, maintains close liaison with related organizations in this country.

The relationship between Japanese space rocket research and COSPAR is, in short, to coordinate observations and launchings of Japanese space rockets with worldwide projects as closely as possible, and get necessary coordinations from the other countries through COSPAR. Most of the Japanese observation space rockets launched so far were dated in or near the "World Rocket Week" which was set up by COSPAR. And internationally, the same methods of observation were used where practicable. This is the reason why we use "the sodium method" as the measuring method for the upper atmosphere and this method was recommended by COSPAR.

It is important to develop our own measuring devices and methods and to measure with these devices and methods. However, it is also essential to use the internationally common measuring devices and methods if we wish to better understand the earth.

Developments in the space science field in Japan including space rocket observations were well known through COSPAR symposiums or other international meetings.

It was also through COSPAR that the United States proposed to launch other countries' satellites with U.S. rockets.

COSPAR is unwilling to touch rocket problems themselves such as the problem of the development of a booster. It is mainly due to the fact that booster development is one of the hot spots in the competition between the United States and the Soviet Union. There are, therefore, almost no papers on launch vehicles at COSPAR symposia. However, the situation is entirely different for domestic organizations and it is impossible to stay away from the development of the launching vehicles. In order to set up a space research plan, the development of a booster is an essential aspect of the entire research and, therefore, it is an important mission of SRSC. This difference comes from the fact that we develop space rockets for scientific research not for military purposes as do other nations.

In SRSC, a sub-committee, to study the needs of the Space Research Laboratory (tentative name), was organized and undertook an active study.

One of the international organizations on space is the United Nations' Committee on the Peaceful Use of Outer Space (UN CPUOS). As we often read "Outer space..." in newspapers, it is the era in which we begin to stretch out our hands to the moon and Venus. What a challenge is outer space!

As the United Nations is a kind of governmental organization, the problems in the UN are not matters which an academic organization can tackle; rather, they are to be handled by the Ministry of Foreign Affairs.

UNCPUOS is a committee of the United Nations' General Assembly. It has two subcommittees, the Science and Technology Sub-committee and the Law Sub-committee in order to perform its mission.

The author has attended the committee meetings at New York during March to April, 1952, and the Science and Technology Sub-committee at Geneva during May to June 1962. Many representatives were acquaintances of the author in connection with COSPAR.

There is the Space Development Council in the Cabinet of Japan. The Council is not only to advise the Prime Minister but also to submit recommendations. This council is not limited to the space science but its function extends to the entire area of space development including the applied field.

(Received on April 3, 1963)

KAPPA-8L ROCKETS

By Hideo Itogawa

Presently, three programs are being carried out by SE Research (or Working) Group in conjunction with upper-atmosphere research rockets. They are:

A. Various research in high-altitude space by use of rockets already completed.

B. Performance improvement, modification, and refinement of the rockets being used for space research.

C. Planning for future research, development and construction of new rockets, and carrying out test flights.

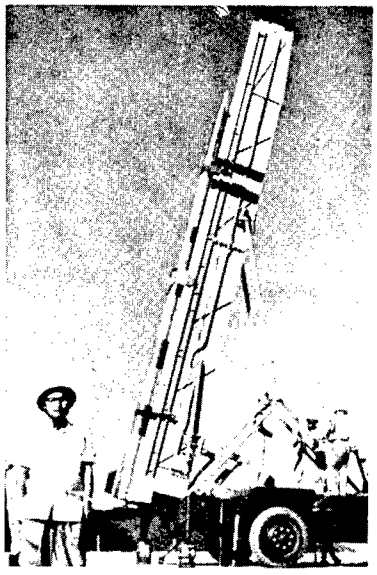

Fig. 1. K-8L type

The summary of the projects in A is given in this magazine by the respective researchers. C, which includes Lambda-type and Mu-type, is also described in this magazine under the title, "A Schedule for Observation

Rockets in 1963" (p. 28). Studies of K-8L fall into B. Its prototype is K-6 which has been used many times during the IGY. As mentioned in volume 11, number 8 of this series (Seisan Kenkyu), the K-6 was later improved in its performance to get the K-6H type rocket (H stands for High Performance). K-8L is the one that had further improvement in its performance and whose original name was K-6S (S stands for Super High Performance). The basic dimensions as well as differences in performance of K-6, K-6H and K-8L rockets are given in Tables 1 and 5 of the paper "A Schedule for Observation Rockets in 1963."

The main differences are in weights and lengths. The weights are 260 kg, 330 kg and 337 kg for K-6, K-6H and K-8L, respectively, while the respective lengths are 5.6 m, 6.9 m and 7.3 m. Also, the diameter of the second-stage of K-6S was slightly increased from 155 mm to 160 mm. In contrast with the slight increases in dimensions, the performance has remarkably improved; that is, to 60 km altitude for K-6, 85 km for K-6H and 175 km for the K-8L-1 rocket (one of the K-8L rockets). By choosing the proper firing conditions (wind dispersion, launch angle, etc.) and with small modifications, K-6S rockets may reach an altitude of 200 km, the same as that of the K-8 rocket. However, the payload of K-8L is 12-15 kg while that of K-8 is 40-50 kg. Since both K-8 and K-6S can attain the same altitude, the name K-8L was given to K-6S. Number 2 rocket of the K-8L type was scheduled to be launched in June 1963 to study the winds in the upper-atmosphere by use of a sodium grenade and Thermit grenade. Also, there is a possibility of the flight of the number 3 rocket of this type in 1963, which may indicate that the K-6 type used during the IGY is replaced by the K-8L for the IQSY (International Quiet Sun Year). One more thing is that the K-8L rocket may be the most suitable to be used for South Pole observations, assuming that Japan resumes its research and supposing that rocket observation research is possible at the South Pole.

The K-8L-1 rocket was also used by KSC (Kagoshima Space Observation Station of Tokyo University) for the first time. Compared with K-6, the K-8L has the following improvements resulting in higher performance: more powerful propellant, weight reduction in various parts of the rocket and other refinements. It may be said that the K-8L (K-6S) is the final model of the K-6 series rockets. K-6S (or K-8L) was planned since September 1961, and its first flight test was made August 25, 1962. For more details on this matter, the author refers to the paper by Assistant Professor Mori on page 87 of this magazine.

(Received on May 20, 1963)

KAPPA-9M ROCKETS

By Hideo Itogawa

Like the K-8L rocket mentioned previously, the study of the K-9M falls into plan B of the SE working programs. K-9M is an improved model of the K-8 in its performance; K-8 has been used as a standard vehicle for space observations.

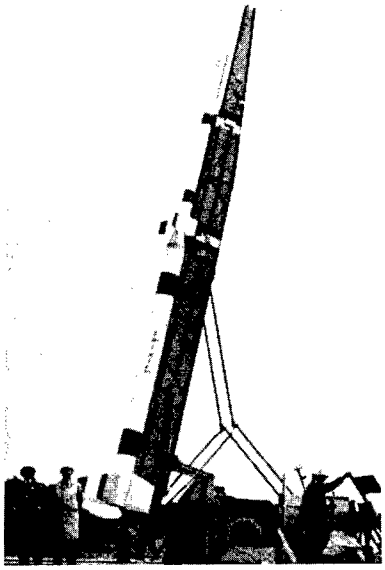

Fig. 1. K-9M

K-8 rockets are stable. Except for the K-8-10 rocket, all rockets of this type have high flight reliability and good characteristics with regard to the effects of acceleration, vibration and temperature on payload and have been considered very useful rockets for space observations. However, as with K-6 rockets, there was a possibility for improving performance. The first such work was planned and carried out since March 1961. The name K-8H was given to the improved rocket.

The main changes were the same as on the K-6H or K-6S type, that is, using a relatively more powerful propellant, developing structural material with high tensile strength, refining the structural design and increasing the loading density.

The dimensions of K-9M are almost the same as those of K-8 in total length, outside diameter and weight (see Table 5, p. 33 of this journal). However, the performance is greatly improved; for example, instead of 200 km altitude of K-8 obtained with a launching angle of 80°, the altitude attainable by K-9M is expected to be approximately 400 km.

The first flight operation to test the rocket's performance was carried out at 15:12 JST, on November 12, 1962, at KSC, with a launching angle of 78°. The flight of the two-stage rocket was normal at the beginning, but the second-stage ignition failed and unfortunately the flight test ended up as though a single-stage rocket with a dummy rocket on the second stage had been launched. Consequently, the comparison between theoretical or inferential values and observed or experimental values had to be postponed until May 17, 1963, when the K-9M-2 rocket is scheduled to be launched. This paper was written before that date.

Even though K-8H has almost the same dimensions as K-8, including the payload of 40-50 kg, and is a two-stage rocket, it reaches an altitude of 350-400 km which is a characteristic height of the K-9L type, the three-stage rocket. This fact leads to the name of K-9M for the K-8H during the research. The letter L in K-9L stands for lower performance while M in K-9M stands for middle-class performance. Even though the maximum altitude of the K-9M is the same as that of the K-9L, the payload of the former is approximately four times that of the latter which is 12 kg and 25 kg for second and third stage payloads, respectively. Besides, the larger space capacity for instruments in K-9M will probably cause a replacement of K-9L with K-9M in the future. Further improvement in the performance of K-8H or K-9M has been studied in conjunction with a more powerful propellant, high tensile steel materials and reducing the structural weight. Most of the fundamental work has been finished and it has resulted in the improvements making the K-9M possible. A very crude projection is that the new rocket may reach a height of 1200 km with a payload of 15 kg. Even though the new rocket is apparently a two-stage rocket, it will carry a spherical rocket in the nose cone of the second-stage rocket as its payload. It will presumably be some time in 1964 before this new rocket is finished and launched in an actual flight. In 1964, the first year of IQSY, the following three rockets, whose design altitudes are more than 1000 km, may be launched:

	Payload	Altitude
L-3	40 kg	1300 km
L-3S	15 kg	2000 km
K-9S (or K-10)	15 kg	1200 km

At the present time, a systematic study is being carried out with respect to the K-9S or K-10 rocket.

(Received on May 20, 1963)

NOS. 8 AND 9 ROCKETS OF KAPPA-8 TYPE

By Akio Tamaki and Shigebumi Saito

1. Program

A program was prepared for research observations in the ionosphere, made during the fall and at midday with the K-8-8 rocket. In this way, we would participate in the International Rocket Week (October 16-25). Also, it was planned to make observations of the ionosphere and airglow during the nighttime with the No. 9 rocket. Ionosphere-observation apparatus consists of devices for measuring positive ion densities, electron densities and electron temperatures. The number of probes used in the rocket increased from K-8-3 and K-8-4 to 5. Consequently, the nose-cone section of the rocket became longer. Therefore, instead of casting as before, metal plates were used in the construction. Thermometers and accelerometers for transverse motion were also installed in the rocket.

The apparatus for observation of airglow was the same as that used in the K-8-5 and K-8-6 rockets. This apparatus measured the altitudes of the luminous layers of the oxygen atom and sodium atom. The apparatus consisted of the phototube, filter and amplifier, and was behind the ionosphere-observation instruments.

The following shows several important characteristics of the rockets:

K-8-8 Rocket (Fig. 1)

Total length: 10,482 mm
Total weight: 1,513 kg
Payload (weight of instruments loaded): 31 kg
Instruments: Telemetry transmitter, radar transponder, timer for opening nose cone, ionosphere measuring device with five probes, thermometer, horizontal accelerometer

K-8-9 Rocket (Fig. 2)

Total length: 10,928 mm
Total weight: 1,540 kg
Payload: 47 kg
Instruments: Telemetry transmitter, radar transponder, timer for opening nose cone, ionosphere measuring device with five probes, airglow measuring device, timer for phototube.

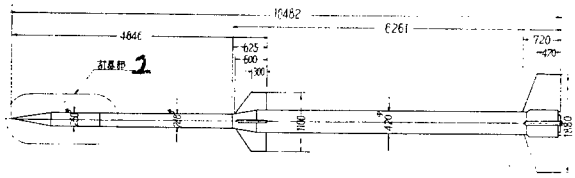

(a) K-8-8 Rocket

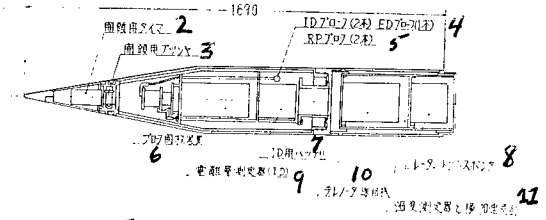

(b) Instrument section of K-8-8 rocket

Fig. 1.

1 - Instrument sections; 2 - Timer for opening nose cone; 3 - Nose cone actuator; 4 - ID probe (2), ED probe (2); 5 - RP probe (2); 6 - Probe opening device; 7 - Battery for ID; 8 - Radar transponder; 9 - Ionosphere measurement device (ID); 10 - Telemetry transmitter; 11 - Temperature measuring device and horizontal accelerometer

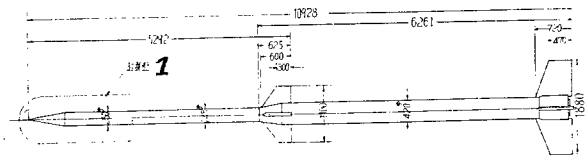

(a) K-8-9 Rocket

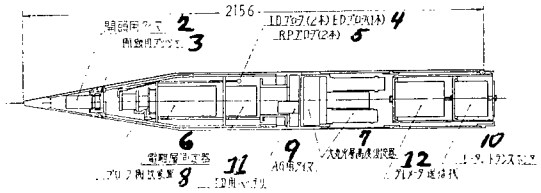

(b) Instrument section
of K-8-9 rocket

Fig. 2.

1 - Instrument section; 2 - Timer for opening nose cone; 3 - Nose cone actuator; 4 - ID probe (2), ED probe (1); 5 - RP probe (2); 6 - Ionosphere measurement device; 7 - Airglow altitude measuring device; 8 - Probe opening device; 9 - Timer for AG; 10 - Radar transponder; 11 - Battery for ID; 12 - Telemetry transmitter

2. Flight Tests

Place: Akita Rocket Range
K-8-8 Rocket: Date, October 24, 1961; time, 12:59 JST
Launch angle: 81° ; Wind: N 4m/sec; Atmospheric temperature: 10.5°C; Highest altitude: 200 km; Horizontal distance: 290 km; Flight period: 434 sec

As expected, the nose cone of the rocket was opened 58 sec after the launch and five probes, i.e., positive-ion probes (a perfect sphere and a boom-shaped one), electron probe and resonance probes (2) were exposed to obtain the data in ionosphere of the D, E and bottom of F regions. Also determined were the temperature rise along the wall of the instrument section and horizontal acceleration during the flight.

K-8-9 Rocket: Date, October 30, 1961; time, 20:13 JST
Launch angle: 80° ; Wind: NE 4 m/sec; Atmospheric temperature: 9°C; Highest altitude: 175 km; Horizontal distance: 230 km; Flight period: 408 sec

In the measurement of airglow, the phototube for the visible-ray region was extended within 65 sec after the launching and measured the intensities of the green line of oxygen and yellow line of sodium up to the highest altitude. From this measurement, it was possible to determine the altitude of the luminous layer of airglow. The photon tube for the infrared region was extended within 53 sec after launching and worked for about 12 seconds before it failed. Therefore, it was not possible to study the luminous layer of the infrared region.

Unfortunately, the nose cone did not open due to some defect in the opening device, and it was not possible to get data for the ionosphere observations although it was certain that the measuring devices were working properly throughout the flight.

(Received on May 2, 1963)

KAPPA - 8 - 10 ROCKET

By Tamiya Nomura and Daikichiro Mori

1. Introduction

The purposes of launching the K-8-10 rocket were to study the ionosphere during the night time by measuring positive ion density, electron density temperature, and to test the function of a newly developed geomagnetic aspectmeter which utilizes terrestrial magnetism. Unfortunately, however, the booster engine and rocket body exploded immediately after the launching and the test failed completely. In the following, the development of the rocket launching is described. The rocket was launched at the Akita Rocket Range.

2. Flight Conditions

The rocket was launched at 7:50 in the afternoon on May 24, 1962, with a launching angle of 81°. As soon as it was fired, the first stage rocket went into trouble and after approximately 0.3 seconds, when the rocket rose 3 or 4 m, the back-half portion of the chamber broke off so that the thrust was reduced a great deal. With the second-stage rocket still connected, the rocket reached the height of 115 m before it fell into the sea 15 m from the coast and 160 m in North-North-West direction from the launching position after 12 seconds. The ignition of the second-stage rocket was supposed to be carried out automatically 31 seconds after the launching use of a time-delay igniter. In spite of the defect of the first-stage rocket, this ignition system worked properly.

At the time the rocket fell into water, it looked like the engine of the second-stage rocket did not have any trouble because the second-stage rocket, separated from the first-stage, flew normally in the eastern direction until it hit a sandhill approximately 100 m from the point where the first-stage rocket fell. Because of this collision, however, the second-stage engine suddenly lost its thrust and it flew only about 80 m before it landed under the bank behind the rocket range where the rest of the propellant ignited. There were no injuries

to the people in the range but it was of great regret that a number of houses near the range received damages from the flying pieces of the exploded rocket.

3. The Investigations

(1) Recovery of the parts:

For 3 days after the accident, all the members searched the area near the range and recovered almost all the parts except the consumed propellant.

(2) Flight condition:

By studying the photographs taken, movie films, sound recordings, memory of the observers, the locations of the fallen parts and the condition of the launcher wreckage, the conclusions given in section 2 above were reached.

(3) Investigation of the recovered parts:

The recovered parts were examined at Tokyo. Main attention was put into the examination of the cause of the first explosion. Especially, the chamber of the booster propellant, and nozzle were examined very carefully and in detail. The investigation of those 3 parts included their dimensions, appearance, intensity, hardness, Young's modulus, microscopic photos and analyses of components.

(4) Investigation on the manufacture and transportation:

The manufacturing process of the chamber and propellant was studied by records in conjunction with the materials, construction, transportation and handling. Then the result of the study was compared with other records of the same series rockets. Also the records were checked with the data obtained from the recovered parts.

(5) The search of the cause:

As for the chamber, many specialists studied it by using various mechanical test devices with respect to tensile strength, safety factor, local stress concentration, intensity of welded joints, impact value, effect of heat, variation of plate thickness, and the cross-section of the wreckage piece. Also, simulated destruction tests of combinations of model chamber and propellant were carried out. Regarding the propellant, a series of tests were made to study the effect of curing temperature on the physical properties of the propellant as well as on the characteristics of the combustion and the effect of transformation of the propellant on the characteristics of the combustion. For the nozzle, an investigation of the characteristics of the material was carried out in addition to the experiments of applying an equal amount of impact pressure to the same type nozzle.

(6) Revisions of the manufacture, process control and inspection process:

Although the booster engine used in this rocket was a highly reliable engine since it was manufactured after 15 such engines worked successfully, some revisions were made after this failure in connection with the propellant, manufacture-process control, inspection technique, material test of the chamber and the measurement of strain. A part of these revisions was already utilized in the manufacture of 8L, 9M, and K-8-11 rockets.

(7) Developing a method to increase the safety of rocket operation:

To increase the degree of safety of a flight test and to minimize any damage, all possible methods were studied. As the first step, a series of studies were made hopefully leading to a safe ignition of the second-stage engine. The studies considered the combustion conditions in the booster-engine and also the first-stage flight conditions. Such a plan was already established and used in the manufacture of the small test-type SO-150-1 rocket and a flight test was made in December, 1962. In the near future, a command series rocket, SO-150-2 will be tested.

4. Principal Items of the Rocket

Total length:	10,936 mm
Total weight:	1,545 kg
Payload:	53 kg in total
Instruments:	Telemetry transmitter Radar transponder Timer for opening nose Ionosphere measuring device (6 probes) Geomagnetic aspectmeter (with a coil to detect the terrestrial magnetism)

Figure 1 shows the main dimensions while Figure 2 gives the locations of the instruments.

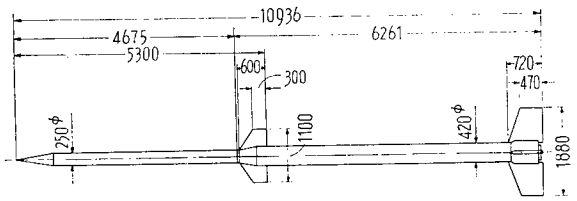

Fig. 1. K-8-10 Rocket

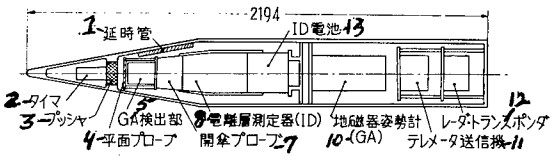

Fig. 2. Instrument section of K-8-10

1) Time-delay igniter
2) Timer
3) Actuator
4) Plane Probe
5) GA Detector
7) Parachute-probe (sic) (for opening)
8) Ionosphere-measuring device (I.D.)
10) Geomagnetic Aspect-meter (G.A.)
11) Telemetry-transmitter
12) Radar-transponder
13) Battery for ID

5. Conclusion

The failure of the flight test of K-8-10 rocket is described above in conjunction with its history and investigations after the test. The reason for the failure has not been found and the investigation is being continued for some items. However, several suspicious points have been raised and have resulted in changes in the manufacture of the rockets in order to prevent the same type of accident. The author is in debt to many people in addition to the SE research group, such as Professor Masao Yoshishiki (Engineering College), Sakae Watanabe, the head of the research section (Prince Automobile Industry Co., Ltd.), Yukihaku Takahashi, Assistant professor, and Otomaru Takagi, vice chief (Shin Mitsubishi Ship Building Co., Ltd.).

(Received on May 2, 1963)

K-8-11 ROCKET

By Shigebumi Saito and Akio Tamaki

1. Program

It was the purpose of launching the K-8-11 rocket to determine the aspect of the rocket during flight by use of the geomagnetic aspectmeter which utilizes terrestrial magnetism, to observe cosmic rays with a Geiger-counter, and to test the function of a newly developed receiver which determines radio noise propagation in the ionosphere.

The program started in August 1962. After having met three times for design purposes and for a number of small committee discussions, the design was completed. The general view of the rocket and the instrumental arrangement are shown in Figures 1 and 2, respectively.

The principal items on the rocket are:

Total length: 10,926 mm
Total weight: 1,499 kg
Instruments: Telemeter transmitter; radar-transponder; cosmic-ray measuring device (CR 3 Geiger-counters); geomagnetic aspectmeter (GA, 3 coils to detect the terrestrial magnetism); receiver for radio noise propagation (RN, loop-antenna, external antenna); timer
Payload: Net 29 kgs

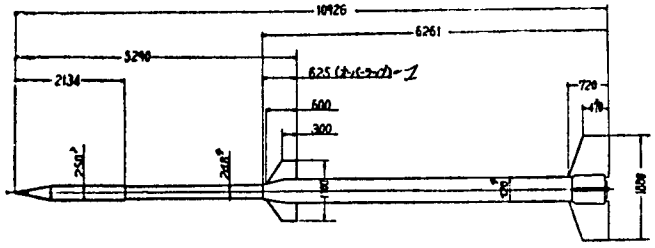

Fig. 1. K-8-11 rocket
1 - (Overlap)

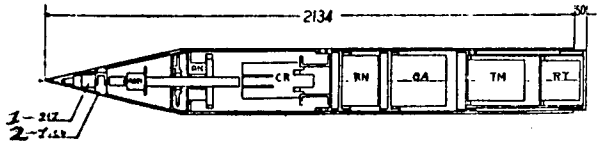

Fig. 2. Instruments in K-8-11 rocket
1 - Timer; 2 - Pusher

2. Flight Test

Place:	Kagoshima Space Observatory
Date:	December 18, 1962
Time:	14:03 JST
Launch angle:	79°
Wind:	W 1 m/sec
Atmospheric temperature:	13° C
Highest altitude:	202 km
Horizontal range:	247 km
Flight duration:	443 sec

The main part of the rocket as well as the booster flew properly and the rocket reached its highest altitude of 202 km in 230 sec after launching. During the whole flight period, the 3 Geiger counters measured the change in intensity of cosmic rays with altitude and observed the directions of the cosmic rays.

The geomagnetic aspectmeter with utilization of the terrestrial magnetism determined the orientation of the rocket from launching to descent. Especially, the data obtained for the aspect of the main rocket after the rocket nose was opened, are important for future works.

The electromagnetic noise was measured by external and loop antennas after the rocket nose was opened in 79.6 sec. The intensity of the noise in and out of the ionosphere at 17.44 kc, 100 kc and 105 kc was measured together with the intensity of the signal waves at 17.44 kc from the Yosami radio station. From the measurement of the latter, it was possible to confirm how well the apparatus worked.

In conclusion, it can be said that all the objectives were successfully achieved with the Number 11 rocket — (K-8-11).

(Received on May 2, 1963)

KAPPA 8L-1 TYPE SPACE ROCKET

By D. Mori and T. Nomura

1. 8L Type Space Rocket Development Plan

Kappa 6H type space rocket, made in September 1960, was a rocket which could carry 12 kg of payload and reach a maximum altitude of 70 to 90 km. It was in September 1961 that the decision to develop 8L type space rocket as a modified rocket 6H type, was made. Nearly the same time, a plan to develop the 9M type space rocket as an improved rocket of the 8 type was underway. Consequently, the 8L type space rocket would not only have value as a modification of the 6H type but also as a model rocket for the development of the 9M type.

Policies on performance improvement were as follows:

(1) Total length, total weight, outside shape, and the weight of payload would be kept to that of the 6H type.

(2) New propellant would be used.

(3) Aerodynamic changes on the outside shape would not be involved except for minor changes and the main booster shroud for better performance.

(4) Structural improvements and lightness would be sought.

After five design meetings, the final design of the space rocket was completed in February 1962. The outside shape of the designed rocket is shown in Figure 1. Locations of the various devices in the rocket are shown in Fig. 2.

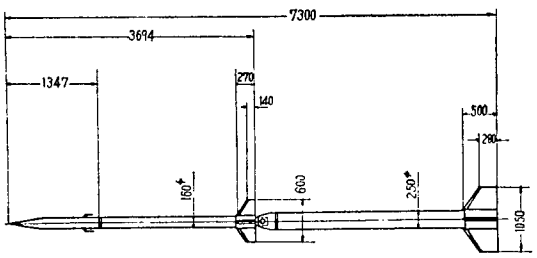

Fig. 1. K-8L-1 type space rocket

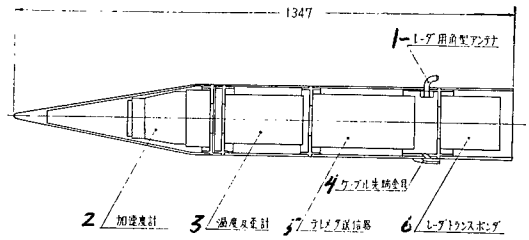

Fig. 2. Layout of instruments in the K-8L-1 type rocket

1 - Bar antenna for radar; 2 - Accelerometer; 3 - Thermometer and strain gauge; 4 - Cable terminal; 5 - Teletransmitter; 6 - Radar transponder

In the meantime, actions were taken on policies. On (2) — see above — it was decided that both engines of the main rocket (second-stage) and booster would use a new propellant. The ground test of the engines with new propellant was performed. On (3), the connection area of the booster to the main rocket was remodeled to have the shape of a cone with flat top. Therefore, several of the main rocket-tail connections on the booster disappeared. The tail of the main rocket was also faired to have a smooth cylindrical shape.

On (4), tail, combustion chamber, tail base, nozzle, and connecting area of the booster were re-evaluated to make them lighter and better as reported in "Structural Strength" (page 112 of this volume). These modified components were tested with respect to strength, elasticity and heat resistance. As a result of the tests, it was known that the weight could be reduced in spite of the increased dynamic pressure and heat which would be due to the higher velocity of the improved rocket.

Along with the modifications, small model rockets, RT-150 and HT-150 were made according to the results of the ground tests. They were launched in December 1961 and March 1962 to test the propellant, aerodynamic performance, and dynamic pressure. Detailed information on the model rockets is discussed under "Model Rockets."

Data for the 8L type space rocket launch are as follows:

Total length: 7,300 mm
Total weight: 48 kg (sic)
Weight of main rocket: 92 kg (sic)
Weight of payload: 12 kg
Payload: Teletransmitter, radar transponder, accelerometer, decelerometer, normal component accelerometer, thermometer, and strain gauge

Maximum acceleration: Main rocket - 24 g; booster - 43 g
Booster combustion time: 7.2 sec
Main rocket combustion time: 5.3 sec
Time to booster takeoff: 7.5 sec

2. Launch:

Test place: Kagoshima Space Center
Test time: 16:50 (JST) August 23, 1962
Launch angle: 80°
Surface wind: 0 m/sec E (sic)
Temperature: 30° C
Maximum altitude: 173 km
Horizontal distance: 160 km
Time of flight: 420 sec

There was no trouble in engine combustion and rocket flight except the rocket had a spiral motion while the main rocket engine fuel was burning. It reached the maximum altitude, 173 km, in 195 seconds. Consequently, the 8L type rocket showed much better performance than the 6H type.

Radar could track the rocket until 270 seconds after launching and measured acceleration, stress and the temperature of the rocket during the entire flight. Maximum temperature at the outside temperature-measuring point of the rocket was 400° C.

The booster was found floating on the sea and was recovered by a patrol boat with the help of some fishing boats which were near the booster. The recovery could be said to be unexpected good fortune.

This was the first two-stage space rocket ever launched at Kagoshima Space Center.

(Received on May 2, 1963)

KAPPA 9L-2 TYPE SPACE ROCKET

By D. Mori and T. Nomura

1. Plan

Kappa 9L-1 type space rocket was launched on April 1, 1961 to test its body. For the test flight, the plan established July 1961 was to develop a 9L-2 type space rocket and observe the ionosphere and determine the flight path of the rocket. The previous rocket flight path was lost during tracking.

Since the diameter of the 9L-type rocket head was small, 150 mm, it was planned to load into it a small ionosphere detector having a probe to measure the density and temperature of the electrons in the ionosphere. Window opening device was newly designed. And a thorough environmental test was performed on each component to determine the durability of the parts under excessive aerodynamic heat and vibration.

9L-1 type rocket failed to be tracked because the radar transponder was loaded in the booster. For the 9L-2 type, the radar transponder was to be loaded in the main rocket as we had a new radar system with an antenna of 4 m in diameter located at the launching ground.

In addition to it, a thermometer and a potentiometer type normal-component accelerometer were loaded in the nose of the main rocket to determine the surface temperature of the nosecone and the normal component acceleration, respectively.

Figure 1 shows the outside of the entire rocket and Fig. 2 is the diagram of the rocket nose.

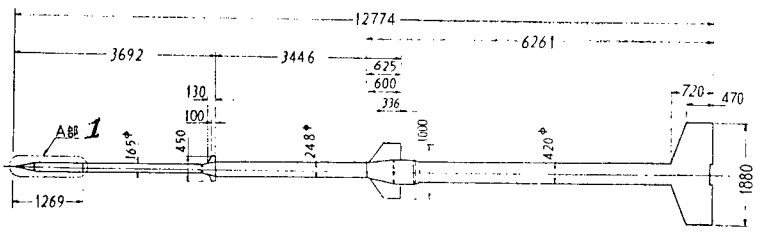

Fig. 1. K-9L-2 type space rocket

1 - Part A (rocket nose)

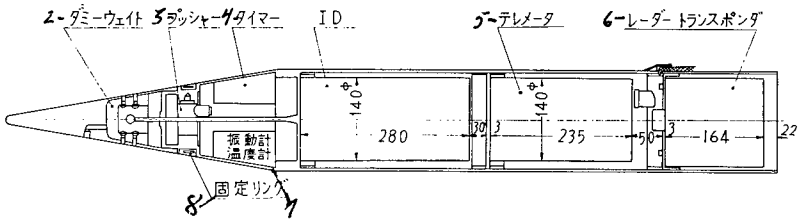

Fig. 2. Layout of devices in the rocket nose of 9L-2 type space rocket

2 - Dummy weight; 3 - Pusher (sic); 4 - Timer; 5-Teletransmitter; 6 - Radar transponder; 7 - Thermometer and normal component accelerometer; 8 - Bulkhead

Data for 9L-2 type space rocket:

Total length: 12,774 mm
Total weight: 1,591 kg
Weight of payload: 17 kg
Payload: Teletransmitter, radar transponder, window opening timer, ionosphere detector, and normal component accelerometer

Total length of the rocket is 260 mm longer than that of 9L-1 type space rocket and the weight of the main rocket is 11 kg heavier than that of the previous rocket.

2. Results of the Launching Test

Launching time: 14:05 (JST) December 26, 1961
Launching angle: 81°
Surface wind: 5 m/sec NNW
Temperature: 4° C
Maximum altitude: 348 km
Horizontal distance: 600 km
Time of flight: 581 sec

The functioning of each of the three stages was perfect, and it was known through telemetry that the window was opened and ionosphere observations were made until 40 seconds after the launching when the ground telemetry receiver began picking up excess noise and the signals became garbled. 160 seconds after the launch, the signals faded out.

During the 40 seconds, ionosphere measurements were made at 100 to 120 km, 160 to 190 km, and 210 to 230 km. Measured data agreed with the data which were obtained at the ground. All of the radar transponders on the rocket

and the radar, new and old ones, at the ground functioned perfectly; and the entire track of the space rocket was traced. From it, the performances of both new radar and the space rocket were known exactly. Also, the thermometer and normal-component accelerometer took their respective data until the window was opened.

Since the weather at Akita in December was very poor, launching preparations and the launch were very difficult.

(Received on April 9, 1963)

REFERENCE

1. Hogawa, J. Prod. Research 13, 10, pp. 319-321, 1961.

KAPPA 9M-1 TYPE SPACE ROCKET

By K. Tamaki and N. Saito

1. Plan

The K-8 type space rocket, made in July 1960, is a medium sized rocket, can carry 50 kg of payload, and reach a maximum altitude of 200 km. The three-stage K-9L type space rocket, consisting of a K-8 type rocket nose and a K-150 type booster, can reach a maximum altitude of 350 km. However, the rockets were not suitable to be used to get data about various phenomena in the upper atmosphere because they could only carry a payload of less than 12 kg to the desired altitude. Therefore, it was thought to be of great significance and value for future space research to develop a two-stage space rocket able to carry about 50 kg of payload and reach at least the maximum altitude of the 9L type rocket by improving the K-8 type. For this purpose, the K-9M type space rocket development plan was made in August 1961.

The plan for performance improvement was as follows:

(1) Total weight, total length and layout of payload in the rocket would be kept to that of the K-8 type space rocket.

(2) Main rocket engine would use a new propellant. Booster would use the same propellant as the K-8 type.

(3) The method of connecting the main rocket to the booster would be simplified. Aerodynamic revisions such as a smaller tail and a wedge-type aft end of booster would be made.

(4) Structural lightness and strength would be sought. Particularly, the booster chamber would be made with a special steel which had high tensile strength in order to reduce the thickness of the chamber wall.

Along with this plan, the design of the K-8L type space rocket, a modification of the K-6H type, was undertaken. Since the K-8L type was actually a smaller rocket of the K-9M type space rocket, the design meetings for each rocket were held one after another. And with the test results from launching the HT-150 model rocket, which used the new propellant, the design of K-8L type was completed first followed by the complete design of the K-9M type. After eight design meetings, the design of the K-9M type space rocket was completed in April 1962.

Figures 1 and 2 show the outline of the rocket and the layout of the payload. Main payload devices in the rocket were the accelerometer, thermometer, and strain gauge since this rocket was to be used to test the performance of the rocket itself. However, an ionosphere detector was also loaded for there was enough space for it.

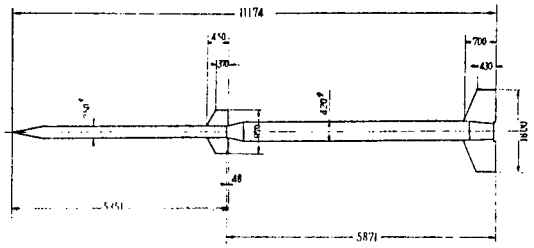

Fig. 1. K-9M-1 type space rocket

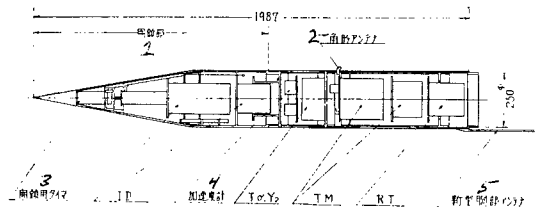

Fig. 2. Layout of payload in K-9M-1 type space rocket

1 - Cutaway of nose; 2 - Bar antenna; 3 - Window opening timer; 4 - Accelerometer; 5 - New rear antenna

Standards for environmental test were also received along with the improved performance. Combustion test of the main rocket engine on the ground, model booster chamber test, and structural strength tests on each part of the rocket such as tail and its connection were performed throughout the developmental period.

Data for 9M-1 type space rocket are as follows:

Total length: 11,174 mm
Total weight: 1,439 kg
Weight of main rocket: 320 kg
Payload: Teletransmitter, radar transponder, decelerometer, vibration meter, thermometer, strain gauge, window opening system, and ionosphere detector (two resonance probes, one spherical-net type probe, and one plane trap).

Total weight of payload: 51 kg, net 21 kg
Test Place: Kagoshima Space Center
Test time: 1101 (JST) November 25, 1962
Launch angle: 78°
Surface wind: 2 m/sec NNW
Temperature: 15.5° C
Maximum altitude: 58 km
Horizontal distance: 54 km
Time of flight: 230 sec

Combustion of the booster engine, and the main rocket flight were good. However, the combustion of the main rocket engine was not started and the rocket went up only to the altitude of 58 km with the impulse obtained from the booster. Teletransmitter, radar, and payload functioned smoothly, but ionosphere observations were not made because the rocket did not reach the estimated altitude of 350 to 400 km.

The cause of the failure of the main rocket engine combustion was thought to be because the new propellant had a higher ignition point under the lower pressure of the higher atmosphere, and the ignition method was later revised. It can be said, however, that the design of the K-9M-1 type space rocket was good because the rocket flight, until the time when the main rocket engine failed to ignite, was normal.

(Received on May 2, 1963)

AERODYNAMIC CHARACTERISTICS OF K-8L AND K-9M TYPE SPACE ROCKETS

By F. Tamaki and S. Mitsuishi

K-8L and K-9M type space rockets are the improved models of K-6H and K-8 type space rockets, respectively. The main changes were made on the rocket engine and body. And the changes which affect the aerodynamic characteristics are as follows:

1) Main-booster connection area cover was removed from the base of the tail of the main rocket. Previously, the cover reached to the base of the tail of the main rocket.

2) The area of the tail was shortened.

3) The end of the booster of the K-9M type was modified to the shape of a wedge and its body was made more slender than the K-8 type. Since these changes have no significant effect on the aerodynamic characteristics of the rockets, the author estimated the stability of the rocket by calculation instead of wind-tunnel experiment. However, low-speed wind-tunnel experimentation on the K-9M type main rocket was performed to evaluate the aerodynamic effects of the telemetry antenna which stretched out on both sides from the main rocket body.

1. The Effect of the Stretched-Out Antenna

If there is a lift force plane in front of the rocket tail, it reduces the function of the tail and if the plane is large, the normal force of the entire rocket may be unstable.

Data on the actual antenna were reported separately (on page 173 of this volume by Yamashita). Since the dimension of the antenna was not fixed until after the wind-tunnel experiment, the experiment was performed with plates which were actually larger than the real antenna.

The model rocket and antenna for the wind-tunnel experiment are shown in Fig. 1. The experiment was performed at the Aviation Research Laboratory's 3-meter wind-tunnel. The wind speed was 35.1 m/sec and the Reynold's number of the wind-tunnel was 2.4×10^6 per meter.

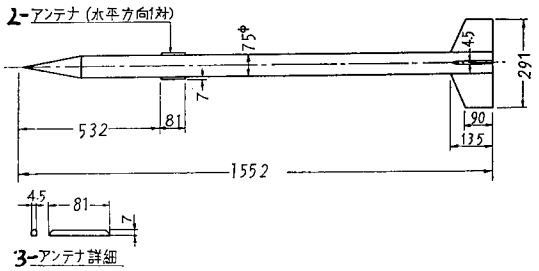

Fig. 1. Model rocket with antenna

2)—Antenna (horizontal pair); 3)—Antenna details

The experimental results are shown in Fig. 2 and Fig. 3, and the notations are as follows:

α = The angle between the center line of the rocket and a horizontal line
q = Dynamic pressure
S = Cross-sectional area of the rocket body,
l = Total length of the rocket,
C_L = Lift force/qS,

C_d = Drag/qS,

Cm (x-o) = Moment/qSl,
CP = Distance from front tip to pressure center/l

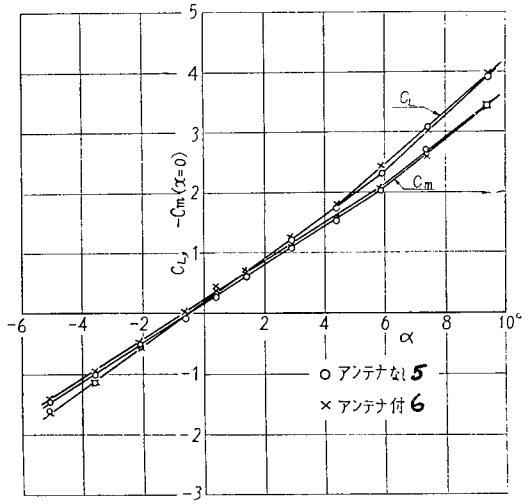

Fig. 2. Lift coefficient and moment coefficient vs α

5) Without antenna; 6) With antenna

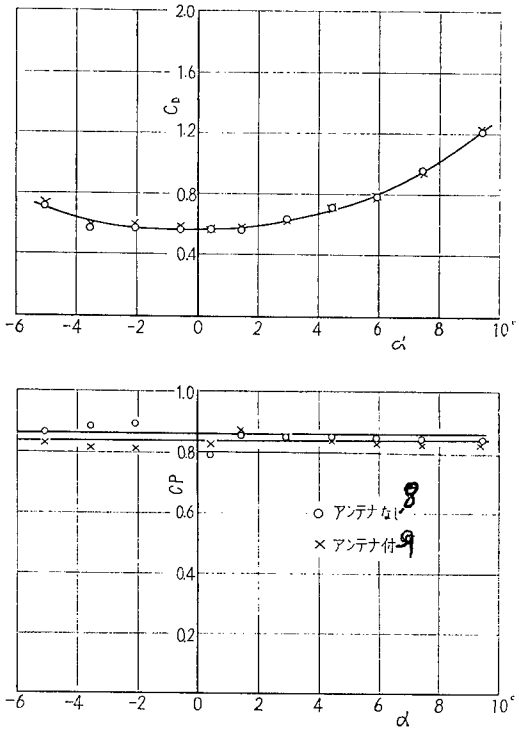

Fig. 3. Drag coefficient and pressure center vs α.

8) Without antenna; 9) With antenna

Data without antenna are also shown in the figures.

According to the experiment:

Near $\alpha = 0°$,

$\frac{dC_L}{d\alpha} = 21.0/\text{rad}$,

$dC_m(x = 0)/d\alpha = -18.0$ rad,

C_D min $= 0.56$,

CP = 0.86 without antenna and
CP = 0.84 with antenna.

This size antenna effects CP but there is almost no effect on $dC_L/d\alpha$, dC_m $(x = 0)/d\alpha$, or C_D min.

We also performed experiments for the cases when the antenna was placed at the point aft of the nose 61 percent of the total length of the rocket and 14 per cent of the total length of the rocket; the latter point is the front end of the equi-diameter part of the rocket body. But we could not find any differences in the aerodynamic data.

Furthermore, the CP shift forward will be less than one percent since the antenna actually used was smaller than the one we used for the experiment.

2. K-8L-1 and K-9M-1 Type Space Rockets

Although K-8L and K-9M type space rockets were designed similarly, the ratio of the area of the tail to the cross-sectional area of the K-8L type is smaller than that of the K-9M type; the tail of the K-8L type was exactly the same tail used in the single-stage AT-150 rocket.

Tables 1 and 2 show the slope of the normal force coefficient C_{Na} curve and the pressure center CP for both rockets.

Table 1

Aerodynamic characteristics of K-8L-1 type space rocket

2 ロケット	M	$C_{N\alpha}$	CP	備考 5
3 ブースタ・メイン	0	27.9	0.765	発進時 6
〃	4	12.5	0.70	ブースタ燃焼おわり 7
4 メイン	0	20.8	0.87	
〃	2	15.4	0.81	コースティングおわり 8
〃	4	9.0	0.675	コースティングはじめ 9
〃	7	6.3	0.58	燃焼おわり 10

2) Rocket
3) Booster and main rocket
4) Main rocket
5) Remarks
6) Start of ascent
7) End of booster engine combustion
8) Start coast phase
9) End coast phase
10) End of main-rocket combustion

The method of calculation was reported previously [1]. C_{NA} and CP for a cone and cylinder, as a function of Mach number, were assumed as follows:

$M = 2$

$C_{NA} = 3$

$CP = 0.15$

Table 2

Aerodynamic characteristics of K-9M-1 type space rocket

ロケット	M	$C_{N\alpha}$	CP	備考
ブースタ・メイン	0	27.8	0.755	発進時
〃	4	12.7	0.67	ブースタ燃焼おわり
メイン	0	23.1	0.860	
〃	3	12.7	0.745	コースティングおわり
〃	4	10.7	0.68	コースティングはじめ
〃	9	5.1	0.62	燃焼おわり

12) Rocket
13) Booster and main rocket
14) Main rocket
15) Remarks
16) Start of ascent
17) End of booster engine combustion
18) Start coast phase
19) End coast phase
20) End of main-rocket combustion

These values are assumed according to shock tunnel experiments of the Production Research Institute [2], from foreign experiments [3] and [4], and according to the theoretical values characteristic of a supersonic fluid at high Mach number. The values of K-9M type in Table 1 are derived with the assumption that the forward shift of CP is 0.01.

Furthermore, we planned to obtain stability of the main rocket of the K-9M-2 type by bending the aft ends of the tail and smoothly spinning the main rocket once it reached very high altitudes (about 35 km), when the combustion is finished.

(Received on May 1, 1963)

REFERENCES

1. F. Tanaki, J. Production Research 12, 12, p. 509 (1960).

2. F. Tamaki, S. Mitsuishi and S. Nagai, Proc. 2nd ISRA Tokyo, 1960, p. 137, Yokendo, Tokyo (1961), Proc. 3rd ISRA Tokyo, 1961, p. 209, Yokendo, Tolyo (1962).

3. W.E. Buford, J. Aero. Sci., 25, 2, p. 103 (1958).

4. G. Grimminger, E.P. Williams and G.B.W. Young, J. Aero. Sci., 17, 11, p. 654 (1955).

PERFORMANCE CALCULATIONS OF KAPPA-8L, -8, -9L, -9M TYPE SPACE ROCKET

By R. Akiba, H. Hirozawa and A. Kitasaka

Along with the improvement of the space rocket and the installation of a digital computer at the Production Research Institute, the performance calculations of the later models of space rocket since K-86 type was done by electronic computer rather than by manual computations. Professor Watanabe had reported on the calculation method for the K-9L-1 type space rocket using the electronic computer and the Aviation Research Institute. The calculation method and other problems in calculating the performance of a space rocket using the electronic computer at this institute will be reported under separate cover in this volume. Therefore, the author will only review the equations involved and evaluate the calculation results.

1. Analysis of the Equations

Input equations are as follows:

$$\frac{dV}{dt}=\frac{T-D}{m}-\sin\theta\, g_0\left(\frac{R_0}{r}\right)^2 \qquad \frac{dz}{dt}=V\sin\theta$$
$$\frac{d\theta}{dt}=-\frac{g\cos\theta}{r}+\frac{V\cos\theta}{r} \qquad \frac{d\varphi}{dt}=\frac{V\cos\theta}{r} \tag{1}$$

These equations are valid only for the coordinate system which rests on earth and with the following assumptions:

(1) Revolution and rotation of the earth are ignored.

(2) The axis of a rocket is parallel to the velocity vector of the rocket.

(3) There is no wind.

(4) The motion of the rocket with respect to its center of mass is ignored.

These equations describe the two dimensional motion of a rocket at the outer circumferences of the earth. In considering the effect of Eq. (1), without regarding the effect of the revolution of the earth, the forces from the rotation of

the earth are the Coriolis force $2V\times\Omega$ and $-\Omega\times\Omega\times r$ (Ω is the rotational angular velocity of the earth). And the maximum values of the two forces are $2V\Omega$ and $\Omega^2 r$. Therefore the ratio of the two forces to the gravitational force of the earth are as follows:

$$\frac{2V\Omega}{g_0\left(\frac{R_0}{r}\right)^2}=V\left(\frac{r}{R_0}\right)^2\frac{2\Omega}{g_0}=V\left(\frac{r}{R_0}\right)^2\frac{2\times 7.25}{9.8}$$

$$=1.48\times 10^{-5}\cdot V\left(\frac{r}{R_0}\right)^2$$

$$\frac{\Omega^2 r}{g_0\left(\frac{R_0}{r}\right)^2}=\frac{R_0\Omega^2}{g_0}\left(\frac{r}{R_0}\right)^3=\frac{6370\times(7.25\times 10^{-5})^2\times 10^3}{9.8}$$

$$\times\left(\frac{r}{R_0}\right)^3=3.42\times 10^{-3}\left(\frac{r}{R_0}\right)^3$$

They show that the Coriolis force for the K-9 type space rocket is relatively large, 3% of g_0 when V = 3000 m/sec. This force has the value of one smaller order-of-magnitude at the surface of the earth, but it becomes 3% of the gravitational force where $r = 2R_0$.

It is, therefore, possible to ignore the rotational effect of the earth for the rocket up to K-9 type, but this effect must be counted in future calculations for L and M type rockets since they will have a much higher velocity.

After a rocket has escaped from the atmosphere, Eq. (1) can be used as it is applicable to a coordinate system whose origin is at the earth's center. Then the equation can be solved with the value of initial velocity plus escape velocity as an initial condition. But the thrust force term must be modified in this case since it normally occurs that the attitude of a rocket is controlled and the adjusted attitude affects the velocity of the rocket. Of course, it is most desirable to solve the equation as it has six degrees of freedom (six independent variables) — if we have enough time to solve it.

When we solve Eq. (1) with the assumptions (1), (2) and (3), the longitude X and latitude Y of the landing point is found by spherical trigonometry, as follows:

$$X=X_0+\arcsin\frac{\sin\frac{H}{R_0}\cdot\sin\beta_0}{\cos Y}$$

$$\beta=\arcsin\frac{\cos Y_0\sin\beta_0}{\cos Y}$$

$$Y=\arcsin\left[\sin Y_0\cdot\cos\frac{H}{R_0}-\cos Y_0\cdot\sin\frac{H}{R_0}\cdot\cos\beta_0\right]$$

where β_0 is the launching direction and H is the surface distance from launching point to landing point.

When we apply this equation to the K-9M type space rocket, taking Uchino-ura, Kagoshima as the launching point, the results are as follows:

$H=420$ km $\quad X_0=131°04'45''$

$\beta_0=54°30'0'' \quad Y_0=31°15'0''$

$\beta-\beta_0=-1°44'4''$

It shows that the rotational effect of the earth is larger than the wind effect or the effect of the changes of the axis of the rocket for this kind of space rocket.

Since the Coriolis force affects the trajectory of the rocket but has no effect on its energy, the force should be considered separately.

In considering the motion of rocket with respect to its center of mass, the force becomes larger immediately after a rocket is launched and when it escapes from the atmosphere. According to Eq. (1), the force has a uniform acceleration in the tangential direction when a rocket is taking off from the launcher. And from the following approximation:

$$\frac{dV}{dt}\simeq G \qquad \frac{d\theta}{dt}=-\frac{g\cos\theta_0}{V}$$

We get $\frac{\Delta\theta}{g/G\cdot\cos\theta_0}=1.15\log\frac{S}{P}$. On the other hand, we get $\frac{\Delta\theta}{g/G\cdot\cos\theta_0}=G_1(S\cdot P)$ from Eq. (2), when we consider the motion of rocket with respect to its center of mass. Where S is flight distance, P is the value of the length of the rocket in terms of a dimensionless unit converted by wavelength, and G_1 is rocket function. Figure 1 shows the two values of $\frac{\Delta\theta}{g/G\cdot\cos\theta_0}$. As shown in the figure, the deviation between

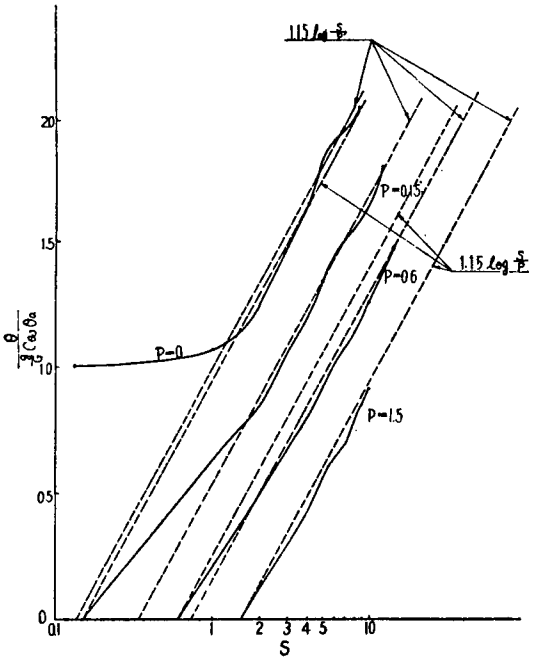

Fig. 1

the two values becomes large when the length of a rocket is large, and therefore the wavelength is large. But it shows that $\frac{\theta}{g/G \cdot \cos\theta_0}$ can be calculated, without significant error, from Eq. (1) when the wavelength is more than unity, even if $P = 0$.

2. Analysis of Results of Calculations:

(1) K-9L-2 type space rocket.

Table 2 and Fig. 2 show the data and results of calculations for the rocket. The pressure thrust is taken into account by the method of conventional graphical calculation. But the difference of gravitational forces at each altitude and the curvature of the earth are ignored.

Table 1. Data of K-9L-2 Type Space Rocket

	1st Stage	2nd Stage	3rd Stage
Total length (mm)	12774	7138	3692
Outside diameter(mm)	420	248	165
Total weight (kg)	1546.8	382.2	108.9
Combustion time (sec)	15.1	9.25	5.3
Payload weight (kg)			18.8

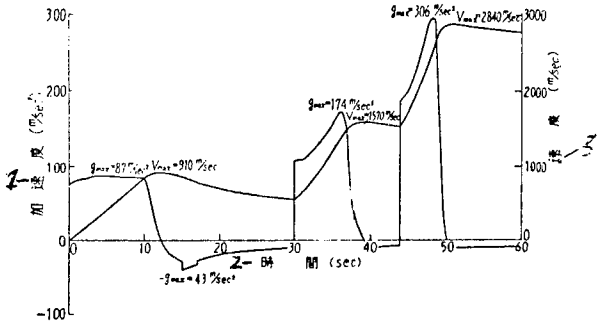

(a) Acceleration and velocity curves of K-9L-2 space rocket (for launch angle of 80°).

1 - Acceleration; 2 - Time; 3 - Velocity

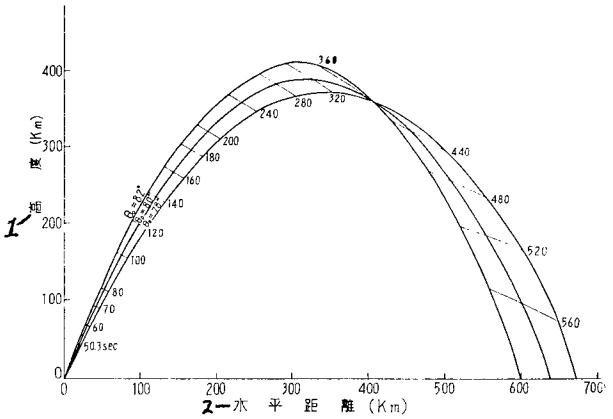

(b) Trajectory of K-9L-2 type space rocket.

1 - Altitude; 2 - Horizontal distance; 3 - Time to the end of the first-stage booster combustion; 4 - Time to the first stage booster take-off; 5 - Time to the beginning of the 2nd stage booster combustion; 6 - Time to the end of the 2nd stage booster combustion; 7 - Time to the 2nd stage booster take-off; 8 - Time to the beginning of main rocket combustion; 9 - Time to the end of main rocket combustion

Fig. 2.

(2) K-8L-1 type space rocket.

Table 2 and Fig. 3 show the data and calculation results; they show that the actual performance obtained from flight test was not reached in the calculation results. The reason can be thought of as follows:

(a) The air resistance was larger than expected at the moment of booster take-off from the main rocket because there was large air turbulence at the moment.

(b) For the same reason, the attitude of the rocket was changed.

(c) There was some propellant residue in the main rocket.

In analyzing the effects of the above causes on the performance of the rocket, it is assumed that the effect on the maximum altitude dZ_{max} is given by the following equation:

$$dZ_{max} = D\ dC_X + \textcircled{H}\ d\theta_M + P\ dW_{PM} \qquad (2)$$

When dC_X, $d\theta_M$ and dW_{PM} are substituted into Eq. (2), the coefficients D, ⊕, and P are obtained as follows:

$$D=\frac{15}{0.05}=300\text{ km} \qquad \oplus=\frac{11}{5}=2.2\text{ km/°}$$

$$P=\frac{35}{5}=7\text{ km/kg}$$

The difference dZ_{max} = 30 km between calculated and actual values is examined and a reasonable explanation was found.

Table 2. Data of K-8L-1 Type Space Rocket

	Booster Stage	Main Rocket
Total length (mm)	7300	3816
Outside diameter(mm)	250	160
Total weight (kg)	338.6	93.6
Combustion time(sec)	7.3	5.17
Payload weight (kg)		11.8

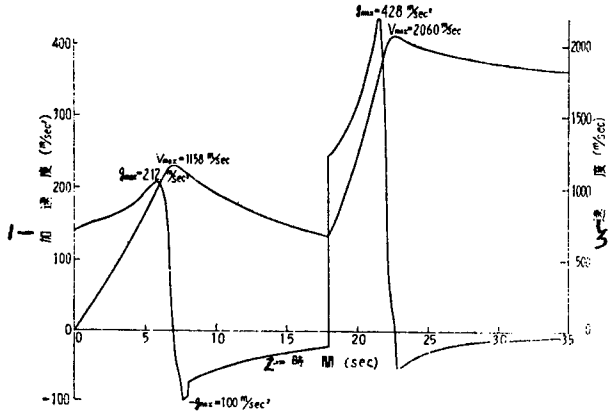

(a) Acceleration and velocity curves of K-8L-1 type space rocket (for launch angle of 80°)

1 - Acceleration; 2 - Time; 3 - Velocity

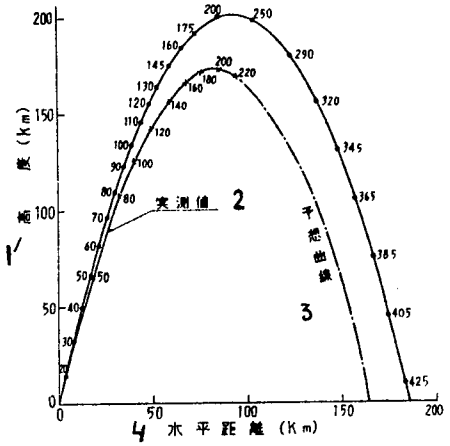

(b) Trajectory of K-8L-1 type space rocket (for launch angle of 80°)

1 - Altitude; 2 - Observed value; 3 - Calculated value; 4 - Horizontal distance; 5 - Time to the end of booster combustion; 6 - Time to the booster take-off; 7 - Time to the beginning of the main rocket combustion; 8 - Time to the end of main rocket combustion

Fig. 3

(3) K-9M-1 type space rocket.

Table 3 and Fig. 4(a) and (b) show the data and results of calculations. Fig. 4(c) is θ vs t curves. In calculating Eq. (1) in which the rocket is regarded as a point, the angle of attack of the rocket is decreased by one degree; and a normal-direction wind up to 1 km of altitude has the effect of drifting the K-9M-1 type space rocket 0.64° per meter (sic) of wind velocity in the direction of the wind.

Table 3. Data for K-9M-1 Type Space Rocket

	Booster Stage	Main Rocket
Total length (mm)	11174	5351
Outside diameter (mm)	420	250
Total weight (kg)	1438.8	331.8
Combustion time (sec)	17	7.6
Payload weight (kg)		27.3

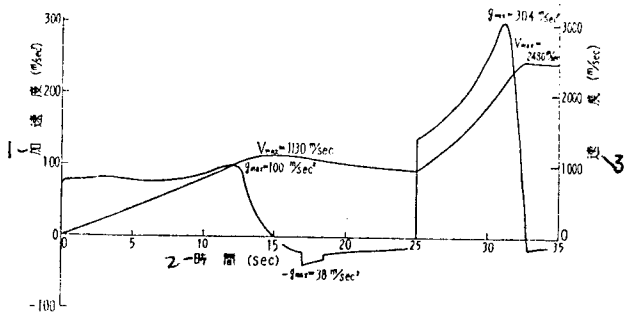

(a) Acceleration and velocity curves of K-9M-1 type space rocket (for launch angle of 80°)

1 - Acceleration; 2 - Time; 3 - Velocity; 4 - Time to the end of booster combustion; 5 - Time to booster take-off; 6 - Time to beginning of main rocket combustion; 7 - Time to end of the main rocket combustion

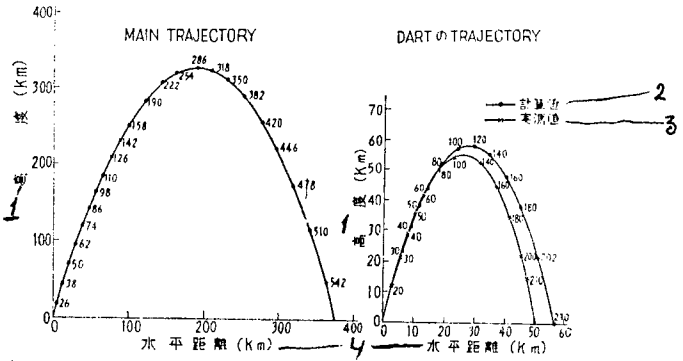

(b) Trajectory of K-9M-1 type space rocket (for launch angle of 80°)

1 - Altitude; 2 - Calculated value; 3 - Observed value; 4 - Horizontal distance

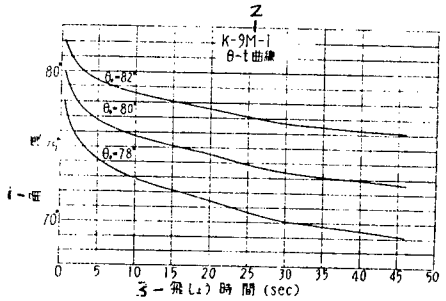

(c) θ vs t curves of K-9M-1 type space rocket

1 - Angle; 2 - θ vs t curves of K-9M-1 type; 3 - Time of flight

Fig. 4

Main rocket engine of the K-9M-1 type space rocket did not ignite when the booster took off and the main rocket went up without the thrust force of its engine. The trajectory of the rocket, observed by radar, compared with the calculated value is shown in Fig. 4(b).

(4) K-8-11 type space rocket.

Table 4 and Fig. 5(a) and (b) show the data and calculated results.

Table 4. Data for K-8-11 Type Space Rocket

	Booster Stage	Main Rocket
Total length (mm)	10930	5290
Outside diameter (mm)	420	248
Total weight (kg)	1529.9	331.9
Combustion time (sec)	16.0	9.715
Payload weight (kg)		29.2

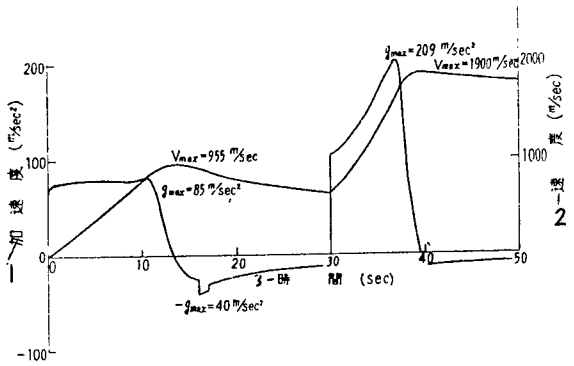

(a) Acceleration and velocity curves for K-8-11 type space rocket (for launch angle of 78°)

1 - Acceleration; 2 - Velocity; 3 - Time

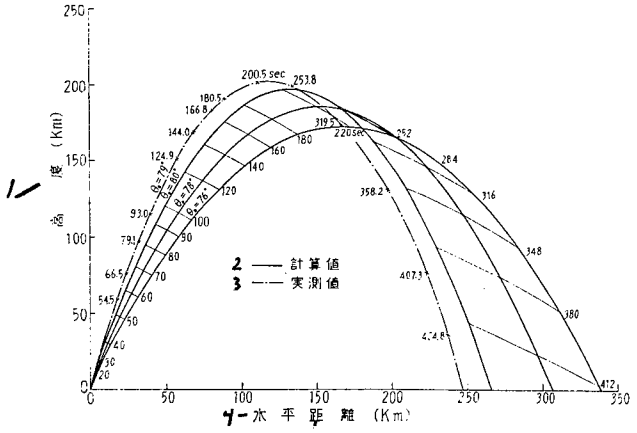

(b) Trajectory for K-8-11 type space rocket

1 - Altitude; 2 - Calculated value; 3 - Observed value; 4 - Horizontal distance; 5 - Time to end of booster combustion; 6 - Time to booster take-off; 7 - Time to beginning of main rocket combustion; 8 - Time to end of the main rocket combustion

Fig. 5

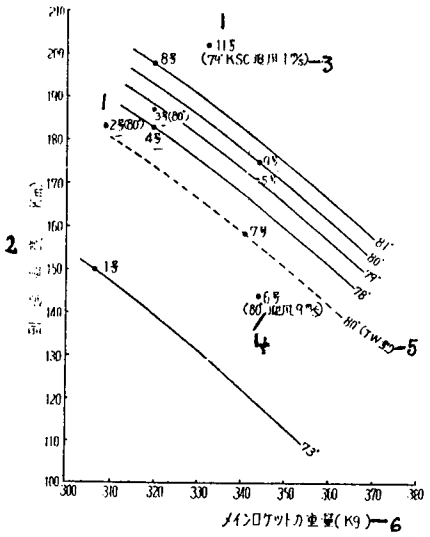

Fig. 6. Weight vs altitude curves for K-8 type space rocket (radar observed values)

1 - Number; 2 - Altitude attained; 3 - (79° KSC, 1 m/sec of tail wind); 4 - (80°, 9 m/sec of head wind); 5 - (TW type); 6 - Weight of main rocket

If the motion of the rocket with respect to its center of mass is included in the calculations, the trajectory will change as much as by the effect of the launch angle being increased by 1.5°. And a normal-direction wind existing up to 1 km altitude has the effect of causing the rocket to drift 0.6° per meter of wind velocity to the direction of the wind. Finally, we show in Fig. 6 the altitudes the K-8 type space rocket reached.

We express our thanks to Professors Watanabe and Nomura and to members in this institute who have helped us in the performance calculations.

(Received on April 22, 1963)

REFERENCES

1. Watanabe, M. Special Issue on Observation Rocket, Production Research, 13, 10.

2. Rosser, J.B. et al. "Mathematical Theory of Rocket Flight," McGraw-Hill, 1947.

STRUCTURAL STRENGTH OF KAPPA-8L AND -9M TYPE SPACE ROCKETS

By Daikichiro Mori and Noboru Uakano

1. Introduction

Kappa-8L and -9M type space rocket development, based on Kappa-6 and -8 type space rockets, were reported on by Professor Itogawa (on page 75 of this issue). In this report, the author will discuss on a part of the development plan, mainly on the better and lighter structure for the rockets.

Out of the rockets which were tested from October 1961 to date — two-stage rockets 8L and 9M type, small rockets HT-150 and LT-150 type, rocket engines L-735 2/3 and L-735 3/3 type which were the engines for the ground combustion test, and K-8-10 type space rocket — all have important considerations in regard to structural strength.

2. HT-150

As a test rocket for the 8L and 9M type space rocket, the HT-150 model rocket was developed to have a similar structure and performance in order to find out the characteristics of aerodynamic heat and pressure. Tail, tail base, connecting part, and nozzle were modified and lightened more than the 6M and 8 type space rocket. And aerodynamic smoothness was particularly emphasized because this rocket was only one step away from the 8L and 9M type space rocket. Results of the flight test were satisfactory. It had new temperature-measuring devices to replace the temperature measuring gauges since the gauge attachments were not reliable. Imazawa and Wanami had reported on this subject on page 241 of this issue.

3. K-8L Type

Main improvements of K-8L type space rocket from 6H type are as follows:

(a) Thickness of the chamber was reduced.

(b) Honeycomb type structure was introduced for the main rocket and booster tails. Thickness of the metal sheet of tail was also reduced. In this way, the weight of the tail was considerably reduced.

(c) Exterior of the tail base cylinder was smoothened, and inside, the cylinder was made so that it could hold the tail.

(d) Connecting part of the booster was given the shape of a cone cut on the top in order to hold the rear end of the main rocket cylinder and not to stretch out to the main rocket tail. With this weight reduction, structural balance could be achieved even though a light connection was somehow lost.

(e) Main rocket nozzle was made from aluminum alloy and phenolic resin FRP.

A new temperature measuring method, which was discovered during the HT-150 type rocket test, was also adapted.

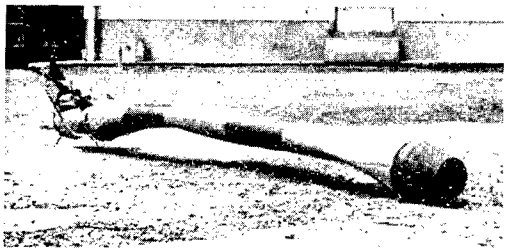

Fig. 1. Recovered 8L type booster

As one may see, two opposing factors of lightness in structure and better performance made the design extremely difficult and forced us to design a unique model. From the results of the launch test, it can be estimated that the rocket was not hurt by the anticipated severe heat and pressure. The recovered booster, which was found floating, had almost no damage on the chamber, nozzle, and connecting part; it is shown in Fig. 1. The tail was stripped out from its frame.

4. K-9M Type

The K-9M type space rocket was developed based on the 8-type space rocket. And its area of improvement is similar to the 8L type space rocket.

Bending stiffness of the rocket body was re-evaluated because the connection part was modified and therefore the body was flattened. The following equation can be applicable as a first approximation to bending stiffness of this kind of moving body.

$$K=\frac{fl}{\sqrt{q}}$$

where K: measure of quality, f: primary bending vibration frequency of the body, l: total length of the body, and q: dynamic pressure

The booster tail was developed at Prince Automobile Industrial Co. under the supervision of Mr. Itahasi and the company made a successful honeycomb type tail. Insulation of the measuring devices compartment was made by a double insulating wall and the test results showed the insulating effect was good.

Even though major improvement in the main rocket was not achieved, we had made a large improvement in the booster.

5. L-735 Type

Ground tests of the Lambda series engines were performed in sequence of 1/9, 1/3, 2/3, and 3/3 type engines, according to their length. The author will only call out the problems which were connected with the structure of the engine, the detailed report will be made later.

(a) Welding method and technique of attaching plate to body.

(b) Installation of nozzle-fitting plate to body.

(c) Manufacturing 100 kg/mm^2 uniform steel sheet, and to even-out the stresses; bending and welding the sheet.

(d) Body stiffness.

(e) Design to remove the heat from the nozzle.

(f) Heat problem and strength of the nozzle fitting plate.

(Received on April 3, 1963)

SMALL TYPE ROCKET

By Fusao Tamaki, Okichiro Tamaki and
Iwaho Yoshiyama

It was in October 1958 that a small rocket FT-122 was first used to test the value of a rocket. Since then, many small rockets have been launched as preliminary model rockets and they performed important roles in observation-rocket development.

Small rockets are used for many purposes as follows:

(1) In the development stage of a new space rocket, they are used to test new engines, propellants, aerodynamic characteristics, structural strength, and flutter.

(2) To test electronics systems such as telemetry, radar, antenna.

(3) Preliminary performance test of measuring instruments which will be later loaded into a space rocket.

(4) To test new safety or controlling systems.

(5) To review and research the preparations for a launching test site at a launching ground.

Small rockets which had been launched from September 1961 to December 1962 are listed in Table 1.

Following are brief discussions on each rocket.

FN 50-1, -2 and FN-150 type rocket: In order to find the characteristics of a four-nozzle rocket, FN-50-1 and -2 type rockets were tested in September 1961 because the Lambda series rocket booster was to have four nozzles. FN-50-1 type rocket was a single-stage rocket and -2 type rocket was a two-stage rocket; its second stage was a dummy. Both of the rockets flew without trouble.

Following them, the FN-150 type rocket was launched in October 1961. It flew smoothly also. From the test results of this rocket we were assured that a four-nozzle engine could be used in an actual space rocket.

Table 1
List of Small Rockets

番号	機種	試験項目	実験場	飛しょう日	外型	エンジン	外径	重量	全長	発射角度	最高高度	水平距離	全飛しょう時間	搭載計器
				(昭和 年 月 日)	(段)	(段)	(mm)	(kg)	(mm)	(deg.)	(km)	(km)	(sce)	
1	FN-50-1	4ノズル・エンジン	ATC	36・9・18	1	1	49	2.90	928	30	0.7	3.5	35	
2	FN-50-2	同上	ATC	36・9・18	2	1	49	2.20	993	30	0.7	3.5	35	
3	FN-150	同上	ATC	36・10・26	2	1	150	66	3392	45				RT
4	RT-75S	4mレーダ試験	ATC	36・12・18	1	1	70.5	14.00	1684	60				
5	RT-75-1	同上	ATC	36・12・18	1	1	70.5	14.00	1684	60	2.2	6.1	40	RT
6	RT-75-2	同上	ATC	36・12・18	1	1	70.5	14.00	1684	60	3.0	5.4	50	RT
7	RT-150	同上	ATC	36・12・20	1	1	150	70.1	3036	48	5.6	10	65	RT
8	OT-75-1	オペレーション	KSC	37・2・2	1	1	70.5	14.00	1684	60	3	6	50	発煙剤
9	HT-150	空力加熱(8L模型)	ATC	37・3・29	2	2	160	115.2	5167	60	20	30	141	X_1, X_2 Y,T,TM
10	OT-75-2	オペレーション	KSC	37・8・21	1	1	70.5	14.00	1684	60				
11	AT-150	胴体アンテナ	KSC	37・8・22	1	1	150	71.4	3017	60	13	12	103.3	TM
12	LT-150	吊下発射	KSC	37・11・21	2	1	150	70.0	3474	60	5	9	65	
13	SP-150-3	スピン翼の性能	KSC	37・11・21	2	1	150	68.4	3472	60	6	9	71	
14	SP-150-4	同上	KSC	37・11・25	2	2	150	69.9	3473	65	10	10	94	RT
15	SO-150-1	異常検出装置	KSC	37・12・20	1	1	160	87.8	3541	70	12	9	116	TM.ET ED

注：略号 AT: Antenna Test, LT: Launching Test, SP: Spin Test, FN: Four Nozzles, RT: Radar Test, SO: Safety Operation
ATC: Akita Test Center KSC: Kagoshima Space Center

1 - No.
2 - Type
3 - Test item
4 - Four-nozzle engine
5 - Same as above
6 - 4 m radar test
7 - Same as above
8 - Operation
9 - Aerodynamic heat (model of 8L type)
10 - Operation
11 - Body antenna
12 - Launching from suspended position
13 - Spin-stability test
14 - Same as above
15 - Trouble-shooting system
16 - Test site
17 - Date
18 - Exterior shape
19 - Engine
20 - No. of stages
21 - Exterior diameter
22 - Weight
23 - Total length
24 - Launch angle
25 - Maximum altitude
26 - Horizontal distance
27 - Time of flight
28 - Payload devices
29 - Smoking agent for atmospheric test
30 - Note: Abbreviation
31* - Year Month Day; to obtain the correct year, add 1925 to first column of numbers

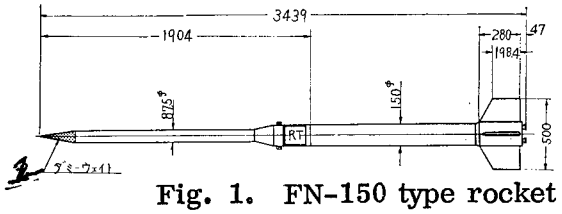

Fig. 1. FN-150 type rocket

1 - Dummy weight

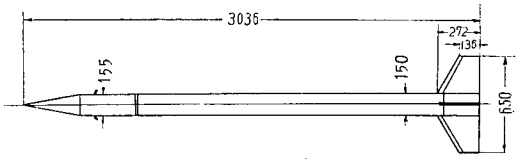

Fig. 2. RT-150 type rocket

RT-75S, -1, -2 and RT-150 type rocket: RT-75-1 and -2 type rocket with small radar transponders were launched to test the tracking performance of the 4 m radar which was newly installed at Akita Test Center. The RT-75S type rocket was launched to determine whether the new radar could be used as the primary radar at the center. Following this, the RT-150 type rocket (see Fig. 2) was launched and its trajectory was tracked by both radars and compared. The RT-150 type rocket had the additional mission of testing a new propellant and body structure. Its flight was smooth.

HT-150 type rocket: The HT-150 type rocket was designed to test the aerodynamic characteristics and heat and structural strength of the new K-8L and -9M type space rockets being developed. It was a two-stage rocket as shown in Fig. 3. It was designed to have high speed in low atmosphere. From the test, design data for the 8L and 9M type space rockets and the performance of the new propellant could be obtained.

As the primary radar, the 4 m radar tracked the flight of the booster, thus, the trajectory of the main rocket was not able to be tracked (refer to the article by Mori on page 112 in this issue).

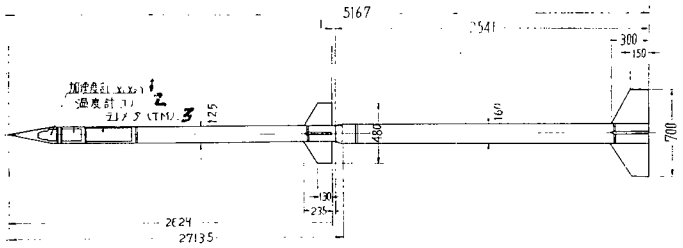

Fig. 3. HT-150 type rocket.

1 - Accelerometer; 2 - Thermometer; 3 - Teletransmitter

OT-75-1 and -2 type rocket: The OT-75-1 type rocket was launched on the day of the ground-breaking ceremony at Kagoshima Space Center. The OT-75-2 type rocket was launched August 1962, in advance of the operational use of the launching ground, to determine the ground and operational conditions and optical observation conditions (see Fig. 4).

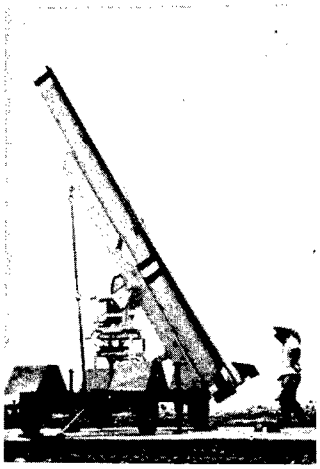

Fig. 4. OT-75-2 type rocket

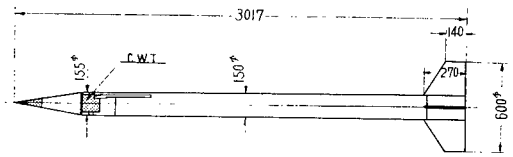

Fig. 5. AT-150 type rocket

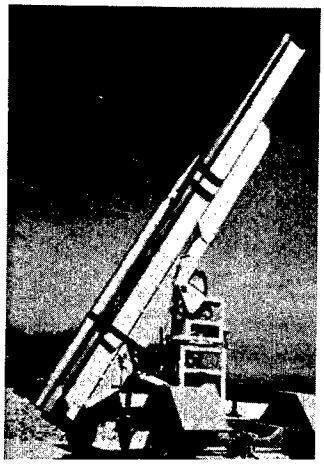

Fig. 6. AT-150 type rocket

AT-150 type rocket: A new teletransmitter antenna, which was stretched along the rocket body was developed to test the performance of the antenna. With it, the AT-150 type rocket was launched (see Figs. 5 and 6 and refer to the article by Yamashita on page 173 in this issue).

LT-150 type rocket: Since Lambda series rockets were designed to launch in the suspended state, the LT-150 type rocket was used to test the launching method (see Fig. 7). As a result of the test, it was found that the launch was smooth and vibration of both rocket and launcher were almost negligible during the launch period.

SP-150-3 and -4 type rockets: They were launched to test the spin tails. Previously, SP-150-1 and -2 type rockets were launched to find the characteristics of the spinning motion of the 9L type space rocket due to the nozzle. This time the rockets were used to find the effect of a rear bent tail on spin, the data to be used as design data for a new space rocket (see Fig. 8).

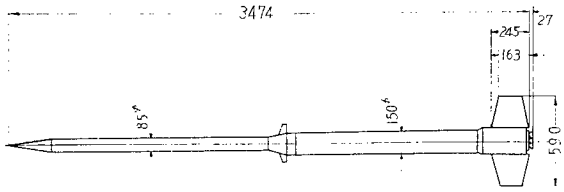

Fig. 7. LT-150 type rocket

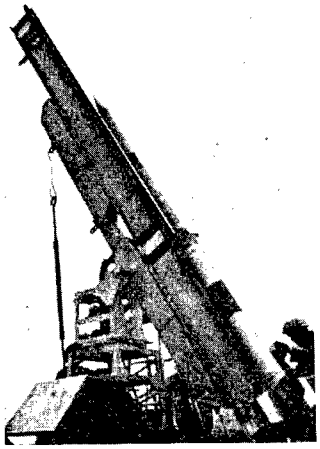

Fig. 8. SP-150 type rocket

SO-150-1 type rocket: It was launched to improve safety operations, particularly the ignition of the second-stage engine of the two-stage rocket (see Fig. 9).

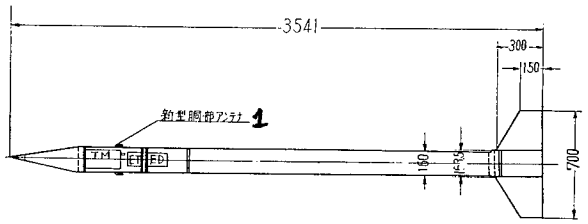

Fig. 9. SO-150-1 type rocket

1 - New type body antenna

As discussed above, about ten small rockets per year were planned, designed, manufactured and launched along with the space-rocket launching and ground combustion test of engines. In performing this complicated and complex project, Prince Automobile Industrial Co., Nippon Electric Co., Mitsubishi Electrical Machinery Co., Akehoshi Electric Co., Matsushita Communication Industrial Co., and Kumatoritani Factory gave much devoted effort.

It can be anticipated that the importance of the small rocket will be much increased in the future.

(Received on May 2, 1963)

DEVELOPMENT OF LAMBDA-735-TYPE ROCKET ENGINE

By R. Akiba

A rocket engine developed by the Production Research Institute is given its type number according to its diameter and so the L-735 type rocket engine's diameter is 735 φ (mm) as its type number suggests. L-735 type rocket engine will be used as the first stage booster for a Lambda series space rocket and its dimensions are listed in Table 1. The engine can be classified as a large engine in comparison with 420 φ boosters which have been used for K-8 and 9 type space rockets or other countires' rocket engines for observation rockets of today. For this reason, and because of the possibility of having a large Mu type booster, the development of a L-735 type rocket engine has significant value. Development of a large rocket engine has been becoming more important for many countries in recent years and there are many difficult problems to be solved for the development.

First of all, whether stable combustion can be obtained is the biggest problem. There are some explanations for unstable combustion. But they are not clear theoretically. Consequently, one must perform a ground combustion test and find the combustion stability of the engine. Particularly, it is difficult to estimate the possibility of a so-called oscillating combustion which is a sonic vibration of the gas in a rocket engine. Therefore, the selection of a fuel and design of an engine have to be based largely upon qualitative or semi-empirical theories and it is common and inevitable to develop a large rocket engine by scaling up step by step from conventional engines. We developed the L-735 type rocket engine in four steps 1/9, 1/3, 2/3 and 3/3 as shown in Table 1.

Table 1

	L-735 1/9	L-735 1/3	L-735 2/3	L-735 3/3
1 直 径 (mm)	735	735	735	735
2 長 さ (m)	1.3	3.4	5.4	7.9
3 重 量 (ton)	—	2.0	3.1	4.5
4 平均推力 (ton)	4.7	14(推定)5	28	40

1 - Diameter; 2 - Length; 3 - Weight; 4 - Average thrust force; 5 - (Estimated value)

Structurally, the biggest problem is to make a large combustion chamber. Such a big chamber is normally made from a steel of high tensile strength and by welding. L-735 type engines were made from HT-100 steel of Nippon Steel Prod. Co. and welded at Kobe Shipyard of Sin Mitsubisi Heavy Industrial Co., Ltd. We will not describe the detailed procedure for welding the steel. Another difference between the 735 φ and 420 φ engines is that the inside wall of the (larger) combustion chamber was not finished after welding.

The bigger rocket engine inevitably has a longer combustion time. This problem of long combustion is particularly important for a solid fuel engine which has a big nozzle to conduct large amounts of heat out of the chamber. Since the combustion time is normally fixed by the diameter of the engine, we had the advantage that we developed and tested the engines step by step from the one which has the smallest ratio of the diameter to length of the booster, 1/n, keeping the same diameter. In order to reduce excessive heat at the nozzle, we walled the inside of the nozzle with heat resisting material to prevent heat conduction from the nozzle gas. And the exit area was covered with a high heat conductive material, mostly by graphite, to help excessive heat to escape and to reduce the temperature at the area.

It is different from the Kappa series rocket engines that the L-735 type rocket engine has four nozzles. One cannot simply say that a single nozzle engine is better than a multiple nozzle engine or the other way around. Considering only the weight of nozzles, we see that an n-nozzle engine has the strength of $1/\sqrt{n}$ of a one-nozzle engine; but it is not practically true because the heat problem must be considered in the same time. In multi-nozzle engines, one nozzle can be a small nozzle and requires only a small amount of graphite. It is therefore of advantage to use multi-nozzle engines since high-quality graphite is scarce these days. On the other hand, during flight, a four-nozzle engine has the disadvantage that some effluent gases from the nozzles overlap when the nozzles are not expanded properly and some of the gas flows toward the side panel. Therefore, some heat preventive method must be applied to the panel. As we will describe later, unexpected heat distribution was found when a ground test had been performed.

The outlines of the ground tests of L-735 -1/9, -1/3, -2/3 and -3/3 and the dimensions of these engines are listed in Table 1.

1. L-735 1/3 Type Rocket Engine

As the first engine test of Lambda series rocket engine, the ground combustion test of L-735 1/3 type rocket engine was performed at Akita Test Center, Michgawa, Akita Province, on April 23, 1961. The engine test stand for the 420 φ was modified at the center for the test.

Test conditions:

Weather: clear; Temperature: 19°C; Atmospheric pressure: 1012 mb.

Measured items: inside pressure, inside vibration, outside vibration, wall temperature, stress, film taken by high-speed movie camera (measuring methods are described in Section 3, L-735 2/3 rocket engine).

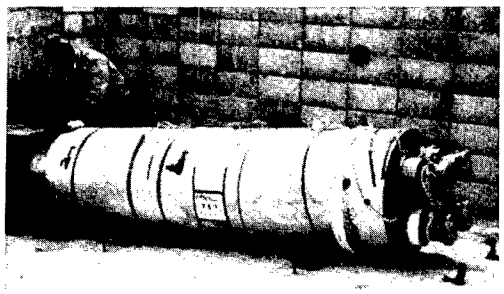

Fig. 1. L-735 1/3 type rocket engine

2. L-735 1/9 Type Rocket Engine

The engine was tested at Kawakoshi test stand of Prince Automobile Industrial Co., Ltd. on February 18, 1961.

Test conditions:

Weather: clear; Temperature of fuel: 15°C.

Measured items: inside pressure, inside vibration, thrust force, temperature of nozzle, outside vibration, film taking.

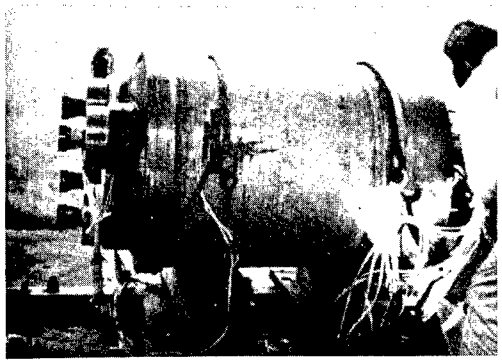

Fig. 2. L-735 1/9 type rocket engine

3. L-735 2/3 Type Rocket Engine

This rocket was designed according to the test results of the L-735 1/3 and 1/9 rocket engines. The expansion end of the four nozzles of the engine was made from a new material, and its structure was changed. That is, two nozzles used ablation cooling and the other two nozzles were coated with a metallic oxide. The ground combustion test of the engine was performed on a new LM test stand at Michigawa Test Center, Akita Province, on March 31, 1962.

Test conditions:

Weather: clear; Temperature: 11°C; Atmospheric pressure: 1022 mb; Temperature of fuel: 20°C.

Measured items and methods are as follows:

(1) Inside pressure. An ordinary resistance type strain gauge was used to measure the inside pressure. However, the combustion oscillations could not be measured because this system uses several kc carriers to amplify the gauge voltage.

(2) Inside vibration. The same resistance type pressure unit (PU) was used. But in this case, unlike the previous case where a carrier was used to amplify the gauge voltage, the voltage was converted into DC and the output was amplified by an RC amplifier and then it was amplified again by a four-channel amplifier. Each channel of the amplifier filtered out all but a certain region of the frequency signals and finally this signal was recorded by an oscilloscope [4]. A capacitance type inside pressure meter was also used to detect the DC and AC components of the gauge voltage due to non-vibrational and vibrational pressure. In this particular case, the recording was done by Brown tube photography.

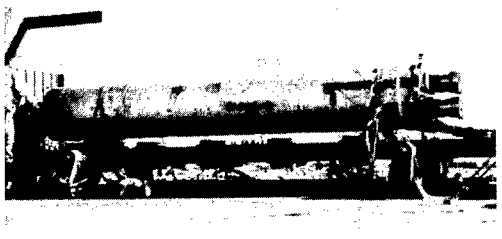

Fig. 3. L-735 2/3 type rocket engine

(3) Thrust force. The thrust force measured by a resistance installed in a high-pressure cylinder. There were some difficulties in designing it and so the accuracy of the gauge was not fully satisfactory. Further details on this measurement will be described in the article "Thrust" (page 136 of this volume).

(4) Temperature. The temperature at the nozzle was measured by a thermocouple of Ni-NiCr, 0.5 φ. Thirty-two thermocouples were scanned by a scanner and the data were amplified by a chopping amplifier, and the amplified data were recorded by an oscilloscope.

(5) Stress and vibration. The stress at the inside of the combustion chamber along axial and radial direction and at the molded section were measured by resistance type strain gauges (DS 6-RX of Shinko Communication Co.). The vibration at the rocket engine test stand was measured by a televibro meter (Akiishi Co.), a vibration meter (Matsushita Communication Co., Ltd.), and a resistance type accelerometer (Sinko Communication Co.). The measurements were recorded by a pen recorder, tape recorder, and oscilloscope.

(6) Optical measurement. The nozzle and body were filmed by a high-speed movie camera (Fastax 500 f/sec) for 9 seconds from ignition, and by a 16 mm movie camera all through the combustion.

(7) The combustion sound was recorded into a tape recorder through a noise meter 200 m away from the stand.

Test results:

The fuel burned almost uniformly for the entire period of combustion. The engine also had a satisfactory structure. And we could obtain important data on the nozzle from the test.

We had to face many difficulties in preventing the data being affected by noise and interference since there were a lot of points which had to be measured and the distance between the computing room and the test stand was more than 100 m. However, it can be said that the resulting data were almost perfect.

4. L-735 3/3 Type Rocket Engine

The L-735 3/3 type engine will be used, almost without changes, as the first stage booster of the L-2 type space rocket. The design of each part of the engine was done according to the test results of the previous L-735 series rocket engines. Since the nozzles had to be enlarged, the thickness of the side reflecting panels were increased. Nozzle structure was selected from that of the L-735 2/3 type which showed up to be the most reliable. And two kinds of nozzles were adopted to compare the effects of coating materials.

2ー燃焼試験中

Fig. 4. L-735 3/3 type rocket engine.
1 - Test stand and engine; 2 - Booster test

Fig. 5

Since the Michigawa test stand, Michigawa, Akita, was not capable of testing this engine, a new LM test stand was constructed at Hama-asa-uchi Beach, Noshiro City, Akita Province, in the summer of 1962. The ground test of the engine was performed on October 29, 1962.

Test conditions:

Weather: light rain; Temperature: 15.5°C; Temperature of fuel: 22°C.

Measured items and methods:

(1) Inside pressure. Method was same as for the L-735 2/3.

(2) Inside vibration. Two methods were adopted, the same method as for the L-735 2/3 type, and the method to record into tape recorder through a wide-band direct amplifier.

(3) Thrust. The method used for L-735 2/3 was revised and a newly developed detector which had the accuracy of 10.5% was used to measure the thrust force.

(4) Temperature. Method was the same as for the L-735 2/3 type test but 44 temperature measuring points were selected.

(5) Vibration and stress. Methods were the same as for the L-735 2/3.

(6) Flame intensity of the effluent gas. The measurement of the flame intensity was the first try in these series of tests. The intensity was recorded by a pen recorder using a CdS converter.

(7) Optical measurement. High speed movie cameras Fastax and 16H were operated in series to take film for the entire period of combustion. Shutter speed was 500 f/sec. And Bell & Howell cameras took the picture with long focus lens and 24 f/sec shutter speed.

Test results:

Combustion test results showed that the engine had sufficiently good performance, both in combustion and structurally, to be used as an actual booster. In other words, it had uniform combustion and enough structural strength.

Conclusion

So far, we described the development of the L-735 type rocket engine. And we found the engine can be used as an actual booster for the L-2 type space rocket without any major changes. In considering the early steps of our rocket engine development and the present situation of large rocket engine developments in the world, we believe that the problems in this area are going to be solved.

Finally, we express our thanks to Prince Automobile Industrial Co., Ltd., and Matsusita Communication Co., Ltd., for their kind help in measuring the performances of the rockets. And we also extend our thanks to Nippon Steel Manufacturing Co., Sin Mitsubishi Heavy Industrial Co., Ltd., for their great contribution in the engine production.

(Received on May 10, 1963)

REFERENCES

1. Y. Ando, J. Mechanics, 65-523, 1159, August 1962.

2. D. Mori, Analysis on the Strength of the Chamber of L-735 1/3, S.E. Report.

3. Y. Tota, Prod. Research, 9-3, 82, March 1957.

4. Wachi, H., Suzuki, M. and Ueno, Z. Proc. of the 3rd ISRA, Yokendo, 319, 1962.

5. Report on Ground Combustion Test of L-735 1/9 type rocket motor, Vol. 22, PM Research Report.

6. Report on Ground Combustion Test of L-735 2/3 type rocket motor, Vol. 42, PM Research Report.

7. Report on Ground Combustion Test of L-735 3/3 type rocket motor, Vol. 110, PM Research Report.

8. Report on the Temperature measurement for Full Size Lambda-Rocket Engine Ground Combustion Test, Matsushita Communication, Research Project No. 21, 74.

9. Extra Issue, Report on the Temperature Measurement for L-735 2/3 Ground Combustion Test, Matsushita Communication Report.

10. Mori Laboratory, Vibration Measurement for L-735 2/3 Ground Test, S.E. Report.

11. Mori Lab., Stress Measurement for L-735 2/3 Ground Test, S.E. Report.

12. Ishikawa Laboratory, Flame Measurement for L-735 2/3 Ground Test, S.E. Report.

13. Akiba Lab., Temperature Measurement results for L-735 3/3, S.E. Report.

DEVELOPMENT OF ROCKET-CHAMBER WELDING TECHNIQUES

By Yoshio Anto

1. Introduction

It was reported by the author that a welded chamber was introduced into use as a rocket chamber for the K-420 boosters which were used on the K-7, -8, and -9 type space rockets; and that HT-85 uniform, high-strength sheet steel had been used mainly to make rocket chamber since September 1950. It was also reported that two of the boosters were made from SAE 4130 sheet steel [1], [2]. In this report, the author will describe development of the L-735 rocket chamber, which was to be used in the booster of the Lambda series rocket; and the K-420H rocket chamber, which was developed to improve the Kappa series booster.

2. L-735 Type

Since HT-85 uniform sheet steel (modified 2H-ultra type, product of Sitsuran Factory, Nippon Steel) showed satisfactory quality for the K-420 type chamber, HT-100 uniform, high-strength sheet steel was selected in making the L-735 type chamber in spite of the difficulties in welding and processing. The fabrication of the chamber was done by Sitsuran Factory, Nippon Steel [3], [4]. One of the important advantages of steel is that it gains strength through annealing and tempering and therefore does not have to have heat treatment, which usually introduces some distortions after welding. Chemical compositions and mechanical properties of HT-85 and HT-100 are listed in Tables 1 and 2.

The L-735 type booster was already made and ready to launch; the launch is scheduled for the summer of 1963. Its engine has already completed four sets of ground combustion tests of the 1/2, 1/9, 2/3, and 3/3 type since 1961. The L-735 type booster has no tail base cylinder and the tails are put directly on the chamber. Since the booster is not launched yet, the author will not discuss this matter here.

The chamber of the L-735 type booster as shown in Fig. 1 is not finished after welding unlike the conventional K-420 type, which was finished to exact dimensions after welding. Fabrication of the chamber was done by Kobe Ship Yard, Sin Mitsukishi Heavy Industrial Co. The first chamber of the 1/3 type was designed to use sheet steel for the entire chamber. But there was cracking at the deflecting plate sides which were the places on them welding heat was affected

Table 1

Chemical Compositions of the Steels Used (%)

鋼種	分析	C	Si	Mn	P	S	Ni	Cr	Mo	Cu	備考
HT-85	仕様	≤.18	≤.55	≤1.35	≤.04	≤.05	≤1.0	≤.60	≤.50	—	
	レードル	.15	.35	1.06	.010	.008	.81	.43	.40	—	
	目標	.18	.40	1.20	≤.020	≤.020	1.30	.60	.45	.30	
	レードル	.17	.46	1.15	.018	.018	1.30	.68	.50	.30	
HT-100	チェック(日鋼)	.17	.49	1.26	.018	.018	1.37	.70	.49	.31	L-735-1/3用
	チェック(新三菱)	.19	.50	1.18	.020	.026	1.39	.64	.46	.28	t=約 4 mm
	レードル	.19	.54	1.26	.028	.011	1.26	.80	.55	.37	K-420H用 t=約 4 mm

3) Type of steel
4) Analysis
5) Specification
6) Result
7) Object
8) Result
9) Check (Nippon Steel)
10) Check (Sin Mitsubishi)
11) Result
12) for L-735-1/3
13) t = about 4 mm
14) for K-420H t = about 4 mm
15) Remarks

Table 2

Mechanical Properties of the Steel Used

鋼種	条件	降伏点 kg/mm²	引張り強さ kg/mm²	伸び (G.L.50mm) %
	仕様	≥65	≥85	≥18
HT-85	板厚 10 mm タテ	84.4	89.9	24.0
	〃	92.3	94.8	19.7
	仕様	≥85	≥95	≥10
HT-100	板厚約 4mm タテ	94.4	100.0	15.1
	〃 ヨコ	97.8	102.3	15.2
	板厚約 2mm タテ	99.1	109.6	10.5

17) Type of steel
18) Condition
19) Specification
20) Thickness of sheet, 4 mm length
21) Specification
22) Thickness of sheet, 4 mm length
23) Thickness of sheet, 4 mm width
24) Thickness of sheet, 2 mm length
25) Immersion point
26) Tensile strength
27) Elongation

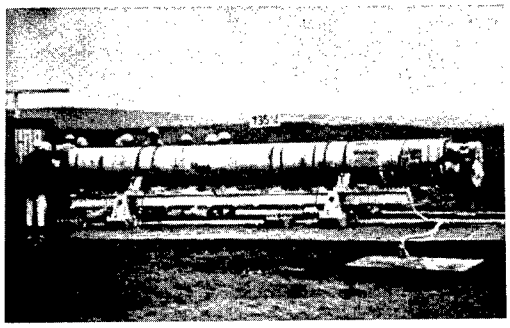

Fig. 1. L-735 3/3 type booster at Noshiro Test Center (October 29, 1962)

Table 3

Chemical Compositions and Mechanical Properties of Molten Metals of the Welding Rods Used

6 名称	7 化学成分 %								8 引張り強さ kg/mm²	9 伸び (G.L.=50mm) %	10 断面収縮 %
	C	Mn	Si	P	S	Ni	Cr	Mo			
LBK 85	.07	1.46	.60	.012	.010	1.83	.05	.65	94.9	18.4	63.9
LBK 100	.08	1.69	52	.012	.009	1.60	.85	.66	106.7	19.0	53.1

6) Nomenclature
7) Chemical compositions
8) Tensile strength
9) Elongation
10) Shrinkage of cross-section

as shown in Fig. 2(a) and it had to be remade. It was quite a time-consuming job to process a material which is highly elastic to a spherical shape. Therefore, for the chambers following 2/3 type, a forged ring of HT80 steel was introduced. With it, and no-overlapping welding and removal of bracket, stress concentrations, weld cracking, and rapid cooling could be avoided. In the 1/3 type, the nozzle was made to insert into the nozzle fitting plate. But it was modified as shown in Fig. 2 (c) and made grooves at the outside of the nozzle as shown in Fig. 2 (a) [5].

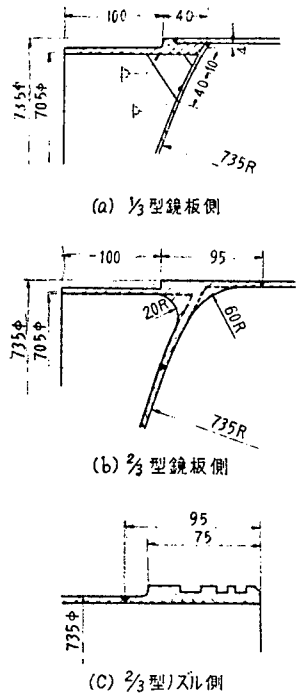

Fig. 2. Design for welding the aft end of the L-735 type chamber. (a)—Side view of the deflecting plate of 1/3 type booster; (b)— Side view of the deflecting plate of 2/3 type booster; (c)—Side view of the nozzle of the 2/3 type booster

The welding rod LBK100 for the welding of the chamber had been especially made by the Welding Rod Department of Kobe Steel. The chemical compositions and mechanical properties of the molten metal compared with those of LBK85, which is the welding rod for HT85 steel, are shown in Table 3.

The initials LB in LBK 85 welding rod denotes the common code of the company's low hydrogen series welding rods, and the K comes from Kappa. Test

results of the tensile strength at the welded portion are listed in Table 4. The breaking point appears outside the welded area except for those areas that were annealed. Hardness test showed that the welded area was harder than the non-welded area [6]. Specifications for the K-420 and K-420H chambers are listed in Table 5. Without a finishing operation, we used rolled steel to make an L-735 type chamber. It had much larger tolerances than the K-420H type chamber with finishing. Allowable stress for the hydraulic pressure test was 60 kg/mm^2.

Table 4

Test of the Tensile Strength at the Welded Area of HT100 Uniform Strength Steel

12 予熱温度 °C	15 引張り強さ kg/mm²	16 破断位置
13 予熱なし	99.7	母材 17
〃	100.0	〃
50	104.8	〃
〃	103.0	〃
100	103.0	〃
〃	101.9	〃
150	104.9	〃
〃	101.3	〃
14 焼なまし(570°C)	98.7	溶接部 18
〃	104.0	〃

12) Pre-heating temperature
13) No pre-heating
14) Annealing
15) Tensile strength
16) Place of tear
17) Base material
18) Welded area

Table 5

20 Outline of Criteria for the Rocket Chamber Test

チャンバ名称	K-420	K-420H	L-735
21 肉厚 mm	$t_1 \pm 0.2$	$t_2{}^{+0.5}_{-0}$	$t_3 \pm 0.5$
22 内径 mm	$420-2t_1 \pm 1.4$	$420-2t_2 \pm 2.0$	$735-2t_3 \pm 2.5$
23 真直度 mm	0 ± 1.75	0 ± 2.5	0 ± 3.0
24 全長 mm	4850^{+3}_{-0}	4850^{+3}_{-0}	7363^{+4}_{-0}
25 両端面の平行度 rad	≦1/1000	≦1/1000	≦1/1000
26 溶接継手の引張り強さ kg/mm²	≧85	≧95	≧95
27 溶接部X線検査シーム(全線)	JIS 1級-31	JIS 1級-31	JIS 1級-31
28 同上パット(シームとの交点)	JIS 2級-31	JIS 2級-31	JIS 2級-31
29 水圧試験圧力 kg/cm²	60	60	60
30 計算重量との許容差 kg	±10	±10	±30

t_1 approximately 3 mm by finishing, t_2 approximately 2 mm thickness by rolling, t_3 approximately rolling to about 4 mm. Each of the above figures indicates first digit after the decimal point.

Key to Table 5:

20) Type of chamber
21) Thickness
22) Inside diameter
23) Straightness
24) Total length
25) Degree of parallel of the bases
26) Tensile strength at welded area
27) Welded area X-ray test, seam (entire line)
28) Welded area X-ray test, butt (junction with seam)
29) Hydraulic test pressure
30) Tolerance in calculated weight
31) Class

3. K-420H Type Booster

The K-420 type boosters have been launched more than ten times with good results since 1959. However, the K-420H type booster was developed to further improve the K-420 booster. Diameter, length, and the structure of the two ends of the booster were similar for both boosters K-420 and K-420H type. The main differences were that chamber material was changed from HT85 steel to HT100 steel. Rolled thin sheet steel was used without finishing unlike the finished chamber of the conventional chamber, and therefore a special rolling method and annealing and tempering treatment had to be adapted. Sitsuran Factory, Nippon Steel who made the steel, had to work hard to avoid introducing some stress during the process. On the other hand, Kobe Ship Yard, Sin Mitsubishi who had fabricated the chamber, had devoted much effort to avoiding the distortion in welding and to overcome the difficulty in the fabrication process. The test criteria for the booster is shown in Table 5. The tolerance of the hydraulic test is 60 kg/mm^2, the same value as for the L-735 type booster. Weight of the booster was reduced 17% below the K-420 type booster.

Even though the size of the K-9M type space rocket, which used the K-420H type booster, was almost the same as that of the K-8 type space rocket, its maximum altitude was increased to 400 km from the K-8 type space rocket's 200 km. It was decided that future boosters would be the K-420H type made from HT-100 steel. Fig. 3 shows the photograph of the K-9M-1 type space rocket, which was launched at Kagoshima Space Center in November 1960.

4. Conclusion

The author outlined the development of the L-735 and K-420H type boosters. Though HT 80 steel is usually used in rocket chambers, highly reliable but inexpensive rocket chambers could be made from HT 100 steel by an all-welding method. We have a plan to develop a chamber with an even stronger steel. But we

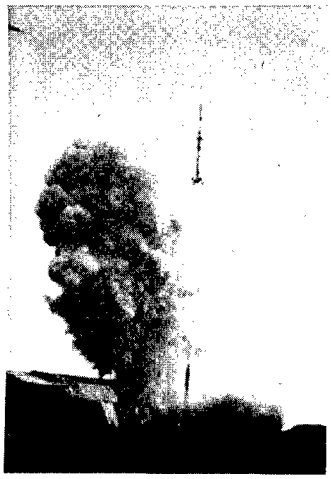

Fig. 3. K-9M-1 type space rocket launching
(at Kagoshima on November 25, 1962)

can anticipate many difficulties in connection with the steel since the steel should be an entirely different kind.

The author expresses sincere thanks to assistant professor Daikichiro Mori who was in charge of the structure, Doctors Simota and Miyano of the Laboratory of Muroran Factory, Nippon Steel who were engaged in sheet steel manufacturing, member of the Welding Division, Kobe Steel Manufacturing who made the welding rod, and Doctor Takagi and Engineers Yano, Kawai, Yamagata, and Nishi who worked in welding and processing the chamber.

(Received on March 28, 1963)

REFERENCES

1. Anto: Prod. Research, 13, 10 (Oct. 1961).
2. Anto: Welding Tech., 10, 2 (Feb. 1962).
3. Simota, Miyano: J. Steel Tech., 7 (June 1961).
4. Miyano: Welding Tech., 10, 2 (Feb. 1962).
5. Anto: J. Mech. Soc. 65, 323 (Aug. 1962).
6. Takaki: Welding Tech., 10, 2 (Feb. 1962).

THE THRUST METER FOR GROUND TEST OF THE LAMBDA SERIES ROCKET ENGINE

By Koshiro Ohi, Owao Yoshiyama,
Kotatsu Kokura, and Takashi Tokimatsu

1. Introduction

The first model of the thrust meter for the Lambda series engine ground-test gave poor repetition of data. However, we could get satisfying results with a modified thrust meter and will report on it.

The required conditions for the thrust meter are as follows: it should be able to measure up to a capacity of 50 tons with an accuracy of 1%. It should have a high spring-constant in order not to be affected by vibrations. And it should be able to maintain the forward gap of the rocket engine to prevent unexpected trouble. Even though the problems are not difficult if faced separately, a combined solution for all the conditions is very hard to get. In other words, it might happen that the center of mass of the load might be shifted in the actual case and the surfaces at the forward gap and the thrust meter might not contact each other squarely. In general, the above factors can act to reduce the accuracy of measurements. If we can hold a rocket in such way that it can move in the direction of its axis and set a joint between the engine and thrust meter, the above troubles can be eliminated. However, this solution does not fulfill the condition calling for a tight hold on the rocket engine. There can be many possible ways to solve the problem. But we could not study the problem extensively because of the time limit and we made only moderate modifications hoping to get accurate measurements. First, we decided to make a model of the thrust meter.

2. Test of the First Model of the Thrust Meter

Figure 1 is the diagram of the pressure-receiving cylinder of the first model for the L-735 1/3 type rocket engine. We will call it Model 1. Cross-type resistance strain gauges are set on both the inside and outside of the cylinder and each gauge is located 90° away from the other. The element of the strain gauge which is parallel to the axis of the cylinder will measure the longitudinal strain, denoted ϵ_z; and the element normal to the above element will be called transverse strain, denoted ϵ_t. This is the way, in the test, that ϵ_z and ϵ_t are measured when a 50-ton load is applied to the model.

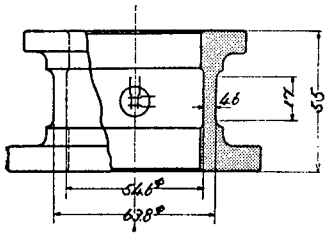

Fig. 1. Model 1 of the thrust meter

When elements are connected as shown in Fig. 2, the strain determined from the outputs of the elements make the bold lines in Fig. 3. As the figure shows, the lines have considerable curvature and large hysteresis and this comes from the friction between the contact faces. It seems impossible to increase the accuracy within one percent when one evaluates Fig. 3, and if we make a slight change on the condition of the contacting faces, the lines in the figure will change considerably and repetition of the measured values will become poorer.

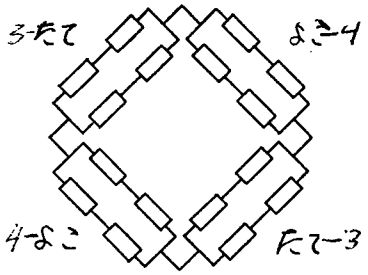

Fig. 2. Method of connection of the gauges

3) Longitudinal; 4) Transverse

Actually, what we need to know is the magnitude of load or the average compressive stress which is the result of the load divided by the cross-sectional area of the cylinder. For instance, if we calculate the average compressive stress according to the following equation using the same data which make the bold lines in Fig. 3, we will get the dotted lines in the figure.

$$\sigma_z = \frac{E}{1-\nu^2}(\varepsilon_z + \nu\varepsilon_t)$$

The result is improved in this case and the result will not change much less than 3%, even if we change the condition of the contacting faces. However, this will not give the accuracy we want.

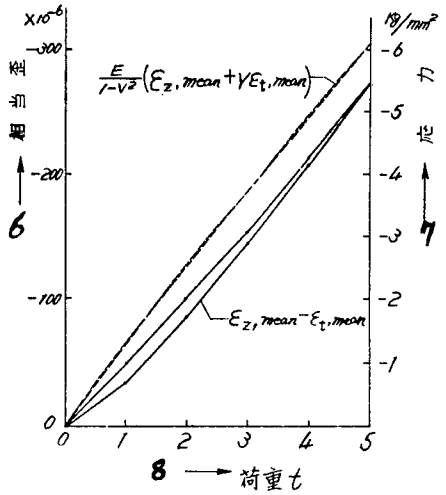

Fig. 3. Test result of Model 1

6) Relative strain, 7) Stress, 8) Load (tons)

Generally, the effect of the edge of a thin-sheet cylinder with axial symmetry decreases according to the following equation:

$$\exp\left\{-\frac{\sqrt{1-\nu^2}\,z}{\sqrt{Rt}}\right\}$$

where z: distance from edge, R: average radius of the cylinder, and t: thickness. Therefore, the effect of the edge can be eliminated when we increase the value of z to several times that of $\sqrt{Rt}$. And we made Model II (see Fig. 4), which has nearly the same dimensions but is longer than Model I, and tested it in the same way. The result is shown in Fig. 5. This time, the effect of the connecting faces does not appear and the bold and dotted lines show the model has the required accuracy.

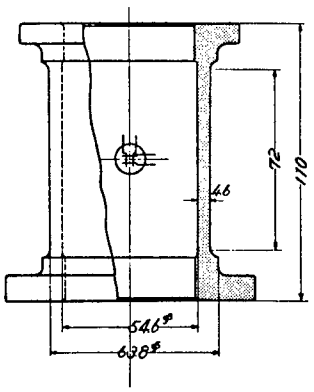

Fig. 4. Model II of the thrust meter

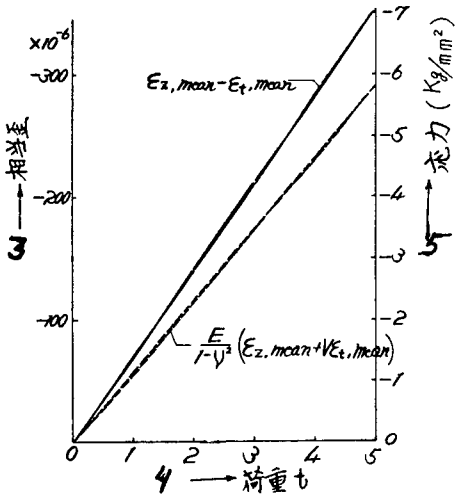

Fig. 5. Test result of Model II

3) Relative strain, 4) Load (tons), 5) Stress

3. 50-Ton Thrust Meter

According to the experimental models' test, we found that the 50-ton size thrust meter can be used as an intermediate size of the two models. However, we made a thrust meter three times bigger than Model II since the most important thing is to measure the thrust force more precisely and accurately even though we knew it would be too big. But the thickness of the cylinder did not increase three times but rather we designed it to have the stress of 15 kg/mm^2. The photograph of the thrust meter is shown in Fig. 6. Midway from the top of the cylinder, cross-type gauges of plotting range of 8 mm are set each $\pi/8$ apart from the other on both inside and outside of the cylinder and they are connected as shown in Fig. 2; and similarly, two more channels are installed. And yet, two more channels are installed, one of which will measure the average longitudinal strain separately and the other will measure the transverse strain separately. In measuring the thrust force, dynamic strain-measuring amplifiers are used and the output sent to electromagnetic oscilloscopes. For accurate calibration of the force, a 50-ton capacity loop-type force gauge, which had recently been inspected at the measuring equipment inspection office, is used (but the gauge did not have to be inspected because the inspection result agreed with a previous value within the deviation of less than 0.2%). The reason a loop-type, force-gauge was used was to determine the sensitivity of the thrust meter under the same conditions as the engine test. From the sensitivity test, we found out that we do not need to measure the longitudinal and transverse stresses separately. When we denote the outputs of each of the three channels of the same structure, each of which is connected as shown in Fig. 2, $\varepsilon_1, \varepsilon_2, \varepsilon_3$ the mean value of the three $\varepsilon_{mean}=(\varepsilon_1+\varepsilon_2+\varepsilon_3)$ $\varepsilon_1-\varepsilon_{mean}$, $\varepsilon_2-\varepsilon_{mean}$, $\varepsilon_3-\varepsilon_{mean}$ becomes as shown in Fig. 7.

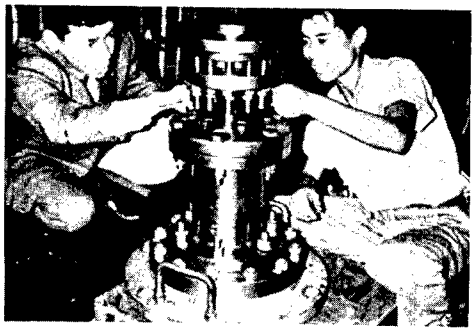

Fig. 6. 50-ton thrust meter

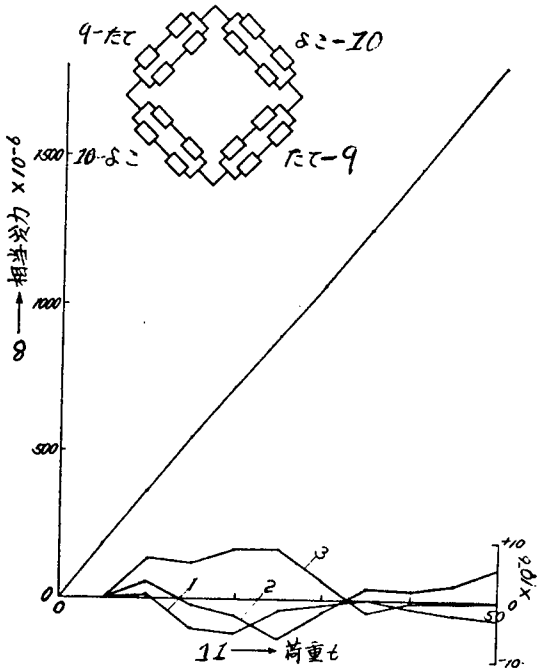

Fig. 7. Static test result of 50-ton thrust meter

8) Relative stress
9) Longitudinal
10) Transverse
11) Load (tons)

4. Thrust Meter Correction

Since a 100-ton capacity oil-pressure-type thrust meter correction system had been made, the thrust-meter-correction was performed under exactly the same conditions of engine test, that is, all strain tubes were fixed at their positions without individual corrections. Corrections were made for every 10 tons of additional load and the outputs recorded by electromagnetic oscilloscope.

And the corrected values of the thrust forces and oscillations of the galvanometer of the electromagnetic oscilloscope were plotted on a graph. In order to get accurate results, a 50-ton loop-type force gauge was connected in parallel with the thrust pick-up (see Fig. 9) and a dynamic strain gauge was set up during the correction test. Fig. 10 shows the correction plots of load and stress.

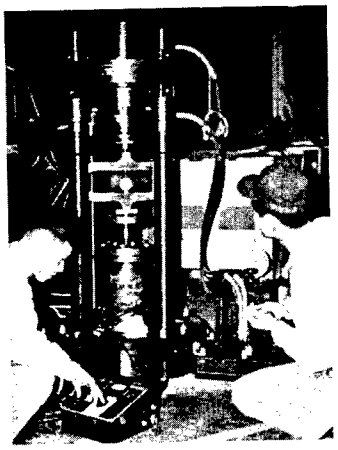

Fig. 8. Thrust-meter correction system

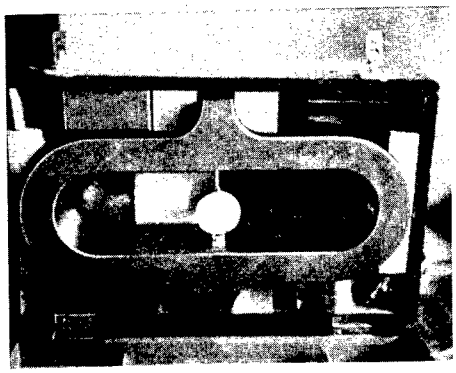

Fig. 9. 50-ton force gauge

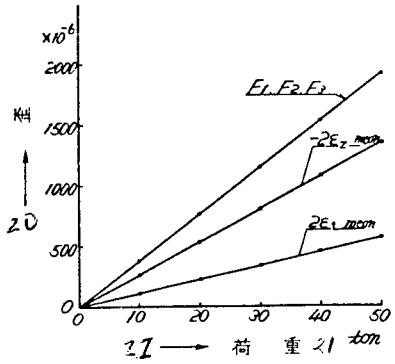

Fig. 10. Experiment results at test site

20) Stress, 21) Load

5. Thrust-Force Measurements and Results

A rubber plate was placed between the thrust meter and the adapter of the rocket engine and was tightened by six emergency bolts and six locating bolts to prevent vibration in the normal direction, as shown in Fig. 11.

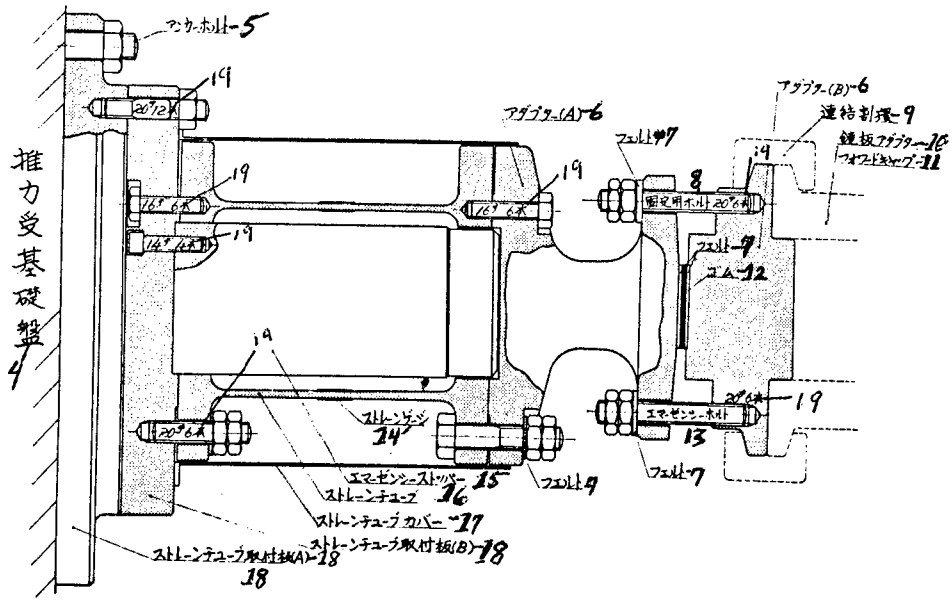

Fig. 11. Connecting the thrust meter

4) Thrust-force base
5) Anchor bolt
6) Adapter
7) Fillet
8) Connecting ring
9) Connecting ring
10) Deflecting plate adapter
11) Forward gap
12) Rubber plate
13) Emergency bolt
14) Strain gauge
15) Emergency stopper
16) Strain tube
17) Strain tube cover
18) Strain tube-receiving plate
19) Number of volts

Figure 12 shows the actual connection of the thrust meter and rocket engine. The combustion test was performed under light rainfall. There was no trouble in combustion and thrust measuring. Correction plots made by the electromagnetic oscilloscope agreed with the corrections of earlier tests with a difference of less than 1.5%. Measured values of each channel showed almost no fluctuation. The ratio of the longitudinal stress ($\varepsilon_{z,\,mean}$) to transverse stress ($\varepsilon_{t,\,mean}$) was known to be 1 : 0.3 as the result of the analysis of the measured values. This means the functioning of the thrust-force pick-up was perfect and therefore the thrust-force determination need not take the steps from measuring ϵ_z and ϵ_t, and then from strain to stress, and from stress to thrust force; but can go directly from the correction plot of the load vs the output of the oscilloscope.

Fig. 12. Connection of thrust-meter to engine

6. Conclusion

We have reported briefly on the thrust-meter development. We express our thanks to the members of Okura Machinery Co., who had to work day and night to manufacture the thrust-force pick-up to meet the combustion test date.

(Received on April 3, 1963)

COMPUTATION OF PERFORMANCE BY USE OF A DIGITAL COMPUTER

By Masaru Watanabe and Michiko Okamoto

1. Introduction

To calculate the trajectory of a rocket by use of a digital computer, the equations of the motion of the rocket should be solved step-by-step with respect to short intervals of time. Hence, the problem is essentially to solve the differential equations and thus there is no particular difficulty in the procedure. In a previous paper, the fundamental programming for the Runge-Kutta integration method was given [1]. However, various techniques should be further studied in order to improve the precision of the solution obtained within a certain time period.

Since last year, a digital computer was available near us and the authors had opportunities to carry out a program of improving the precision of trajectory analysis on computer. The result of this work may contribute a great deal in the computation of rocket performance. In this paper, the progress and improvements made since the last paper is presented.

For reference, the types of computers and their computing time will be given: the computer used for the previous paper was Datatrom B-205 of Aeronautics and Space Technical Research Institute. That computer employed drums for the memory and was somewhat slow in the computation, took approximately one hour even though a floating-point apparatus was used. For this paper, the OKITAC computer was used, which had a magnetic core as memory, and was faster in that the same amount of time was sufficient even without a floating-point apparatus.

2. Interval Control due to Critical Time

In the integration of a motion equation, the problem of determining the size of the time interval (sub-interval of integration) arises. Increasing or decreasing the size of the interval is also called control of interval. In the practical case, the interval changes by doubling (twice) or halving (1/2) the original interval. Therefore, this method is also called the halving-doubling method. It is a necessary technique in order to keep the precision of the solution or the magnitude of the relative error within a certain range of error. For instance, when the velocity of a rocket is low, immediately after the launching, it is necessary to make the time interval small enough so that even a rapid change of the

orientation angle of the rocket could be determined correctly. On the other hand, as the velocity of the rocket increases, the time interval may increase, too. Especially, after combustion, the effect of an error is not very significant and the time interval may be taken as a large value to shorten the computation time. This is called "interval control by an error" or "error control". Error control is actually an optimization of calculation because it is designed to obtain a solution with a desired degree of precision within the shortest possible time. More details on this control are presented in a previous paper.

The above considerations may be taken into account not only for the case of motion of a rocket but also for any general differential equations. However, the rocket requires another particular control especially at the combustion stage. This is given in the following: at the beginning and completion of combustion or when the booster separates, a discontinuance change appears in the thrust, resistance and weight. Suppose no special consideration is made at this instant of discontinuity and only error control is introduced in the computation, it may happen that the instant (point) of discontinuity lies within the sub-interval of the integration and thus the exact change before and after the discontinuity point, such as change in the thrust, can not be computed precisely. At the lower part of Figure 1 is shown the point of combustion which is located within the sub-interval of the integration in the sample computation with the 9L-1 rocket.

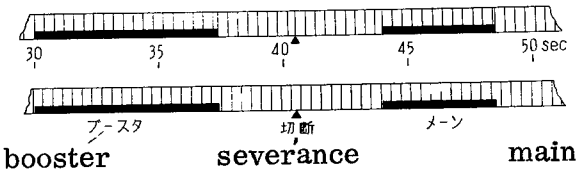

(Upper)—The case with an interval control
(Lower)—The case without an interval control

Fig. 1. The sub-interval of integration and the instant of discontinuity in the thrust schedule

This kind of trouble, i.e., the disagreement between the start of a sub-interval and the discontinuous instant, causes certain errors which will be explained later. To eliminate this type of errors, the sub-interval of the integration should be modified so that the start of a sub-interval coincides with the discontinuous point (Fig. 2). This is called an "interval control due to critical time." In this case, not only the interval of the integration is modified but also the value of some variables should be changed in the integration before and after this discontinuous point. Fig. 3 shows a flow chart summarizing the above principles. The comparison of results with and without interval control is shown in Fig. 4. The largest error is seen at the end period of combustion in the main rocket. At this point, the error in the computation of maximum speed is 0.08 km/s or approximately 3% and the highest altitude 20 km or approximately 6%. This

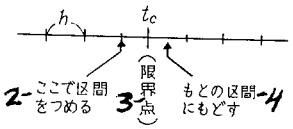

Fig. 2. Change of sub-interval in the interval control (due to critical time)

2) Terminate the interval here; 3) Critical time point; 4) Resume the original interval

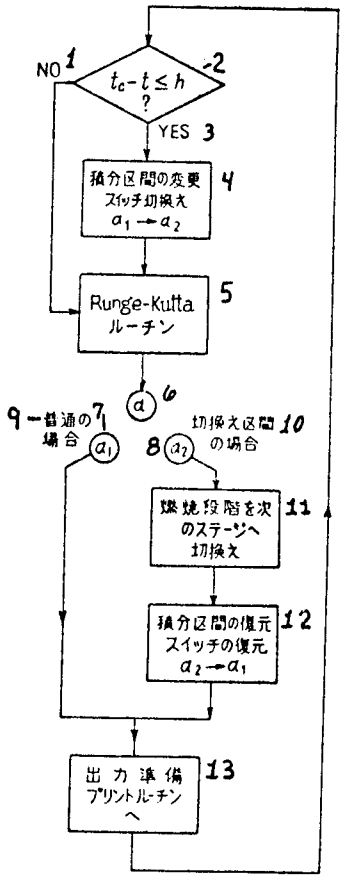

Fig. 3. Flow Chart for Interval Control

1) No
2) $t_c \leq h$
3) Yes
4) Change of sub-interval of integration. Switch change $a_1 - a_2$
5) Runge-Kutta routine
6) a
7) a_1

Coding for Figure 3 continued—

8) a_2
9) Ordinary case
10) Change of sub-interval case
11) Change the combustion steps into next stage
12) Resume the sub-interval. Switch change $a_2 - a_1$
13) Output system to print routine

kind of large error does not always exist. Sometimes, the computation with and without interval control may be in good agreement. In the following a quantitative analysis with respect to the size of error will be discussed. As an example, the time of burning in the main rocket will be considered in a case with a rectangular-type thrust curve, which would show the largest effect.

Let us assume the time of burning, t_c lies in a sub-interval between t_{n-1} and t_n. According to the Runge-Kutta method, the thrust, T in the interval of (t_{n-1}, t_n) can be expressed in the form:

$$\frac{1}{6}\left[T(t_{n-1}) + 4\,T\left(\frac{t_{n-1}+t_n}{2}\right) + T(t_n)\right]$$

Consequently, the effective thrust in this interval is:

$$(1/6)\ \mathrm{T} \text{ if } t_{n-1} \le t_c < \frac{t_{n-1}+t_n}{2}$$

or

$$(5/6)\ \mathrm{T} \text{ if } \frac{t_{n-1}+t_n}{2} \le t_c < t_n$$

This gives the apparent completion time of combustion as (b) or (c) in Figure 5. This disagreement in the computed combustion times causes the error in the computed result of other values. In Figure 6, the amount of disagreement with respect to the position of t_c in the sub-interval is given for a clear demonstration of the error. In the above, only a rectangular-type thrust was considered. However, the interval control can be considered in the case where the value of thrust is actually measured. In this case, the change of the weight is obtained by integrating the equation,

$$\frac{dm}{dt} = -\frac{T}{I_{sp}}$$

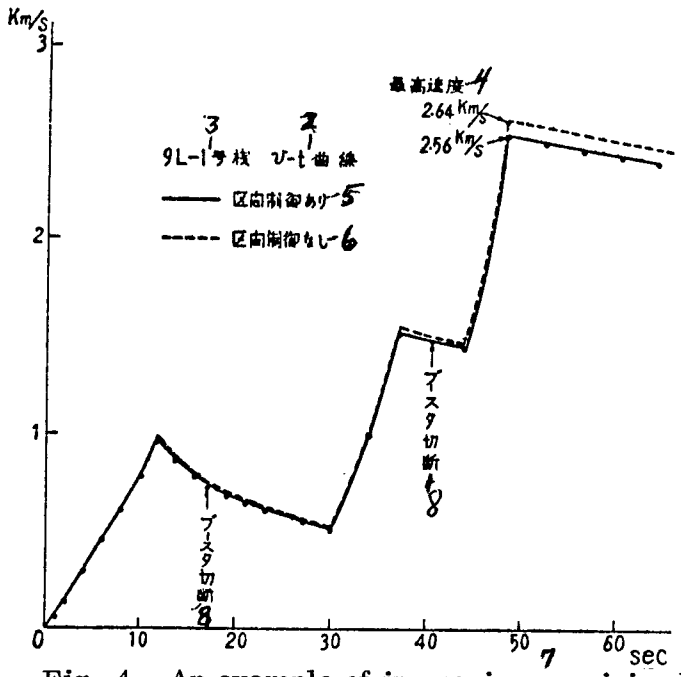

Fig. 4. An example of improving precision by an interval control

1) Velocity
2) v-t curve
3) 9L-1 rocket
4) Maximum velocity
5) With interval control
6) Without interval control
7) Time
8) Booster severance

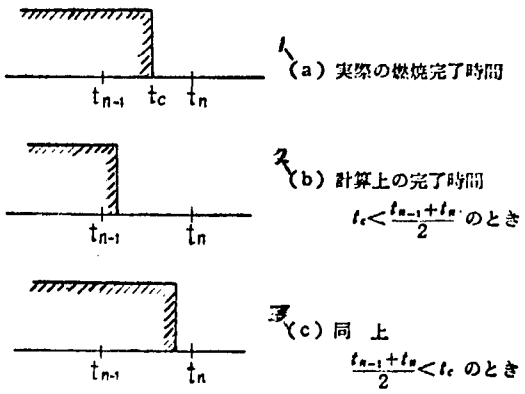

Fig. 5. The apparent completion time of combustion in the case without interval control

1) (a) The actual completion time of combustion
2) (b) The calculated completion time of combustion
$t_c < t_{n-1}+t_n/2$
3) (c) The calculated completion time of combustion
$t_{n-1}+t_n/2 < t_c$

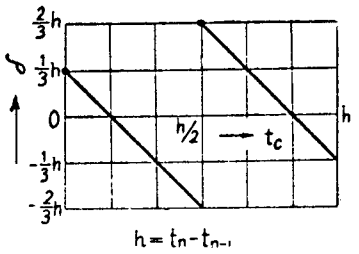

δ = The error in the combustion time (Prolongation is signed positive)

Fig. 6. The error between the apparent completion time of combustion in the case without interval control and the actual completion time

where T = Thrust
I_{sp} = Specific impulse.

Also, the change of weight at the moment of separation of the booster should be considered in the interval control.

A general method used in conjunction with interval control at the discontinuity point or any build-up point in the solution of differential equation is given by Lesh of Jet Propulsion Laboratory, California Institute of Technology in his paper [3] together with a program for an IBM 704 digital computer. He called this scheme an "Automatic Interruption." In contrast to his method, the method by the authors provide:

(1) dynamic change of sub-interval according to the combustion time determined by the thrust schedule, and

(2) utilization of both error control and interval control.

Also, the program by the authors is simpler than that of Lesh and can be used in a smaller sized computer.

3. Normalization of Thrust

The computations with the assumption of rectangular-type thrust is simple and rapid but it gives an uncertain value for the time of burn-out. Therefore, this method cannot be used in the calculations (Fig. 7). It is well known that the specific impulse, I_{sp} is a characteristic value for a propellant and is

calculated by dividing the total impulse (obtained by integration of curve such as in Fig. 7) by the weight of the fuel. Sometimes, however, the computed I_{sp} is

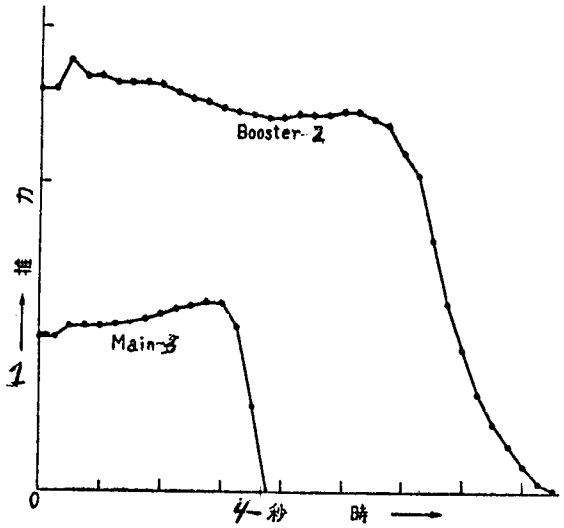

Fig. 7. Thrust Curve (measured) of 9M-1

1) Thrust
2) Booster
3) Main
4) Time

somewhat different from the actual value of that particular propellant due to some kind of error introduced in the thrust curve and it is necessary to correct this thrust before further computations are carried out. This process is called "Normalization of thrust". The authors fed the original thrust data to the computer and then integrated by a trapezoidal rule, i.e.,

$$\left\{\frac{1}{2}T(t_0)+T(t_1)+T(t_2)+\cdots\cdots+T(t_{n-1})+\frac{1}{2}T(t_n)\right\}\times h$$

where T = thrust, t_0, t_1, . . . t_n = coordinate points with sub-interval size h.

By dividing the result by the weight of fuel, a crude value of I_{sp} is obtained.

Finally, by multiplying the original thrust data by a certain ratio to make the computed I_{sp}, a new set of thrust data is obtained.

This new set of data is fed into the computer for further computation. In Fig. 8, the result of computations with the original thrust data and the normalized thrust data are compared. At the maximum velocity, approximately 10% error is seen which indicates the need for normalizing.

4. Checking the Solution from an Analog Computer

The solution by use of an analog computer has certain advantages such as

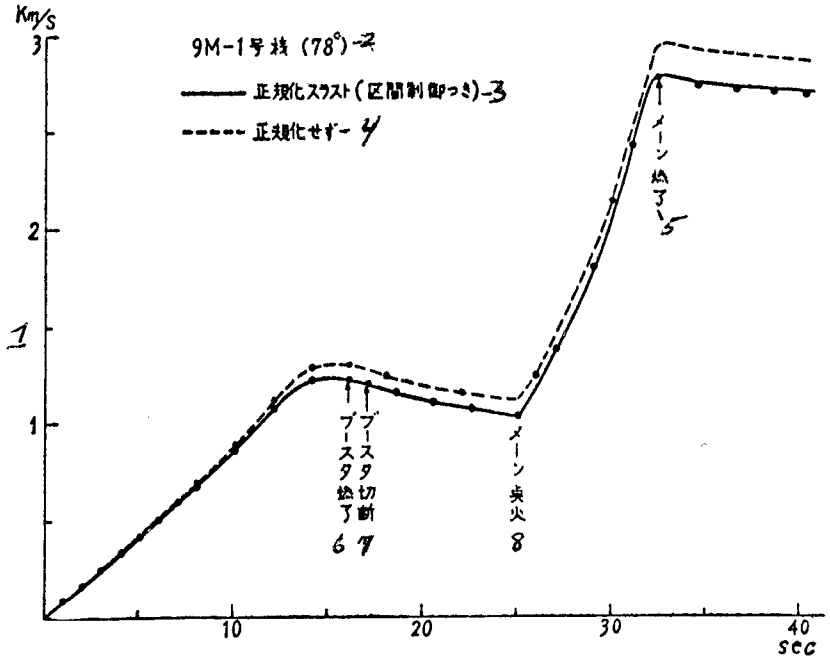

Fig. 8. The effect of normalizing thrust

(1) Velocity
(2) 9M-1 rocket (78°)
(3) Normalized thrust (interval control)
(4) No normalization
(5) Completion of combustion in main rocket
(6) Booster burn-out
(7) Booster separation
(8) Ignition in main rocket

rapid calculation and easy understanding of the results because the trajectory is shown as a graphical figure. However, there exists some inherent errors in the computer and it is not possible to obtain the high precision desired. Therefore, we may solve the same equation by use of a digital computer and determine the precision of the analog computer by checking the results from the two computers. Two cases may be considered in checking the accuracy. One is the case with the inherent error due to the precision of the computer itself, and the other, with the errors due to the simplification of the equations because of the limit of the machine as well as using non-rigorous (or simplified) data. These errors are determined independently. First, the same equation as well as the same data used in the analog computer are used in the digital computer so that the inherent error in the analog machine is determined by comparing the two results. This solution may contribute as an index in the improvement of the precision of the analog computer. Next, the error due to the simplification of the equation or due to insufficient data will be determined. Since this is a purely mathematical problem, it can be done by the method of simulation on a digital computer. The exact solution, by using the rigorous equation and the exact data, is obtained as in the first case. Then, by introducing simplified equations or insufficient data

one by one, the solution is obtained and compared with the exact solution to determine the errors.

The simplified equation used in the analog computer assumes:

(1) there is no variation in the gravity with respect to the altitude and the averaged value over the total flight range may be used as the acceleration of gravity for the whole course. The assumptions due to insufficient data are as follows:

(2) The density of air above 25 km is negligible

(3) The residence coefficient is calculated from the formula, $C_D \times M^2$ (M: mach number). This makes a difference in the computing operation rather than in the numerical values of data. However, this number and the air density of (2) are related through the function generators of the analog computer, and their delicate variations cause certain errors in the result.

(4) Beside these, it was found that the speed of sound used in the computation of mach number was 340 m/s for the analog computer and 310 m/s for the digital computer by an accident. It can be corrected since it is merely a difference in the data but, as shown later, this fact caused the largest error. The respective solution with each of the (1) - (4) assumptions is marked as G, Z, C, and S. The comparison between these solutions and the exact solution E is shown in Figure 9. In this figure, only the part of the velocity curve near the completion time of combustion is shown to give a clear indication of the errors. The result may be summarized as below:

G: The effect of the gravity is the least. That is, it is necessary to consider the variation of gravity along the altitude but the averaged value may be used without too much danger. Of course, this can be said only for rockets reaching altitudes close to this sample run.

C: Next, the difference in the resistance coefficient owing to the function generator is not significant.

Z: The error arising from the assumption that the density of air above 25 km is negligible is considerably large.

S: The largest error is due to the different values taken for the speed of sound.

5. The Effect of the Change in Speed of Sound Due to the Altitude

Since it is realized that a change in the value of the speed of sound causes a large effect on the computed result, it becomes necessary to consider the

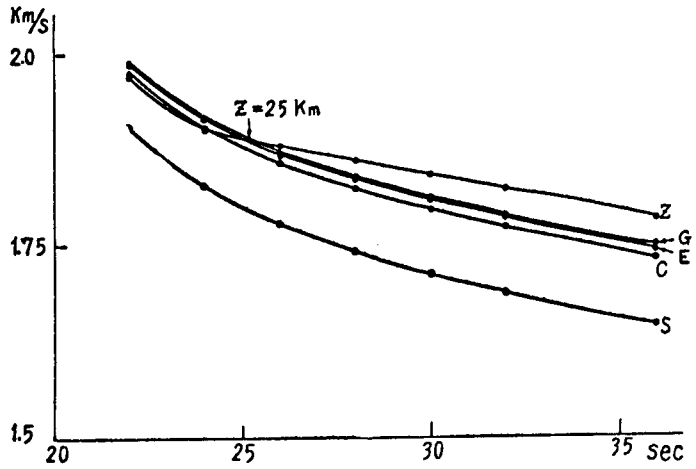

		Zmax (km)	ΔZmax
E:	Exact solution	193	
G:	Only gravity is changed	191.5	-1.5
Z:	Air density is changed	200	7
C:	Resistance coefficient changed	191	-2
S:	Sound speed (and resistance coefficient) are changed	174	-19

Fig. 9. Analysis of causes of error-enlargement of velocity curve near burn-out

change of the speed of sound along the altitude axis in the computation. In Fig. 10, the change of the speed of sound with altitude is presented. It is cited from the material [4] published by the preparatory group of the COSPAR International Reference Atmosphere (CIRA) according to the most recently observed data. Using these data, we made a sample calculation involving the L-2 rocket whose highest altitude was 450 km and the altitude at the time of burn-out was 52 km. We used the resistance coefficients calculated from the corresponding exact mach number along the altitude. The result, then, was compared with that calculated by using the averaged sound speed of 310 m/s over the total range of altitude.

Surprisingly, the two results were almost identical. This may indicate that the averaged sound speed can be taken over the total range without too much error.

Acknowledgements:

The authors would like to express their gratitude to Professor Nomura and Assistant Professor Akiba for their suggestions. Also, the authors are in debt to

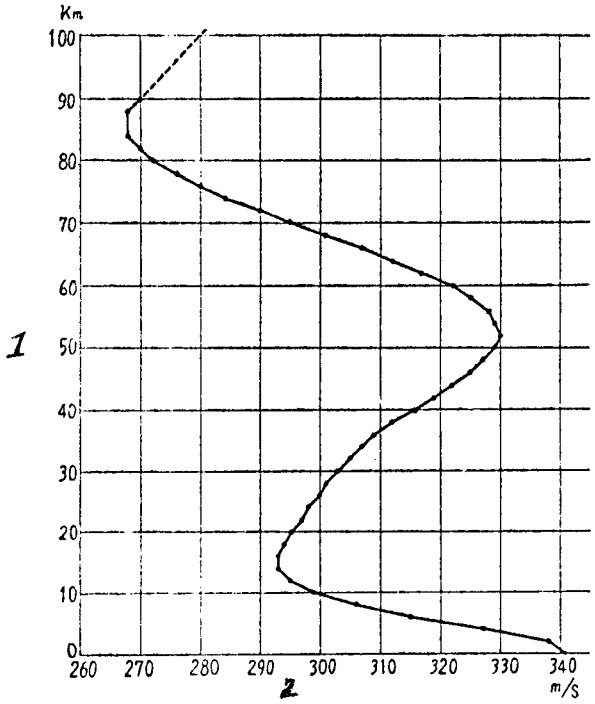

Fig. 10. Change of sound speed along the altitude (CIRA)

1) Altitude; 2) Speed of sound m/s

Yasuo Suzuki, Akihite Kitasaka and Chieko Matsuoka for their help in the arrangement of the material and operation of the computers.

(Received on April 27, 1963)

REFERENCES

1. Watanabe, Higuchi and Togawa: Industrial Research 13, 10, 1961; p. 57-61 (Japan).

2. Akiba, Hirazowa and Kitasaka: Industrial Research 15, 7, 1963 (Japan).

3. F. Lesh: JP DEQ (Differential Equations Solver) 1959, Jet Propulsion Laboratory, California Institute of Technology.

4. H. Kallmann-Biji, R.L.F. Boyd, H. Lagow, S.M. Poloskov and W. Priester: CIRA (COSPAR International Reference Atmosphere) 1961, North-Holland, Amsterdam.

5. Nomura: Performance Computation by use of an Analogue Computer.

TELETRANSMITTER

By Katsuhiko Ohi, Masoich Hakui, and Mitsuo Kazitani

1. Introduction

When the K-6-1 space rocket was launched March 1958, a K-6 type transmitter was carried. The K-6 type transmitter was developed by modifying the conventional K-4B type transmitter. The details of the K-6 type transmitter were reported on in Production Research Vol. 11 No. 8. It was used several times for measuring and observing upper atmospheric phenomena. Through those experiments, we tried to prevent troubles due to the low atmospheric pressure at the very high altitude, the high temperature of the rocket body, and also the evaporation of the battery solution and decrease of the stability of the unit. In the meantime, the K-8 type rocket became one of most effective space research rockets. The rocket could reach a very high altitude and could carry a big payload. With these improvements in a space rocket, a four-channel teletransmitter was definitely required. Having advantages in operation and production, a RK-9/T was used for the actual experiment. In this equipment, four units of subcarrier are plugged in: the shape of the equipment is rectangular. Because of the functional and geometric properties, all components can be effectively arranged within a small volume, which, in turn, ensures an easy way to get an airtight seal.

Along with the increase in space rocket size, the conventional method of direct control of the electrical power supply caused a great deal of difficulty and danger, so that many remote control methods were studied; and finally, a lagging relay method was adopted.

2. Improvement of the K-6 Type Transmitter

The K-6 type transmitter, which was developed to be used for the Kappa series space rocket, was able to get its weight cut down by using highly reliable transistors.

The first time, we transistorized the oscillator of the subcarrier transmitter, improved the shielding and heat insulation of the case, and replaced the on-off switch of the power supply by a remote control lagging relay. This was used in a K-8L No. 1 space rocket.

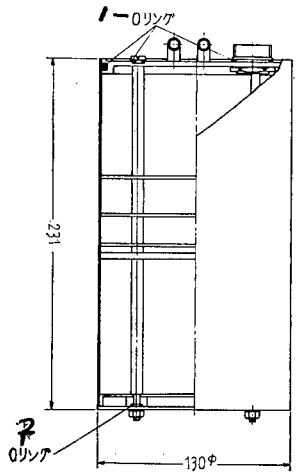

Fig. 1. The improved K-6 transmitter

1) O-ring, 2) O-ring

(1) Airtight and heat insulating enclosure.

In order to achieve a simpler airtight enclosure than the conventional one, we arranged all connectors in one panel and using O-rings, they were made airtight; and thus, a totally airtight enclosure was designed. To eliminate any possible effect on the transmitter of the high temperature of the surroundings, several methods were tried with satisfactory results: for instance, we used a multilayer board of copper and paper, and asbestos board was used to insulate from the heat. However, in both cases, many difficulties in manufacture were involved so that finally we reached the conclusion that it would be better to decrease the thickness by 10 φ and get the same insulation effect from the air layer: also, a heat reflection effect was hopefully expected by using a baffled enclosure surface.

(2) The remote control switch.

The primary requirements for a remote control switch are simplicity, accuracy and endurance for various environmental conditions. Examining carefully many experiments, we found that a sigma-lagging relay showed very satisfactory results. The important features of the relay are as follows:

Circuit: transfer 2 circuits
Capacitance of connecting point: 2A 28 VDC/120 VAC
Resistance of winding: 3,100 Ω
Operating voltage: 24-28 VDC
Operating time: 2-20 ms
Size and weight: 0.8 x 0.9 x 0.4 in. 18 gm

3. RK-9/T Type Transmitter

Through increasing the maximum altitude of a rocket, many kinds of observation were made possible by (a) single space rocket and in turn, this required many channels in a transmitter. The RK-9/T type transmitter was designed to carry 10 channels to meet the basic requirements of the Kappa-8 type space rocket. The central peak frequency of the transmitter is 960 c/s-14.5 kc which is an assigned frequency by IRIG and has a frequency deviation from the central peak of ±7.5% and a response of 14 c/s-220 c/s. The main carrier frequency is 225 Mc/s, its deviation is ±100 kc/s and total output power is about 0.5 w.

(1) Structure.

The oscillator of the subcarrier is transistorized and each channel is a completely independent unit and all channels are plug-in type modules. With such advantages it is very easy to check and adjust the units. Fig. 3 shows a unit of the subcarrier oscillator, and the completely assembled whole unit is shown in Fig. 4.

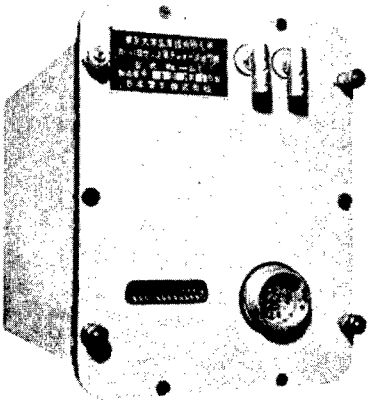

Fig. 2. RK-9/T type transmitter

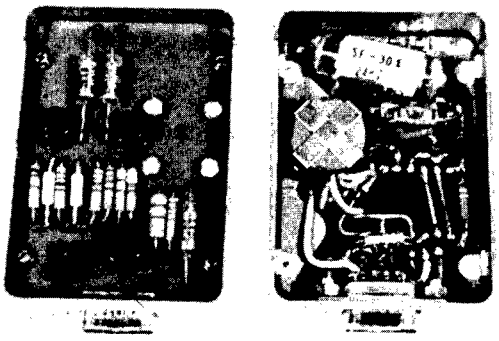

Fig. 3. Subcarrier oscillator unit

(2) Characteristics.

Difficult problems such as cross-talk and SN (signal-noise) ratio came about when we increased the number of channels. We could overcome the cross-talk problem by putting a band-pass filter circuit in front of the output terminal.

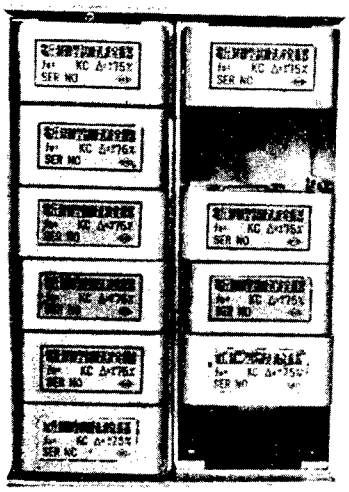

Fig. 4. An arrangement of sub-carrier oscillator units

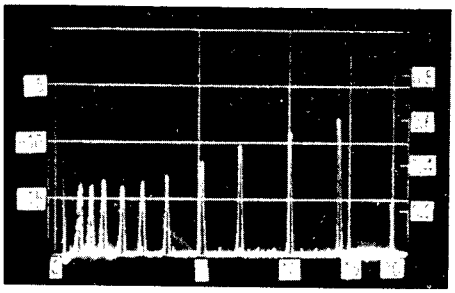

Fig. 5. The pre-emphasis characteristics

And by changing the circuit such that the unit had a 6 dB/oct of pre-emphasis from 8 kc/s on, we could improve the SN ratio to a satisfactory level.

4. The Crystal Control Type Transmitter for the L-2 Space Rocket.

As the space rockets reached higher altitudes and soared for longer times, we had to improve the S/N ratio of the radio receiver by narrowing the signal band. Thus, the conventional transmitter had to face up to practical problems. To overcome the problems, we built a crystal-control-type transmitter to be used in the L-2 space rocket.

(1) Characteristics and circuit.

Significant features are as follows:

Modulation method: FM-FM

Main-carrier section

Frequency: 298.1 Mc
Frequency deviation: $\pm 5 \times 10^{-5}$
Maximum deviation: about ± 100 kc
Output power: about 1.5 w
Type of output: 50Ω coaxial (equilibrium)

Subcarrier section

Number of channels: 10
Type of input: voltage control type

Input impedance: more than 250 Ω
Central peak frequencies: 0.96, 1.3, 1.7, 2.3, 3.0, 3.9, 5.4, 7.35, 10.5, and 14.5 kc
Linearity in modulation: less than ± 2.5%
Maximum deviation: ± 7.5% of central peak frequency
Maximum regulating time: more than 30 minutes
Environmental conditions

Temperature: 0 - 40°C (for more than 30 minutes) and 150°C (500 seconds)
Shock along body axis: 40 g (more than 5 ms)
Vibration along body axis: 5 - 35 c/s 1 mm 35 - 2000 c/s 5 g
Acceleration along body axis: + 40 g - 10 g
Pressure: 1 mm Hg for 3 minutes

The output of the ten-channel subcarrier oscillator is the same type as the conventional one. Its circuit is shown by Fig. 6.

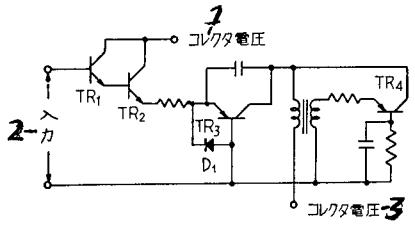

Fig. 6. The circuit diagram of the subcarrier oscillator

1) Collector voltage, 2) Input, 3) Collector voltage

In the circuit, TR_1 and TR_2 are connected by the Darlinton (sic) connection method, and this section acts as input circuit. Its impedance is big enough to neglect any change in impedance due to temperature change, and generally its value is about 1 M Ω. Base bias circuit of modulation transistor TR_3 is coupled with a thermostat and a variable resistor. By adjusting the bias voltage according to the temperature change, we could improve the temperature characteristics of the resonant frequency. Fig. 7 shows an example of our experimental data on the characteristics of modulation and temperature. The modulation sensitivity seems to change with this temperature correction method. And also, the thermostat does not function linearly over a large temperature range. Therefore, it is impossible to use this correction method over a wide temperature range, but it is reasonably easy to correct for the temperature effects sufficient for our purpose where the temperature varies from 0 to 40°C.

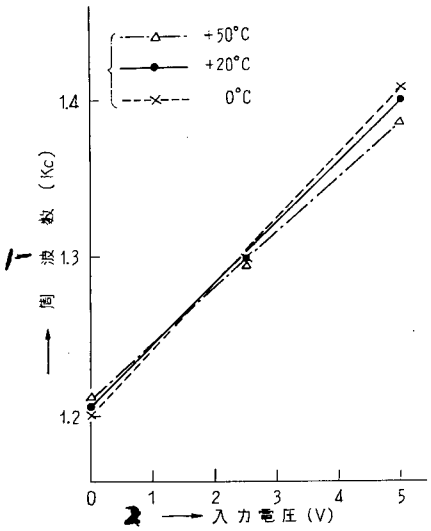

Fig. 7. An example of characteristics of modulation and temperature of a subcarrier oscillator

1) Frequency, 2) Input voltage

The principle carrier has the system shown in Fig. 8. It employs a bridge-type phase modulation method using a two terminal tube. The total amplification factor is 108 times the original signal. Because of the airtight case, air circulation is impossible; therefore, a somewhat high temperature of the modulation circuit due to the vacuum tube is unavoidable. However, through our experience, it turned out that the heat is not any trouble in practical use.

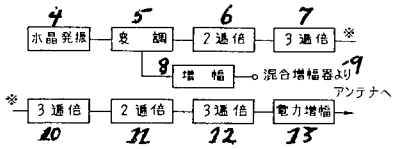

Fig. 8. A system diagram of a principle-carrier section

4) Crystal oscillation
5) Modulation
6) Multiplied by 2
7) Multiplied by 3
8) Amplification
9) From mixing amplifier to antenna
10) Multiplied by 3
11) Multiplied by 2
12) Multiplied by 3
13) Power amplification

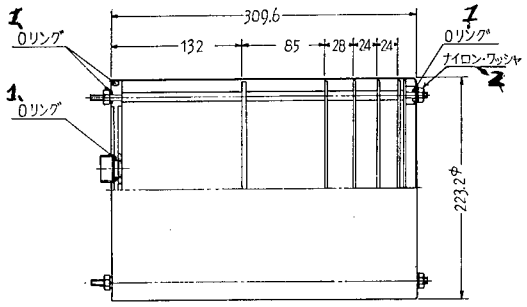

Fig. 9. Structure of transmitter

(1) O-ring, (2) Nylon washer

The shape and structure of the unit is like the one shown in Fig. 9. Special attention was paid to airtightness and strength. To obtain good airtightness, we used O-rings and nylon washers. All panel connectors are hermetically sealed. And the unit was a very satisfactory one. The internal structure consists of two units each of which are the power section and principle-carrier section: ten-channel subcarrier oscillator, and mixing amplifier. The ten-channel subcarrier oscillator and mixing amplifier are built on three circular disks of printed circuitry, and the three printed circuits are stacked one over one. Connectors are used as far as possible to connect power source and signals. Since the over-all shape is cylindrical, there are many open spaces due to the various shapes of components and arrangements; and sometimes it is difficult to check the operation of each part. With respect to this point, there are several problems left for the future. We hope that through practical experiences we shall be able to obtain electrically and mechanically much more satisfactory equipment.

5. Conclusion

With many improvements, the K-6 type transmitter became an almost complete piece of equipment. The RK-9/T type transmitter, however, should be carefully studied for use in a K-8 type space rocket. And further work should be done on the equipment to fit other standard space rockets. We should keep close cooperation with people working on other parts of the payload in order to have room for the crystal control transmitter in the L-2 and L-3 space rockets.

We express our sincere thanks to Professor Takagi and Nomura of Production Research of Tokyo University. We are also grateful to Mr. Tanaka and others for their great help.

(Received on April 15, 1963)

HIGH-RESPONSE RADIO RECEIVER (PART 2)

By Kenich Takahashi

1. Introduction

As a result of the increased distance between ground tracking stations, a very sensitive, high-response telemetry radio receiver was urgently needed. With such a need, we built a high response radio receiver and got satisfactory results in an experiment involving a rocket flight in March 1961. This receiver had the following six sections: (1) a coaxial pre-amplifier of 225 Mc/s; (2) frequency converter; (3) middle frequency amplifier and FM feedback phase detector; (4) video amplifier; (5) indication dial panel; and (6) constant voltage power source.

Detailed discussion of this equipment was reported in Vol. 13, No. 10 of this issue (production research). We shall discuss in this report the significant characteristics of this equipment such as the noise factor and limits on improvement.

2. Coaxial Type Pre-Amplifier

In order to obtain low noise from the vacuum tube amplifier, we built a coaxial input and an output resonant circuit. And we particularly used the low-noise ceramic vacuum tube GL-6299.

The design specifications are as follows:

Resonant frequency range: 220 - 230 Mc/s
Band width: More than 2 Mc/s
Gain: More than 14 db
Noise factor: 5 db (our final aim)
Input impedance (Z_i): 50 Ω

Output impedance (Z_0): 50 Ω

Vacuum tube: GL-6299

$g_m = 12$ m℧
$r_p = 9.6$ kΩ
$\mu = 115$
C_p in $= 1.7$ PF
C_k in $= 4$ PF

Figure 1 is an equivalent circuit of the amplifier. Based on this equivalent circuit, the following theoretical values are calculated, where the resonant frequency is fixed at 225 Mc/s

Z_{01}: 50 Ω

Z_{02}: 75 Ω

Anode resistance (R_0): 9.5 k Ω

Length of coaxial anode (l_1): 30 cm

Output loop area (A): 2.6 cm^2
(Electric angle of center of loop is 10°)
Resistance applied to cathode input (R_k in): 152 Ω

Admittance applied to cathode input (Y_k in): 1/152 + j 1/202 x S'

(S' = 1.5, correction factor due to C_s)

Length of coaxial cathode (l_2): 14.9 cm

Length of coaxial to obtain equilibrium (l_3): 13.7 cm

Correction capacitance: (C_s): 0 ~ 4 μf

Amplification gain (at equilibrium): about 15 db
Noise factor (at equilibrium): about 3.4 db

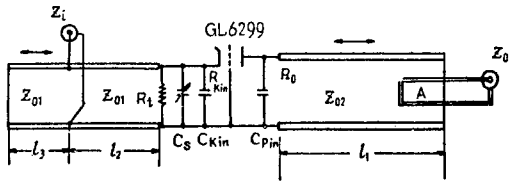

Fig. 1

Based on these theoretical data, the actual amplifier was designed with the size and structure shown in Fig. 2.

Testing the amplifier, we obtained the following experimental data:

Resonant frequency: 225 Mc/s
Frequency adjusting range: 220 - 230 Mc/s (including 2nd stage amplifier)

Output loop: 0.8 cm x 2.5 cm
Gain: about 18 db (power ratio)
Band width: about 2 Mc/s
Noise factor: 4.8 db - 5.0 db

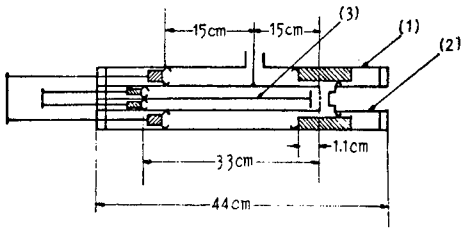

(1) 60.5φ/57.5φ (2) 25φ/21φ (3) 6φ/4φ

Fig. 2

For the 2nd stage of the coaxial amplifier, a one-stage 225 Mc/s frequency converter and 30 Mc middle wave amplifier are connected in parallel. The overall noise factor of the 2nd stage amplifier is about 8 db.

3. Limitation of the FM Negative Feedback Phase Detecting Section

Previously, we reported on the problem of constructing an FM high-response radio receiver. Later on, we studied the signal-noise ratio for an FM output and its limits for improvement. We shall briefly discuss these problems.

There are many approaches to the FM sideband. We shall, however, discuss only the maximum frequency deviation and the first sideband. In this case, the receiving signal band width B_i is:

$$B_i = 2(\Delta F + f_h) = 2(m_f + 1) f_h \tag{1}$$

m_f = modulation factor = $\Delta F / f_h$

ΔF = maximum frequency discrepancy
f_h = maximum modulation frequency

The SN ratio of the input for the phase detection section at the limiting point for improvement is:

$$\left[\frac{S_i}{N_i}\right]_T = 0.86 \frac{\sqrt{m_f}}{m_f + 1} |\eta(t)|^2 \tag{2}$$

$\eta(t)$ is the instantaneous amplitude of the noise which can be calculated based on the effective value.

Generally, the decreasing ratio (A_T) of the limit of improvement in FM modulation is given by

$$A_T = 9.3\frac{m_f+1}{\sqrt{m_f}} \cdot |\eta(t)|^2 \tag{3}$$

When the SN ratio of the input is larger than the level of the limit of improvement, the SN ratio of the output is

$$\left[\frac{S_0}{N_0}\right] = 3\, m_f^2 (m_f+1)\left[\frac{Si}{N_i}\right] \tag{4}$$

If the SN ratio of the input decreases, then it may happen that synchronization can disappear at the noise peak point. In this case, let (1 - r) be the probability that the amplitude of the noise is within the noise level. Then,

$$(1-r) = \frac{2}{\pi}\int^{\eta(t)\sqrt{2}} e^{-x^2}dx \tag{5}$$

In other words, if synchronization disappears at an amplitude greater than $|\eta(t)|$ times the effective value of the noise, then the probability of synchronization disappearing becomes r.

Now we assume that at a certain point of output pulse, the synchronization has disappeared; then at that portion there is neither the output signal component S_0 nor the usual output noise component N_0. And a totally different noise N_x is assumed to appear. In this case, the SN ratio is

$$\left[\frac{S_0}{N_0}\right]_r = \frac{S_0(1-r)^2}{N_0(1-r)^2 + N_x r^2} = \frac{S_0}{N_0 + N_x r^2/(1-r)^2} \tag{6}$$

where N_x takes following value

$$N_X = \frac{S_0}{8\sin^2\left(\frac{\pi}{2}\cdot\frac{D_s}{D_M}\right)} \tag{7}$$

where D_s is the frequency displacement for the usual output signal S_0, and D_m is the frequency displacement within the synchronization limit when noise does not exist.

Substituting equations (4), (5), and (7) into equation (6) we can calculate the SN ratio of output.

An an example, let us assume that D_m = 400 kc, D_s = 100 kc, mf = 3.3; then for a certain fixed value of $|\eta(t)|$ we can calculate the SN ratio of input and output from equations (2) and (6), respectively. From this fact we get a certain relation between the SN ratios of input and output. An example is shown in Fig. 3. From this curve we determine the limit of improvement.

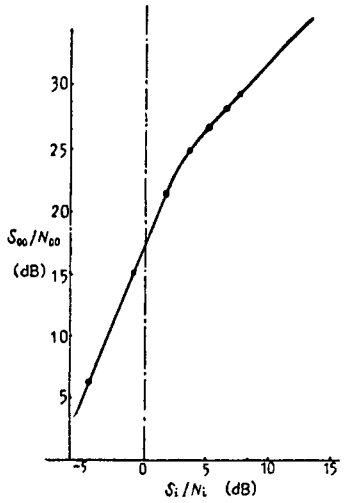

Fig. 3

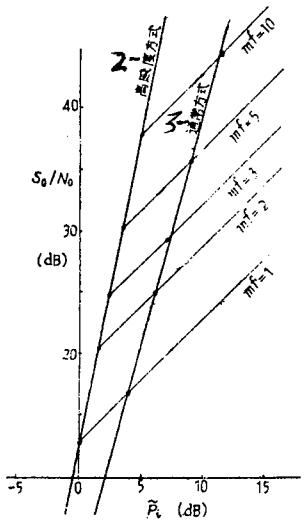

Fig. 4

2) High-response method; 3) Ordinary method

Now, we discuss the decrease of the limit of improvement by varying the parameter m_f for FM and ordinary modulation methods. For these two methods, we calculate the SN ratios of outputs from Eq. 4, the SN ratios at the limiting point of improvement for inputs from Eq. (2), and the decreasing rates of the limit of improvement from Eq. (3). Tracing limiting points of improvement, we get curves of limits of improvement like those shown in Fig. 4.

Where $\tilde{P}_i$ is the relative value of the input normalized with the input at the limiting point of improvement for $m_f = 1$. From this curve, we can see the limit of improvement and its rate of decrease as a function of m_f.

Finally, the author expersses his great thanks to professors Tokagi, Saido, and Nomura for their great help in developing this radio receiver.

(Received on November 4, 1963)

DEMODULATOR-RECORDER SYSTEM

By Katsuhiko Ohi and Shisato Torii

1. Introduction

The IIS-TM-3 radio receiver has been in use since the Kappa-3 rocket experiments and was described in Production Research Reports, Vol. 9, No. 11. The sensitivity of the receiver has since been improved. Development of a system with special demodulation recording equipment was begun in 1961 and is now in the final stages. The present report deals mainly with the demodulator and the tape recorder of the system.

A conventional demodulator employs a voltage-division frequency discriminator. In the discussed equipment, however, we employed a pulse-delay type frequency discriminator and the tape recorder response was improved to record a 14.5 kc subcarrier.

We intend to increase the recording frequency response and report on this in detail after completing the system.

2. Demodulator

(1) Block Diagram. A 15-channel demodulator unit with frequency range of 400 cycles to 30 kc (assigned by IRIG) is planned. It is expected that we could have a maximum 450 cps signal with DC source. The signal frequency depends largely on the center frequency; the higher the center frequency we use, the higher the signal frequency we can obtain. The telemeter-demodulator system now in use contains 15 demodulators, each functioning as a frequency filter with a specified passband. These frequency filters separate the subcarrier signals according to frequency. As seen in Fig. 1, the demodulator consists of an amplifier, peak limiter, Schmitt circuit, phantastron and square-wave shaper.

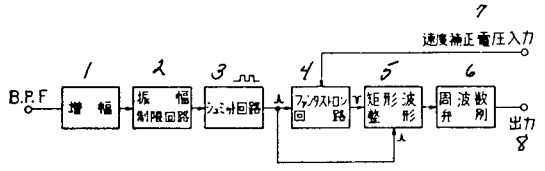

Fig. 1. Block diagram of demodulator

1) Amplifier; 2) Peak limiter; 3) Schmitt circuit; 4) Phantastron; 5) Square-wave shaper; 6) Frequency discriminator; 7) Rate correction input voltage; 8) Output

The operational details are as follows. The discriminated signal from the filter is fed to an amplifier with 40 db gain and then to a peak limiter. After limiting to a certain fixed amplitude the signal is stabilized in the Schmitt circuit. Thus, with a sine-wave input at the peak limiter, bidirectional limiting yields a nearly square-wave output which is further squared by the Schmitt circuit. The latter circuit is so designed that the threshold can be set for a specified input signal level below which the circuit has a squelching characteristic. The output of the Schmitt circuit is differentiated into positive and negative pulses. Only the negative pulse is passed by the phantastron circuit to the square-wave shaper. Thus, the phantastron and square-wave shaper are triggered by a pulse of the same frequency as the signal. The square-wave shaper is used to shape and amplify the square wave. This unit is switched on by a trigger pulse and off by a hold pulse applied to the phantastron. The phantastron is used to obtain a constant amplitude pulse. Only the negative pulse, with a certain delay (achieved by control of the pulse rise time) is obtained. The rectangular pulse output from the square-wave shaper is applied to a Zener diode limiter and finally to a low-pass filter from which we obtain a signal of desired frequency.

If the signal frequency is exactly the same as the center frequency and pulse width is so regulated that a square pulse is obtained, then the output becomes zero at the center frequency and by changing the frequency by $\pm 7.5\%$, we obtain $\pm$ output voltages. The major specifications of the demodulator are as follows:

Output voltage:	± 1 v for $\pm 7.5\%$ change in frequency
Linearity:	Less than 1% for $\pm 8\%$ change in frequency
Output change due to input change:	Less than 0.2% of maximum output for input change of 50 mv to 1 v
Stability of output:	Warm-up after 45 min., less than 0.5% drift for 45 min
Output impedance:	Less than 1.5 kilohms

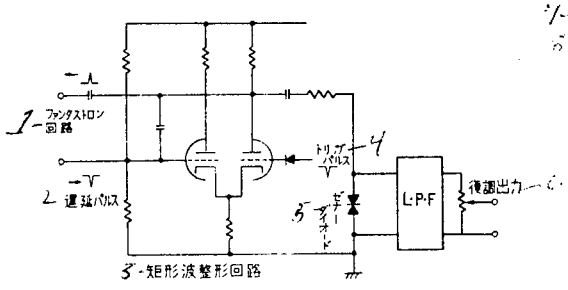

Fig. 2

1) Phantastron circuit; 2) Delay pulse; 3) Square-wave shaper; 4) Trigger pulse; 5) Zenar diode; 6) Demodulator output; 7) Demodulator output $E = kE_pfT$; 8) Where: E_p = Pulse amplitude; T = Phantastron pulse width; K = Proportionality constant; f = Signal frequency

(2) Physical Layout. As seen in Fig. 3, all the demodulator components are installed in a rack 2 m high. Operation is achieved from control panel switches. Each demodulator section contains two channels, one on the right and one on the left.

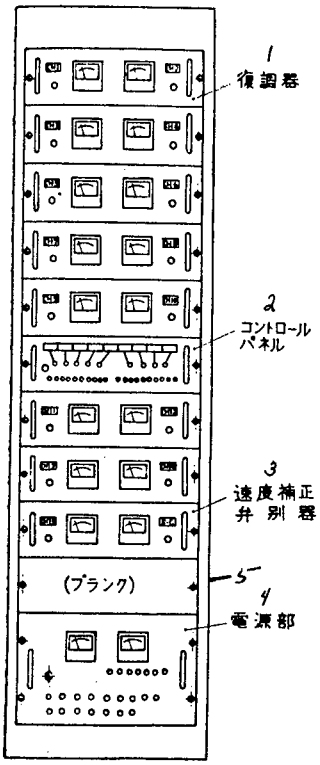

Fig. 3. Demodulator rack.

1) Demodulator; 2) Control panel; 3) Rate corrector; 4) Power supply; 5) Spare

Receiving, recording, and playback are easily controlled from the control panel switches. The signal separated through the band-pass filter is easily externally controlled from the control panel switches. The demodulator output is connected to the recorder by patch plug.

3. Tape Recorder

A tape recorder is added to record the mixed signal which enters the demodulator. This is done mainly to prevent any loss of data and also for data storage.

(1) Performance. The operating specifications are as follows:

Recording method:	AC-bias direct recording
Tape width:	1/4 inch
Speeds:	7-1/2, 15, 30 ips
Number of tracks:	Recording and playback each 2 tracks
Wow and flutter:	Less than 0.13%
S/N ratio:	More than 40 db for input 0 vu (1 v rms)
Separation of track:	46 db (at 1 kc, 0 vu)
Input impedance:	50 kΩ
Output impedance and level:	100 Ω, + 12 db (3 v rms)
Frequency response:	200 cps to 50 kc ± 3 db at 30 ips 200 cps to 30 kc ± 3 db at 15 ips 200 cps to 15 kc ± 3 db at 7-1/2 ips

In order to minimize wow and flutter, a crystal oscillator is used for supply voltage control. After stepping down the supply voltage at the crystal oscillator, it is applied to a power amplifier to drive the capstan motor. Maximum wow and flutter of 0.13% are obtained at 7-1/2 ips; however, this value decreases as tape speed increases and is 0.06% at 30 ips.

The frequency response drops out below 200 cps and is very flat over the higher frequencies because the low-frequency region is not used.

(2) Physical Layout. The monitor amplifier, tape deck, recording and playback amplifiers, and power supply are installed in a rack 2 m high. The monitor amplifier (with external speaker) permits monitoring of the signal being recorded or played back. Microphone input permits voice recording. The signal input and output terminals are mounted on the front and back sides of the panel. The rear terminal connections can be switched from the front. The capstan motor rotates as long as the main power is on, thus reducing the time needed to obtain uniform rotation after operation has started. This unit can accommodate 10" and 7.5" reels. Figure 4 shows the arrangement of the various units of the tape recorder.

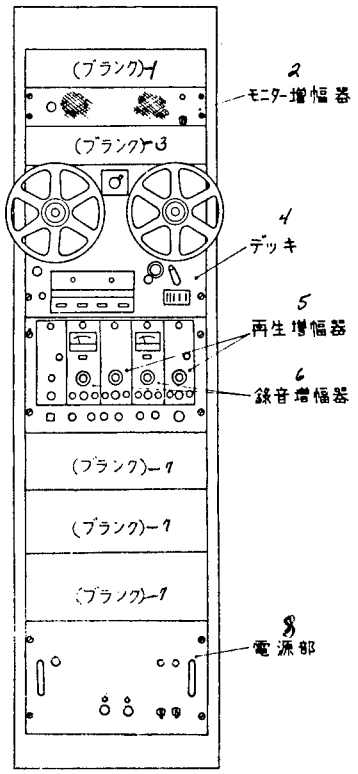

Fig. 4. Tape recorder rack.

1) Blank; 2) Monitor amplifier; 3) Blank; 4) Deck; 5) Playback amplifiers; 6) Recording amplifiers; 7) Blank; 8) Power supply

4. Conclusion

In previous sections we have described the various features of the demodulator and tape recorder. Stability and linearity of the demodulator were improved. The present tape recorder is functioning very well for the present 10-channel demodulator.

We plan to increase the number of channels to 15. A monitor and tape recorder suitable for 15-channel operation will be completed within the near future.

Finally, we express our thanks to Professor Naboru Takagi of Tokyo University Production Research Institute for his useful discussions throughout the design and construction of the ground receiving and recording equipment. We are also very grateful to the chief of the business section of Tanaka Radio Communication Equipment of Japan Electric Co., Ltd. and other members of the company.

(Received on May 7, 1963)

TELEMETRY ANTENNAS

By Fujio Yamashita and Yoseki Inane

1. Introduction

The basic requirements for an antenna suitable to be used as a telemetry antenna are: (1) its shape should be such that it is not seriously affected by the motion of the rocket and it should be mechanically strong enough to withstand the very high speed of the rocket flight, and (2) it should have an optimum radiation pattern which is determined by the relative positions of the rocket and the ground tracking station. Frequently these conditions can not be fulfilled in the overall design because the particular structure of a rocket and an antenna and often we used antennas which were not quite suitable as ideal antennas. In the current report, we will classify antennas by their shapes and describe changes we made in them and also their characteristics found in actual experiments.

2. A Stretched-Out Hoop Type

This type of antenna was used for the K-6 type space rocket. Its shape is sketched in Fig. 1. It consists of a pair of metal wires stretched out parallel to the rocket body from the trailing edge of the rocket tail. Its length is about 1/4 of the wavelength of the employed wave. And oppositely phased electric power is applied to each insulated leg.

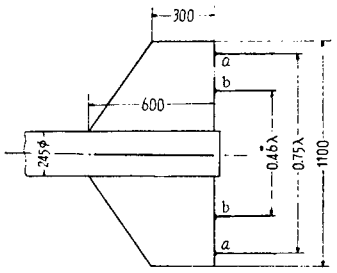

Fig. 1. The structure of the stretched-out hoop type antenna installed at the tail of a rocket

Such an antenna emitted very favorable radiation backward when it was installed in the K-6 type rocket. About the time when K-6 type rocket was

launched, it was generally believed that the tail of a rocket always pointed toward the launching point. And the signal level at the tracking station was intense enough. Therefore, that antenna was used as a very useful type. However, the K-8 type space rocket had a much longer flight distance and for that rocket it was possible to observe the signal level during its flight. It was found that the input signal level is much lower than the theoretical value for free transmission level (refer to the article of "The Telemetry Experiments" for more details). Therefore, we were much concerned about insufficient response of the radiowave receiving equipment. The K-8 type space rocket was supposed to have a much wider and longer tail than K-6. In the meantime, the radiation pattern of the antenna was theoretically calculated, and showed that if the distance between the two hoops were increased, the backward radiation pattern would decrease. And this fact was proved experimentally, too. Originally, the tail hoop antenna was installed far from the axis of the body to avoid exhaust flames, however, based on the previous arguments, the hoops were brought closer to the axis for the K-8-7 space rocket. The change in point is shown by point b of Fig. 1. In this case, the radiation patterns were significantly changed as seen from Fig. 2. As the result of the decreased distance between the two hoops, however, there occurred very violent changes in input signal at the ground tracking station due to the exhaust flame during the booster rocket separation and main rocket ignition. The antenna data for this case is shown in Fig. 3.

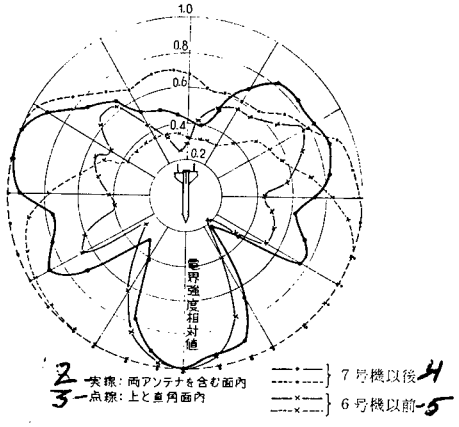

Fig. 2. K-8 type No. 6 and No. 7 rocket tail—stretched-out hoop antenna

2) Solid line: in a plane which includes both antennas
3) Dotted line: in a plane which is perpendicular to the above plane
4) No. 7 rocket onward
5) Up to No. 6 rocket

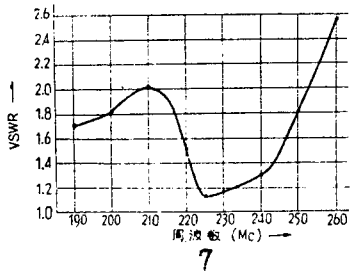

Fig. 3. Data for the K-8-7 rocket stretched-out hoop antenna

7) Frequency (Mc)

This later type antenna had several disadvantages: for example, it was easily affected by the exhaust flame; and the insulating material in the power supply line and antenna supporting points became very poor because the surface temperature of the tail sometimes rose to as much as 200°C; also it required long connecting lines from the transmitter to the antenna. Having such disadvantages, this type of antenna was used only in special cases and for many other cases we used another type (hook type) of antenna.

3. A Hook Type Antenna (Body-Antenna)

A hook type antenna was developed to replace the stretched-out hoop type antenna. And the hook type antenna is expected to be used for command purposes. Its structure consists, as shown in Fig. 4, of a pair of hook type antennas installed symmetrically on the surface of a rocket about the body axis near the teletransmitter.

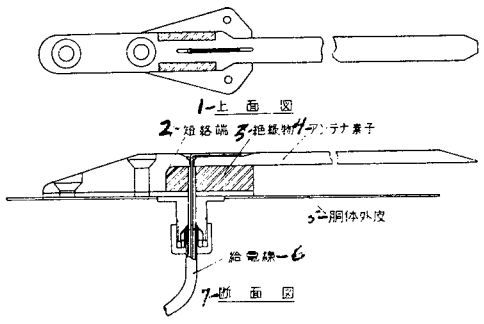

Fig. 4. Structure of the hook antenna

1) Top view
2) Ground terminal
3) Insulator
4) Antenna element
5) Outer surface of the rocket body
6) Power supply line
7) Side view

The total length of the antenna is 1/4 wavelength. Opposite phased electric currents are supplied to each antenna leg. To match impedance, it is desirable to have the power supply terminal near the grounding terminal. There are three components of electric current which contribute to radiation: the first is the parallel component along the antenna; the second is opposite to the first component and is distributed along the body surface; and the third component is perpendicular to the first two components and distributed along the body surface perpendicular to the body axis. Therefore, by choosing the proper diameter of rocket body and wavelength in the experiment, we can obtain an almost isotropic radiation pattern for the antenna. In the K-8 type space rocket, this particular radiation pattern has very useful characteristics (see Fig. 5).

This antenna is very suitable even if the space rocket does not keep its aspect all through the flight such as the K-8-11 whose aspect changed irregularly during its flight.

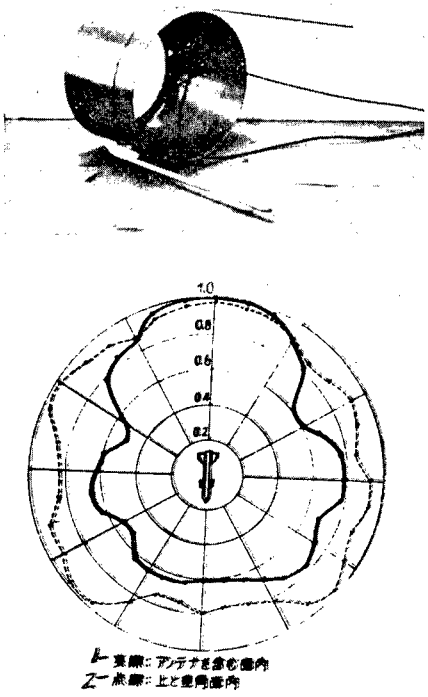

Fig. 5. The radiation pattern of the body hook antenna used for the K-8 type space rocket

1) Solid line: surface including the antenna
2) Dotted line: surface perpendicular to the above surface

This antenna is also not affected by the exhaust flame and booster rocket separation, which are very serious problems in tail hoop-type antennas. On the other hand, this antenna has a few disadvantages, namely, once the diameter of the rocket body is fixed, then the radiation pattern is automatically fixed once and for all, and there is no room to adjust it; and since the power input terminals are near the grounding terminal, the frequency characteristics are very steep because of the large reactance of the grounding wire. The coordinates of this antenna is shown in Fig. 5. If we assume the one antenna is connected to a large conductor cylinder, the equivalent circuit is shown in Fig. 7. From this equivalent circuit, we can see that the reactance of l_1 has a large effect. For an actual antenna, we have to take account of the mutual impedance between the two antennas. In the equivalent circuit of Fig. 7, β is a constant determined by the rate at which the electric current, which contributes the radiation, divides into two parts; one flows through the antenna and the other flows through the rocket body.

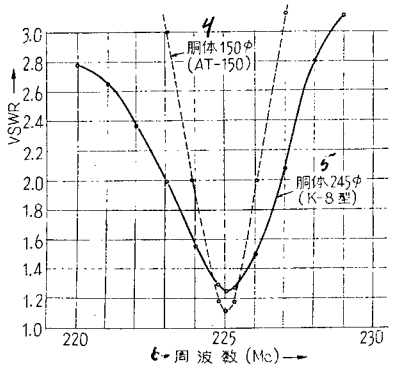

Fig. 6. Data for the body hook antenna

4) Body
5) Body
6) Frequency (MC)

This antenna was installed to an antenna testing rocket AT-150 to test it for aerodynamic aspects and electrical characteristics and its results were very satisfactory. Taking into account the future plan of using a crystal control system, this antenna holds promise because we do not need worry about the narrow waveband property of the control system. And also, it has a short power input wire, so that mechanical damage and electrical loss can be cut down by a large amount. With all these advantages, this antenna is very desirable as a future telemetry antenna.

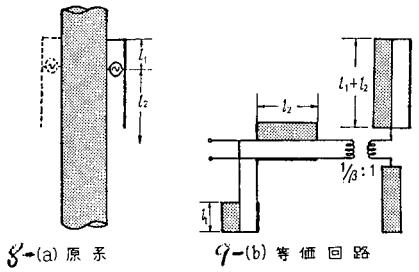

Fig. 7. The equivalent circuit of the body hook antenna (for the case of one antenna)

8) Original system. 9) Equivalent circuit

4. Conclusion

In this article, we discussed the two recent rocket antennas used for telemetry. The tail stretched-out hoop antenna has advantages such as wide frequency band characteristics; it is easy to control the radiation pattern; its cost is low, etc. On the other hand, a body hook antenna has advantages such as an ideal radiation pattern and strong mechanical strength; short power input line; and it is not affected by exhaust flames, etc. Therefore, the former is useful for a small space rocket such as the K-6 type space rocket. And, with some improvements, the latter can be used in a much larger space rocket.

Finally, we express our great thanks to Professors Takagi, Saido, and Nomura and Associate Professor Kurokawa for their help in developing those antennas. And we are also grateful to many people of Prince Motor Co. for constructing the body hook antenna.

(Received on April 11, 1963)

THE TELEMETRY EXPERIMENT DURING KAPPA 8 TYPE NO. 8 THROUGH NO. 11 SPACE ROCKET FLIGHTS

By

Noboru Takagi, Tamiya Nomura, Sachetsugu Yokayama, Sigehito Yokoyama, Kosoburo Inoue, Yukio Murada, Katsuhiko Ohi, Kenich Takahasi, and Nohio Katayama

During the period October 1961 to December 1962 telemetry was used a total of ten times in space rocket experiments carried in the rockets Kappa 8 types 8-11, Kappa 9L-2, Kappa 8L-1, Kappa 9M-1, HT-150-1, SO-150-1, and AT-150-1.

Throughout these experiments the telemetry was successful except for the experiment with the rocket 9L-2 in which we obtained only partial data because of the troubles with the teletransmitter and the transmission antenna. The data obtained in the above experiment will be reported by the responsible groups. Thus, we report only on several problems and the main improvements which have been made on the teletransmitter during the period of the above experiments.

1. Transistorization of Subcarrier

Oscillator of teletransmitter.

It had been a long standing plan to use transistors in order to minaturize teletransmitters. In 1957 transistorized subcarrier oscillators were already used experimentally for the rockets Kappa 4-1 and 122-S-1. However, there were many difficult problems with transistor technology in those days. The IGY was on its way, and we were badly in need of flight and observation data. For such reasons, the transistorization of a teletransmitter was put aside for a while.

The flight success of the K-8 type space rocket had proved its ability to carry a big payload. Thus, it was quite possible to make multipurpose observations, and in turn, this single factor called our attention to the need for a multichannel telemetry. Using conventional tube method, it was impossible to achieve miniaturization of electronics equipment. Therefore, once again the old transistorization idea became popular. In the K-8-8, a transistorized teletransmitter was actually used for the first time.

Heat is the most difficult problem for all transistorized equipment. However, as we described in the article on the teletransmitter (current issue, page 155) by means of temperature correction of the circuit itself the temperature characteristics of the subcarrier oscillator were able to be stabilized; and with particular designs of the structures of the transmitter and rocket chamber, we obtained fairly good heat insulation. Thus, so far we had no serious problem concerning heat.

For conventional vacuum tube telemetry 0 - 5V input was required for 500 kΩ impedance; but in transistorized telemetry, the impedance usually decreased by a large amount. However, we fixed the input impedance at larger than 100 kΩ and the input voltage for a range of 0 - 5V, just as in the conventional vacuum-tube case, because a very low impedance telemetry gave large loads to the detecting instruments. Generally, there is an inductive coupling between the input terminals of transistorized equipment and the output terminal of detecting equipment. Therefore, we had to fix the upper limit of the output impedance of a detecting instrument, and as of now, we have roughly set the upper limit of output impedance at 10 kΩ .

2. Increasing the Number of Channels

To meet the increased capacity of the payload of the Kappa-8 type space rocket, the number of telemetry channels was subject to increase. Because of conditions at the ground-tracking station, we used an 8-channel teletransmitter; for a while and, for the time being, we now use 10-channel teletransmitter. The standard IGIR channels: No. 4, No. 5, No. 12, and No. 13 were newly added to the conventionally used channel. Table 1 shows the teletransmitter channels and their characteristics, both original ones and the newly added ones.

Ten kc/s signals were used to calibrate the speed of the tape recorder for the conventional radiowave receiving and recording equipment. However, the ten kc/s signal band was within the channel No. 12 of IRIG which was added to our telemetry as an independent channel. Therefore, it was impossible to record 10 kc/s signals and a subcarrier signal in the same track of tape. To overcome this, we installed a new two-track tape recorder and the two tracks were used to record a subcarrier signal and 10 kc/s signal.

3. Problems in the Telemetry Used in the Kappa 8 Type Space Rocket

During the Kappa 8 type 1-6 space rocket experiment, we found the following difficulties:

(i) The signal reaching the receiver was much weaker than what was theoretically expected.

Table 1

Telemetry Channels

2 IRIG チャネル番号	3 副搬送波中心周波数 (c/s)	4 周波数下限 (c/s)	5 周波数上限 (c/s)	6 周波数レスポンス (c/s)	7 備考
4	960	888	1,032	14	
5	1,300	1,202	1,398	20	増設チャネル — 8
6	1,700	1,572	1,828	25	
7	2,300	2,127	2,473	35	
8	3,000	2,775	3,225	45	従来のテレメータチャネル — 9
9	3,900	3,607	4,193	60	
10	5,400	4,995	5,805	80	
11	7,350	6,799	7,901	100	
12	10,500	9,712	11,288	160	増設チャネル — 10
13	14,500	13,412	15,588	220	

2) IRIG channel number
3) Central peak frequency of subcarrier wave
4) Frequency lower limit
5) Frequency upper limit
6) Frequency response
7) Remarks
8) Added channel
9) Original telemetry channel
10) Added channel

(ii) The transmitting frequency changed rapidly over a large band.

Special attention was paid to solve these problems for the experiments on K-8-7 and its successors.

Figure 1 shows the correlation of the input signal level of the receiver with range, measured by K-8-5 and -6 space rockets. As seen from the figure, the input signal level is much lower than the theoretically acceptable value. And as seen from Fig. 2, for the majority of the flight time, the input signal level was barely above the possible detecting input signal level. The main reason for this fact is supposed to come from the propagation pattern of the antenna fixed on the tail of the rocket, which was reported on in detail in the article "Telemetry Antennas" (page 173 of current issue). Improvements were made on this matter from the K-8-7 experiment onward. Their experimental results are shown in Figs. 3 and 4. As seen in Fig. 4, during most of the flight, the input signal levels were well above the possible detecting input signal level. Thus, the communications system achieved its optimum operational condition. Even with such improvements, as seen from Fig. 3, the input signal level measured

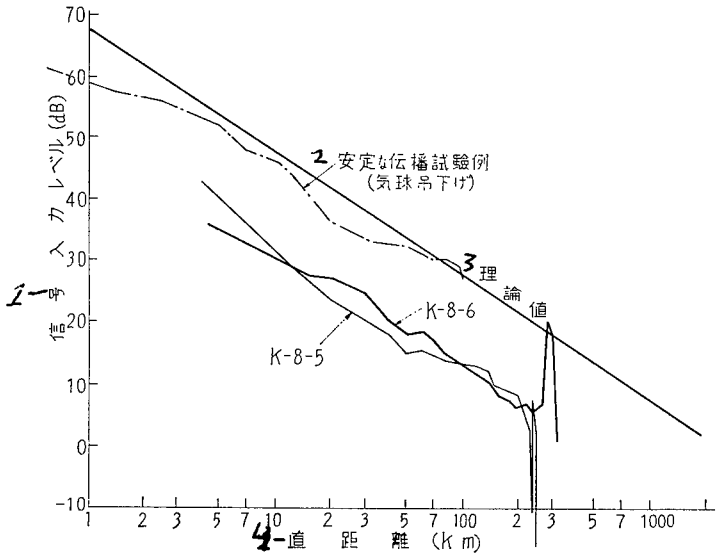

Fig. 1

1) Input signal level
2) An example of stable transmission experiment (balloon flight)
3) Theoretical value
4) Straight distance (km)

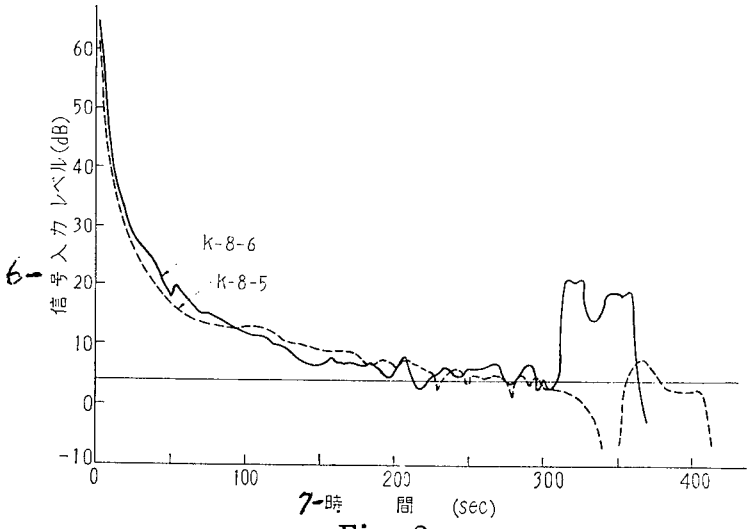

Fig. 2

6) Input signal level, 7) Time (sec)

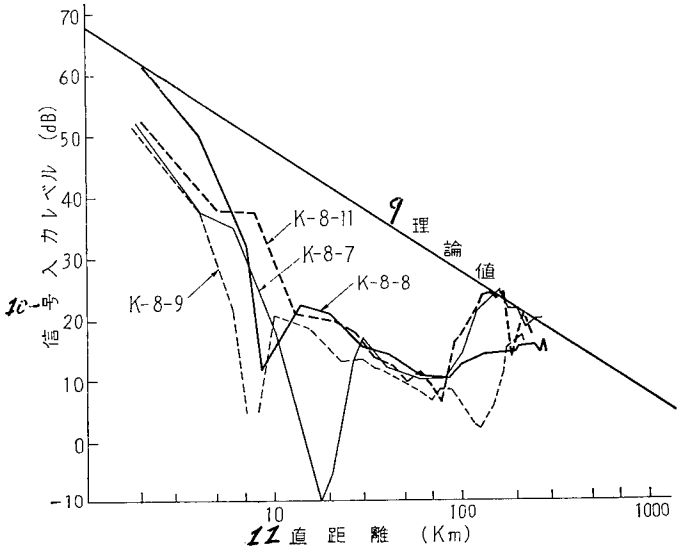

Fig. 3

9) Theoretical value
10) Input signal level
11) Straight distance

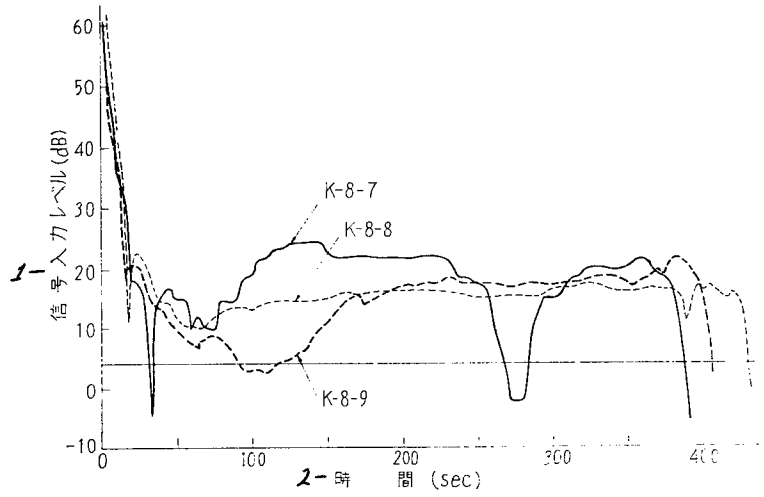

Fig. 4

1) Input signal level
2) Time (sec)

with respect to range were far lower than what was expected by theoretical calculations. This effect was mainly a result of the pattern of the antenna fixed at the tail of the rocket, which turned out not to be suitable for the K-8 type space

rockets. To improve it, we developed a new hook type antenna to be installed at the body—not the tail—of a rocket. The advantage of this new antenna was well proved by the AT-150-1 space rocket experiment. A telemetry antenna, which was installed at the tail of a rocket, was originally designed to be used for the K-6 type space rocket. The experimental data for the K-L-1 rocket, which is essentially the same as the K-6 rocket, are shown in Fig. 5, by which we can see that the input signal level reached almost the theoretically expected values. Judging from those data, we think it is reasonable to install antennas at the tail for the 150 type rocket and at the body for the 245 type rocket in the future.

(b) Changes of transmitting frequency.

We noticed large changes in the transmission frequency during main rocket ignition and separation of the booster rocket. On the other hand, we could not detect such changes in 3-direction acceleration experiments. Therefore, we reached the conclusion that the changes in transmission frequency resulted not from shock and other mechanical conditions but rather were from changes of antenna impedance during separation of the booster rocket. This argument was verified by several other experiments. Based on this finding, we made a loose connection between the output terminal and the antenna for the K-8-10 and follow-up rockets. By this, we could eliminate the impedance change of an antenna up to a satisfactory level even though it inevitably cost some output power.

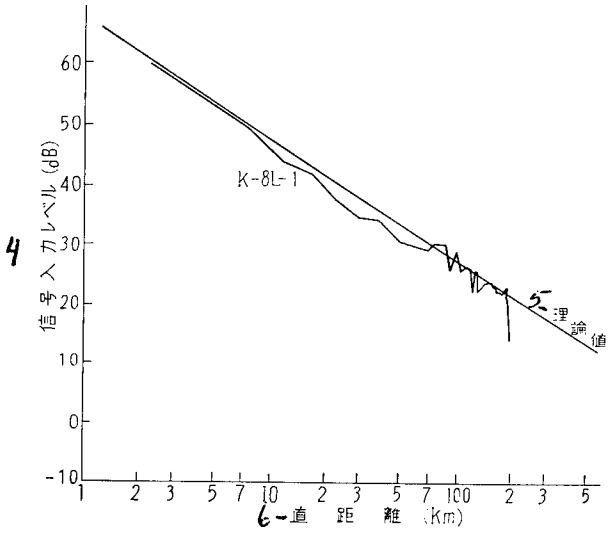

Fig. 5

4) Input signal level
5) Theoretical value
6) Range

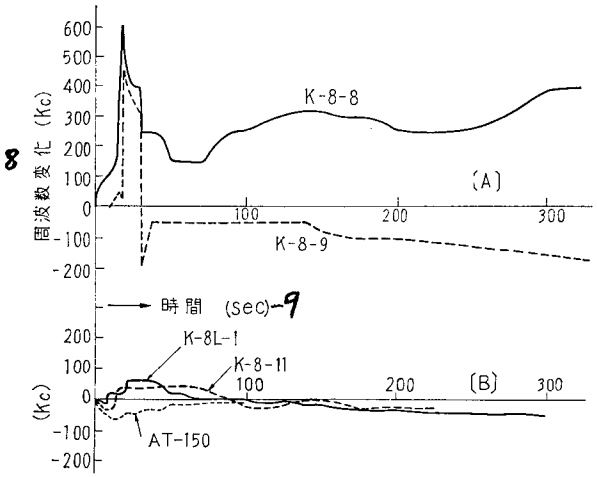

Fig. 6

8) Frequency change
9) Time (sec)

4. Conclusion

As seen in the previous sections, many problems concerning telemetry for the K-8 type space rocket have almost been solved. We can summarize the problems remaining for the future as follows: in order to obtain more stable operation of the transmitter, a crystal control should be adopted. And to increase channels, we are scheduled to get four more telemetry frequencies by dividing the 300 Mc/s band by 600 kc/s sub-wave-bands. In the latter case we are not able to use the crystal control device. As of now, intense research is on the way concerning these subjects and we expect, in the near future, to be able to realize a crystally controlled and totally transistorized teletransmitter.

(Received on May 7, 1963)

4 mφ RADAR SYSTEM

By Tamiya Nomura, Junsho Kashimoto
and Masaru Watabe

1. Introduction

In the early days of the Kappa series space rocket tests, a modified GMD-1A type weather observation tracking was used to get data on rocket trajectory. However, with the improvements of the rocket, we faced a rocket such as the K-9 type, and anticipated having larger, longer range space rockets in the future. Thus, it became necessary to have a new radar system.

For this reason, we developed a radar system which should be the most suitable one for rocket research. The 4 mφ radar system with a parabolic antenna is the result.

This radar system has wide applications in rocket tracking, that is, it can track either a large rocket carrying a radar transponder or a small rocket without transponder and it can track a rocket whether the rocket flies long distances or short.

2. Characteristics of the Radar System

(1) It is highly accurate and can track long-range rockets. In order to track a large space rocket which can fly up to 1500 km, the radar has a 4 mφ parabolic reflecting mirror as its antenna; its transmitting power is 500 kw; and its receiver has a low-noise parametric amplifier as the pre-amplifier to reduce noise.

(2) The response of the angular tracking servo system is extremely rapid and, therefore, it can track any kind of rocket.

Because the response of the antenna servo system is extremely sensitive, the radar system can track not only a large rocket but also a small rocket which has a large velocity and acceleration. It can "see" a rocket on the launcher and then continuously track the rocket even during a high-acceleration take-off from the launcher. Therefore there is no chance to mistrack by the side lobe of the antenna. It means that the radar system can completely follow the initial motion of a rocket.

In order to have these characteristics, the parabolic antenna is made of welded light-metal alloy to reduce weight without losing stiffness. A high-pressure, oil pressure motor is installed to operate the large antenna swiftly. A new angular signal conversion method is adopted to make the servo system respond with high sensitivity, thereby making it possible to track for long distances with high accuracy.

(3) It can be used not only as a secondary radar (transponder tracking radar) but also as a primary radar (passive reflecting body tracking radar).

Conventional radar can only track a rocket on which a transponder is mounted. But this radar can track a reflecting body by switching from the secondary function. It is also a wind-measuring device when a rocket dispatches a large number of metallic foils, which are called chaff, and the flow pattern of the foils are measured. The radar system as a primary radar can measure the chaff, too.

(4) It can swiftly convert linear polarization to circular polarization.

When it is tracking a rocket as a secondary radar, its antenna has circular polarization. Therefore, with a linear polarization antenna as the transponder antenna of the rocket, transmitting and receiving are safely done regardless of the attitude of the rocket.

On the other hand, there is a large power loss when the radar is operating as a primary radar and the radar antenna has circular polarization rather than linear polarization. So, it is better to convert to linear polarization. This function can be done without delay simply by turning a switch.

(5) The rocket trajectory is drawn out on graph paper.

The position of a rocket at any time is plotted with distance horizontal and altitude vertical.

So far, the main characteristics of the rocket have been explained. It may be possible to say that the rocket is unique in its field for its large parabolic antenna, quick response, long-range tracking ability, high sensitivity, tracking ability for every kind of rocket including chaff, and, as a multi-purpose automatic radar.

3. Structure of the System

The radar system consists of the following elements:

Antenna unit

Transmitting and receiving unit

Direction and control unit

Data photographing system

Vertical and horizontal trajectories pen-writing system

Oil pressure generator

400 c/s power source

Automatic voltage controller

Power distribution panel

The function of each element is as follows:

(1) Antenna unit (Fig. 1).

The parabolic reflecting mirror is 4 m in diameter, 150° in angle of vision, net type, and up to 400 Mc/s of mirror face accuracy. Primary radiator is the cylindrical horn type. Conical scanning is of the eccentric, semispherical, reflecting mirror rotating type. There is a switch to convert circular polarization to linear polarization between the mirror and filter. And there is a high-power adjustable power reducer to protect both the receivers of the radar and transponder when the rocket is near the radar.

The antenna is mounted according to elevation-azimuth and operated by an oil-pressure motor in order to be operated as swiftly as possible or as slowly as possible.

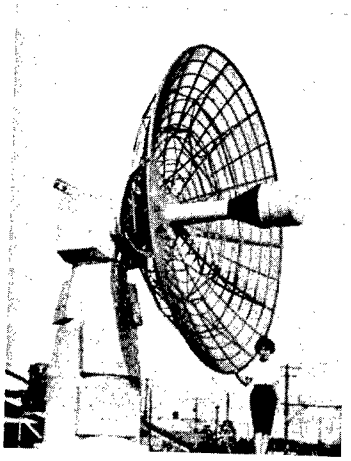

Fig. 1. 4 mφ radar antenna

(2) Transmitting and receiving unit (Fig. 2).

It has a transmitting magnetron, modulator, TR system for transmitting and receiving, parametric amplifier, local oscillator, mixer, intermediate frequency amplifier.

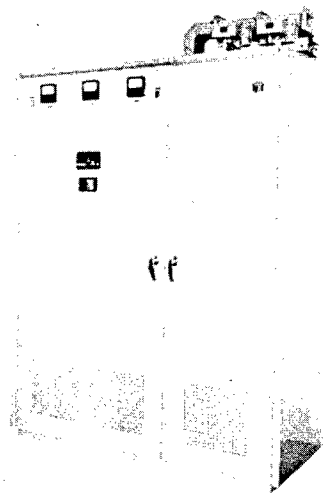

Fig. 2. Transmitting and receiving unit

(3) Direction and control unit (Fig. 3).

It has or performs the following: data conversion to the angles of azimuth and elevation of tracking, the servo circuit which produces the electronic signals to control the oil-pressure servo system and valves, range tracking system from bit signals, AGC circuit, measurements based on crystal, timing device for the entire pulse system including the transmitting trigger, A/R scope, converting primary radar to secondary, converting circular polarization to linear polarization, starting operation of recording camera. And all these functions can be controlled by remote controls. In addition to these, synchronization of receiver, gain adjustment, manual control or range measurement system and angle tracking system, indication of the errors of range measurement and tracking angles for each axis of the coordinates, indication of receiving level, and other functions of surveillance, coordination, and control for the entire radar system are performed in this unit.

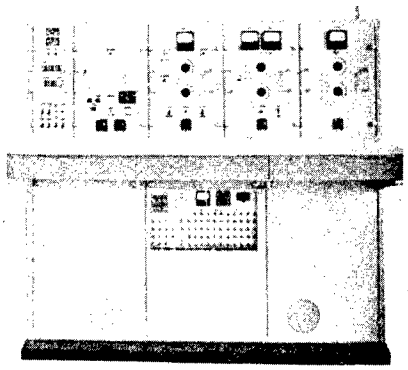

Fig. 3. Direction and control unit

(4) Data Photographing System (Fig. 4).

This unit records the data which will be used to calculate the trajectory. Angles of azimuth and elevation, digital indication of elapsed time from launching with date, condition of tracking, and others are shown on the dial panel and they are photographed by a 16 mm cine-camera.

This system also has a computer which calculates the altitude and horizontal distance (absolute and longitudinal and latitudinal component values) of the rocket from the angles and range measured by the radar system. The resultant output (values) are sent to the vertical and horizontal trajectories pen-writing system.

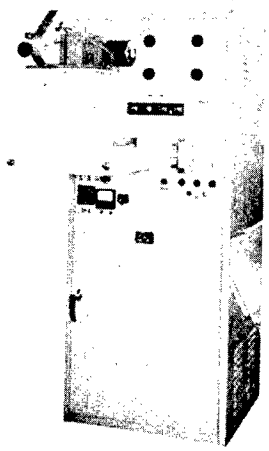

Fig. 4. Data photographing system

(5) Vertical and horizontal pen-writing system (Fig. 5).

Outputs of the computer in the data photographing system are led to X and Y plotters. The plotters draw the trajectories of the rocket on horizontal and vertical planes.

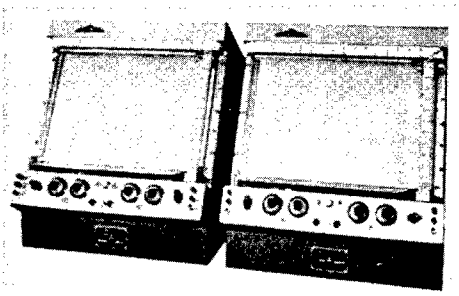

Fig. 5. Vertical and horizontal pen-writing system

(6) Oil pressure generator (Fig. 6).

It is the system from which high-pressure oil is supplied to the oil-pressure motor which drives the azimuth and elevation axes of the antenna. The generator includes the oil pump which generates the high-pressure oil, a motor which drives the pump, oil control valves, oil tank, accumulator, and oil pressure gauge.

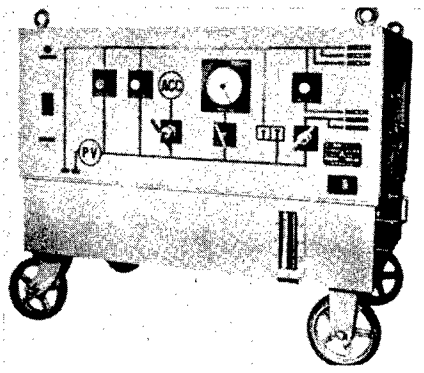

Fig. 6. Oil-pressure generator

(7) Others.

The radar system also includes 400 c/s power source for the synchro and servo systems, automatic voltage controller for commercial power source, and power distribution panel.

4. Dimensions and Performance

(1) Antenna unit

Parabolic reflector:	Diameter: 4 m Angle of vision: 150°
Mount:	Elevation-azimuth type Limit of rotation: Elevation axle: -5 ~ +85° Azimuth axle: all direction (continuous)
Operation:	Oil pressure motor driving Oil pressure: 100 kg/cm^2 Flow rate of oil: 76 l/sec
Scanning:	Conical eccentric semi-spherical rotating type Scanning rate: 12 cps
Polarization:	Vertical linear polarization - counterclockwise circular polarization Switchable
Antenna gain:	Between linear polarizations: 33 db Linear to circular polarizations: 30 db
Beam width:	Half value width: 4°
Side lobe:	For circular polarization: 12 db
Beam separation angle:	1.5°
Directivity cross point gain:	2 db

(2) Transmitting and receiving unit

Transmitting unit

Type:	Pulse modulating, magnetron oscillation type

Transmitting frequency:	Primary radar: 1678 Mc/sec Secondary radar: 1687 Mc/sec Both can be pre-set and convertible
Transmitting power:	500 kw (wave front value)
Pulse width:	1 μsec
Pulse recurrence frequency:	83-1/3 c/sec

Receiving unit

Type:	Parametric high-frequency amplifier, superheterodyne type
Parametric amplifier:	Pump frequency: 11,000 Mc/sec With APC and AFC Gain: 20 db Bandwidth: 10 Mc/sec Equi-frequency (for input and output) with circulator type
Intermediate frequency (IF):	30 Mc/sec
IF bandwidth:	3 Mc/sec
IF amplifier gain:	115 db
AFC:	Receiving frequency automatic tracking type Time constant: 2 sec Hold period: over 5 min
Overall noise index:	2.3 db
Minimum trackable receiving signal:	-95 dbm

(3) Direction and control unit

Range-measuring unit

Type:	Crystal frequency base, pulse tracking type
Max. measurable range:	1,500 km
Min. measurable range:	600 m

Max. range measuring speed:	8.5 km/sec
Max. range measuring acceleration:	32 km/sec^2
Overall range measuring accuracy:	40 m (rms)

Angle tracking unit

Type:	Conical scanning, oil pressure servo type
Max. tracking speed:	EL: 22° /sec AZ: 14° /sec
Max. tracking accelerator:	EL: 9° /sec AZ: 6° /sec
Servo loop range width:	EL and AZ: 16 rad/sec
Overall angle tracking accuracy:	0.05° (rms)

Direction unit

Limits of A scope:	0-150 km, 0-500 km and 0-1,500 km
Limit of R scope:	± 5 km
Angle and range direction:	Same as that of the data photographing system

(4) Data photographing system

Angle, range and time recording:	Both angle and range are indicated on rough and fine indicating scales Time is shown by digital number These are photographed by a 16 mm cine-camera
Recording scale:	Angle: fine scale: 10° /revolution min. scale: 0.1° rough scale: 360° /revolution min. scale: 10°

Range:
fine scale: 50 km/revolution
min.scale: 500 m
rough scale: 1800 km/revolution
min. scale: 50 km

Time: 4 digits, decimal system
min. number: 0.1 sec

(5) Vertical and horizontal trajectories pen-writing system

Type:	Oscillograph records altitude, horizontal distance (on vertical plane) and trajectory projection on horizontal plane
Recording accuracy:	±0.5% of full scale

5. Technical Problems With the Radar System

Following are the problems we encountered in developing the radar system:

(1) Problems at short distance.

(a) Quick-response for the tracking of initial angle.

For operational necessity we have to set the launcher and the radar close to each other. This makes the initial angular velocity of a rocket large as seen from the radar. The relationship with the pre-determined flight courses of the K-9L type space rocket is shown in Fig. 7. At Michigawa, the distance from the radar ro the launcher was only 0.75 km. Using the above value of distance, the velocity as a function of time changes in the way shown in Fig. 8.

In radar design, it is important to design a radar which can track the initial path of a rocket even though it has high velocity and acceleration, and which will not lose the rocket from its beam. For the rocket system, we used the following transform function to give the above qualification:

$$G(S) = \frac{124.6\ (s+1)}{S\ (17.8\,s+1)\ (1+s/55)}$$

According to experience with conventional radar, this will be the best value we can have for the operation of a 4 mφ antenna. Errors from the value are calculated and shown in Fig. 9.

There were many difficulties to give these characteristics to the antenna.

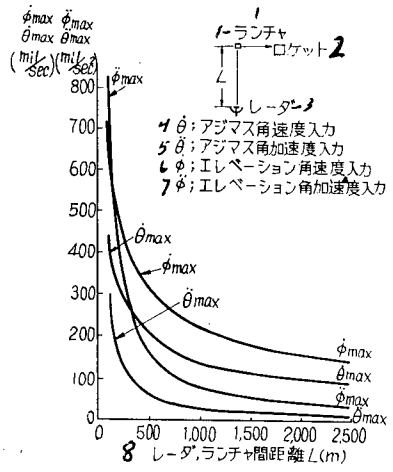

Fig. 7. The relationships between the distance from radar to launcher and maximum values of angular velocity input and angular acceleration input

1) Launcher; 2) Rocket; 3) Radar; 4) Angular velocity input in azimuth; 5) Angular acceleration input in azimuth; 6) Angular velocity input in elevation; 7) Angular acceleration input in elevation; 8) Distance between launcher and radar

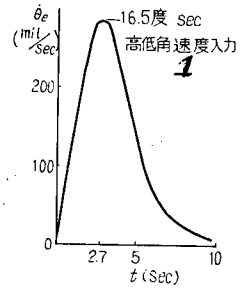

Fig. 8. Angular velocity input in elevation

1) Angular velocity input in elevation

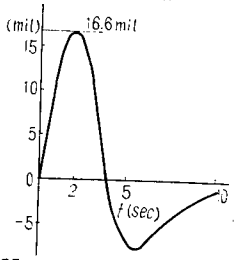

Fig. 9. Overall errors of the angle of elevation

(b) Excessive, initially receiving input.

The limiting value of initial input to the transponder receiver was about 20 dbm and that to the parametric amplifier of the radar was about 25 dbm. In the actual case, the inputs were about +26 dbm and -14 dbm and we had to develop an adjustable power reducer which was durable to high power and install it in between the waveguide. The detail of the device is shown in Fig. 10.

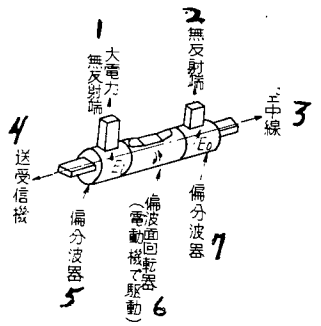

Fig. 10. The theory of a high power, adjustable power reducer

1) High-power no-reflection end; 2) No-reflection end; 3) Antenna; 4) Transmitter and receiver; 5) Polarization component divider; 6) Polarization rotator (operated by motor); 7) Polarization component divider

(2) Problems at long distance.

(a) Low angular velocity tracking.

When a rocket is far away, the angular velocity is small. In this case, it is important that the antenna system should not have an unsmooth motion due to friction. For this reason, an oil-pressure operation system was adopted.

We found from actual rocket tracking that an antenna would vibrate because the incoming wave was interfered with by the lobing frequency of the direction detector if the incoming wave was not stable due to the spinning and fading of the rocket. In order to prevent this interference, we made a design change to reduce the width of the servo band at long-range tracking. We had no chance to test the idea.

(b) Maximum effective range.

In order to increase the maximum range, we take an antenna of large diameter, 500 kw of transmitting power, and parametric amplifier to reduce the

noise index. For the relationship between the parametric amplifier and transmitting range, refer to Figs. 11 and 17.

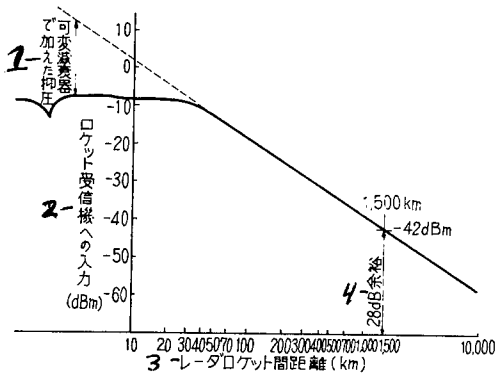

Fig. 11. Diagram of input level to rocket receiver (secondary radar)

1) Power reduction by the adjustable power reducer; 2) Input to rocket receiver; 3) Distance between radar and rocket; 4) 28 db of power reserve

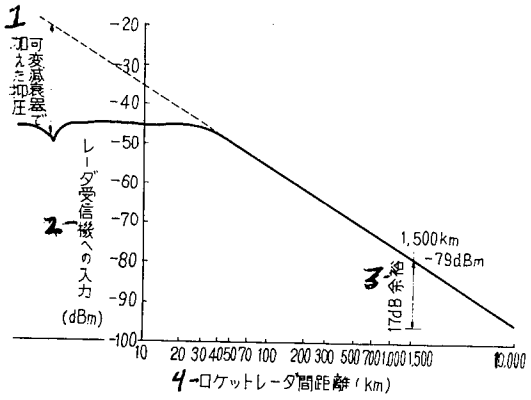

Fig. 12. Diagram of input level to tracking radar receiver (secondary radar)

1) Power reduction by the adjustable power reducer; 2) Input to radar receiver; 3) 17 db of power reserve; 4) Distance between radar and rocket

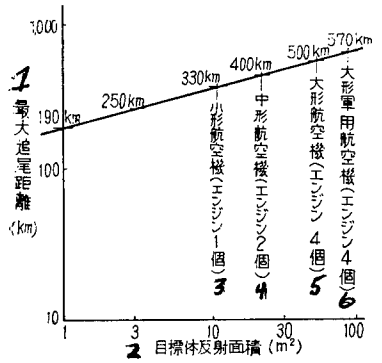

Fig. 13. The relationship of maximum tracking range to the reflecting area of the object at passive object tracking (primary radar)

1) Maximum tracking range; 2) Reflecting area of the object; 3) Small aircraft (single engine); 4) Middle class aircraft (two engines); 5) Large aircraft (four engines); 6) Large military aircraft (four engines)

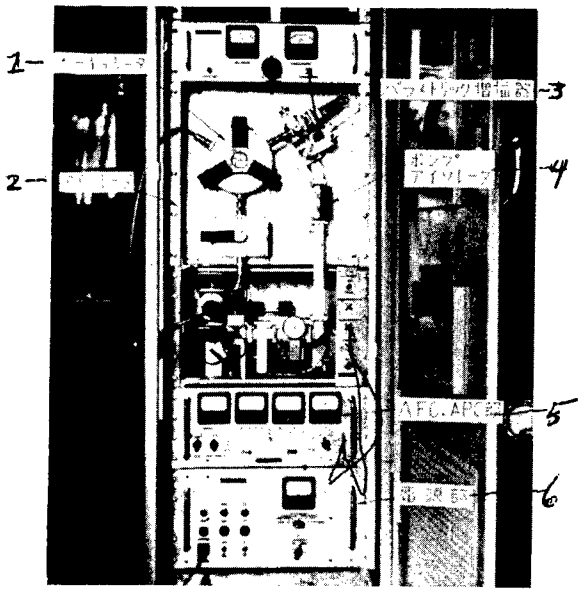

Fig. 14. Outside of the parametric amplifier

1) Circulator; 2) Isolator; 3) Parametric amplifier; 4) Pump isolator; 5) AFC-APC unit; 6) Power source

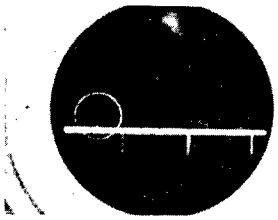

Fig. 15. S/N without parametric amplifier

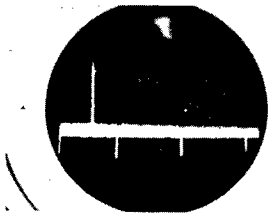

Fig. 16. S/N with parametric amplifier

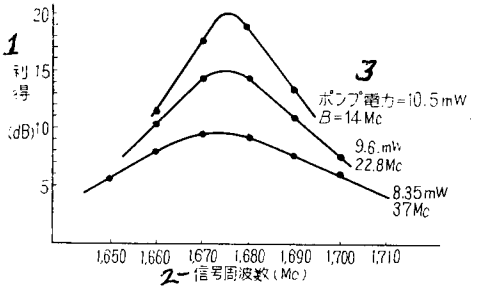

Fig. 17. The amplification characteristics of 1680 Mc parametric amplifier

1) Gain; 2) Signal frequency; 3) Pump power

(c) The problem of data conversion in the angle-tracking system.

In order to obtain the maximum tracking range of 1500 km, we had to have low values, 83-1/3 pps for pulse recurrence frequency and 12 cps for conical scanning rate. Therefore, we had to take the small time-constant method which would give stability, and smooth operation of the angle-tracking system. And we had to develop and adopt a method which performs sampling, integration, and hold-on for each cycle of pulse and scanning.

(d) Switch between primary radar and secondary radar.

In order not to make the system complicated, we adopted the idea of using a fixed receiving frequency, and by switching the transmitting frequency, one to the other, the conversions were performed.

(e) Switch the circular polarization to and from the linear polarization.

Linear polarization is better for primary radar and circular polarization is better for secondary radar. For these conversions, a particular switch system which holds up under high power was adopted and its structure is shown in Fig. 18.

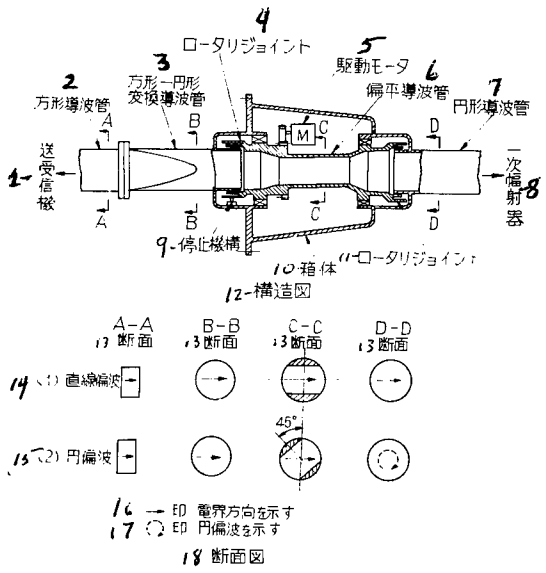

Fig. 18. Polarization switch system

1) Transmitter and receiver; 2) Rectangular waveguide; 3) Rectangular to circular converting waveguide; 4) Rotary joint; 5) Driving motor; 6) Edge flat waveguide; 7) Circular waveguide; 8) Primary amplifier; 9) Stopper; 10) Cover; 11) Rotary joint; 12) Structure; 13) Cross-sectional area; 14) Linear polarization; 15) Circular polarization; 16) Direction of electric field; 17) Circular polarization; 18) Cross-sectional area

(f) High accuracy in range measurement.

In order to measure the range accurately up to 1500 km, we designed a three-stage, time modulation system based on crystal oscillation. The circuit

and measured errors are shown in Figs. 19 and 20, respectively.

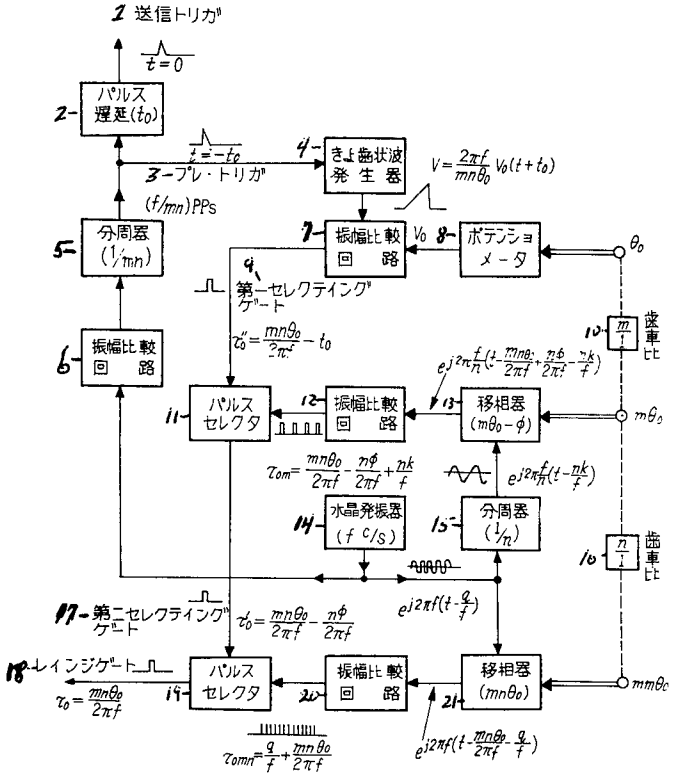

Fig. 19. Block diagram of three-stage time modulator unit

1) Transmitter trigger; 2) Pulse delay (t_0); 3) Pre-trigger; 4) Saw-tooth type wave generator; 5) Frequency divider; 6) Amplitude comparison circuit; 7) Amplitude comparison circuit; 8) Potentiometer; 9) Selecting gate No. 1; 10) Ratio of the toothed wheel; 11) Pulse selector; 12) Amplitude comparison circuit; 13) Phase converter; 14) Crystal oscillator; 15) Frequency divider; 16) Ratio of the toothed wheel; 17) Selecting gate No. 2; 18) Range gate; 19) Pulse selector; 20) Amplitude comparison circuit; 21) Phase converter; 22) k: any integer, q: any integer, t_0: certain time gain, φ: certain phase gain

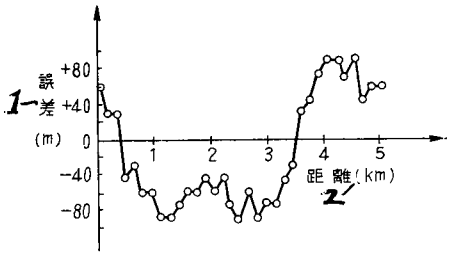

Fig. 20. Errors in range interval of 5 km (measured values)

1) Error; 2) Distance

(g) Structure of antenna.

As stated above, a 4 mφ antenna was used to track at a long distance. But it had to have high stress resistance and a small moment of inertia in its parabolic reflector because the antenna had to be driven swiftly during the initial period of rocket launch, and the antenna system had to have a gear system which would have minimum backlash and friction.

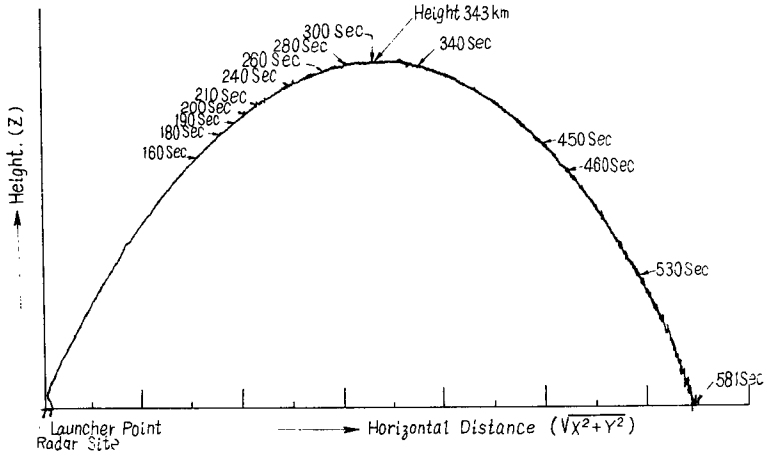

Fig. 21. Entire trajectory of K-9L type space rocket when radar was used as secondary radar (maximum altitude = 343 km, total flight time = 581 sec)

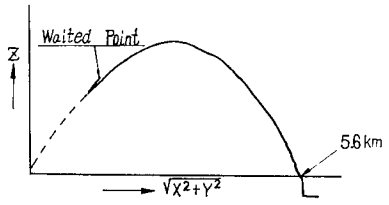

Fig. 22. A small rocket tracking record when radar was used as primary radar (the radar tracked the rocket only at altitude in order not to be influenced by ground reflections)

6. Conclusion

So far, we explained the newly manufactured 4 mφ tracking radar system. The radar has been installed at Michigawa Test Center and tracked the K-9L type space rocket from the moment of launch to 600 km, the maximum flight distance. Fig. 21 is the trajectory of the K-9L type space rocket which was drawn on the vertical trajectory pen-writing system. And as illustrated in Fig. 22, the radar system showed that it could track as primary radar a small rocket which has no transponder.

We wish to thank Professors Takagi, Zawai, Saito and Assistant Professor Mori who have contributed many helpful suggestions in developing the radar.

(Received on April 27, 1963)

RECEIVING LEVEL CHANGE CAUSED BY THE ANTENNA MOUNTED IN THE ROCKET BODY

By Radar Research Team: Noboru Takagi,
Kaneyuki Kinokawa, Motomi Nagatani,
Mitsum Ichigawa and Minoru Sekikuchi

1. Introduction

It is desirable that there should be no level change at the ground receiver due to relative changes in phases of the ground antenna and the radar antenna on the rocket. Thus, an ideal antenna on a rocket should have absolutely no directivity in radiation pattern. However, it is impossible to make an antenna which has no directivity at all. And the radiation surface area is inevitably large as it has to be mounted on the metallic surface of a rocket, and this makes a cut-off in directivity. Furthermore, an antenna should have a certain shape and structure and it should be mounted at a particular place on the rocket. For these reasons, it is extremely difficult to make an ideal antenna. Consequently, we have to compromise.

The author will report on the design of the radar antennas for K-8, K-9L-1 and -2, K-8L-1, and K-9M-1 type space rockets.

2. Current Radar Antenna

There are two kinds of antennas, as shown in Figs. 1 and 2, which were mounted on K-8-1 to -11, K-9L-1 and -2, K-8L-1, and K-9M-1 type space rockets, that is, the notch antenna at the tail and pole antenna at the body.

(1) Notch antenna at tail. For the K-8-11 and K-9L-1 type space rocket, notch antennas, as shown in Fig. 1, were used as radar antennas, and we got good results. As shown, Fig. 1a and b, K-9L type and K-8 type antennas have notches at 94 mm and 35 mm from the front end of the tails, respectively. The input impedance can be easily adjustable to 50 Ω when the power is supplied at the point shown in Fig. 1c. The measured values of frequency vs voltage standard wave ratio (VSWR) of K-8 type and K-9L type antenna are shown in Fig. 3. The difference in the locations of an antenna at the tail does not influence the input impedance unless there is a notch at the base of the front end of the tail. However, the radiation pattern changes as a result of different locations of the notch,

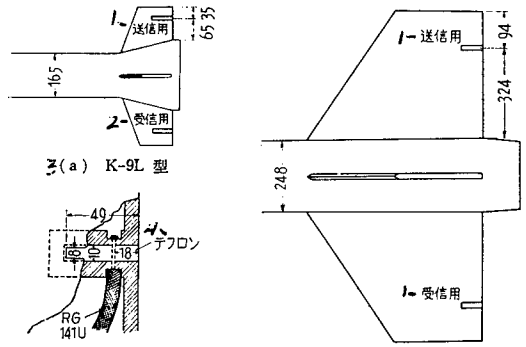

Fig. 1.

1) Transmitting (antenna); 2) Receiving (antenna); 3) K-9L type; 4) Teflon; 5) Structure of the notch antenna at tail, 1680 Mc type; 6) Notch antenna at the tail of K-8M type space rocket

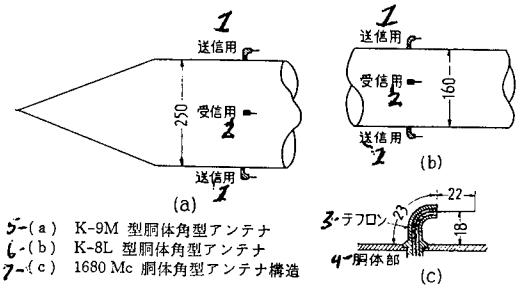

Fig. 2.

1) Transmitting (antenna); 2) Receiving (antenna); 3) Teflon; 4) Body; 5) Pole antenna at the body of K-9M type space rocket; 6) Pole antenna at the body of K-8L type space rocket; 7) Structure of the pole antenna, 1680 Mc type

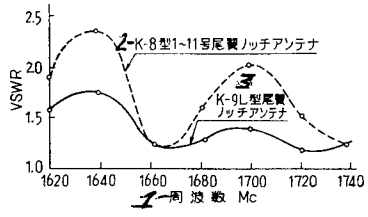

Fig. 3.

Fig. 3. Characteristic curve of the frequencies of the tail antennas of K-8 and K-9L type

1) Frequency; 2) Notch antenna for K-8-1 to -11 type space rockets; 3) Notch antenna for K-9L type space rocket

the shape of the tail, and the distances between the notch antenna, body and tail. And this should be considered in the design of a notch antenna.

Since a rocket antenna has quite a complicated radiation surface area, the measurement of the radiation pattern for a rocket antenna cannot be done the same way as for other antennas, and one has to measure the patterns for the planes: horizontal E_θ(X-Y), vertical E_φ(Z-X), and the plane normal to the rotational axis of the rocket E_ρ (Y-Z).as shown in Fig. 4.

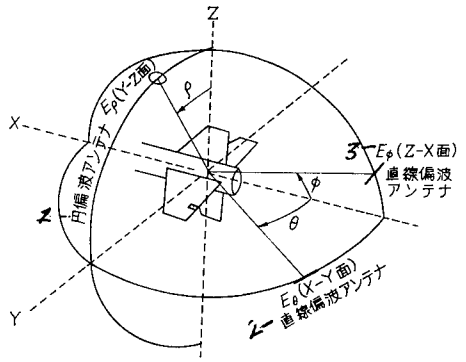

Fig. 4. Measurement of radiation pattern of a rocket antenna

1) Circular polarization antenna E_ρ(Y-Z) plane); 2) Linear polarization antenna E_θ (X-Y) plane); 3) Linear polarization antenna E_φ (Z-X plane)

Figure 5a, b and c show the measured radiation patterns E_θ, E_φ, and E_ρ of the K-8 type antenna for the horizontal and vertical planes and the rotational axis of the rocket. E_θ of the horizontal plane and E_φ of the vertical plane are measured with a linear polarization antenna. And E_ρ of the plane normal to the rotational axis of the rocket is measured with a circular polarization antenna.

Figure 6a, b and c show the radiation patterns E_θ, E_φ, and E_ρ of the K-9L type antenna for the horizontal and vertical planes and the normal to the rotational axis of the rocket. The method of measurement and the antennas used are the same as those of the K-8 type.

The radiation pattern of the K-8 type antenna, as one may know from Fig. 5a, b and c, is similar to the radiation pattern of a dipole antenna which is

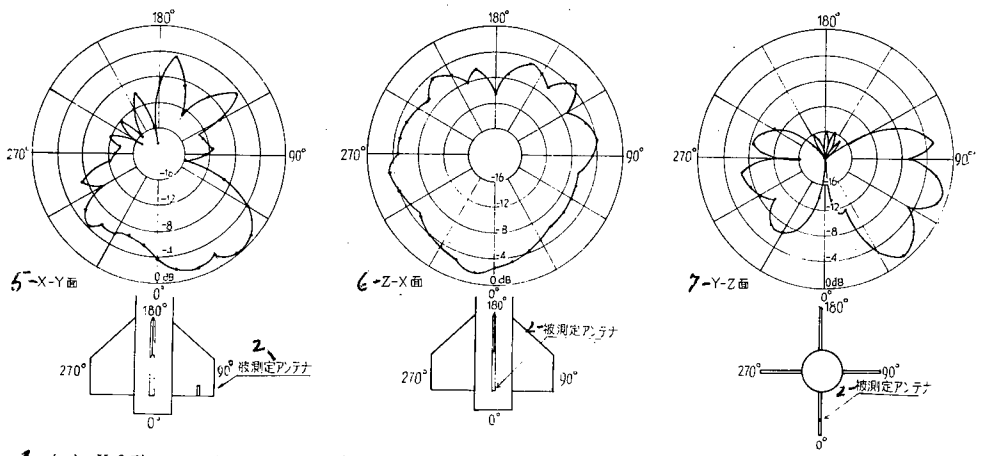

1-(a) K-8 型アンテナ水平面内 E_θ(X-Y 面) 指向特性
3-(b) K-8 型アンテナ垂直面内 E_ϕ 指向特性
4-(c) K-8 型アンテナロケット回転軸面内 E_ρ 指向特性

Fig. 5.

1) Directivity characteristics of E_θ of the K-8 type antenna for the horizontal plane (X-Y plane); 2) Antenna to be measured; 3) Directivity characteristics of E_φ of the K-8 type antenna for the vertical plane; 4) Directivity characteristics of E_ρ of the K-8 type antenna for the plane normal to the rotational axis of the rocket; 5) X-Y plane; 6) Z-X plane; 7) Y-Z plane

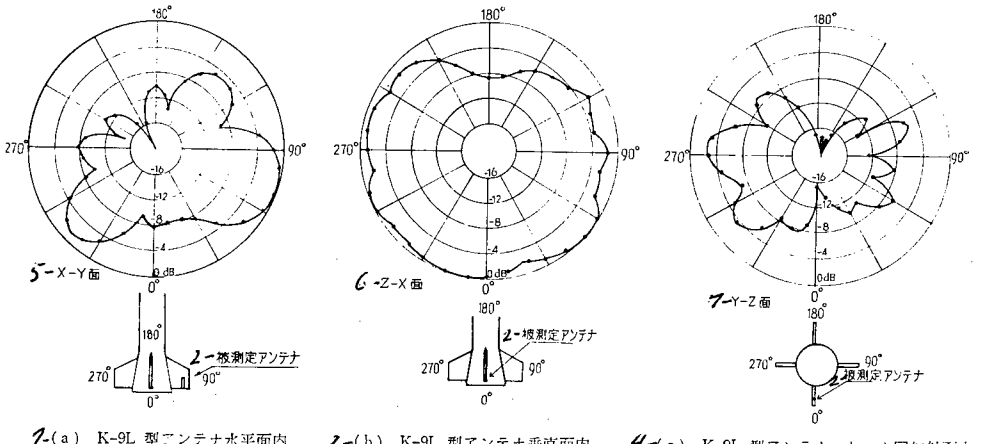

2-(a) K-9L 型アンテナ水平面内 E_θ(X-Y面) 指向特性
3-(b) K-9L 型アンテナ垂直面内 E_ϕ 指向特性
4-(c) K-9L 型アンテナロケット回転軸面内 E_ρ 指向特性

Fig. 6.

Fig. 6 (cont'd.)

1) Directivity characteristics of E_θ of the K-9L type antenna for the horizontal plane (X-Y plane); 2) Antenna to be measured; 3) Directivity characteristics of E_φ of K-9L type antenna for vertical plane; 4) Directivity characteristics of E_ρ of K-9L type antenna for the plane normal to the rotational axis of the rocket; 5) X-Y plane; 6) Z-X plane; 7) Y-Z plane

equivalent and vertical to the notch. However, the radiation pattern of the K-9 type antenna has increased radiation to the horizontal direction of the notch antenna rather than in the vertical direction as shown in Fig. 6a. The reason seems to be that the direction of the radiation current which flows through the tail panel will change by the cut-off for the notch when the area of the tail, which has the notch, is small enough. And the tail of the K-9L type space rocket is much smaller than that of the K-8 type as one can see from Fig. 1. Therefore, it can be said that the position of the cut-off for the notch and the distance from the rocket body will obviously influence the radiation pattern.

The difference between the measured values between locations above and below the tail for the radiation pattern in the plane normal to the rotational axis of the rocket is thought to come from the circular polarization component of the radiating electromagnetic wave from the surface of the tail antenna which has a notch since a circular polarization antenna is used as the measuring antenna.

The antenna which had the radiation patterns shown in Fig. 6 was mounted on the K-9L type space rocket, and we got a satisfactory result from the antenna test. Actually, we could design an antenna better than the one we used for the test. But we did not attempt to make a new one because of the time limitation and because we thought we could get a satisfactory result with the K-9L type antenna.

The advantages of a notch antenna at the tail are that it has a simple structure and it is easy to design a notch antenna which has the radiation pattern of a small cut-off in the rear direction. However, the notch antenna has the disadvantages that the radiation intensity at the portion where it is blocked by the rocket body or tail is extremely reduced because the single notch antenna has to cover all directions around the rocket, and it is inevitable that the antenna will lose several db because the power line to the antenna is very long.

(2) Pole antennas at the body. As shown in Fig. 2, the pole antennas, mounted at the body, are used as K-8L and K-9M type radar antennas. Each of the four inverted L-type antennas is placed 90° away from the other on the circumference of the rocket body. And one of the diagonal pairs is used as a transmitting antenna, and the other pair is for receiving. By supplying currents of opposite phase to each of a pair of antennas, the two antennas of a pair can be made a pair of in-phase antennas.

In the adjustment of input impedance, VSWR can easily be reduced to less than 1.5 as for the notch antenna.

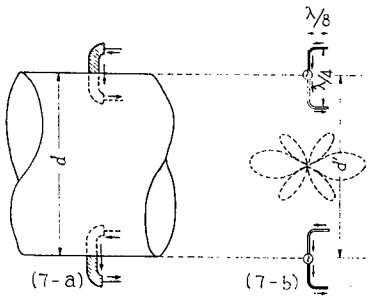

Fig. 7. A series of in-phase antennas by supplying currents of opposite phase

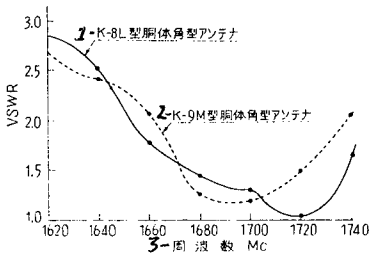

Fig. 8. Frequency characteristics of K-8L, K-9M type pole antennas

1) K-8L type pole antenna, mounted at the body; 2) K-9M type pole antenna, mounted at the body; 3) Frequency

To measure a radiation pattern of the pole antenna at the body, E_θ, E_φ and E_ρ have to be measured for the horizontal and vertical planes, and plane normal to the rotational axis of the rocket body as they were for a notch antenna at the tail. Fig. 9a, b and c show E_θ, E_φ and E_ρ values measured for the planes of the horizontal, vertical and normal to the rotational axis of the rocket body.

The multiple radiation pattern, as shown in Fig. 7b, of the two antennas, having the distance d between them and ignoring the rocket body between the antennas, does not agree with the radiation pattern E_θ for the horizontal plane which is shown in Fig. 9a because of the effect of the rocket body. However, the radiation patterns for the plane normal to the rotational axis of the rocket body become similar to each other when the distance between the antennas d is equal.

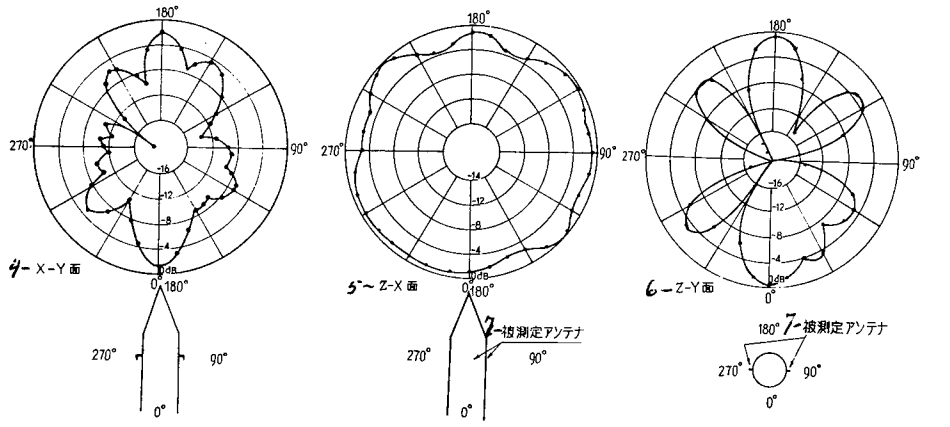

Fig. 9

1) Directivity characteristics of E_θ for the K-8L type antenna for the horizontal plane; 2) Directivity characteristics of E_φ of the K-8L type antenna for the vertical plane; 3) Directivity characteristics of E_ρ for the K-8L type antenna for the plane normal to the rotational axis of the rocket; 4) X-Y plane; 5) Z-X plane, 6) Z-Y plane; 7) Antenna to be measured

Figure 9a and b are the radiation patterns which were measured with linear polarization antennas. However, there are the horizontal and vertical components of the polarization, as shown in Fig. 10a and b, in the electromagnetic wave which is being emitted from the entire rocket body including the antennas. Thus, the radiation patterns measured with linear polarization antenna and with circular polarization antenna are different as shown in Fig. 11a and b.

For the K-9M type antenna, only the radiation pattern for the horizontal plane is shown in Fig. 12. The radiation pattern of the K-9M type antenna had a large cutoff area because the K-9M type space rocket had a larger body than that of the K-8L type. Therefore, it was decided that the pole type antenna would not be used for the K-9M-2 type space rocket. And it was known that in measuring the radiation pattern, a circular polarization antenna should be used as the measuring antenna when the receiving antenna on the ground was a circular polarization antenna.

The advantages of the pole antenna at the body are that it does not need to have a long power-supply line around the rocket engine because it is mounted at the body; and that it has a small phase effect as a result of the change of

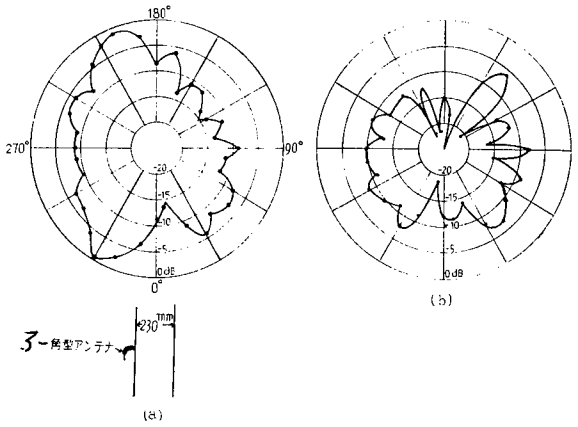

1-(a) 水平面内，水平偏波成分の指向特性　　2-(b) 水平面内，垂直偏波成分の指向特性

Fig. 10.

1) Directivity characteristics of the horizontal component of the polarization for the horizontal plane; 2) Directivity characteristics of the vertical component of the polarization for the vertical plane; 3) Pole antenna

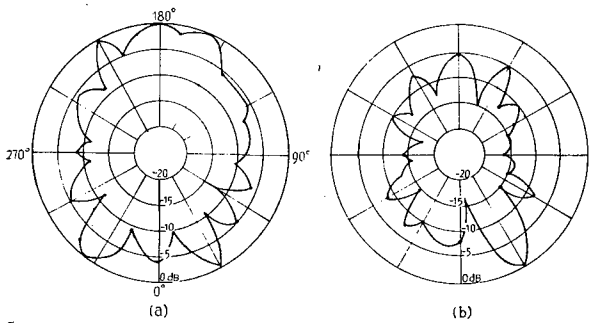

1-(a) 胴体径 180 mm 胴付長 1000 mm 上に角型アンテナを第1図のように取付けた時の水平面内輻射パターン　直線偏波アンテナにて測定

2-(b) 胴体径 180 mm 胴体長 1000 mm 上に角型アンテナを第1図のように取付けた時の水平面内輻射パターン　円偏波アンテナにて測定

Fig. 11.

1) Radiation pattern of the pole antenna which is mounted on the body, 180 mm in diameter and 1000 mm in length. The pattern is measured with linear polarization antenna; 2) Radiation pattern of the pole antenna which is mounted on the body, 180 mm in diameter and 1000 mm in length. The pattern is measured with the circular polarization antenna

distance between the antennas caused by the spin of rocket when the diameter of the rocket is small. So, the pole antenna is a convenient antenna to use. However, it has the disadvantage that it can have a weak radiation rearward for a rocket which has a rapid change in shape; since the antenna is mounted at the body and radiates to the rear direction, the radiation pattern is disturbed by the tail when a rocket has tails.

We will develop tail antenna for a tailed rocket and body antenna for a non-tail rocket.

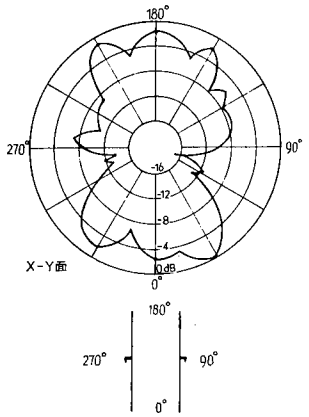

Fig. 12. Directivity characteristics of E_θ for the K-9M type antenna for the horizontal plane

3. Level Change due to the Motion of Rocket

Figure 13 shows the receiving level changes due to the flight of the K-8-11 type space rocket. One may find the level changes together with the relative position change of the mounted antenna as a function of spin and attitude change of the rocket. The receiving level changes from the K-8L-1 type pole antenna are shown in Fig. 14. Comparing the two figures, we know that the receiving level change from the pole antenna due to the spin of the rocket is several $d\beta$ larger than that from the notch antenna of the K-8 type. When double antennas are mounted on a rocket, the phase effect appears due to the changes in the relative distance of the two antennas, and there appears a pattern cut-off which is proportional to the frequency of spin. The amount and frequency of the level change due to the spin motion of the rocket are really important in actual application.

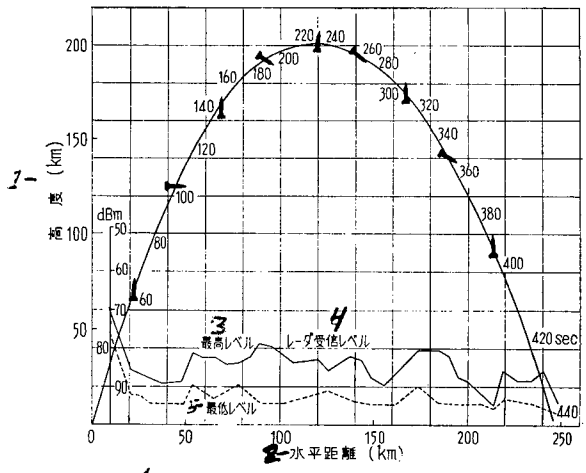

Fig. 13. Records of receiving levels from the K-8-11 type space rocket.

1) Altitude; 2) Horizontal distance; 3) Maximum level; 4) Radar receiving level; 5) Minimum level; 6) Attitude of the rocket is determined based on the results of the geomagnetic aspect meter measurement

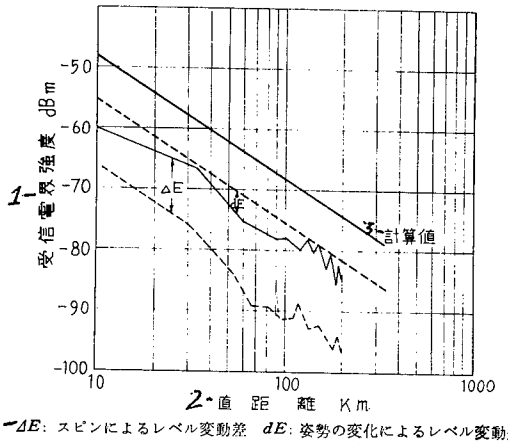

Fig. 14. Records of the receiving levels from the K-8L type space rocket.

1) Intensity of receiving wave; 2) Straight distance; 3) Calculated value; 4) ΔE: level change by spin, dE: level change by different attitude

4. Conclusion

Along with the larger and longer distance rockets of the future, the receiving level changes caused by the attitude of the rocket or the spin motion of the rocket will become a very important problem. Now, we have no definite basis for it. However, it will be convenient to classify space rockets in two categories: one, a rocket that has high-speed spin motion, and the other, a rocket that has low-speed spin motion. For the former type of space rocket, it will be better to design a single element antenna which can cover all direction of the rocket and to take the advantage of the radiation pattern cut-off. To do this, we can avoid the unnecessary increase of the number of changes in the receiving level. For the latter space rocket, multiple element antennas will be more suitable. And in this connection, the relationship between the number of receiving level changes and the frequency of the conical scanning of the receiving side's parabolic antenna on the ground; the method of power supply to the multiple antenna; and the high-speed scanning method should be studied.
We wish to thank Mr. Kurimoto, Akehoshi Electric Co., who designed and manufactured the antennas, and the members of Prince Automobile Industrial Co.

(Received on April 1, 1963)

REFERENCES

1. Kaneyuki Kurokawa, Tokuzo Suda and Nagao Abe, Prod. Research, Vol. 8, No. 6, p. 31, October 1956.

2. Kaneyuki Kurokawa, Tokuzo Suda, Nobuji Urimoto, Prod. Research, Vol. 10, No. 10, p. 42, October 1960.

3. Kaneyuki Kurokawa and Tamiya Nomura, J. Soc. Elec. Comm., Reference on Special Committee on Aerodynamic Electronics Equipment Research, April 1959.

4. Kaneyuki Kurokawa, Hideyo Nagatomo and Huzio Yamamoto, Prod. Research, Vol. 9, No. 4, April 1957.

ROCKET TRAJECTORY PLOTTED BY RADAR

By Radar Research Team: Noboru Tagaki,
Narihumi Saito, Motomi Nagatani,
Toshimichi Kameo, Mitsum Ichigawa,
Minom Sekikuch and Tatake Kurashige

1. Introduction

The rocket trajectories described in this report are the radar-plotted trajectories of Kappa series rockets, which had been launched at Michigawa Test Center and Kagoshima Space Center during July 1961 to December 1962.

2. Method of Plotting and Changes in Ground Facilities

The structure and the operation of the tracking radar were already reported on under other subjects in this issue and we will describe briefly some of the newest changes and other auxiliary equipment.

The rocket trajectories up to May 1962 (K-8-10 type space rockets) are the data for the rockets which were launched at Michigawa Test Center, Akita Province; and those from August 1962 (K-8L-1 to K-8-11 type space rockets) were launched at Kagoshima Space Center. For the Kagoshima Space Center, the following correction calculations should be considered for terrain condition. These calculations could be ignored at Michigawa Test Center.

$$\begin{cases} x = x_0 - r'' \sin \psi' \\ y = r'' \cos \psi' - y_0 \\ z = r' \sin \theta' + z_0 \end{cases}$$

For $r_0 = 0.3$ km and $\delta = 78°49'$

$$x_0 = r_0 \sin \delta = 0.29 \text{ km}$$
$$y_0 = r_0 \cos \delta = 0.06 \text{ km} \quad z_0 = 0.3 \text{ km}$$

r' = distance between radar and $r'' = r' \cos \theta'$.

R: radar point, L: launcher point. The difference of the elevations between the radar point and launcher point is ignored.

The angle of elevation, azimuth angle, and distance from the radar point to the rocket are substituted into the above equations and give the trajectory of the rocket.

With larger rockets, longer range-tracking was required and many modifications and improvements of ground radar facilities were made to extend plotting ability.

In addition to the radar system, an automatic tracking and range measuring system was installed. Through this system, the measurable range was extended and the measurement made automatic. Conventional systems could measure the range up to 400 km, but with the new one, about 600 km became the limit. And the former system had an 8-mm movie camera to record the data and the camera had 430-440 sec of operation-time limitation. Therefore, the system could not track longer than for that time period. But the new system has a recorder and the recorder types out the data without being limited by a time period.

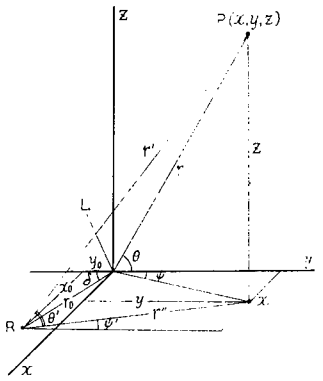

Fig. 1

At another ground facility, a new large automatic-tracking radar system with a parabolic antenna of 4 m in diameter was installed. Since the details of the radar system will be reported on page 186 of this issue, only its characteristics are introduced below.

(1) It can track a rocket which is 1,500 km away. For this, it needs 500 kw of transmission power.

(2) It responds extremely rapidly and has the ability to track every kind of rocket. Maximum tracking speeds are 60° per sec on azimuth axis, 30° per sec on elevation axis, and 25 km per sec for range.

(3) It can be used not only as a secondary radar but also as a primary radar. The switch from secondary to primary or from primary to secondary

Table 1

Data on the Launched Rockets, K-8-8 to K-8-11 Types

1 ロケット名称 カッパ型号	2 打上げ日時 年月日 時分	10 地上風 方向 風速 m/sec 天候	13 発射仰角 度	14 パラボラ待受角 (度) [方位待受角 (度)]	16 航跡標定結果概要 17 頂点 時間 sec	頂点 高度 km	頂点 水平距離 km	18 着水点 時間 sec	着水点 水平距離 km	24 備考
K-8-8	36.10.24 12.59	11 N4* くもり	81	73	230	198.0	143.9	435	288.4	道川 全装置正常
K-8-9	36.10.30 20.13	12 SE4 晴	80	72	216	174.6	102.4	407	207	道川 8ミリカメラ故障 トランスポンダ正常
K-9L-2	36.12.26 14.50	11 NNW5 くもり	80	70	310	347.6	331.0	581.4	625	道川 GMD1 と 4mφ 新型レーダ 同時追跡
K-8-10	37. 5.24 19.05	—	81	73	—	—	—	—	—	道川 正常飛しょうせず
K-8L-1	37. 8.23 16.15	12 0 晴	80	15 76 [Nより CW 129]	203	172.3	82.0	—	(152)*	鹿児島 発射方向Nより CW 132°39′ 270sec にてトランスポンダ電波途絶
K-9M-1	37.11.25 11.01	11 NNW くもり	78	15 73 [Nより CW 123.5]	115	56.0	26.0	229	52.7	鹿児島 発射方向Nより CW 125°30′
K-8-11	37.12.18 14.03	12 W1 晴	79	15 74 [Nより CW 138]	231	202.1	120.0	443	248.0	鹿児島 発射方向Nより CW 150°

32-* ( ) 内の数値は推定値を示す. 33-* N4 は北の風 4 m/sec を示す.

1. Type of rocket
2. Date and time of launching
3. 12:59 Oct. 24, 1961
4. 20:13 Oct. 30, 1961.
5. 14:50 Dec. 26, 1961
6. 19:05 May 24, 1962
7. 16:15 Aug. 23, 1962
8. 11:01 Nov. 25, 1962
9. 14:03 Dec. 18, 1962
10. Direction and speed of surface wind; weather condition
11. Cloudy
12. Clear
13. Angle of elevation of the launching, degrees
14. Preset angle of parabolic antenna (degree); [preset azimuth angle (degree)]
15. [N to CW (clock-wise)]
16. Data for trajectory plotting
17. Peak point
18. Impact point
19. Time
20. Altitude
21. Horizontal distance
22. Time
23. Horizontal distance
24. Remarks
25. At Michigawa: All devices were normal
26. At Michigawa: 8 mm camera had trouble; transponder was normal
27. At Michigawa: GMD1 and new 4 mφ radars were used to track
28. At Michigawa: No normal flight
29. At Kagoshima: Launching direction N to CW 132°39'; at 270 sec after the launch, the radar transponder signal was cut off
30. At Kagoshima: Launching direction N to CW 125°30'
31. At Kagoshima: Launching direction N to CW 150°
32. *The value in the parentheses is the estimated value
33. *N4 means wind of 4 m/sec from north

is made without delay. The transmitting frequency at the ground is automatically converted to receiving frequency.

(4) Conversion of the transmitting frequency and the conversion of the polarization to circular and linear polarizations could be made automatically.

(5) The frequency is 1,680 Mc/s, as before.

(6) The trajectory of a rocket is immediately drawn on graph paper.

3. Results of the Trajectory Plotting

The rockets and its flight results are shown in Table 1. The launching direction at Michigawa Test Center was exactly to the west (4° W to N in magnetic coordination). The launch direction of each of the three rockets which were launched at Kagoshima Space Center took slightly different directions because of topographical conditions.

The times in the tables are the time period from the moment when the ignition switch to the igniter of the rocket was turned on (time = 0). The angle of elevation of the launch is the elevation angle of the launcher. The preset angle of the parabolic antenna means the angle which is set on the parabolic antenna to track the launched rocket from the time a few seconds after it leaves the launcher. The impact point indicates the time when the transponder lost the signal from the rocket, and the distance at which the transponder lost the signal. Tables 2 and 4 show the altitude and horizontal distance vs. time for a particular rocket. The deviating distance from the launch direction in Table 4 means how many kilometers the rocket had deviated from the launch direction at the moment.

Table 5 shows the trajectories of small-type rockets. The results of the tables are shown in Figs. 2, 3 and 4.

The transponder of the K-8L-1 type space rocket was cut off 270 seconds after the launch and hence the signals could not be received by the receiver. But the remaining portion of the trajectory could be estimated because the accident occurred after the rocket had reached maximum altitude.

In case of the K-8-9 type space rocket, the transponder was operating normally but the 8 mm camera was in trouble until 350 seconds after the launch. However, the missing portion of the trajectory could be estimated from the remaining trajectory and the horizontal distance flown.

In small rockets, the FN-150 was launched to determine the flying characteristics of a four-nozzle engine rocket; the RT-150, RT-75-1, -2, and--3 type rockets were launched to test the new type radar; and the SP-150-3 and -4 type rockets were launched to find the spin characteristics of the low-spin Lambda-

Table 2

Trajectories of Kappa Series Rockets

2 2-( ) 内はトランスポンダ電波途絶秒時を示す

時間 sec	K-8-8 高度 km 3	K-8-8 水平距離 km 4	K-8-9 高度 km 3	K-8-9 水平距離 km 4	K-8L-1 高度 km 3	K-8L-1 水平距離 km 4	K-9M-1 高度 km 3	K-9M-1 水平距離 km 4	K-8-11 高度 km 5	K-8-11 水平距離 km 4
0	0	0	0	0	0	0	0	0	0	0
10	—	—	—	—	6.6	1.7	—	—	—	—
20	12.8	3.4	12.3	2.6	14.8	3.5	12.9	3.3	12.6	3.0
30	19.0	5.4	18.7	4.1	34.0	7.9	21.8	5.9	19.9	5.0
40	30.4	9.5	28.4	7.1	51.7	13.0	29.3	8.3	32.9	9.1
50	47.7	16.2	44.5	12.3	66.3	17.4	36.1	10.5	50.0	14.9
60	63.8	23.2	60.0	17.6	80.1	21.6	41.5	12.8	66.7	21.0
70	79.5	30.4	74.2	22.7	93.0	25.8	46.6	15.5	86.8	26.4
80	95.0	37.8	87.6	27.9	104.5	30.0	50.0	17.7	96.4	32.2
90	107.4	44.3	99.7	33.7	115.3	34.2	53.0	20.4	109.8	37.5
100	120.0	51.2	110.9	39.1	125.1	38.7	54.7	22.7	122.9	43.2
110	131.8	58.4	121.5	44.2	133.8	43.0	55.4	24.7	134.4	48.1
120	142.1	65.4	131.0	50.0	141.7	47.2	55.4	27.0	145.0	53.8
130	152.1	71.9	139.6	55.0	148.8	51.8	54.5	29.6	155.1	59.5
140	160.8	79.1	147.0	60.9	154.7	56.0	52.5	32.2	164.0	65.2
150	169.1	86.2	153.7	66.2	160.5	59.1	49.6	34.6	172.0	72.0
160	175.9	93.1	159.2	71.9	164.3	64.7	45.4	37.2	179.0	77.8
170	181.7	100.3	163.9	76.8	167.5	68.7	41.1	39.5	184.6	84.0
180	186.5	108.1	167.9	82.6	169.8	72.4	35.2	41.9	190.0	90.0
190	190.3	115.0	171.2	87.2	171.6	76.4	30.0	43.7	194.3	96.3
200	193.9	122.1	172.8	93.5	172.1	80.3	22.7	46.4	197.5	101.1
210	196.3	129.4	174.2	99.4	172.1	84.3	15.0	48.7	199.6	107.4
220	197.9	136.5	174.5	104.3	170.9	88.6	0	52.7	201.2	113.8
230	198.0	143.9	173.5	110.5	169.0	92.2			202.1	119.5
240	197.3	151.4	171.5	116.1	166.0	96.2			201.3	125.7
250	196.3	158.4	169.9	121.6	161.7	100.6			200.0	132.5
260	193.2	166.2	165.6	127.1	156.8	104.6			198.2	137.7
270	190.1	173.0	159.7	134.0	151.1	108.5			195.0	143.7
280	186.4	180.0	155.9	137.9					191.2	149.4
290	181.1	187.5	149.1	144.0					185.9	156.0
300	175.2	194.6	142.0	149.7					180.0	162.0
310	167.9	202.3	133.5	155.8					173.7	167.8
320	160.4	209.1	124.8	160.8					166.2	173.9
330	151.5	216.4	114.0	165.5					158.6	179.2
340	141.4	223.7	102.7	171.5					149.5	184.6
350	130.6	230.7	90.4	177.3					140.5	190.0
360	118.6	238.0	—	—					129.8	196.0
370	106.5	245.1	—	—					119.9	201.0
380	92.5	252.7	—	—					108.0	207.2
390	76.6	260.5	—	—					93.0	214.2
400	62.7	267.6	(407sec) 0	207					80.2	220.0
410	45.4	274.1							61.9	227.6
420	31.5	281.0							43.1	234.9
430	13.5	286.7							21.1	241.1
440	(435sec) 7.6	288.4							4.3	246.7
450									(443sec) 0	248.0

Table 2 (Cont'd.)

1) Value in the parentheses indicates the time when the transponder signal was cut off;
2) Time; 3) Altitude; 4) Horizontal distance

Table 3

Deviating Distance From the Launch Direction

1

時間 sec	K-8-8 km	K-8-9 km	K-8L-1 km	K-9M-1 km	K-8-11 km
0	0	0	0	0	0
20	N 0.8*		N 1.7		N 0.1
40	2.4		3.1	S0.1	0.5
80	10.3		3.0	0.3	
120			2.4	0.4	0.7
160	27.6	N 2.3	3.1	1.0	1.1
180			3.2	1.2	
220	34.0	3.6	3.3	(229sec) 1.7	1.2
260	49.0		1.1		1.3
300		5.0	(270sec) 0.8		1.4
340	63.5				
380		5.9			1.5
420	(435sec) 81.9	(407sec) 6.0			(443sec) 1.8

2 * N 0.8 は発射方向より北へ 0.8 km ずれたことを示す

1) Time; 2) *N 0.8 means the rocket drifted 0.8 km north from the launch direction

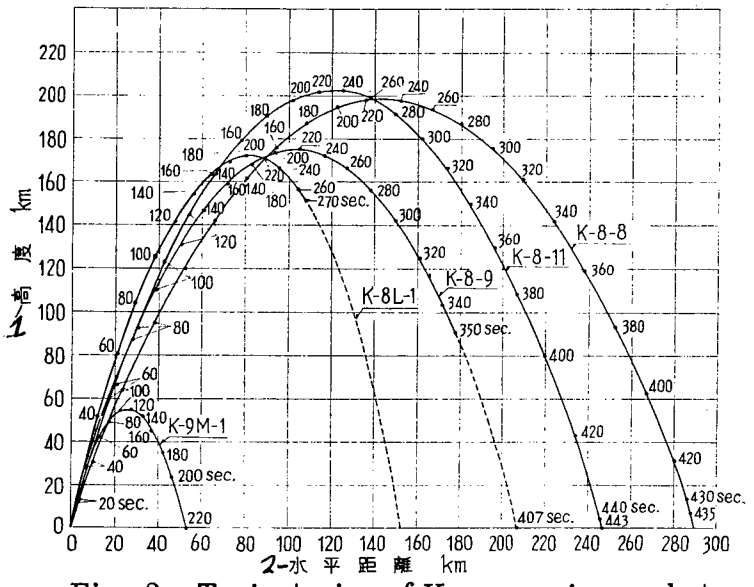

Fig. 2. Trajectories of Kappa series rockets

1) Altitude; 2) Horizontal distance

Table 4

Trajectory of the K-9L Type Space Rocket

1	K-9L-2			1 時間	K-9L-2		
sec	2 高度 km	水平距離 3 km	偏差距離 4 km	sec	高度 2 km	水平距離 3 km	偏差距離 4 km
0	0	0	0	300	347.5	318.4	77.0
10				310	347.6	331.0	
20	11.8	3.4	N 0.8	320	346.8	343.2	83.0
30	18.1	5.8		330	345.3	355.1	
40	27.9	9.8	2.2	340	343.4	366.9	88.8
50	43.9	16.8		350	340.2	379.2	
60	67.3	28.2	6.5	360	335.6	391.5	96.0
70	89.4	39.8		370	330.3	403.5	
80	111.2	52.3	12.2	380	324.6	415.4	102.6
90	131.7	64.5		390	317.4	427.4	
100	151.6	76.9	18.0	400	309.8	439.2	108.5
110	168.4	88.0		410	300.9	451.2	
120	186.1	100.2	23.6	420	291.5	462.9	114.3
130	203.0	112.1		430	280.8	474.8	
140	218.7	124.2	29.2	440	269.6	486.4	120.1
150	~~233.~~5	136.4		450	257.0	498.0	
160	247.5	148.1	34.8	460	243.2	510.0	126.0
170	260.7	160.8		470	228.9	521.6	
180	273.8	172.5	40.3	480	213.2	533.0	131.6
190	284.6	184.1		490	198.0	544.1	
200	295.4	197.0	46.0	500	181.4	555.0	137.1
210	303.9	208.8		510	164.5	566.1	
220	312.2	221.1	52.4	520	146.0	577.0	142.5
230	320.0	233.1		530	128.1	587.7	
240	326.0	245.8	59.1	540	108.8	598.6	147.9
250	331.4	258.0		550	87.8	609.5	
260	336.4	270.5	65.4	560	67.4	620.0	153.1
270	340.9	282.0		570	45.2	630.8	
280	343.6	294.5	71.2	580	22.4	641.0	158.3
290	346.2	306.3					

1) Time; 2) Altitude; 3) Horizontal distance
4) Deviating distance

Table 5

Trajectory of Small-Type Rockets

名称	FN-150		RT-150		RT-75-1		RT-75-2		SP-150-3	
発射日	1961.10.26		1961.12.20		1961.12.18		1961.12.18		1962.11.21	
時間	11.43.		15.05.		10.52.		12.27.		15.09.	
発射角	45°		48°		45°		60°		60°	
時間 sec	高度 km	水平距離 km	高度 km	水平距離 km	高度 km	水平距離 km	高度 km	水平距離 km	高度 km	水平距離 km
0	0	0	0	0	0	0	0	0	0	0
10	3.0	3.1	4.4	5.2					3.2	2.4
15	3.5	4.4	5.1	6.1					4.3	3.3
20	3.9	5.6	5.4	6.8	2.0	3.5	3.0	2.7	5.0	3.9
25	4.4	6.5	5.4	7.4	1.8	4.4	2.9	3.2	5.6	4.5
30	4.6	7.4	5.2	7.8	1.4	5.1	2.7	3.7	6.0	5.1
35	4.4	8.2	4.8	8.2	0.9	5.6	2.3	4.2	6.0	5.8
40	3.9	8.9	4.3	8.4	(39.5sec) 0	6.0	1.7	4.7	5.8	6.4
45	3.2	9.6	3.6	8.7			0.9	5.1	5.5	6.9
50	2.5	10.2	2.9	8.8			(48.5sec) 0	5.3	5.0	7.5
55	1.7	10.8	2.1	9.0					4.4	8.0
60	0.7	11.2	1.2	9.0					3.5	8.5
65	(61.3sec) 0	11.8	(64.5sec) 0	9.0					2.4	8.9
70									1.0	9.2
75									(73sec) 0	9.25

1) Type of rocket; 2) Launch date; 3) Launch time; 4) Launch angle; 5) Time; 6) Altitude; 7) Horizontal distance

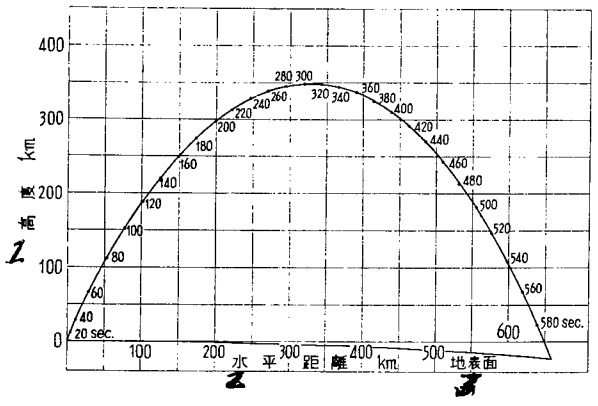

Fig. 3. Trajectory of the K-9L-2 type space rocket

1) Altitude; 2) Horizontal distance; 3) Surface of the earth

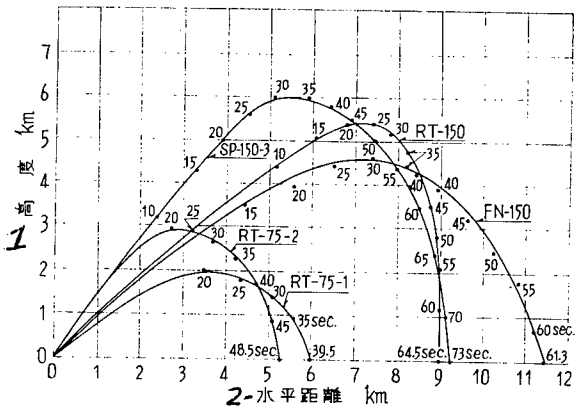

Fig. 4. Trajectories of small-type rockets.

1) Altitude; 2) Horizontal distance

4. Conclusions

In this report, the results of the trajectory plotting for the Kappa series space rockets, which were launched during the period from July 1961 to December 1962, are presented.

Recently, the ground facilities for radar and the radar transponder were quite improved; the plotting of the entire trajectory of a rocket became possible; and we could have confidence in the test.

The new radar system will have a great role in future rocket tests, particularly when space rockets are much larger.

We wish to thank Messrs. Hukushima, Urimoto, Simotoi and Komichi of Akehoshi Electric Co. for their help in the tests.

(Received on March 18, 1963)

REFERENCES

1. Prod. Research, Vol. 13, No. 10.

2. SE Note Akita No. 25, New Type Automatic Tracking Radar System.

SAFETY OPERATIONS AND THE SO-150 TYPE ROCKET

By Tamiya Nomura, Iwaho Yoshiyama
and Hi-iro Nakamura

1. Introduction

The safety operation (SO) research team was organized to perform extensive technical studies to improve the safety and reliability of rocket launchings, to provide for future rocket launchings of large type space rockets, and to provide for the safety of the dense population in Japan against rocket mishaps, as it was stated by Itogawa on page 49 in this issue. There are two aspects to the problem of securing safety in rocket launchings, that is, the passive and active aspects. The former aspect includes preventative action against possible damage to people, livestock or property in or around the test site. For this, some preparations such as appointment of safety officers in observation teams, preparation of protection facilities, and increased fire-fighting facilities were already made. The latter aspect includes establishing measures which can effectively minimize the damage from a possible accident. For instance, it would be an active measure to analyze a safety system such as command destruction, and develop and adopt a similar system which is more effective for our own test ground conditions.

With our present ignition system for rockets, it is almost impossible to prevent damage from any accident if the accident occurs after the ignition switch is turned on. If it is possible to prevent the ignition of the second-stage rocket in multi-stage rockets when the first stage rocket's combustion condition is abnormal or its flying condition is dangerous, the damage can be minimized. The first approach of the safety operation plan is along this line.

2. Technical Problems in SO Plan

Present SO plan which was made by SO team is as follows:

First, the emergency detector (ED) detects whether the combustion of the first-stage rocket is normal or not. If the combustion condition is normal, ED starts the electronic timer (ET) for the second-stage rocket-engine ignition. A certain time later, the ignition circuit for the second stage rocket engine will be connected. The delay tube and pressure switch are also independently used for the ignition.

The rocket carries a remote command system (CM). If the rocket flight does not follow the predetermined course or the combustion condition of the first-stage engine is not normal, CM, which is controlled by ground operator, cuts off the power source of the ignition circuit of the second-stage rocket. However, the first-stage rocket take-off from the main rocket is performed regardless of the flight condition.

The above functions and procedures are shown in Fig. 1. As shown in the figure, ED or CM will prevent ignition of the second-stage rocket engine when the combustion condition of the first-stage rocket engine is not normal or the flight condition is not normal, even if the combustion condition is good.

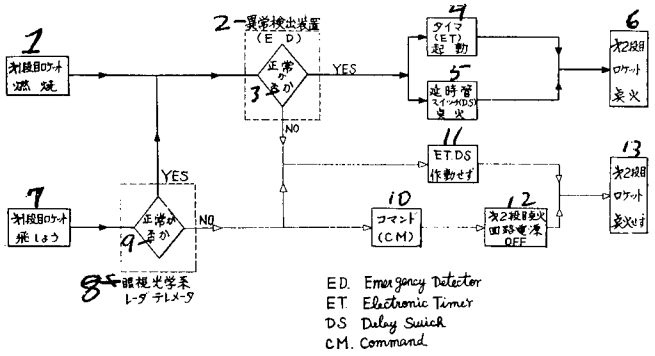

Fig. 1

1) Combustion of first-stage rocket engine; 2) Emergency detector; 3) Normal ?; 4) Electronic timer, start; 5) Delay tube, ignite; 6) Second-stage rocket engine, ignite; 7) First-state rocket, flight; 8) Observe, optic system and radar transponder; 9) Normal ?; 10) Command system; 11) ET and DS don't work; 12) Power source of the second-stage ignition circuit, cut-off; 13) Second-stage rocket engine, no ignition

3. SO-150-1 Type Rocket

In order to test the technical research results for the SO plan, we manufactured a small 150-type rocket and it was called SO-150-1 type rocket.

(1) Emergency detector. First, we had to decide how we were to know when an abnormal condition occurred. We thought we could be almost certain to detect the condition of the rocket from the combustion pressure vs time curve of the first-stage rocket (which was determined during ground combustion tests). This method was adapted to the SO -150-1 type rocket.

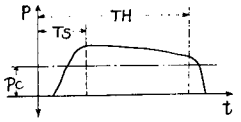

Fig. 2

In Fig. 2, T_S, T_H and P_C are the predetermined values. At $T_S < t < T_H$, if the pressure P is greater than P_C, the combustion is abnormal, and the relay to cut off the power source of the ignition circuit is started. The following are included in the emergency detector:

(a) Bourdon-gauge-type pressure detector with switch
(b) Semi-conductor strain-gauge-type pressure detector
(c) T_S and T_H generating circuits
(d(P and P_C comparison circuit
(e) Relay circuit

Detecting conditions for the rocket are as follows:

P_H: If P rises above P_H, the second-stage ignition circuit is cut off.

P_L: If P falls below P_L, the second-stage ignition circuit is cut off.

P_C: It is the reference point for the semiconductor pressure detector, and the timer of the second-stage ignition system starts when P reaches P_C.

T_S: Delay time from the ignition of the first-stage engine to the start of the power comparison circuit.

T_H: The time from the ignition of the first-stage engine to the moment when the pressure reaches 75% normal pressure.

Figure 3 is the diagram of the emergency detecting circuit. Figure 4 shows estimated outputs from each circuit and the relationships between the circuits.

(2) Electronic Timer. This device performs the same function as the conventional delay igniter, that is, it gets a signal from ED and starts the relay which ignites the igniter of the second stage-rocket engine at a predetermined time.

Among the many kinds of electronic timers, the unijunction transistor type timer was selected because the timer can be safe, reliable and small if the circuit constants are given adequate values. The outline of the circuit is shown in Fig. 5.

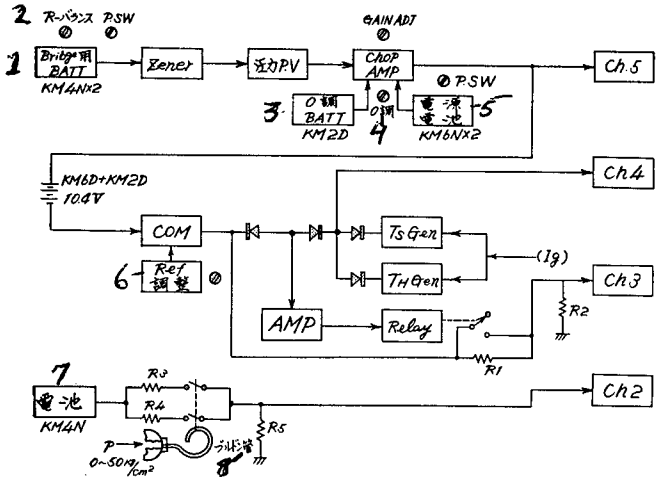

Fig. 3. Block diagram of ED of SO-150-1 type rocket.

1) Battery for bridge; 2) R - balance; 3) 0 - balance battery; 4) 0 - balance; 5) Source battery; 6) Reference balance; 7) Battery; 8) Bourdon gauge

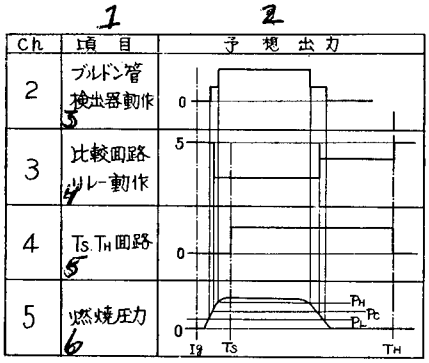

Fig. 4

1) Functions; 2) Estimated output; 3) Bourdon gauge detector starts; 4) Comparison circuit relay start; 5) T_S, T_H circuit; 6) Combustion pressure

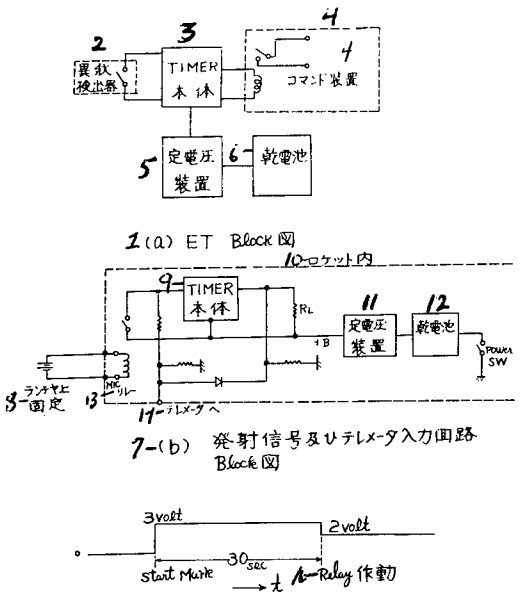

Fig. 5

1) Block diagram of ET; 2) ED; 3) Timer; 4) Command system; 5) Constant voltage generator; 6) Battery; 7) Launch signal and telemetry input circuit block diagram; 8) Fixed at launcher; 9) Timer; 10) Inside of rocket; 11) Constant voltage generator; 12) Battery; 13) MC relay; 14) To telemetry; 15) Telemetry input voltage; 16) Relay starts

(3) Telemetry. The telemetry is the same type used in the K-8L-1 type space rocket. It is five-channel transmitter and uses a body antenna.

Transmission mode	FM-FM
Carrier frequency	225 Mc
Carrier frequency shift	±100 kc
Carrier output	0.5 w
Input signal	0-5 v DC
Input impedance	Above 200 kΩ

Table 1

Secondary Carrier Center Frequency and Frequency Distribution to Channels

Ch	中心周波数	レスポンス	測 定 項 目
1	2,300 c/s	35 c/s	電子式タイマ
2	3,000	45	ブルドン管検出器
3	3,900	60	比較回路
4	5,400	80	T_S, T_H 回路
5	7,350	110	燃焼圧力

1) Center frequency; 2) Response; 3) Circuit to be measured; 4) Electronic timer; 5) Bourdon-gauge detector; 6) Comparison circuit; 7) T_S, T_H circuit; 8) Combustion pressure

(4) SO-150 type rocket. It is a single-stage rocket of 160 φ outside diameter. In order to find the performance of the SO system, we used a propellant with a long combustion time. Fig. 6 shows the outline of the rocket and the layout of the devices.

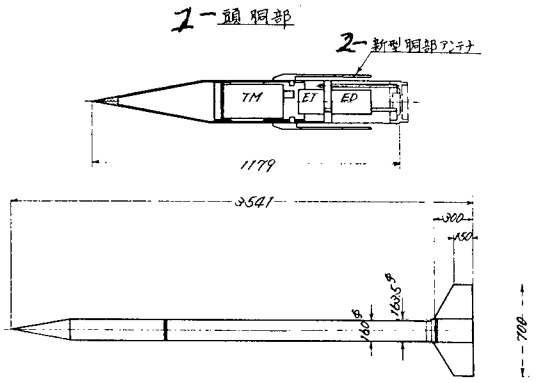

Fig. 6. SO-150-1 type rocket

1) Forward; 2) New body antenna

4. Test Results

(1) Bourdon-gauge-type pressure detector with switch. It did not operate. The cause may be either that the detector was broken or the circuit was disconnected by the launch acceleration.

(2) Semiconductor strain-gauge-type pressure detector. From the telemetry record, we knew the detector's operation almost agreed with that predicted.

(3) T_S, T_H generating circuits. The reason that neither of the circuits worked could be that neither received the starting signal disconnection of the lead or the signal was sent after launch. In any case, it is important for future tests that a method able to transmit starting signals without fail be found.

(4) Comparison circuit. In both periods of pressure rise and pressure fall, the circuit functioned perfectly. We could not find from the record whether it started at a predetermined point because the pressure rise was too steep.

(5) Relay circuit. It was impossible to find the function of the relay because of T_S, T_H circuits' failure.

(6) Electronic timer. It was found from the record that the electronic timer functioned exactly at the preset time.

A portion of the telemetry record is shown in Fig. 7.

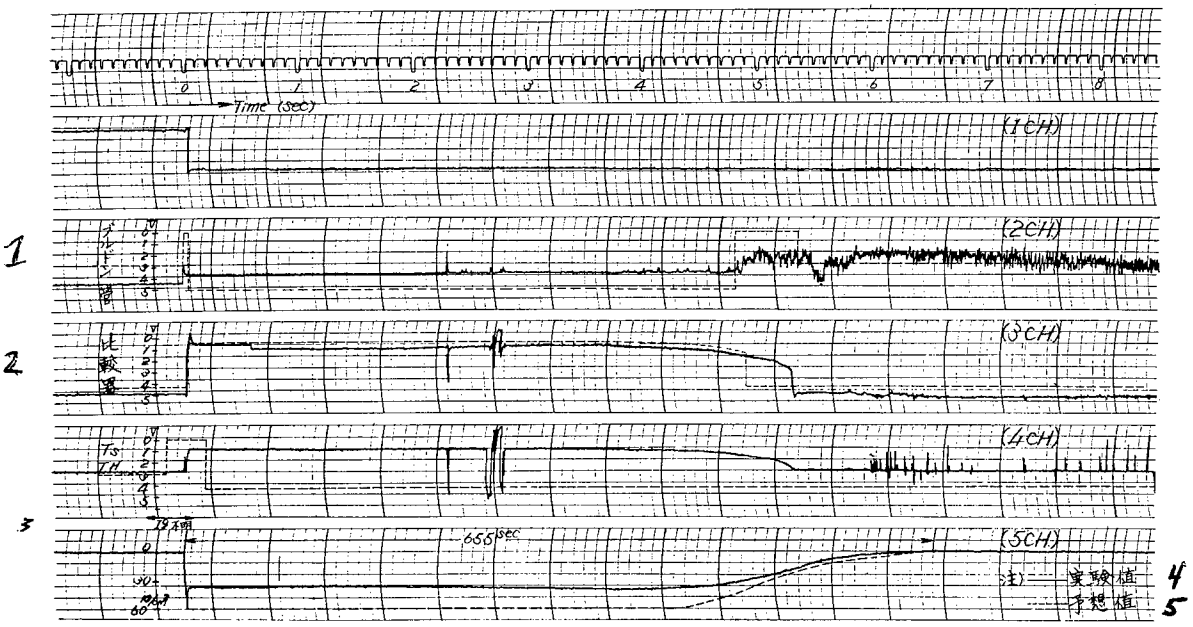

Fig. 7. Data from SO-150-1 type rocket test.

1) Bourdon gauge; 2) Comparison detector; 3) Ignition is uncertain; 4) Test value; 5) Predetermined value

5. Conclusion

An adequate system for safety operations can be made based on the reliability of the system. However, environmental considerations come first; and without knowing these, reliability cannot be found. In case of SO-150-1 type rocket, we found the problem was involved with the method of starting the emergency detector. But, it is impossible to say anything about the value of the emergency detector itself from this single test. And we have a schedule of SO-150-2 type rocket tests in April to test the command system and delay switch.

In order to overcome the limited launching space in this country, we have to depend on a well-developed safety operation plan. And we hope that we shall have the help we need in developing a highly reliable safety operation system.

(Received on April 27, 1963)

ACCELEROMETER AND ITS MEASURED RESULTS

By Iwaho Yoshiyama, Ensei Nakamura
and Motoyoshi Hayashi

1. Introduction

The accelerometer, which had been used in the tests from the HT-150 type rocket to the K-9M-1 type space rocket, is shown in Fig. 1. The theory and circuit of the accelerometer were reported on previously.

2. Measured Results

(1) HT-150 type rocket. It was launched at Akita Test Center at 11:34, May 29, 1962. We got a complete record from the launching to the landing at sea. Figures 1 and 2 show the accelerometer and its location in the rocket.

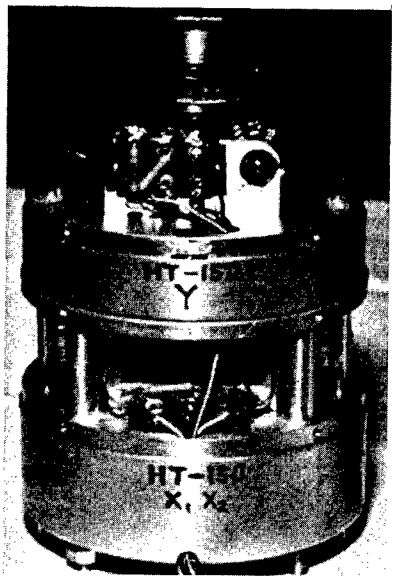

Fig. 1

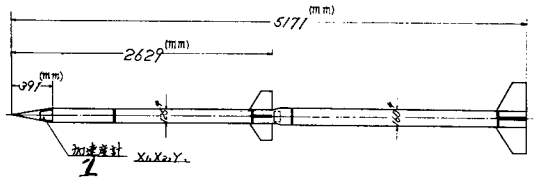

Fig. 2. Location of the accelerometer in the HT-150 type rocket

1) Accelerometer

Table 1

ロケットの種類	加速度計の種類		出力電圧 (V/g)	計測範囲 (g)	大きさ (m/m)	重量 (kg)	写真	加速度計搭載位置
HT-150	推進軸加速度計	X_1	0.09	0～ 53	109φ(max)×152	1.4	第 1 図	第 2 図
	推進軸加速度計	X_2	0.13	0～−37				
	横軸加速度計	Y	0.45	0～± 5				
K-8L-1	推進軸加速度計	X_1	0.09	0～ 52.5	132φ(max)×151	1.7	第 5 図	第 6 図
	推進軸加速度計	X_2	0.31	0～−11.3				
	横軸加速度計	Y	0.55	0～± 4				
K-9M-1	推進軸加速度計	X_1	0.09	0～ 55	122φ×61	0.8	第 10 図	第 11 図
	推進軸加速度計	X_2	0.35	0～−14				
	横軸加速度計	Y_1	0.65	0～±3.5	受感部 72φ×68 電源部 62φ×67	0.55		

19 —— 実測値
20 —— 計算値

計測結果

1. Type of rocket
2. Kind of accelerometer
3. Longitudinal accelerometer
4. Transverse accelerometer
5. Output voltage
6. Range of measurement
7. Size
8. Sensitive part
9. Power source part
10. Weight
11. Photograph
12. Fig. 1
13. Fig. 5
14. Fig. 10
15. Location of the accelerometer
16. Fig. 2
17. Fig. 6
18. Fig. 11
19. Measured value
20. Calculated value

It was found from the record that booster combustion, take-off and main-rocket combustion were normal.

The acceleration curve from the longitudinal accelerometer is shown in Fig. 3. The velocity curve, which was obtained from Fig. 3, is shown in Fig. 4. Some important values from the measured results are listed in Table 2.

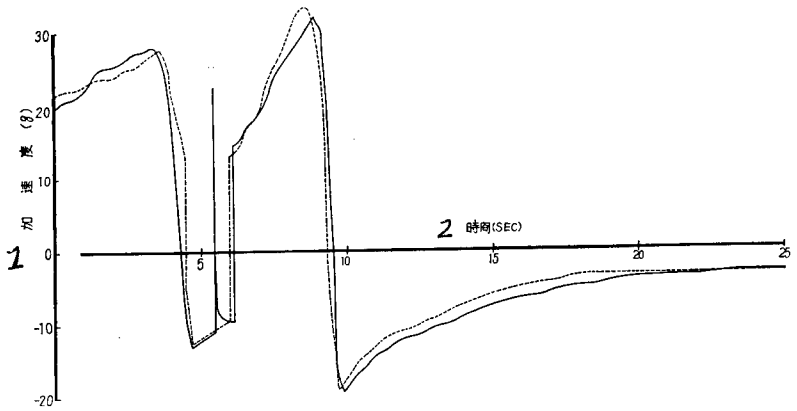

Fig. 3. Acceleration curve of HT-150 type rocket

1) Acceleration; 2) Time

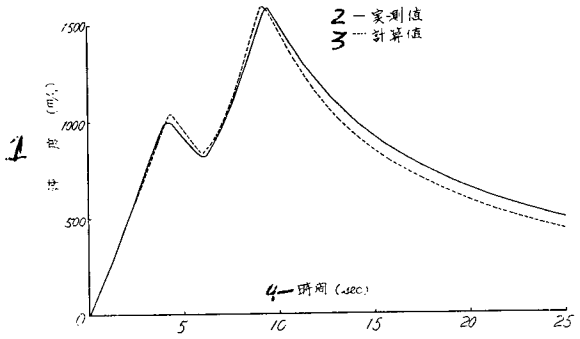

Fig. 4. Velocity curve of HT-150 type rocket

1) Velocity; 2) Measured value; 3) Calculated value; 4) Time

(2) K-8L-1 type space rocket. It was launched at Kagoshima Space Center at 16:15, August 23, 1962. Record was complete.

Its photograph and location are shown in Figs. 5 and 6, respectively. From the record, it was found that booster combustion, take-off, and main-rocket combustion were normal. The measured acceleration curve is shown in Fig. 7 and the velocity curve, which was obtained from Fig. 7, is shown in Fig. 8. Some important values from the measured results are listed in Table 3.

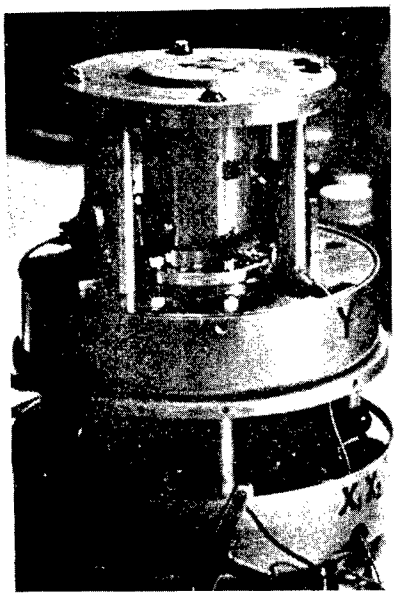

Fig. 5

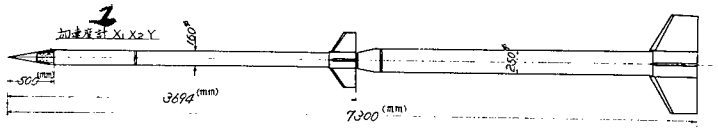

Fig. 6. Location of the accelerometer in K-8L-1 type space rocket

1) Accelerometer

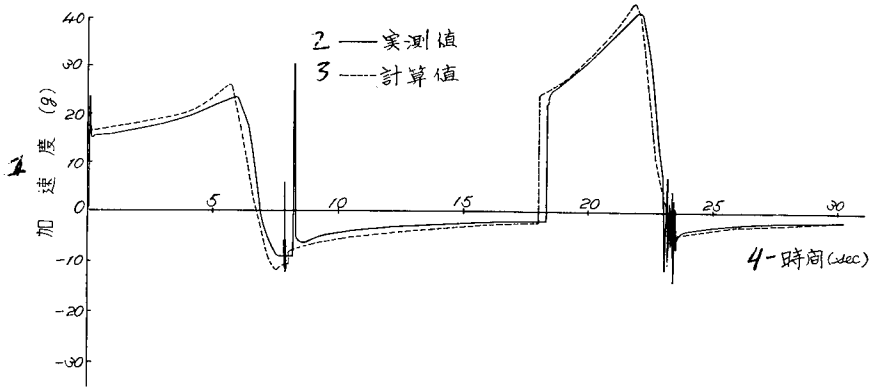

Fig. 7. Measured values of X_1 and X_2 for the K-8L-1 type space rocket

1) Acceleration; 2) Measured value; 3) Calculated value; 4) Time

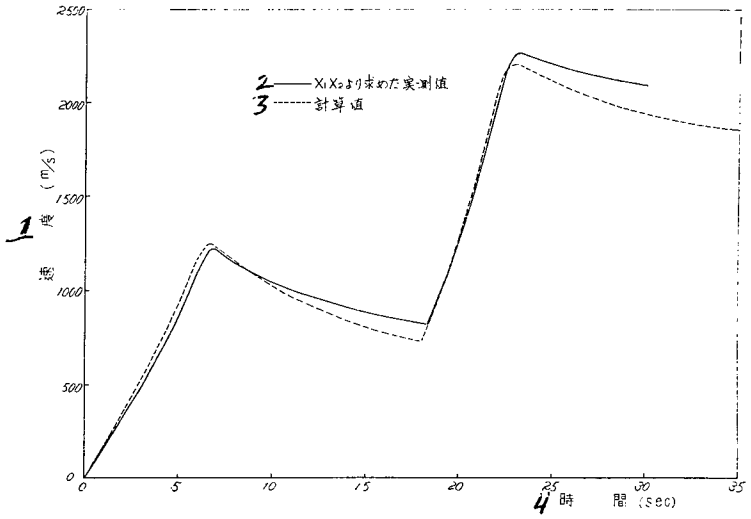

Fig. 8. Velocity curve for the K-8L-1 type space rocket.

1) Velocity; 2) Measured value (obtained from X_1 and X_2); 3) Calculated value; 4) Time

Table 2

		12 計測値	13 計算値および計画値
1—ブースタ	最大加速度 (g) 3	28.0	27.0
	最大減速度 (g) 4	−13.0	−12.6
	燃焼秒時 (sec) 5	4.7	4.6
	切断秒時 (sec) 6	5.45	5.0
	最大速度 (m/s) 7	995.0	1,040.0
2—メイン	点火秒時 (sec) 8	6.1	6.0
	最大加速度 (g) 3	32.0	33.3
	最大減速度 (g) 4	−19.3	−19.0
	燃焼秒時 (sec) 5	3.8	3.7
	点火時速度 (m/s) 9	820.0	835.0
	最大速度 (m/s) 7	1,580.0	1,590.0
	全飛しょう秒時 (sec) 10	141.0	142.0

1) Booster; 2) Main; 3) Max. acceleration; 4) Max. deceleration; 5) Combustion time period; 6) Take-off time; 7) Max. velocity; 8) Ignition time; 9) Velocity at the moment of ignition; 10) Total time of flight; 12) Measured value; 13) Calculated or preset value

Table 3

		計測値 (12)	計算値および計画値 (13)
1 ブースタ (1)	最大加速度 (g) (3)	23.6	26
	最大減速度 (g) (4)	−9.3	−12
	燃焼秒時 (sec) (5)	7.3	7.3
	切断秒時 (sec) (6)	8.23	7.5
	最大速度 (m/s) (7)	1,222.0	1,240.0
2 メイン (2)	点火秒時 (sec) (8)	18.32	18.0
	最大加速度 (g) (3)	41.2	43.0
	最大減速度 (g) (4)	−7.1	−8.8
	燃焼秒時 (sec) (5)	5.17	5.17
	点火時速度 (m/s) (9)	824.2	730.0
	最大速度 (m/s) (7)	2,260.6	2,210.0
	全飛しょう秒時 (sec) (10)	413.2	441.0

1) Booster; 2) Main; 3) Max. acceleration; 4) Max. deceleration; 5) Combustion time period; 6) Take-off time; 7) Max. velocity; 8) Ignition time; 9) Velocity at the moment of ignition; 10) Total time of flight; 12) Measured value; 13) Calculated or preset value

(3) K-9M-1 type space rocket. It was launched at Kagoshima Space Center at 11:01, November 25, 1962.

We obtained the entire record even though the main rocket did not ignite.

The accelerometer was placed at the parallel portion of the body of the main rocket, as shown in Fig. 10, unlike the previous ones which were placed at the front end of their main rocket.

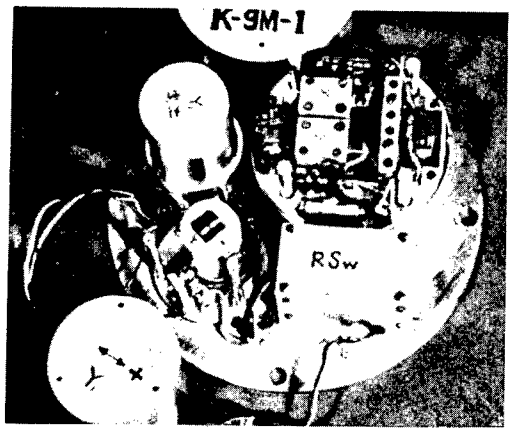

Fig. 9

The booster combustion and take-off were normal. Measured acceleration curve is shown in Fig. 11, and the velocity curve, which was obtained from Fig. 11, is shown in Fig. 12. Some important values from the measured results are listed in Table 4.

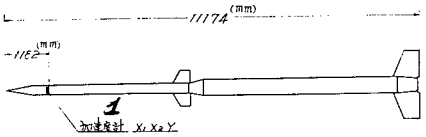

Fig. 10. Location of the accelerometer in the K-9M-1 type space rocket

1) Accelerometer

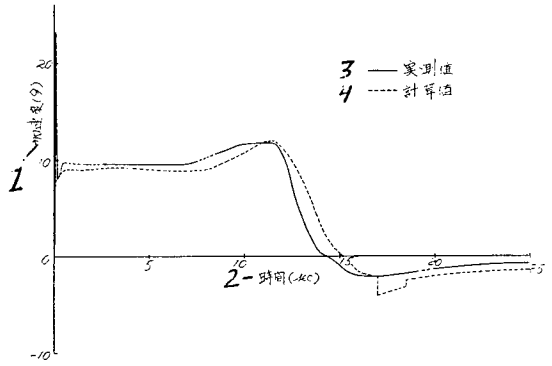

Fig. 11

1) Acceleration; 2) Time; 3) Measured value; 4) Calculated value

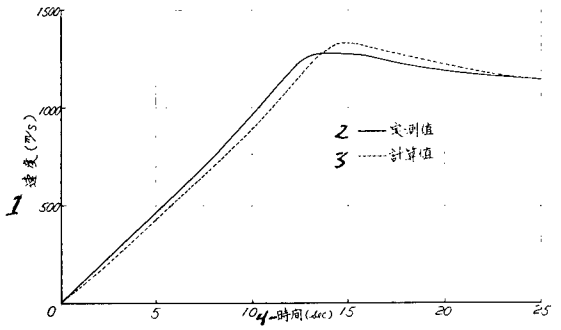

Fig. 12

1) Velocity; 2) Measured value; 3) Calculated value; 4) Time

Table 4

		9 計測値	10 計算値および計画値
1 ブースタ	最大加速度 (g) 2	11.7	11.9
	最大減速度 (g) 3	−2.1	−4.2
	燃焼秒時 (sec) 4	16.2	17.0
	切断秒時 (sec) 5	19.36	18.5
	最大速度 (m/s) 6	1,275.0	1,330.0
	開頭秒時 (sec) 7	45.66	46.0
	全飛しょう秒時 (sec) 8	229.22	

1) Booster; 2) Max. acceleration; 3) Max. deceleration; 4) Combustion time period; 5) Take-off time; 6) Max. velocity; 7) Time of nosecone opening; 8) Total time of flight; 9) Measured value; 10) Calculated or preset value

(Received on April 9, 1963)

REFERENCES

1. Miyazaki, Takeuchi, Imai, Ozka and Oya, J. Prod. Res. 13, 411, 1961.
2. H. Takeuchi, Rep. Ionos. Space Res. Japan 16, 64, short note, 1962.
3. G.H. Ludwig and W.A. Whelpley, J. Geophys. Res. 65, 1119, 1960.
4. W.J. Price, Nuclear Radiation Detection, 136, McGraw-Hill, 1958.
5. K.A. Anderson, Phys. Rev. 123, 1435, 1961.
6. J.I. Vette, J. Geophys. Res. 67, 1731, 1962.

THERMOMETER, STRAIN GAUGE AND TRANSVERSE ACCELEROMETER

By Sigeo Imazawa and Takemi Wanami

1. Introduction

Along with advances in space rockets have been requirements to re-evaluate temperature- and stress-measuring methods. Thermostat-type sensors were used as the temperature-detecting elements of the thermometers. However, the use of the thermostat is not good for temperatures above 350°; and to install the thermostat is another difficulty in the use of a thermostat. On the other hand, the thermoelectric method presents no problem. But it produces a very low signal output and therefore needs a highly sensitive amplifier. This is the reason a thermoelectric temperature-measuring device was not used for the rocket-mounted thermometer. However, the use of a thermoelectric thermometer did become possible with the current development of the transistor, chopper-type DC amplifier. The strain gauge also adopted the new amplification method. The new measuring devices were tested with the K-8L and K-9M space rockets and we got satisfactory results from the tests. For the measurement of transverse acceleration, accelerometer Y_1 was used. We also used a potentiometer-type accelerometer Y_2, which allowed us to compare readings from two different-type accelerometers on the flights of K-8-8, K-9L-2 and K-9M-1 type space rockets. Figure 1 shows the devices which were carried by the K-8L-1 type space rockets.

Fig. 1. Exterior of the devices

2. Thermometer

For rocket-carried thermometers, we used platinum-resistance type thermometers for the K-6 and earlier space rockets and thermostats for the K-8 and -9 type space rockets. These have been reported on previously [1, 2, 3]. Therefore, we will report only the newly developed thermoelectric devices which were used on the K-8L and -9M space rocket tests.

Because a thermostat has a large output voltage and therefore does not need an amplifier, many of the thermostats can be easily used in a rocket, and have been widely used. However, it was inevitable that the temperature-measuring method employing a thermostat be re-evaluated because it had limitations in its measurable temperature and also in its response-time to changes in temperature and adhesiveness to a metal surface. In advance of our re-evaluation, we got suggestions from engineers Nakamura and Kawashima with respect to modifying the method of adhesion of the thermostat. We followed their advice in attaching a thermostat on the HT-150 type rocket, which was tested to get data on aerodynamic heat for the subsequent tests of the K-8L and -9M space rockets. HT-150 had ten temperature-measuring points, and one thermostat was attached by mechanical pressure with asbestos and aluminum plate. The test results are shown in Fig. 2. The figure showed us that the temperature deviations were large, and we reached the conclusion that the thermostat adhesion method was completely inadequate.

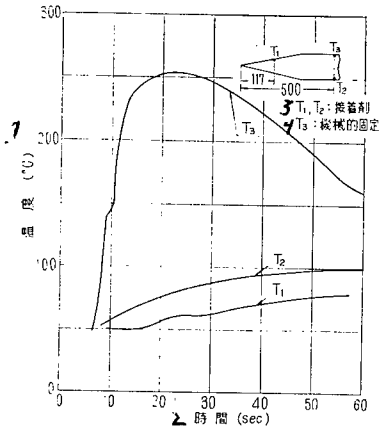

Fig. 2. Temperature-measurement results of the HT-150 type rocket test.

1) Temperature; 2) Time; 3) Mounted with adhesive; 4) Mechanically fixed

Therefore, we undertook development of a thermoelectric sensor as the detecting element and a transistor chopper type DC amplifier in order to get a new temperature-measuring device. For the thermoelectric couple, we used 0.2 mmφ Ni-NiCr plate. The plate was welded directly to the outside body plate of the rocket so there was no error due to the adhesive and to get high response. The transistor chopper amplifier is highly sensitive, stable and has good characteristics with respect to temperature and drift. Figure 3 shows the circuit diagram of the amplifier. With the use of a rotary switch, temperature measurements at many points are possible. Figure 4 is the switch portion of the thermometer.

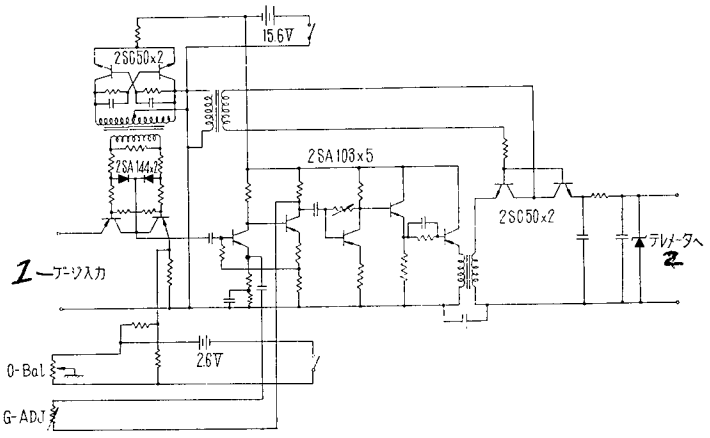

Fig. 3. Circuit diagram of the transistor chopper DC amplifier.

1) Gauge input; 2) To telemetry

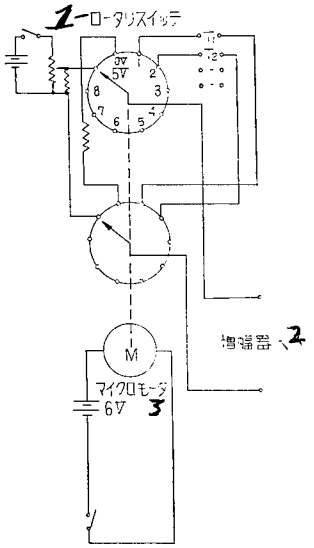

Fig. 4. Switch portion of the thermometer.

1) Rotary switch; 2) To amplifier; 3) Micro-motor

The new thermometers were used in the K-8L and -9M tests and we obtained highly accurate data from these tests. All of the thermoelectric couples at the tail area of the K-8L type space rocket and at one point of the K-9M were torn off. But, we did get information about the aerodynamic heating characteristics of the rocket because the tear-offs occurred when the temperature was falling. From the tests we learned that we should develop an improved welding method for the thermoelectric couple. In Fig. 5, we show the measured temperature values for the K-8L-1 type space rocket.

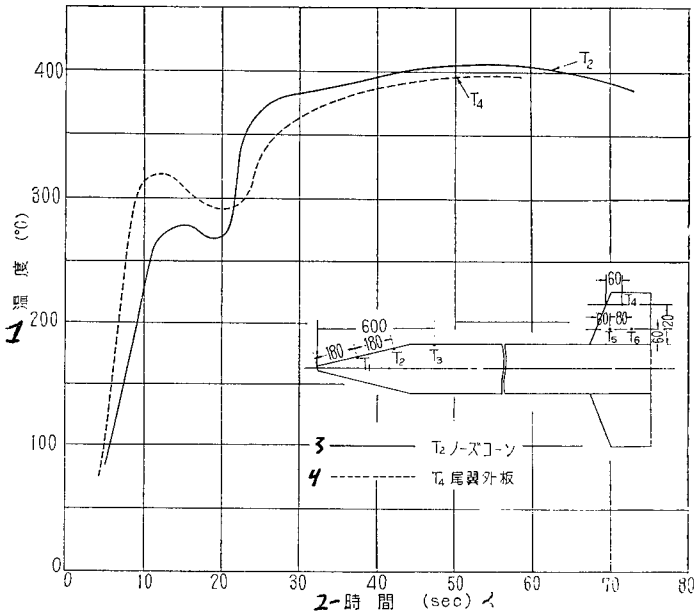

Fig. 5. Results of the temperature-measurements on the K-8L-1 type space rocket.

1) Temperature; 2) Time; 3) T_2: nosecone; 4) T_4: exterior of the tail

3. Strain Gauge

Conventional gauges had been reported [1, 2] and this is the report on the new strain gauge which was developed along with the new amplifier. The gauge uses this same amplifier. With the strain gauge, the stress on the tails of the K-8L and -9M type space rockets were measured. Figure 6 is the circuit of the bridge portion of the strain gauge. Figure 7 shows the measured results of the K-9M-1 type space rocket test.

Through the tests of the K-8L and -9M type space rockets, we found that the aerodynamic heat increased with improvement of rocket performance; in

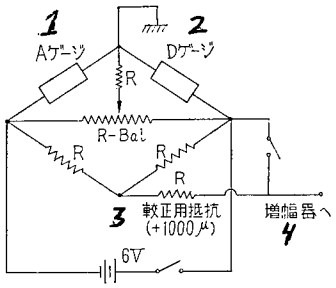

Fig. 6. Circuit diagram of the bridge portion of the strain gauge.

1) A gauge; 2) D gauge; 3) Correction resistance; 4) To amplifier

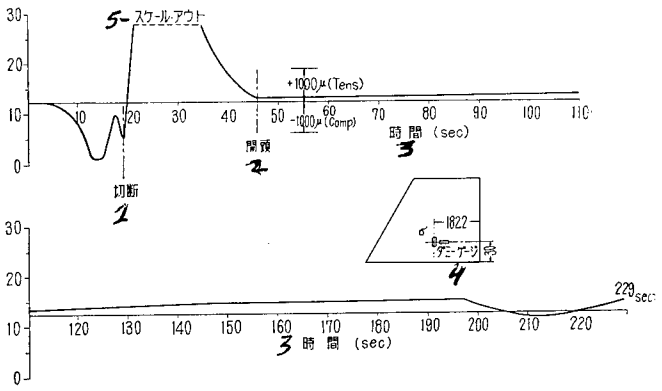

Fig. 7. Results of the stress measurement on the K-9M-1 type space rocket.

1) Cut-off; 2) Nosecone open; 3) Time; 4) Dummy gauge; 5) Off-Scale

particular, the heat increased rapidly during the end of combustion. Therefore, we could not analyze the net stress for that period. It was found that the strain gauge had not functioned right. Therefore, the development of a high-temperature strain gauge which will not be affected by heat is an urgent requirement in the near future.

4. Transverse Accelerometer

Accelerometer Y_1 [4] had been used to measure the transverse acceleration of a rocket. For the K-9L-2, K-8-8 and K-9M-1 type space rocket tests,

we also used a potentiometer-type accelerometer Y_2, the measurement theory of which was different from that of Y_1, in order to compare the data of the two meters, and we obtained satisfactory results.

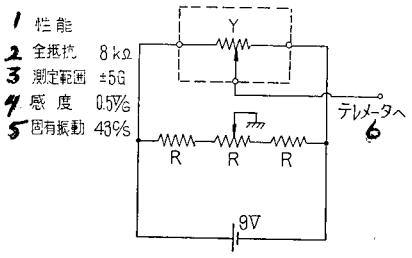

Fig. 8. Straight line potentiometer-type accelerometer

1) Performance; 2) Total resistance; 3) Region of measurement; 4) Sensitivity; 5) Characteristic vibration; 6) To telemetry

Both the theory and circuit of the meter are very simple and its output voltage is high. These make acceleration measurements with the meter easy. Figure 8 is the circuit diagram. The converter was made by Tokyo Measuring Equipment Production Co. According to the data which had been transmitted by the teletransmitter of the K-9M-1 type space rocket, the transverse acceleration was very small and a one-g shock due to the opening of the nosecone was the maximum value. 5.7 cps of rocket bending vibration immediately after the launching was precisely measured.

(Received on April 1, 1963)

REFERENCES

1. Daikichiro Mori and Atsushi Sozi, Prod. Res., Vol. 9, No. 4, 192, 1957.

2. Daikichiro Mori, Humizi Tomita and Sigeru Okada, Prod. Res., Vol. 10, No. 10, 296, 1958, and Vol. 11, No. 8, 341, 1959.

3. Daikichiro Mori, Takemi Wanami and Sigeo Imazawa, Prod. Res., Vol. 13, No. 10, 379, 1961.

4. Iwaho Yoshiyama and Iwaho Nakamura, Prod. Res., Vol. 9, No. 11, 455 1957.

TIMER

By Iwaho Yoshiyama, Hroshi Sakai
and Hakui Kumatorilani

We used seven timers, as shown in Table 1, for the space rocket tests from October 1961 to December 1962. The theory and structure of the timers are all the same, that is, the timer has a floating cam type micro motor (CL-2B-1 type, 6 volt of rated voltage, and 18 ma of driving current) and a micro-switch (OMRON S-5G OIAI type). As its battery source, four 1.3 v MU type mercury batteries are used.

Table 1

1) ロケット型式	2) 飛しょう年月日	3) タイマの種類	4) 重量 (kg)
K-8-8	36.10.24	開　頭　用	0.58
K-8-9	36.10.30	〃	〃
〃	〃	光学系突出用	0.54
K-9L-2	36.12.26	開　頭　用	0.74
K-8-10	37. 5.24	〃	0.60
K-9M-1	37.11.25	〃	0.65
K-8-11	37.12.18	〃	0.60

1) Type of rocket; 2) Date of flight;
3) Purpose of timer; 4) Weight;
5) Nosecone opening; 6) Actuate the opening instruments

Function of the timer is as follows: One end of piano wire is fastened to the launcher and the other end is fixed to the start switch of the timer. When the rocket is launched, the piano wire slips off the start switch, the switch is turned on, and the micromotor begins to rotate. A certain time period later, the motor axle gears into the hook of the cam plate. Thus, the cam plate is rotated by the motor and, in turn, the cam plate turns the microswitch on, and the ignition circuit is connected. Then the nosecone-opener actuator functions. In order to be assured that the circuit is connected, a signal is sent to the tele-transmitter when the circuit is completed. Figure 1 is the circuit diagram.

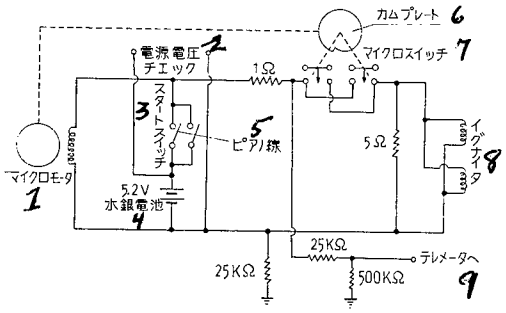

Fig. 1

1) Micro motor; 2) Source voltage checkpoint; 3) Start switch; 4) Mercury battery; 5) Piano wire; 6) Cam plate; 7) Micro switch; 8) Igniter; 9) To teletransmitter

Table 2

1 ロケット型式	2 用途	3 セット秒時（秒）	4 作動秒時（秒）	
K-8-8	5 開頭用	58	58	
K-8-9	〃	62	7 確認せず	
〃	6 光学系突出用	64	65	
K-9L-2	5 開頭用	60	60	
K-8-10	〃	61		8 ロケットに異常を生じ早期作動
K-9M-1	〃	46	45.7	
K-8-11	〃	76	79	

1) Type of rocket; 2) Purpose; 3) Time set for start of operation (sec); 4) Actual time of start of operation (sec); 5) Nosecone opened; 6) Projection of optical system; 7) Unidentified; 8) Premature function due to faulty operation of the rocket

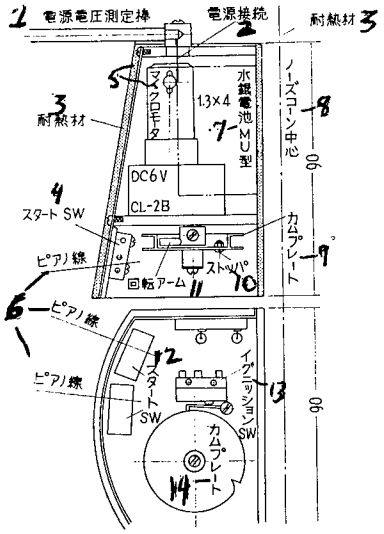

Fig. 2

1) Source voltage measuring rod; 2) Source connection; 3) Heat insulating material; 4) Start switch; 5) Micro motor; 6) Piano wire; 7) MU type mercury battery; 8) Center line of nosecone; 9) Cam plate; 10) Stopper; 11) Rotating arm; 12) Start switch; 13) Ignition switch; 14) Cam plate

Table 2 shows the time set and actual operation time. Figure 2 is the figure of the timer which was placed inside the open portion of the nosecone of the K-9L-2 type space rocket.

(Received on April 18, 1963)

LIGHT DETECTOR FOR SOUND BOMB

By Iwaho Yoshiyama, Sigeo Imazawa
and Takemi Wanami

1. Introduction

To measure the wind and temperature of the atmosphere by the sound bomb method requires high accuracy in measuring the time period of the illumination of the sound bonb.

For the K-6 type rocket, the illumination time period was measured by an infrared light detector (Pb cell) from the ground. But it was extremely difficult to identify the light of the sound bomb from other lights — from the sun, reflected from cloud to cloud, or from the earth. In order to eliminate this difficulty, we installed phototransistors in the body of the K-8-7 type space rocket and the illumination-time-period detected was sent by the teletransmitter.

2. Problem area

There were the following difficulties with the new method.

(a) Effects of the vibration, shock, pressure and aerial currents.

(b) Heat.

(c) Interference or masking of the light from the sound bomb firing to the light of the sound bomb explosion.

(d) Response of the phototransistor.

(e) Directivity and the effect of the sun.

(f) Explosion powder protection.

Each item was thoroughly examined in advance of the test. Preliminary tests were performed at Chiba test ground and the results were good. In actual flight test, item (f) was treated with particular caution.

3. Structure and Circuit

The sound bomb is to be fired to the rear of the rocket with an angle of 10° from the rocket direction axis and it will explode 20 to 30 m away from the rocket. With this consideration of the directivity of the sound bomb, the phototransistor is set to face rearward with about an angle of 15° to 20°. The structure is shown in Fig. 1.

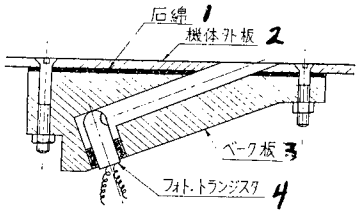

Fig. 1. Structure of the detector

1) Asbestos; 2) Outside panel of the body; 3) Bakelite sheet; 4) Phototransistor

Four phototransistors are set on the circumference of the rocket body. Two of the transistors are covered by heat resistant crystal glass. The four transistors are connected in series (sic) so they can offer data even if some of them are destroyed. The circuit diagram is shown in Fig. 2. The relative positions of the phototransistors and sound bombs are shown in Fig. 3.

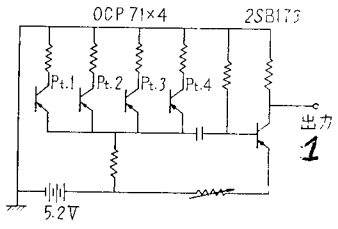

Fig. 2. Circuit diagram

1) Output

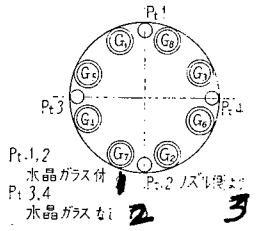

Fig. 3. Relative positions of the sound bombs

1) With crystal glass; 2) Without crystal glass; 3) Viewed from nozzle

4. Results of the Measurement

A portion of the teletransmitted data are shown in Fig. 4. The two pulses from the lights of the firing and explosion were detected separately without interference or masking. All sound bombs had exploded and were detected.

Among the four phototransistors, two transistors were, as explained previously, covered by heat resistant crystal glass. In considering the relative positions of the sound bombs, G's, and the transistors, Pt's, we decided that the reason G_1, G_2, G_3 and G_4 showed low light sensitivity is that the detectors near the bombs were covered by glass. It was also found by the spin of the rocket that the detectors were being operated until X + 36 sec ~ X + 190 sec.

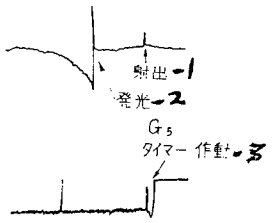

Fig. 4. A portion of the record from the teletransmitter

1) Fire; 2) Explosion; 3) Timer start

The measured results of the time periods are listed in Table 1. Timer operations are also included in the table for reference. From the table, we know that the time duration from the timer start to the detect of the firing light was 0.04–0.09 sec and from the timer start to the detect of the explosion light was 0.63–1.04 sec.

Table 1

Measured Result of the Illumination Time Period of the Sound Bomb

	タイマー作動秒時			発光検出器		タイマー作動～発光秒時
	計画	最終調整	作動秒時	射出	爆発発光	
	sec	sec	sec	sec	sec	sec
G_1	41.2	41.40	41.70	41.74	—	—
G_2	45.6	45.85	46.02	46.06	46.78	0.76
G_3	50.0	50.15	50.29	50.38	51.08	0.79
G_4	54.4	54.60	54.68	54.75	55.71	1.03
G_5	58.9	58.80	58.89	58.99	59.50	0.61
G_6	63.4	63.30	63.43	63.45	64.19	0.76
G_7	68.1	68.10	68.22	68.25	68.96	0.74
G_8	73.0	73.00	73.03	73.08	73.91	0.88

1) Time of timer start; 2) Plan; 3) Final adjustment; 4) Actual time period; 5) Light detector; 6) Firing; 7) Explosion; 8) Time period from the timer start to the detection of the explosion light

We had limited the time period to prepare and check the plan and there were many difficulties. But we could get an unexpected good result from the test and get an assurance for the future successful use of the method. We wish to thank Mr. Hi-iro Nakamura, Matsushita Communication Industrial Co., for his help in the development of the detector.

(Received on April 1, 1963)

COLORIMETER

By Iwaho Yoshiyama, Akio Hirozawa
and Susumu Matsusima

1. Introduction

It uses electron tubes which have large resistance change for different brightness of lights, that is, the electron tube detects the brightness of the combustion flame of a rocket engine and converts the brightness of the light into the magnitude of the current.

We developed a rocket-borne-type colorimeter. The colorimeter, in connection with the timer, was to detect the booster cut-off, main rocket engine ignition and abnormal combustion of the engine. As a preliminary test, we used the colorimeter at the ground combustion test of the L-735 3/3 rocket engine test and obtained satisfactory results.

2. Colorimeter for the L-735 3/3 Type Engine Test and the Measured Results

The electron tube, as a kind of semiconductor, is cadmium sulfate and sensitive to light of wide wavelength, particularly 7000-5000 Å. Because we did not know the sensitivity of the tube to the combustion flame of the L-735 3/3 type engine, we examined two kinds of filters to find out the references based on the light from the sun. Figure 1 shows the circuit diagram. The test was performed at Noshiro Test Center, the Institute of Production Research of Tokyo University on October 29, 1962 and the colorimeter was placed as shown in Fig. 2. The measured results are shown in Fig. 3. We could find the following from the results:

(1) 2-5 sec. and 13-15 sec. after ignition, there were vibrations. We don't know if these were internal pressure vibrations.

(2) The combustion time was 33.4 sec. But the meter detected combustion at the injector after the flame from the exhaust had died out.

(3) The reason that the curve was increasing from about 20 sec. is due to the color of the flame and that the flame composition had changed.

(4) In the test, the sensitivity of the colorimeter was higher to the red flame of the injector than to the main flame. And, therefore, research on filters is needed.

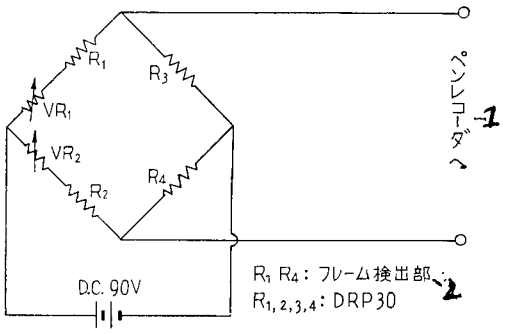

Fig. 1

1) To pen recorder; 2) Flame detecting parts

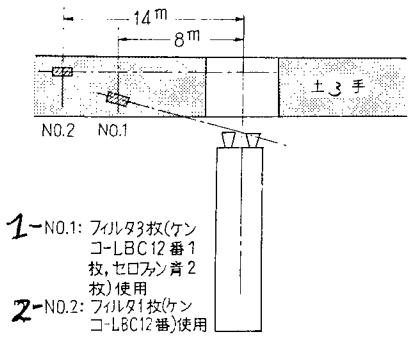

Fig. 2. Set-up

1) No. 1: three filters (one Kenko-LBC 12, two Cellophane blue); 2) No. 2: one filter (Kenko-LBC 12); 3) Bank

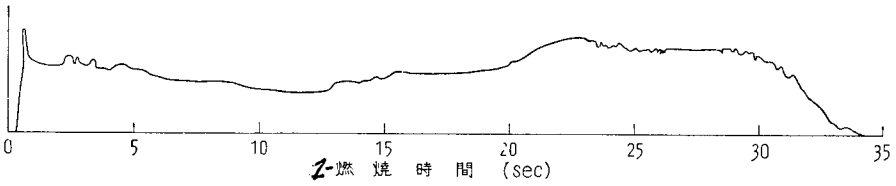

Fig. 3. Measured result of the colorimeter No. 1

1) Combustion time

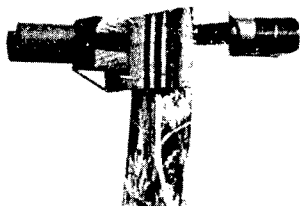

Fig. 4. The colorimeter

We will perform research on filters and examine the position and number needed to measure internal pressure vibrations, temperature of gas, and the velocity of gas.

(Received on April 17, 1963)

THE NOSECONE OPENING SYSTEM

By Muneo Itabashi, Iwaho Nakamura and
Iwaho Yoshiyama

1. Introduction

The instruments for atmospheric observations are placed in the rocket nosecone portion and carried to the upper atmosphere by the rocket. Therefore, when the rocket engine has completed its mission, the vehicle is not necessary any more. Sometimes it can even be an obstacle as in the case of an earth satellite, therefore it is cut off from the payload section. The same thing can be said about the outside wall of the rocket nosecone. In other words, it is better to take off the outside wall when it is not needed. The role of the outside wall is to protect the instruments from the outside force and frictional heat until the rocket escapes from the layer of air around the earth. Beyond that point, the outside wall has no use or it may even become an obstacle to the measuring devices.

According to the phenomena under observation, there are some instruments that cannot function unless the wall is taken away; some instruments will have lower sensitivity and some will even effectively use the outside wall.

Among the instruments, the detecting units which should not be shielded by the wall are held separate from others and assembled in the front part of the payload compartment; and the front portion of the outside wall (which is normally the nosecone and a portion of the parallel portion of the rocket body) is shorn away from the rocket body.

2. Structure of the Nosecone Opening System

The first nosecone opening system was made in July 1960. Since then, modification and improvement were made continuously, and ten 250 φ types and a 160 φ type nosecone opening systems were made.

As shown in Fig. 1, the open nosecone consists of two separated half cones. In order to put the half cones together, a couple of split rings are placed over the cone at about one-third of the cone length and the ring is tightened by a shear pin (see Fig. 1). The actuator which will push the walls apart is put in the nosecone in advance. The connection of the open cone to the rocket body is made by a slip joint which will be safe under the bending load. In this connection, the rocket body holds the nosecone from the outside and therefore the cone

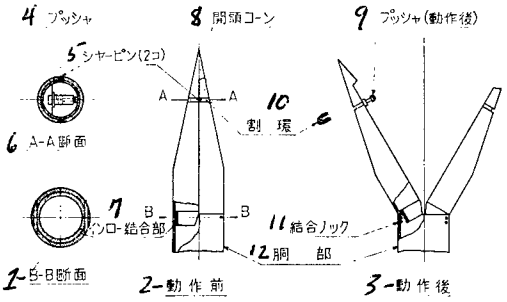

Fig. 1. Nosecone opening system (left one is before it functioned).

1) B-B cross-sectional area; 2) Before functioning; 3) After functioning; 4) Actuator; 5) Shear pins (two); 6) A-A cross-sectional area; 7) Slip joint portion; 8) Open nosecone; 9) Actuator, after functioning; 10) Split ring; 11) Joint lock; 12) Body

can move only in the axial direction. To minimize the axial direction movement, joint locks are used between the connecting parts. The nosecone opening process is as follows: The actuator gets its signal from the nosecone-opening timer (refer to page 247 of this issue) or nosecone-opening delay tube, then starts to function (see Fig. 1). First, the black powder in the actuator is ignited, the piston is then pushed out. By this movement, the shear pin in the split pin is broken and the nosecone is opened. Because the nosecone opening takes place when the rocket is flying, the relative velocity of the nosecone with respect to the rocket is zero and the cone gradually flies away in a direction normal to the rocket. Therefore, there is no possibility that the nosecone will hit the rocket body.

3. Open Nosecone

The first model of the nosecone was molded and had two actuators to make sure there was no failure. The nosecone had the shape shown in Fig. 2 for there were not many devices to be placed in the nosecone portion then. Since then, the nosecone has been improved mainly by Professor Daikichiro Mori. Current nosecones are made from sheet metal by welding instead of molding. Figures 3 and 4 show the open nosecones. As shown in Fig. 4, the nosecone opening timer is set at the front end of the nosecone, and an actuator is placed under the timer. In this case, it has only one actuator. But, considering that the important part is the black powder and is the power source of the actuator, we placed two ignition ends in the black power to increase its reliability.

Recent nosecone opening systems also have a nosecone-opening-delay-tube to support the function of the timer, so that if the timer does not function, the

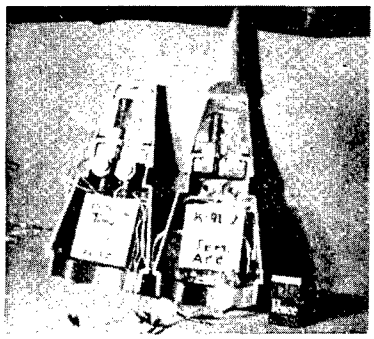

Fig. 2. First model of open nosecone (160 φ type)

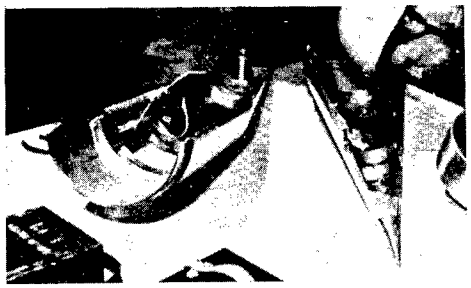

Fig. 3. Current open nosecone (welded sheet metal)

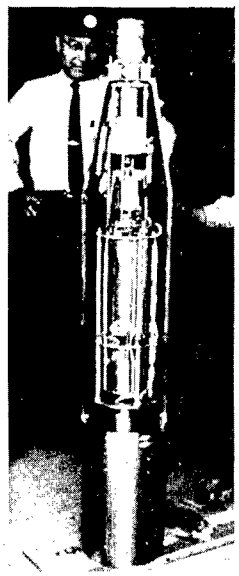

Fig. 4. Open nosecone with instruments loaded

delay tube will ignite the actuator powder. Standard open nosecone is that of the K-8 type space rocket, which has total length 1 to 1.5 m and outside diameter 250 φ, and ten cones of this type have been produced so far. Besides these, nosecones of 0.5 m total length and 160 φ outside diameter are being produced for the K-9L type three-stage space rocket.

4. Actuator

The latest actuator is shown in Fig. 5. The actuator powder placed as shown in the figure is ignited by the timer or the delay tube, which sends electric current to the ignition end and heats the platinum line in the black powder. By the explosive force of the black powder, the piston is actuated breaking the lock pin. And the force of the piston breaks the shear pins and separates the nosecone as stated above.

In designing the actuator, we had taken particular care since it was desired that the explosive gas not contaminate the instruments or the surroundings.

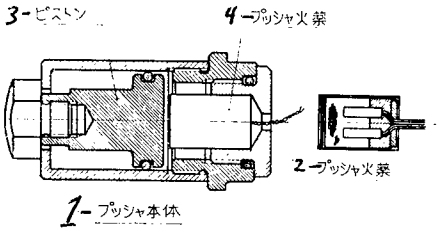

Fig. 5. Actuator and actuator powder

1) Actuator; 2) Actuator powder;
3) Piston; 4) Actuator powder

5. Nosecone Opening Delay Tube

There is no definite place at which the nosecone opening tube should be placed and it depends on the shape of the tube, but the tube is normally placed at a place as shown in Fig. 4. The role of the delay tube is, as stated before, to take over the function of the timer when the timer has trouble and to ignite the actuator powder. Therefore, the delay tube was made to function a little bit later than the timer. As the name "nosecone-opening-delay tube" suggests, the main body of it is the time delaying powder.

The ignition end of the delay powder is ignited at the moment the rocket is launched. A certain time later (the time length is determined by the length of the delay powder), the delay powder's fire reaches the end and ignites the fuse. Then the fuze ignites the black powder. By the explosion of the black powder, the air pressure rises and turns on the pressure switch. By this, the

current from the source battery flows to the actuator and makes the actuator function. The structure of the delay tube is shown in Fig. 6.

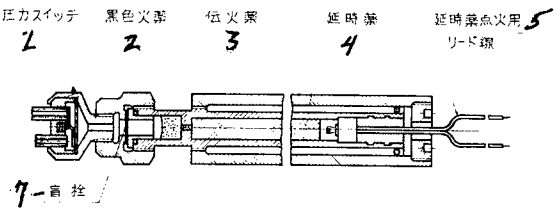

Fig. 6. Structure of the nosecone opening delay tube

1) Pressure switch; 2) Black powder; 3) Fuse powder; 4) Delay powder; 5) Lead line for the ignition of delay powder; 7) Blocking cock

6. Actuator Powder Ignition Circuit

Figure 7 shows the diagram of the ignition circuit for the actuator powder. The nosecone opening timer and cone opening delay tube are connected to the actuator powder in series. Therefore, if the switch of the timer, which had started when the rocket was launched and would turn on at a preset time, does not turn on due to trouble, the nosecone-opening-delay-tube will ignite the actuator powder. In the figure, the lead line (line from the ignition end of the delay tube) will be connected to the rocket engine ignition circuit. Thus, the delay tube will be ignited at the time the rocket is launched. And the delay tube will function later than the timer since the length of the delay powder is so adjusted.

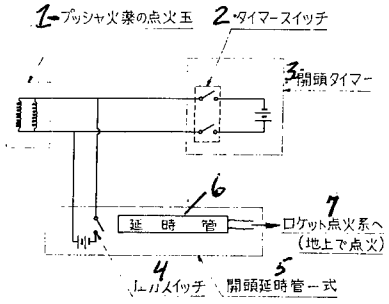

Fig. 7. Actuator powder ignition circuit

1) Ignition end of the actuator powder; 2) Timer switch; 3) Nosecone opening timer; 4) Pressure switch; 5) Entire unit of the nosecone-opening delay tube; 6) Delay tube; 7) To the rocket engine ignition system (ignited on the ground)

7. Conclusion

We wish to thank Assistant Professor Mori, members of the Institute of Production Research, Tokyo University, and members of Teikoku Explosives Industrial Co. for their help in design, production, and test of the system.

(Received on March 30, 1963)

GROUND TEST OF LAMBDA TYPE ENGINES

(735 φ -1/3, -2/3 and -3/3 TYPE)

— 37th report on research of the optical tracking of a high-speed, moving body —

By Hisaaki Uemura, Katsuya Tanaka, Kazuo Kanezawa, Yutaka Kikusato and Sei-ich Okamiya

1. Introduction

Along with large space-rocket development, the ground combustion tests of the Lambda type rocket engines were performed in Akita Province. These tests involved putting a rocket engine on an engine test bed, called a test stand, and performing the ground combustion tests. L-735-1/3 and -2/3 type rocket engines had been tested at Michigawa Beach, Akita Province, on April 23, 1961 at 2:35 p.m., and on March 31, 1962 at 4:05 p.m., respectively. And the combustion test of the L-735-3/3 type rocket engine was performed at Hama-asa-uchi Beach, Noshiro City, Akita Province, which was newly outfitted for the test on October 29, 1962 at 2:15 p.m. In the tests, 80 items including internal pressure, internal pressure-vibration, thrust, stress, vibrational sound, humidity, and optical observations were measured. We, the optical observation team, filmed the flame at the nozzle of the rocket engine with a 16-mm high-speed camera and a 35-mm cine-camera (exposure time 1/500 sec per frame). Developed films were sent to the experts on rocket engines, explosive technology and other sciences to be examined. Here, we will report on the filming and the observation results.

2. Equipment and Method of Filming

The camera used to film the ground combustion tests of the Lambda type rocket engines are a 16-mm prism type high-speed camera (maximum film speed, 10,000 frames/sec) and a 35-mm cine-camera. In the test of the L-735-1/3 type rocket engine, the prism-type high-speed camera (Fastax) filmed the nozzle area of the rocket engine, and the 35-mm cine-camera (Bell and Howell camera) filmed the entire flame. For the L-735-2/3 type rocket engine test, the cameras were used the same way as in the previous test. The film speed of the high-speed camera was adjusted according to the phenomenon. For the Lambda type rocket-engine test, the film speed was taken at 500 frames per second in order to film

Table 1

使用カメラ		735 1/3 L	735 2/3 L	735 3/3 L
16 mm Fastax 高速度カメラ	5レンズ	Raptar 101 mm	Raptar 153 mm	Raptar 153 mm
	6絞り	f: 3.5	f: 8 よりやや絞る	f: 4.5
	7カメラ電圧	AC 33 V	AC 27 V	AC 27.5 V
	8フィルタ	Wratten No. 85	なし	なし
	9同期	手動	手動	手動 ×−2 sec SW on
	10撮影速度	800 f/sec	500 f/sec	500 f/sec
	11画面	ロケットエンジンのノズル部分	ロケットエンジンのノズル部分	ロケットエンジンのノズル部分
	12フィルム	Eastman Color Negative (ASA 50) (5250)	Eastman Ektachrome (7257) (ASA 160)	Eastman Ektacerome (7257) (ASA 160)
16 mm 日立 Himac 高速度カメラ	5レンズ			Nikkor 180 mm
	6絞り			f: 2.8
	8フィルタ			なし
	9同期			手動によるカウント×＋6秒 SW on
	10撮影速度			500 f/sec
	11画面			ロケットエンジンのノズル部分
	12フィルム			Eastman Kodak (Reversal) Type 7257 (ASA 160)
35 mm Bell & Howell カメラ	5レンズ	Tessar 80 mm f: 2.7	Tessar 80 mm f: 2.7	Tessar 80 mm f: 2.7
	6絞り	f: 5.6	f: 6.3	f: 2.7 開放
	8フィルタ	Wratten No. 85	Wratten No. 85	Wratten No. 85
	9撮影速度	24 f/sec	24 f/sec	24 f/sec
	13コマ露出時間	1/500 秒	1/500 秒	1/500
	12フィルム	Eastman Color Negative (ASA 50) Type 5250	Eastman Color Negative (ASA 50) Type 5250	Eastman Color Negative (ASA 50) Type 5250

1. Camera used
2. High-speed camera
3. 16-mm Hitachi Himac high-speed camera
4. Bell & Howell camera
5. Lens
6. Aperture setting
7. Camera voltage
8. Synchronization
9. Film speed
10. Objective
11. Picture area
12. Film
13. Exposure time per frame
14. Nozzle area of rocket engine
15. Sec
16. Smaller than f:8
17. None
18. Manual
19. Count x + 6 sec and turn switch on by manual control
20. Open to f:2.7

the nozzle and flame as long as possible. With this film speed, 100 feet of film would last ten seconds. Therefore, we used two high-speed cameras in series and operated them successively in the L-735-3/3 type rocket-engine test in order to film continuously as long as possible.

The two high-speed cameras filmed neon-tube time marks and an overlapping flash when they were filming pictures near the end of their film rolls. By

the overlapping flash, the time basis of the two cameras could be matched. The 35-mm cine-camera had a small aperture setting and 1/500 sec per frame of exposure time. Both cameras used color films. For details, refer to the camera data (Table 1).

The filming method was the same for both tests of the L-735-1/3 and -2/3 type rocket engines, that is, we took the film-start flash when we got a "zero" signal from the controller. Both high-speed and 35-mm cameras were started manually. The 35-mm camera was arranged so that it shot the dial plate of a clock which had two needles, one showing revolutions per second and the other, revolutions per minute. Camera and subject arrangement are shown in Fig. 1.

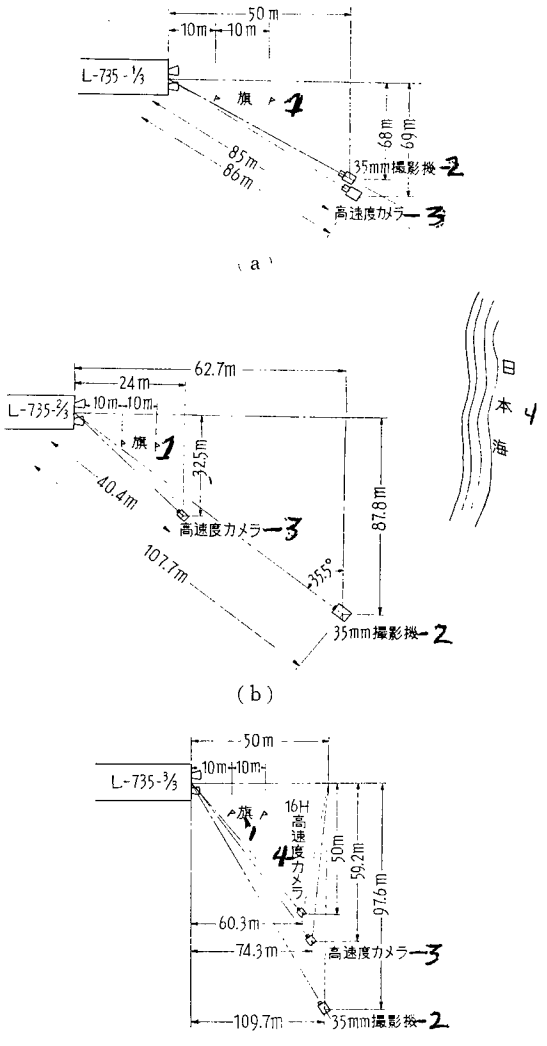

Fig. 1. Diagram of camera and subject arrangement.

1) Flag; 2) 35-mm cine-camera; 3) High-speed camera (Fastax); 4) 16-mm Hitachi high-speed camera

In filming the L-735-3/3 type rocket engine test, high-speed cameras were arranged so they could take film as fast as possible in order to catch completely the nozzle area of the rocket engine. First, the Hitachi camera was started manually. One second before the film of the Hitachi camera was completely exposed, film-start flash light was actuated by an event pulse to link the time axes of the Hitachi and Fastax cameras. The Fastax camera was started manually about two seconds before the Hitachi camera finished its filming. An electric circuit could be designed to operate the high-speed cameras automatically. However, we operated the cameras manually because the test required a considerably low film speed. The 35-mm cine-camera was operated the same way for the L-735-1/3 and -2/3 type rocket engine tests. The camera arrangement is shown in Fig. 1.

3. Results of the Filming

Because we used color film in both cameras, we could see the flame and smoke clearly. We paid particular attention to aperture setting because the color film had a limited choice of f-settings. And we determined the aperture setting from the background light because we had no data on the light intensity of the flame. It was cloudy for the L-735-1/3 test, clear for the L-735-2/3 and rainy for the L-735-3/3, but the pictures were almost adequate except that the flame was a little over-exposed. Analytical results will not be discussed here.

4. Summary

From April 1961 to October 1962, three Lambda type (L-735 type) rocket-engine combustion tests were performed. We were able to film the tests with high-speed cameras. Because the films were color films, they showed combustion conditions clearly. Normally, a black-and-white film does not show the flame portion and transparent portion of the gas separately, but a color film shows them clearly. The effect was particularly good for the L-735-3/3 type rocket engine test when there was extremely bad weather. In order to take complete and continuous film of a combustion which lasts more than 10 to 20 seconds, we had to set two cameras in series. The 35-mm cine-camera, which used a short shutter speed, was effective in filming the entire phenomenon.

(Received on May 2, 1963)

OPTICAL TRACKING OF KAPPA-8 TYPE ROCKETS

(-7, -8, -9 and -11 TYPE)

—39th report on the research of the optical tracking of a high-speed body—

By Hisaaki Uemura, Katsuya Tanaka, Kazuo Kanezawa and Yoshiaki Kurokawa

1. Introduction

The launch test of the K-8-6 type rocket had been performed previously. And we tested K-8-7 to -11 type rockets successively.

The launchings at Michigawa Beach, Akita Province, were of the K-8-7 type and occurred at 11:42 a.m., July 21, 1961 with the angle of launch elevation 80°; K-8-8 type at 12:59 p.m., October 24, 1961 with the angle of launch elevation 81°; and K-8-9 at 8:13 p.m., October 30, 1961 with the angle of launch elevation 80°. The K-8-11 type rocket was launched at the new rocket test site in Kagoshima at 2:03 p.m., December 18, 1962. K-8-7 and -8 were launched to observe cosmic rays and the ionosphere. K-8-9, the rocket tested on the second night, was launched to observe the ionosphere and air glow. As the first rocket test at Kagoshima, the K-8-11 was launched to observe cosmic rays by Geiger counter, rocket attitude, by a geomagnetic aspect meter, and the performance of a newly developed receiver to detect noise in the ionosphere.

We set our optical tracking equipment at central and high-speed observation points at Akita and at No. 1 and No. 2 optical observation points at Kagoshima, to film the rockets. We will report the characteristics of K-8 type rockets here.

2. Equipment for Filming

Figure 1a and b show the layout for filming. We, the optical observation team, set a 16-mm high-speed camera to take the film when a rocket leaves the launcher, and a 35-mm Bell & Howell cine-camera at the high-speed observation point. A 15-times magnified tracking system was set at the central observation point to film the track. Details are listed in the camera data (Table 1).

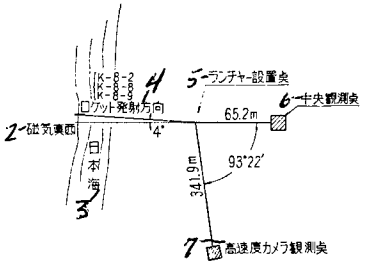

1 (a) 秋田実験場観測点配置

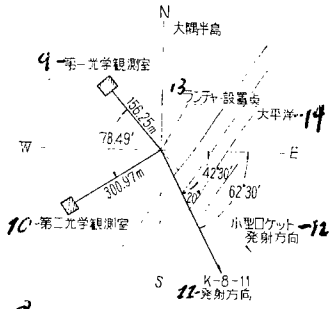

8 (b) 鹿児島観測室配置

Fig. 1

1) Observation point layout at Akita Test Center; 2) West in magnetic coordinates; 3) Sea of Japan; 4) Launch direction of rocket; 5) Launch point; 6) Central observation point; 7) High-speed-camera observation point; 8) Observation point layout at Kagoshima Space Center; 9) Optical observation point No. 1; 10) Optical observation point No. 2; 11) Launch direction of K-8-11 type rocket; 12) Launch direction of small type rocket; 13) Launch point; 14) Pacific Ocean

3. Flight Observations

We filmed the K-8 type space rocket flight by means of a 16-mm prism-type high-speed camera. And the rocket's launch and ascent were filmed by a 35-mm Bell & Howell cine-camera. As it was clear when the K-8-7 was launched, we could track the rocket for 50 seconds from the central observation point. Because it was cloudy when the K-8-7 type was launched, the rocket was tracked only 7 seconds. The K-8-9 type was launched at night, but we could track it for 43 seconds because it was clear and there were no clouds in the sky. The K-8-11 type was launched at Kagoshima with clear weather and tracked for 43 seconds. We could not obtain the trajectories of the rockets for we could not set the south observation point at Akita and the optical observation point No. 4 at Kagoshima for some reason.

Table 1

使用カメラ			K—8—7	K—8—8	K—8—9	K—8—11
15倍手動追跡装置 (中央観測点) (第1観測室)	5 追跡撮影カメラ	7 本体	18 35 mm Mitchell 改造カメラ	18 35 mm Mitchell 改造カメラ	18 35 mm Mitchell 改造カメラ	18 35 mm Mitchell 改造カメラ
		8 レンズ	Raptar 254 mm F: 4.5	Raptar 254 mm F: 4.5	Raptar 254 mm F: 4.5	Raptar 254 mm F: 4.5
		9 絞り	F: 8	F: 5.6	F: 4.5 開放	F: 5.6
		10 フィルタ	Fuji No. 7	19 — なし	19 — なし	Fuji No. 7
		11 撮影速度	24 f/sec	24 f/sec	22 f/sec	24 f/sec
		12 同期	20 目盛カメラと同時 1 PPS	20 目盛カメラと同時 1 PPS	20 目盛カメラと同時 1 PPS	5/6 PPS
		13 一コマの露出時間	1/500 sec	1/500 sec	1/500 sec	1/500 sec
		14 フィルム	Fuji Negative Film (ASA 80)	Fuji Negative Film (ASA 80)	Fuji Negative Film (ASA 80)	Fiji Negative Film (ASA 80)
	6 目盛撮影機	8 レンズ	1″	1″	1″	1″
		9 絞り	f: 5.6	f: 5.8	f: 5.6	f: 5.6
		10 フィルタ	19 なし	19 なし	19 なし	19 なし
		11 撮影速度	16 f/s	17 f/s	17 f/s	15 f/s
		12 同期	1 PPS	1 PPS	1 PPS	5/6 PPS
		13 一コマの露出時間	21 1 m sec 以下 (ストロボ照明による)	21 1 m sec 以下 (ストロボ照明による)	21 1 m sec 以下 (ストロボ照明による)	21 1 m sec 以下 (ストロボ照明による)
		14 フィルム	16 mm Fuji Negative Film (ASA 80)	16 mm Fuji Negative Film (ASA 80)	16 mm Fuji Negative Film (ASA 80)	16 mm Fuji Negative Film (ASA 80)
16 mm Fastax 高速度カメラ (高速度カメラ観測点) (第二観測室)		8 レンズ	Raptar 153 mm	Raptar 180 mm	Raptar 180 mm	Raptar 153 mm
		9 絞り	f: 4.5	f: 3.5	f: 4	f: 4
		16 カメラ電圧	AC 40 V	AC 40 V	AC 40 V	52 V
		10 フィルタ	Wratten No. 85	19 なし	19 なし	19 なし
		12 同期	22 手動 X—2 sec ・ SW on	22 手動 X—1.5 sec SW on	22 手動により X—1.5 sec SW on	22 手動 X—1.5 sec SW on
		11 撮影速度	1,000 f/s	1,000 f/s	1,000 f/sec	2,000 f/s
		15 画面	23 ランチャ離脱付近	23 ランチャ離脱付近	23 ランチャ離脱付近	23 ランチャ離脱付近
		14 フィルム	Eastman Color Negative (5250) (ASA 50)	Eastman Ektachrome (7257) (ASA 160)	Eastman Tri-X (ASA 320)	Eastman Ektachrome (7257) ASA 160
35 mm Bell & Howell カメラ (高速度カメラ観測点) (第二観測室)		8 レンズ	Nikkor 250 mm f: 4	Nikkor 250 mm f: 4	Nikkor 250 mm f: 4	Nikkor 250 mm f: 4
		9 絞り	f: 5.6	f: 4 開放	f: 4	f: 5
		10 フィルタ	Fuji No. 7	Wratten No. 85	Wratten No. 85	Wratten No. 85
		11 撮影速度	24 f/s	24 f/sec	24 f/sec	24 f/sec
		13 一コマの露出時間	1/500 sec	1/450 sec	1/500 sec	1/500 sec
		17 モータ	24 シンクロナスモータ	24 シンクロナスモータ	24 シンクロナスモータ	24 シンクロナスモータ
		15 画面	25 ランチャ付近より上空へ追跡	25 ランチャ付近より上空へ追跡	25 ランチャ付近より上空へ追跡	25 ランチャ付近より上空へ追跡
		14 フィルム	Fuji Negative Film (ASA 80)	Eastman color Negative(5250) (ASA 50)	Eastman color Negative(5250) (ASA 50)	Eastman Color Negative (5250) (ASA 50)

1. Camera used
2. 15 times magnified tracking system (central or No. 1 observation point)
3. 16-mm Fastax high-speed camera (high-speed camera or No. 2 observation point)
4. 35-mm Bell & Howell camera (high-speed camera or No. 2 observation point)
5. Track filming camera
6. Scale filming camera
7. Camera
8. Lens
9. Aperture setting
10. Filter
11. Film speed
12. Synchronization
13. Exposure time per frame
14. Film
15. Picture area
16. Object
17. Motor
18. Modified 35-mm Mitchell camera
19. None
20. 1 PPS (same to the scale filming camera)
21. Less than 1 millisec (by stroboillumination)
22. Manual (switch on at x-2 sec)
23. Rocket launch
24. Synchronous motor
25. Rocket's ascent from launcher to sky

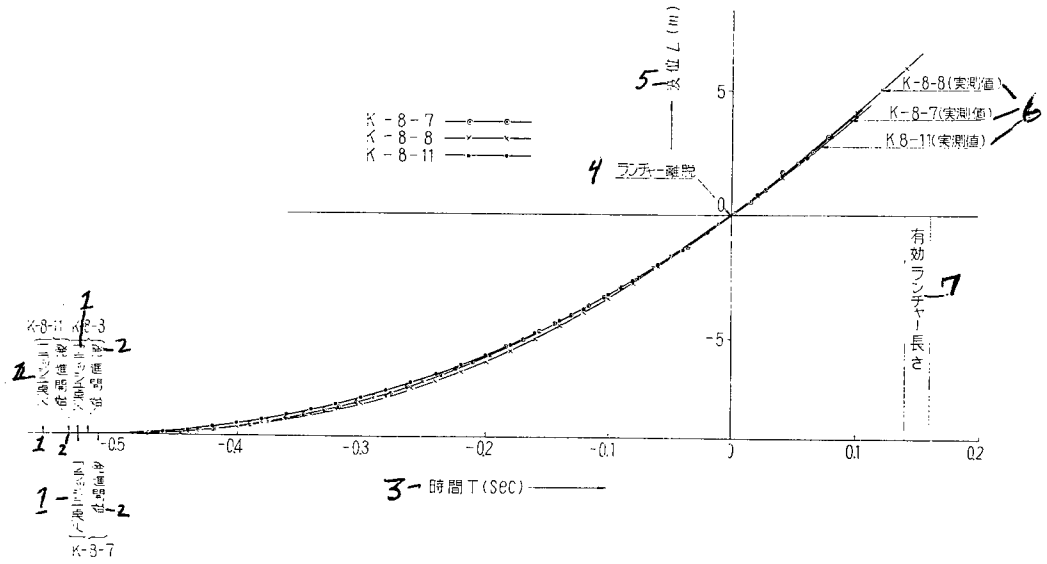

Fig. 2. Displacement vs time curve

1) Ignition point; 2) Starting time; 3) Time; 4) Launch point; 5) Displacement; 6) (Observed value; 7) Effective launch length

4. Observation Result and its Analysis

(a) The characteristics of the rocket motion near the launcher.

The rocket motion when it is leaving the launcher was filmed by the prism-type high-speed camera. Film speed was set about 2000 frames/sec according to

the launch velocity of the rocket. The analytical result is shown in Fig. 2. Figure 2 is the displacement (L) vs time (T) curve and the displacements were measured for each frame of the film. K-8-7 and -8 type rockets had left the launcher about 0.53 sec after the ignition flash. For the K-8-11 type, it took about 0.56 sec. The time length from the ignition flash to the moving of a rocket depends upon the total weight (including the measuring devices) and launch angle of the rocket, and the K-8-8 type had the longest time, 0.02 sec. The three displacement vs time curves agree well with anticipated values. We could not analyze the initial motion of the K-8-9 type rocket which had been launched at night at Akita because the illumination on the rocket at the launching moment had failed. However, we could estimate from the flame and later motion of the rocket that the initial motions of the rocket were quite similar to those of the other rockets.

(b) Trajectories obtained from the tracking system.

In the K-8 type space rockets test both at Akita and Kagoshima, rockets were tracked from behind for we had set only one observation point, the central observation point at Akita and the optical observation point at Kagoshima. From the tracking, we obtained the angle of elevation α vs time (T) and the angle of rotation θ vs time (T) curves. Figure 3 shows the curves which were drawn from the tracking film taken at the central observation point, Akita Test Center. The launch direction of the rockets was 4° north from the direction of the line which connected the launcher and the central observation point. The altitude of the K-8-7 type space rocket was higher than the calculated value. The angle of rotation of the rocket at 44 sec after the launch was 1°15' north of the launching direction. K-8-8 type space rocket disappeared a few seconds after the launch and we could not observe it further.

The K-8-9 type space rocket, launched at night, drifted 4° north from the launch direction 44 sec after the launch. The angle of rotation θ vs time (T) and the angle of elevation α vs time (T) curves of the K-8-11 type rocket is shown in Fig. 4. Optical observation point No. 1 was located at a mountain top which was 26 m higher than the launch point. The angle of elevation from the launch point to the optical observation point was about 8°50'. Therefore, the angle of elevation vs time curve in Fig. 4 starts from -8°50'. And the curve is higher than the calculated value. The launch direction of the rocket was 20° south from the line which connected the optical observation point No. 1 and the launch point. Therefore, the positions were so arranged that we could not accurately observe the rocket from behind. And the calculated angle of rotation vs time curve asymptotically approaches to 20° line as shown in Fig. 4. The K-8-11 type rocket drifted 3° south from the direction of the launch 40 sec after the launching.

5. Summary

In the K-8 type space rocket tests at Akita and Kagoshima, we filmed the launch of the rocket and the flight of the rocket. We obtained the above results.

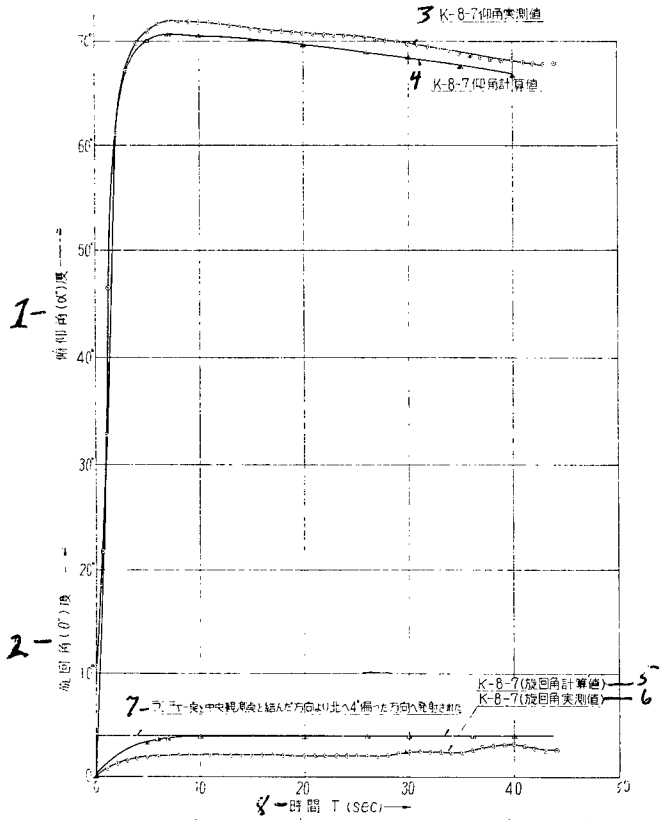

Fig. 3. Angle of rotation vs time and angle of elevation or depression vs time curves

1) Angle of elevation or depression (α); 2) Angle of rotation (θ); 3) Observed value of the angle of elevation of K-8-7 type space rocket; 4) Calculated value of the angle of elevation of K-8-7 type space rocket; 5) (Calculated value of the angle of rotation); 6) (Observed value of the angle of rotation); 7) The rocket was launched to the direction of 4° North from the line which was connected between the launcher point and the central observation point; 8) Time

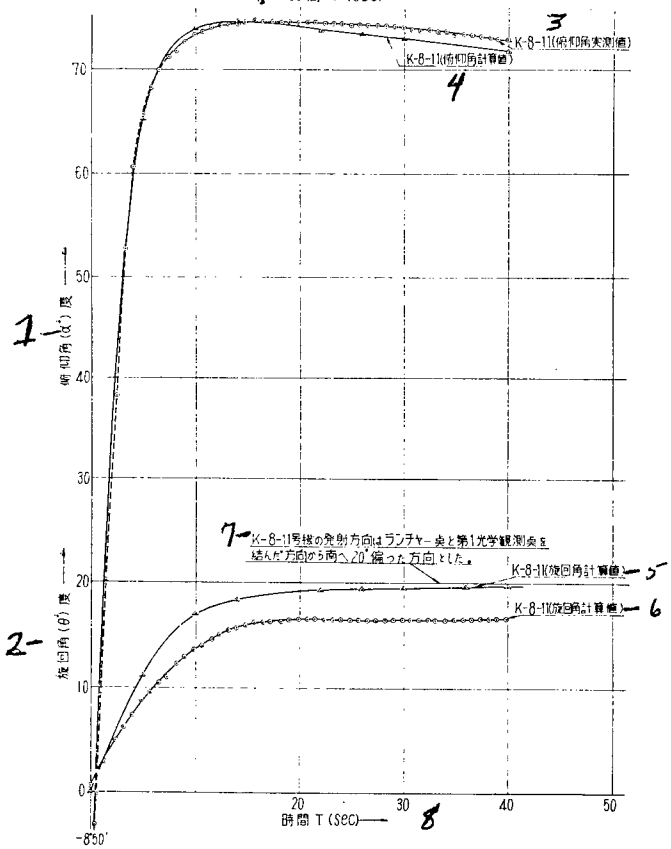

Fig. 4. Angle of rotation vs time and angle of elevation or depression vs time curves

1) Angle of elevation or depression (α); 2) Angle of rotation (θ); 3) Observed value of the angle of elevation of K-8-11 type space rocket; 4) Calculated value of the angle of elevation of K-8-11 type space rocket; 5) (Calculated value of the angle of rotation; 6) (Observed value of the angle of rotation); 7) The launch direction of the K-8-11 type rocket was 20° south from the line which was connected between the launch point and the optical observation point No. 1; 8) Time

We understand that complete rocket trajectory tracking by present observation equipment is not feasible, but we know that we can track a rocket about 50 km if the observation conditions are good. We wish we could improve our observation equipment and get more useful data.

(Received on May 2, 1963)

OPTICAL TRACKING OF THE K-9L-2, -8L-1 AND -9M-1 TYPE SPACE ROCKETS

—39th report on research on the optical tracking of a high-speed, moving body—

By Hisaaki Uemura, Kanzi Ito, Katsuya Tanaka,
Yoshitaka Yamamoto and Kazuo Kanezawa

1. Introduction

The K-9L-2 type space rocket was launched at Michigawa Beach, Akita Province, at 2:05 p.m., December 26, 1961, with 81° angle of launch elevation. The rocket was to detect the density and temperature of electrons in the ionosphere. The rocket consisted of three stages, 420 B, 245 B and 150 M and reached a maximum altitude of about 350 km. The K-8L-1 type space rocket was launched at Kagoshima test ground at 4:15 p.m., August 23, 1962, with 80° angle of launch elevation. It was an improved K-6H type space rocket and consisted of two stages, 245 B and 150 M. The purpose of the launching was to test the flight performance of the rocket. The K-9M-1 type space rocket was launched at Kagoshima at 11:01 a.m., November 25, 1962, with 78° angle of launch elevation. It was an improved K-8 type space rocket and consisted of two stages, 420 B and 245 M. During the launching, the flight performance of the rocket was tested and the ionosphere observed. During the launch tests, we took film of the rockets. For the K-9L type, we filmed from the central and high-speed observation points. For the K-8L type, we used optical observation points No. 1 and No. 2. For the K-9M type, we used another observation point just beside the launch point to take film of the lift-off of the rocket by means of a high speed camera in addition to the optical observation points No. 1 and No. 2.

2. Equipment for Filming

The K-9L-2 type space rocket was filmed by a 15 times magnified tracking system from the central observation point and by a Bell & Howell camera from the high-speed camera observation point. The K-8L-1 type space rocket was filmed by a 15 times magnified tracking system and a 16-mm Filmo camera from optical observation point No. 1 and by a prism-type high-speed camera and Bell & Howell camera from optical observation point No. 2. And for the K-9M-1 type space rocket test, in addition to the cameras for the K-8L-1 type, a high-speed camera was set near the launch point and the lift-off of the rocket from the launcher was filmed by the camera. For details, refer to the camera data (Table 1).

Table 1

使用カメラ 1		K-9 L-2	K-8 L-1	K-9 M-1
15 倍手動追跡装置 27	6本体	16 35 mm Mitchell 改造カメラ	16 35 mm Mitchell 改造カメラ	16 35 mm Mitchell 改造カメラ
	7レンズ	Raptar 254 mm f: 4.5	Raptar 254 mm f: 4.5	Raptar 254 mm f: 4.5
	8絞り	f: 4.5	f: 5.6	f: 4.5
	9フィルタ	17 なし	Fuji No. 7 Geratine	17 なし
	10撮影速度	22 f/sec	24 f/sce	24 f/sec
	11同期	18 目盛カメラと同時 1 PPS	18 目盛カメラと同時 5/6 PPS	18 目盛カメラと同時 5/6 PPS
	12一コマの露出時間	19 約 1/500 sec	19 約 1/500 sec	19 約 1/500 sec
	13フィルム	35 mm Fuji Nega (ASA 80)	35 mm Fuji Nega (ASA 80)	35 mm Fuji Nega (ASA 80)
(中央観測点)(第1観測室) 目盛撮影機 28	7レンズ	1″ f: 1.8	1″ f: 1.8	1″ f: 1.8
	8絞り	f: 5.6	f: 5.6	f: 5.6
	9フィルタ	17 なし	17 なし	17 なし
	10撮影速度	17 f/sec	15 f/sec	15 f/sec
	11同期	1 PPS	5/6 PPS	5/6 PPS
	12一コマの露出時間	20 1 msec 以下 (ストロボ照明による)	20 1 msec 以下 (ストロボ照明による)	20 1 msec 以下 (ストロボ照明による)
	13フィルム	16 mm Fuji Nega (ASA 80)	16 mm Fuji Nega (ASA 80)	16 mm Fuji Nega (ASA 80)
16 mm Fastax 高速度カメラ (第2観測室) 5	7レンズ		Nikkor 180 mm	Raptar 101 mm
	8絞り		f: 4 と 5.6 の間	f: 4.5
	14カメラ電圧		50 v	50 v
	9フィルタ		21 17 なし	21 17 なし
	11同期		手動により X-1.8 sec SW on	手動により X-1.5 sec SW on
	10撮影速度		2,000 f/sec	2,000 f/sec
	15画面		22 ランチャ離脱付近	22 ランチャ離脱付近
	13フィルム		Eastman Ektachrome (7257) (ASA 160)	Eastman Ektachrome (7257) (ASA 160)
16 mm 日立 Himac 高速度カメラ (高速度カメラ観測点) (第2観測室) 4	7レンズ	Nikkor 180 mm		Topcor 58 mm
	8絞り	f: 2.5		f: 4.5
	9フィルタ	17 なし		23 17 なし
	11同期	23 手動 X-1.7 sec SW on		23 手動 X-1.5 sec SW on
	10撮影速度	1000 f/sec		2,000 f/sec
	15画面	24 ランチャ		25 ロケットのノズル部分
	13フィルム	Eastman Ektachrome (7257) (ASA 160)		Eastman Ektachrome (7257) (ASA 160)
35 mm Bell & Howell カメラ (第2観測室) 5	7レンズ		Nikkor 250 mm	Nikkor 250 mm
	8絞り		f: 5	f: 5
	9フィルタ		Wratten No. 85	Wratten No. 85
	10撮影速度		30 f/sec	30 f/sec
	12一コマの露出時間		26 約 1/500 sec	26 約 1/500 sec
	13フィルム		Eastman Color Negative (ASA 50) (5250)	Eastman Color Negative (ASA 50) (5250)

1. Camera used
2. 15 times magnified manual tracking-system (the central observation point or optical observation point No. 1)
3. 16 mm Fastax high-speed camera (optical observation point No. 2)
4. 16 mm Hitach Himac high-speed camera (the high-speed camera observation point or optical observation point No. 2)
5. 35 mm Bell & Howell camera (optical observation point No. 2)
6. Camera

7. Lens
8. Aperture setting
9. Filter
10. Film speed
11. Synchronization
12. Exposure time per frame
13. Film
14. Camera voltage
15. Object
16. Modified 35 mm Mitchell camera
17. None
18. 1 PPS (same moment with the scale filming camera)
19. About 1/500 sec
20. Less than 1 m sec (by strob-illumination)
21. Manual SW (switch) on at x-1.8 sec
22. Manual SW on at x-1.5 sec
23. Lift-off motion
24. Manual SW on at x-1.7 sec
25. Manual SW on at x-1.5 sec
26. Launcher
27. Nozzle area of rocket
28. About 1/500 sec

3. Flight Observation

(a) K-9L-2 type space rocket.

The film of the rocket from ignition until it went 5 m above the launcher was taken from the high-speed camera observation point. The tracking film was taken by the 15 times magnified tracking system from the central observation point. But the rocket disappeared behind a cloud because the weather was bad. However, the film taken of the rocket until it disappeared showed no abnormality in the flight.

(b) K-8L-1 type space rocket.

It was the first launching test at Kagoshima. The rocket's lift-off was filmed by high-speed cameras from the optical observation point No. 2 and the tracking film was taken by the 15 times magnified tracking system from optical observation point No. 1.

(c) K-9M-1 type space rocket.

The 15 times magnified tracking system took the tracking film from optical observation point No. 1, 117 m behind the launching point. But the rocket was hidden by a cloud and further tracking was not possible. High-speed cameras took film of the rocket from its ignition until it went 5 m above the launcher from optical observation point No. 2. And another camera set at its side, 3 m away from the launcher, filmed the moment when the rocket lifted off.

4. Analysis of the Measured Results

(a) K-9L-2 type space rocket.

Figure 1 shows the analytical result of the displacement (L) and time (T) relation of the K-9L-2 type space rocket when the rocket was leaving the launcher. Because a lens of 180 mm focal length was used, the camera could take film of the rocket only when it was more than 5 m above the launcher. On the other hand, the accuracy of the film was high due to the long focal length lens. The K-9L-2 type space rocket started to move 15 m sec after the flash ignition and left the launcher 460 m sec after ignition. The velocity change was almost linear during the period.

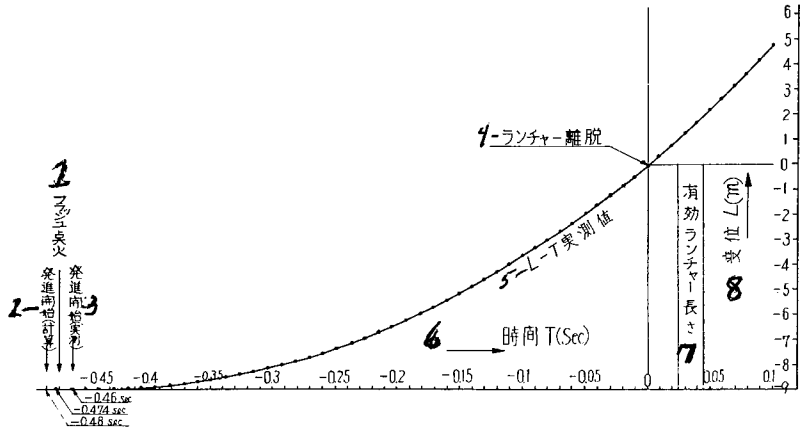

Fig. 1. Displacement (L) vs time (T) curve

1) Flash ignition; 2) Start moving (calculated value); 3) Start moving (observed value); 4-Lift-off; 5) Observed values of L vs T curve; 6) Time; 7) Effective length of launcher; 8) Displacement

(b) K-8L-1 type space rocket.

Figure 2 shows the displacement (L) vs time (T) curve of the K-8L-1 type space rocket. In the filming, a camera with a 180 mm focal length lens was used just as for the K-9L-2 type space rocket. This camera has approximately the same view and accuracy as that used for the K-9L-2 type space rocket.

(c) K-9M-1 type space rocket.

Figure 3 shows the displacement (L) vs time (T) curve of K-9M-1 type space rocket. In the filming, a 110 mm focal length lens was used, and we could take film of the rocket until it went 8 m above the launcher because the lens had a wider sight than that of the camera for the K-8L-1 type.

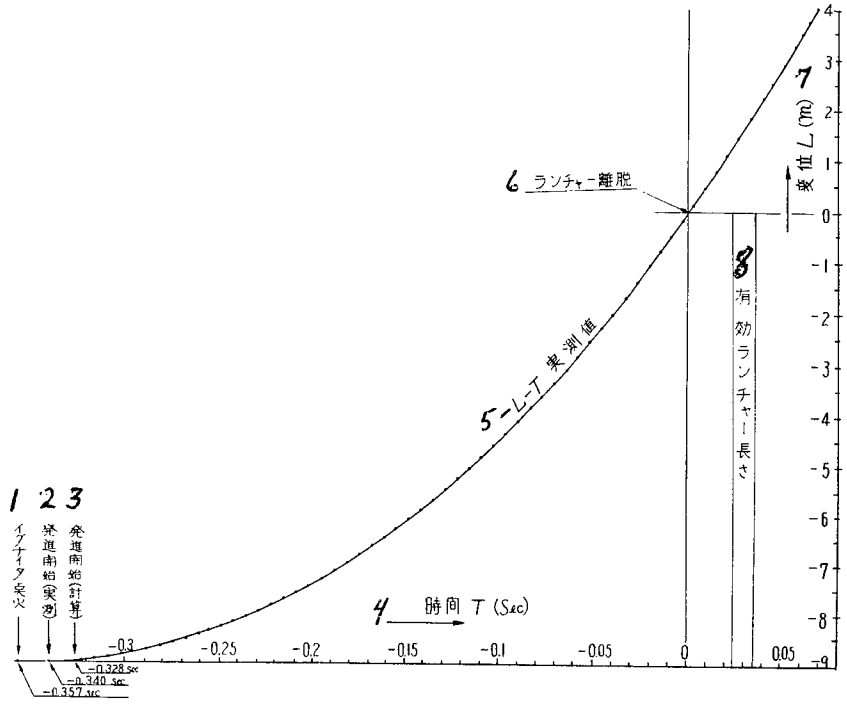

Fig. 2. Displacement (L) vs time (T) curve

1) Igniter ignition; 2) Start of moving (observed value); 3) Start of moving (calculated value); 4) Time; 5) Observed values of L vs T curve; 6) Lift-off; 7) Displacement; 8) Effective length of launcher

(d) K-9L-2 type space rocket.

In comparing the accelerations of K-8L-1, K-9M-1 and K-9L-2, the order of accelerations of the rockets were K-8L-1 — K-9L-2 — K-9M-1. This order agrees with the calculated values. The calculated value was larger than the observed value for the K-8L-1. But, for the other two rockets, the calculated values were smaller than the observed values. The differences between the calculated values and observed values were very small and we can say that the rockets began lift-off at the moments that were calculated.

5. Summary

The K-9L-2 type space rocket was the second three-stage rocket ever launched. Because of the bad weather, we could not track the trajectory

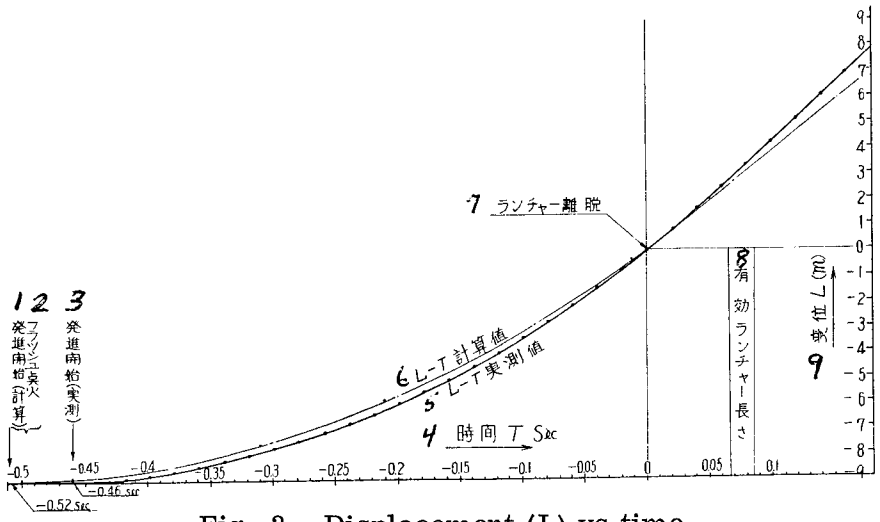

Fig. 3. Displacement (L) vs time (T) Curve.

1) Start of moving (calculated value); 2) Flash ignition; 3) Start of moving (observed value); 4) Time; 5) Observed values of L vs T curve; 6) Calculated values of L vs T curve; 7) Lift-off; 8) Effective length of launcher; 9) Displacement

of the rocket. However, we could get some films of the rockets, part of their trajectories and lift-off. And we did find that the rockets were stable when they were leaving the launcher.

We had bad weather for many launch tests. But we hope that we will have better data when we have optical observation point No. 4 from which we can observe a rocket as long as possible without any cloud interference, unlike the southern observation point at Akita.

(Received on May 2, 1963)

OPTICAL TRACKING OF SMALL MODEL ROCKETS

—High-speed Optical Tracking Research Report No. 40—

By Hisaaki Uemura, Ketsuya Tanaka,
Kazuo Kanezawa and Tokio Kitahara

1. Introduction

Small model rockets are launched to obtain basic information concerning rocket parts and accessories. At Michigawa Beach in Akita Province a four-nozzle FN-150-1 rocket was launched on October 26, 1961 (11:43 a.m.) (with 40° launching angle) to check the flying stability of such rockets. On December 20, 1961 (3:05 p.m.) an RT-150-1 rocket was launched (with 48° launching angle) to test the tracking performance of the radar system. On May 29, 1962 (11:34 a.m.) an HT-150-1 rocket, which was the K-6S prototype, was launched (with 60° launching angle) to obtain basic data on the aerodynamic heat of the rocket. At the Kagoshima rocket test ground an AT-150-1 rocket was launched on August 22, 1962 (1:00 p.m.) (with 60° launching angle) to test the new body antenna. On November 21, 1962 (11:09 a.m.) an LT-150-1 rocket was launched (with 60° launching angle) to check the launching characteristics of an undersling launcher. On November 24 (3:12 p.m.) and 25 (3:11 p.m.), 1962 an SP-150-3 rocket (with 60° launching angle) and an SP-150-4 rocket (with 65° launching angle) were launched to study methods of imparting spin to a rocket. And on December 20, 1962 (11:09 a.m.) an SO-150-1 rocket was launched (with 70° launching angle) in order to test an electronic system for improvement of operational reliability in a multistage rocket launching.

We, the optical observation team, photographed the rockets from the central and high-speed camera observation points at Akita and from optical observation points No. 1 and 2 and from the launch site at Kagoshima.

2. Photographic Equipment

We installed a 15-power tracking system at the central observation point and a 16-mm high-speed camera at the high-speed camera observation point for the tests at the Akita test ground. At Kagoshima we installed a 15-power tracking system at optical observation point No. 1, a high-speed camera and Bell & Howell camera at optical observation point No. 2, and another high-speed camera at the launch site. For details, refer to the camera data (Table 1).

Table 1

使用カメラ			FN-150-1	RT-150-1	HT-150-1
15 倍手動追跡装置 (中央観測点) (第1光学観測室)	追跡撮影カメラ 6	本体	Mitchell 改造カメラ	Mitchell 改造カメラ	Mitchell 改造カメラ
		レンズ	Raptar 254 mm f: 4.5	Raptar 254 mm f: 4.5	Raptar 254 mm f: 4.5
		絞り	f: 8	f: 4.5	f: 5.6
		フィルタ	Fuji No. 7	なし	Fuji No. 7
		撮影速度	24 f/sec	22 f/sec	24 f/sec
		同期	目盛カメラと同時 1PPS	目盛カメラと同時 1 PPS	目盛カメラと同時 1 PPS
		1コマの露出時間	約 1/500 sec	約 1/500 sec	約 1/500 sec
		フィルム	Fuji Negative Film (ASA 80)	Fuji Negative Film (ASA 80)	Fuji Negative Film (ASA 80)
	目盛撮影機 7	レンズ	1"	1"	1"
		絞り	f: 5.6	f: 5.6	f: 5.6
		フィルタ	なし	なし	なし
		撮影速度	17 f/sec	17 f/sec	17 f/sec
		同期	1 PPS	1 PPS	1 PPS
		1コマの露出時間	1 msec 以下 (ストロボ照明による)	1 m sec 以下 (ストロボ照明による)	1 m sec 以下 (ストロボ照明による)
		フィルム	16 mm Fiji Negative Film (ASA 80)	16 mm Fuji Negative Film (ASA 80)	16 mm Fuji Negative Film (ASA 80)
16 mm Fastax 高速度カメラ (高速度カメラ観測点) (第2光学観測室)		レンズ	250 mm	250 mm	250 mm
		絞り	f: 4	f: 4	f: 5.6
		カメラ電圧	AC 45 V	AC 45 V	AC 53 V
		フィルタ	Wratten No. 85	なし	なし
		同期	手動により X—1.5 sec SW on	手動による X—1.5 sec SW on	手動により X—1.3 sec SW on
		撮影速度	1300 f/sec	1700 f/sec	2,000 f/sec
		画面	ランチャ離脱付近	ランチャ離脱付近	ランチャ離脱付近
		フィルム	Eastman Kodak Negacolor Type SO—285 (ASA 50)	Eastman Kodak Tri—X (ASA 320)	Eastman Ektachrome (7257) (ASA 160)
16 mm 日立 Himac 高速度カメラ (16 H) (ランチャ点)		レンズ		250 mm	
		絞り		f: 4	
		フィルタ		なし	
		同期		手動により X—1.5 sec SW on	
		撮影速度		1700 f/sec	
		画面		ランチャ離脱付近	
		フィルム		Eastman Kodak Tri—X (ASA 320)	
35 mm Bell & Howell カメラ (高速度カメラ観測点) (第2光学観測室)		レンズ			
		絞り			
		フィルタ			
		撮影速度			
		1コマの露出時間			
		フィルム			

1. Camera used
2. 15-power tracking system (central observation point or optical observation point No. 1)
3. 16-mm Fastax high-speed camera (high-speed camera observation point or optical observation point No. 2)

Table 1 (Cont'd)

AT-150-1	LT-150-1	SP-150-3	SP-150-4	SO-150-1
35 mm Mitchell 改造カメラ	35 mm Mitchell 改造カメラ	35 mm Mitchell 改造カメラ	35 mm Mitchell 改造カメラ	35 mm Mitchell 改造カメラ
Raptar 254 mm	Raptar 254 mm	Raptar 254 mm	Raptar 254 mm f: 4.4	Raptar 254 mm f: 4.5
f: 5.6	f: 4.5	f: 4.5	f: 4.5	f: 4.5
Fuji No. 7	なし	なし	なし	なし
24 f/sec	24 f/sec	24 f/sec	24 f/sec	24 f/sec
5/6 PPS	5/6 PPS	5/6 PPS	5/6 PPS	5/6 PPS
約 1/500 sec	約 1/500 sec	約 1/500 sec	約 1/500 sec	約 1/500 sec
Fuji Negative Film (ASA 80)	Fuji Negative Film (ASA 80)	Fuji Negative Film (ASA 80)	Fuji Negative Film (ASA 80)	Fuji Negative Film (ASA 80)
1″	1″	1″	1″	1″
f: 5.6	f: 5.6	f: 5.6	f: 5.6	f: 5.6
なし	なし	なし	なし	なし
16 f/sec	16 f/sec	16 f/sec	15 f/sec	15 f/sec
5/6 PPS	5/6 PPS	5/6 PPS	5/6 PPS	5/6 PPS
1 msec 以下（ストロボ照明による）	1 msec 以下（ストロボ照明による）	1 msec 以下（ストロボ照明による）	1 msec 以下（ストロボ照明による）	1 msec 以下（ストロボ照明による）
16 mm Fuji Negative Film (ASA 80)	16 mm Fuji Negative Film (ASA 80)	16 mm Fuji Negative Film (ASA 80)	16 mm Fuji Negative Film (ASA 80)	16 mm Fuji Negative Film (ASA 80)
180 mm	35 mm	35 mm	35 mm	180 mm
f: 5.6	f: 3.5	f: 3.5	f: 4.5	f: 2.8
DC 50 V	AC 50 V	AC 50 V	AC 50 V	AC 52 V
なし	なし	なし	なし	なし
手動により X—1.5 sec SW on	手動により X—1.5 sec SW on	手動により X—1.5 sec SW on	手動により X—1.5 sec SW on	手動により X—1.8 sec SW on
2000 f/sec	2000 f/sec	約 2000 f/sec	2000 f/sec	2000 f/sec
ランチャ離脱付近	ランチャ離脱付近	ランチャ離脱付近	ランチャ離脱付近	ランチャ離脱付近
Eastman Kodak Tri—X (ASA 320)	Eastman Ektachrome (7257) (ASA 160)	Eastman Kodak Tri—X (ASA 320)	Eastman Kodak Tri—X (ASA 320)	Eastman Kodak Tri—X (ASA 320)
	58 mm	58 mm		
	f: 4	f: 3.5		
	なし	なし		
	手動により X—1.5 sec SW on	手動により X—1.5 sec SW on		
	2000 f/sec	2000 f/sec		
	ロケットノズル部分	ロケットノズル部分		
	Eastman Ektachrome (7257) (ASA 160)	Eastman Kodak Tri—X (ASA 320)		
Nikkor 250 mm f: 4	Nikkor 250 mm f: 4	Nikkor 250 mm f: 4	Nikkor 250 mm f: 4	Nikkor 250 mm f: 4
f: 8	f: 4 開放	f: 4	f: 5	f: 5.6
Fuji No 7	Wratten No. 85	Wratten No. 85	Wratten No. 85	Wratten No. 85
24 f/sec	24 f/sec	24 f/sec	24 f/sec	24 f/sec
1/5000 sec	1/500 sec	1/500 sec	1/500 sec	1/500 sec
35 mm Fuji Negative Film (ASA 80)	Eastman Color Negative Type 5250 (ASA 50)	Eastman Color Negative Type 5250 (ASA 50)	Eastman Color Negative Type 5250 (ASA 50)	Eastman Color Negative Type 5250 (ASA 50)

4. 16-mm Hitachi Himac (16H) high-speed camera (launch site)
5. 35-mm Bell & Howell camera (high-speed camera observation point or optical observation point No. 2)
6. Track filming camera
7. Scale filming camera

8. Camera
9. Lens
10. Aperture setting
11. Filter
12. Film speed
13. Synchronization
14. Exposure time per frame
15. Film
16. Camera voltage
17. Subject
18. Modified 35-mm Mitchell camera
19. None
20. 1 PPS (same moment with scale filming camera)
21. About 1/500 sec
22. Less than 1 msec (by strobe light)
23. Manually
24. Take-off
25. Open
26. Picture of nozzle of rocket

3. Observation of the Flights

Since the rockets had very high flying speed, take-offs were filmed mainly by high-speed cameras. Beside them, the rocket ascents were filmed by a 15-power tracking system and 35-mm Bell & Howell camera. Both at Akita and Kagoshima, rocket drift measurement was based on the direction of the line connecting the 15-power tracking system and the launch site.

Since most of the rockets were launched under cloudy or rainy weather conditions, the tracking times did not last more than several seconds. Trajectories of the rockets were not obtained since we could not set the south observation point at Akita and optical observation point No. 4 at Kagoshima, which was located to the side of the rocket trajectory.

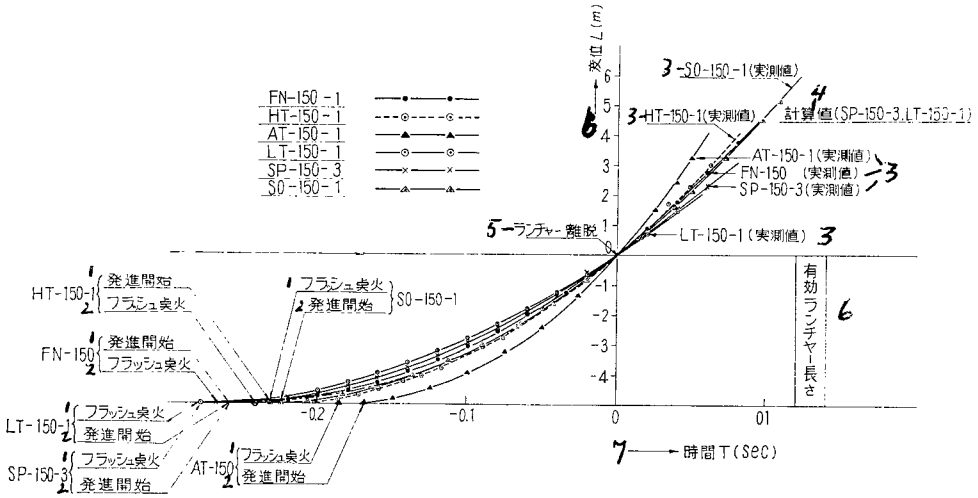

Fig. 1. Disposition (L) vs time (T)

1) Start; 2) Ignition; 3) Observed value; 4) Calculated value; 5) Take-off; 6) Disposition; 7) Time

4. Analysis of Observed Results

(a) Analysis of characteristics of rocket motion near the launcher.

The films were taken with a 16-mm prism type high-speed camera with speed of about 1300-2000 frames per sec. The lenses used were 35 mm, 180 mm, or 250 mm, depending on the purpose of the film analysis. A long-focus lens is good for detail, but a short-focus lens, on the other hand, gives a wider field. From the film, disposition (L) vs time (T), velocity (V) vs time (T), and disposition (L) vs velocity (V) characteristic curves were obtained. Figure 1 is the disposition (L) vs time (T) curve. A launcher with overall length of 5 m was used for all rocket launchings. The FN-150 rocket had the longest time (0.02 sec) from ignition to start. It took about 0.187 to 0.267 sec from ignition to take-off from the launcher. The AT-150 was the first of the rockets launched at Kagoshima and left the launcher in the shortest time, 0.187 sec. In the figure, the calculated value is shown only for the LT-150 rocket. The calvulated value differs for each rocket according to launching direction and total weight. Each model rocket had a different calculated value.

Figure 2 is the velocity (V) vs time (T) and was obtained from Fig. 1 (disposition (L) vs time (T) curve) by graphical differentiation. The velocities of the rockets at take-off were 34.6 m/sec for the LT-150, 35.7 m/sec for the SP-150, 37.6 m/sec for the FN-150, 41.1 m/sec for the SO-150, and 57 m/sec for the AT-150. "SP-150-3, LT-150-1 (calculated value)" in Fig. 2 means that the calculated disposition of the LT-150 rocket, which was first launched at Kagoshima by the undersling launcher, was the same as that of the SP-150 rocket launched by the ordinary launcher.

Due to poor weather at the time of launching of the SP-150 rocket the film was quite inaccurate. The AT-150 rocket left the launcher very rapidly. The velocity of the rocket was 14 to 19 m/sec higher than the other rockets. Graphical differentiation of the velocity vs time plots yields the average accelerations of the rockets. They are 163 m/sec^2 (164 m/sec^2) for the FN-150, 176 m/sec^2 (212 m/sec^2) for the HT-150, 334 m/sec^2 (343 m/sec^2) for the AT-150, 133 m/sec^2 for the LT-150, 136 m/sec^2 for the SP-150, and 164 m/sec^2 (183 m/sec^2) for the SO-150 type. The values in parentheses are the calculated values (normally larger than the observed values).

Figure 3 is the plot of disposition (L) vs velocity (V) as obtained from Fig. 1 [disposition (L) vs time (T)] and Fig. 2 [velocity (V) vs time (T)]. In the figure, the X-axis is the effective length of the launcher and the Y-axis is velocity. The AT-150 had the highest velocity at all times (velocity at moment of take-off was 57 m/sec).

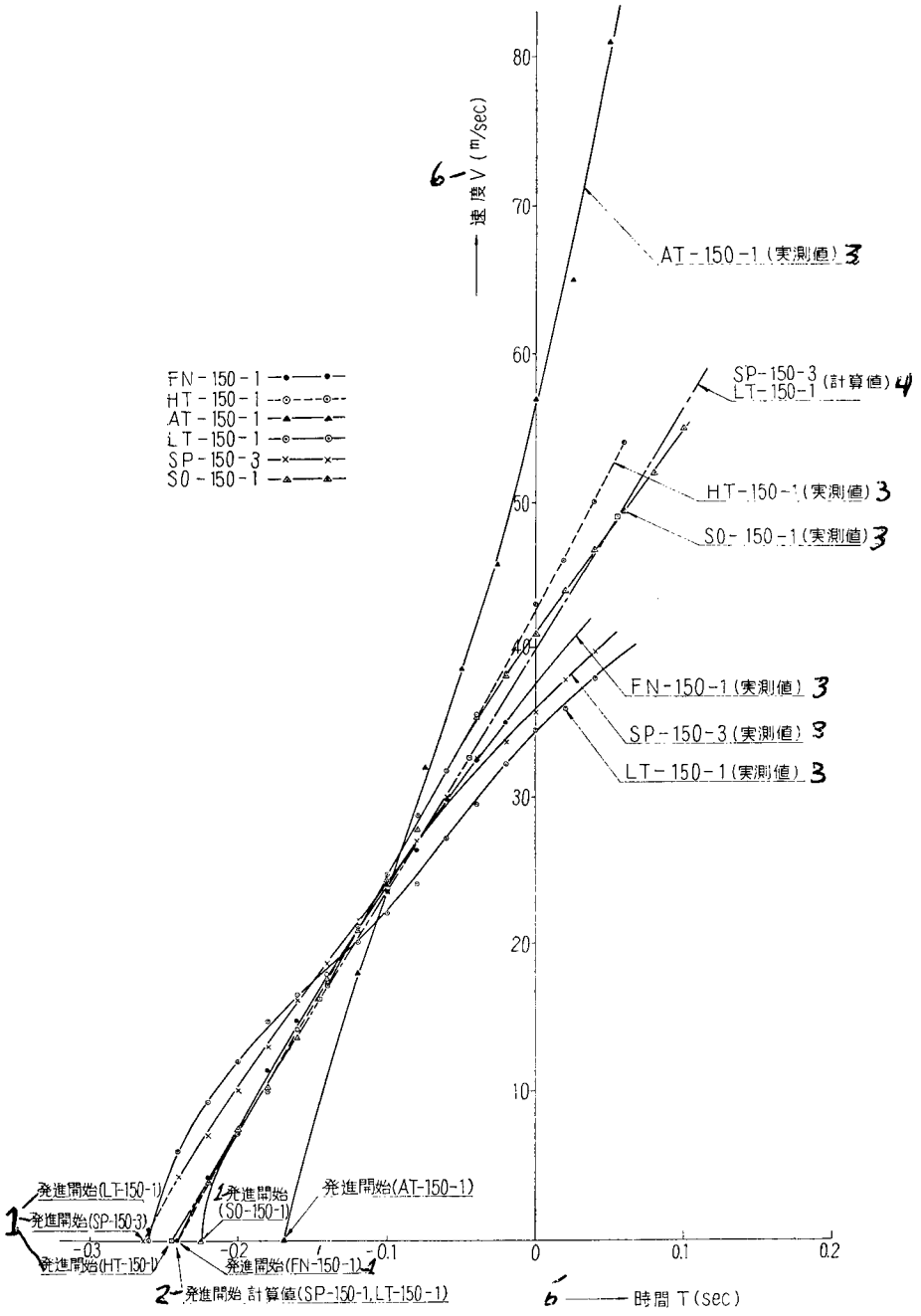

Fig. 2. Velocity (V) vs time (T).

1) Start; 2) Calculated start position;
3) Observed value; 4) Calculated value;
5) Time, T; 6) Velocity, V

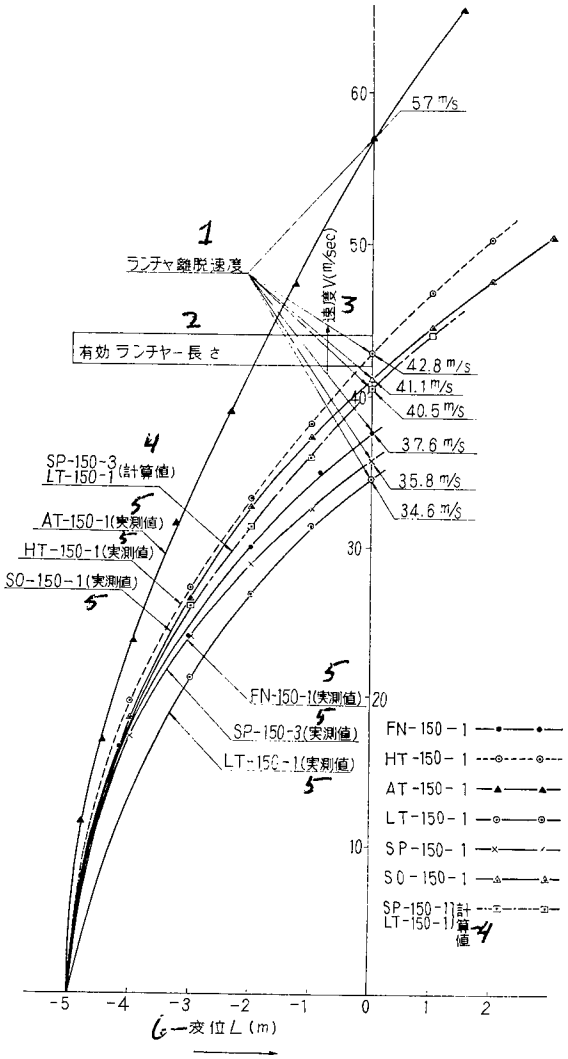

Fig. 3. Disposition (L) vs velocity (V).

1) Take-off velocity; 2) Effective length of launcher; 3) Velocity, V; 4) Calculated value; 5) Observed value; 6) Disposition, L

(b) Tracking film from the tracking system.

Since we tracked the small rockets with only one 15-power tracking system from the central observation point at Akita and from optical observation point No. 1 at Kagoshima, we could not obtain the trajectories of the rockets. Among the rockets which were launched at Akita, the FN-150 had drifted 4° south of the launching direction 8 sec after launching; the RT-150 was tracked for only 3 sec due to snowfall; the HT-150 had drifted 3.5° north from the

launching direction 5 sec after launching. Among the rockets launched at Kagoshima, the AT-150 had drifted 5.5° south from the launching direction 4 sec after launching; the LT-150 was launched in the rain and had drifted 0.5° north from the launching direction 4 sec after launching; the SP-150-3 had drifted 3° north from the launching direction about 4 sec after launching; the SP-150-4 was also in bad weather and had drifted 0.6° north from the launching direction 6 sec after the launching; the SO-150 was launched under cloudy conditions and tracked only 3 sec. Eight out of ten small rockets were launched under bad weather conditions, and that was the main reason we could not obtain useful data.

5. Summary

Launching tests with small model rockets were performed at Akita and Kagoshima test grounds. The objective of the launching tests was to check the performance of rockets and rocket-borne instruments as well as the launcher. We, the optical observation team, recorded the rocket flights, particularly at take-off, and obtained the above data. Since small rockets have much higher velocities than large space rockets, we had to film with natural background. We think that at least two observation points are required in order to obtain the trajectory of a rocket.

(Received on May 2, 1963)

SUPPORTING TOWER FOR 18-mφ TRACKING TELETRANSMITTER ANTENNA

By Takakazu Maruyasu, Hideo Nakamura

1. Introduction

This is a brief report on the supporting tower designed by us for the 18-mφ parabolic antenna under construction at the Kagoshima Space Center.

In designing the tower the following factors were given particular consideration.

(1) The tower site (the top of a mountain on Okuma Peninsula facing the Pacific Ocean) is located in the typhoon belt. The antenna will have no dome for wind protection, hence the structure of the tower must be such that it can withstand the severe stresses encountered during typhoons.

(2) The tower site is remote from sources of construction materials, equipment and skilled labor, hence the tower design must not be unduly complex.

(3) The structural tolerances are quite narrow, that is, the surface on which the antenna base is to be installed must be horizontal within less than ±1 minute and elastic deformation at the antenna base must be less than 10 seconds.

(4) The soil survey revealed that the foundation for the supporting tower was unexpectedly bad and that measures must be adopted to prevent differential settlement of the tower.

2. Composition and Structure

The tower is a reinforced concrete cylindrical structure. There are anchor bolts on top of the tower by which the antenna system is fixed in place. The antenna can rotate from 0° to 360° on the vertical axis (azimuth) and from -9° to 185° on the horizontal axis (elevation). There is a door at the bottom of the tower; a spiral stairway and ducts for feed lines are installed within the tower. The upper part of the tower will be used as the power distribution room, from which a door opens onto the catwalk to a spiral stairway for access to the rear of the rotary housing (see Fig. 1).

These facilities determine the inside and outside diameter of the cylindrical concrete body.

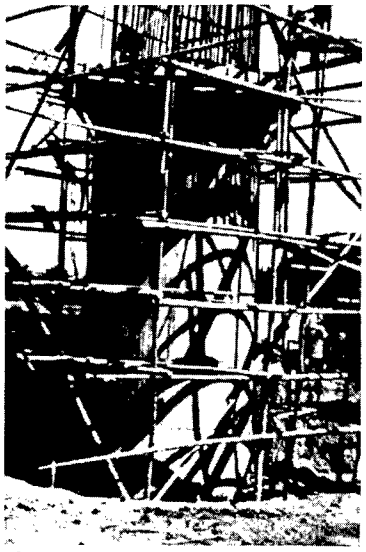

Photo. 1. Tower concrete work in progress

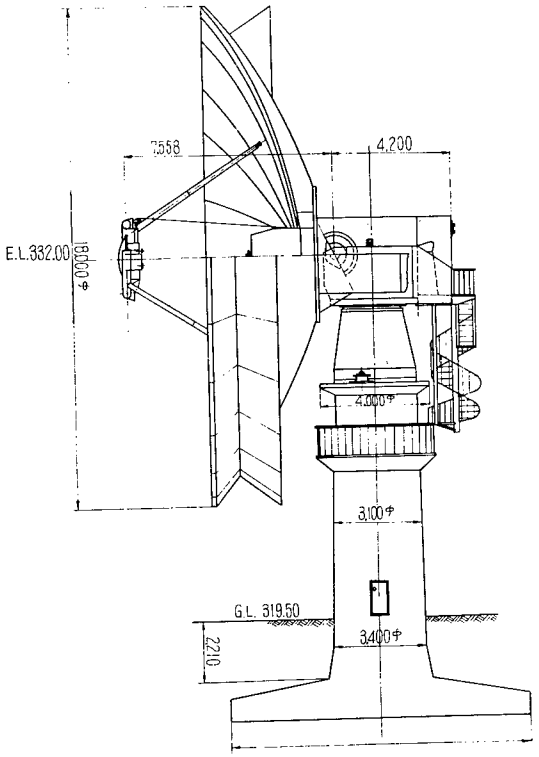

Fig. 1. Sketch of 18-mϕ parabolic antenna and its supporting tower

3. Load conditions

(1) Weights of antenna system

Weight of reflector (including counterpoise) : 30.3 ton

Weight of rotary compartment (including stairs) : 27.7 ton

Weight of stationary compartment: 16.3 ton

(2) Wind load

In testing a model of the installation at the Mitsubishi Electrical Machinery Co. it was assumed that the average wind velocity under normal weather conditions is 10 m/sec and the plane of the reflector is perpendicular to the wind direction (elevation 0°). The following values were obtained for normal wind load.

Horizontal force: 2.5 ton

Moment through elevation: 40.8 ton-m

Moment through azimuth: 20.4 ton-m

In the event of a typhoon, the reflector will be directed skyward (elevation 90°). In testing the model under these conditions (see Fig. 2) the following values were obtained.

Horizontal force: 40 ton

Moment through elevation: 100 ton-m

Moment through azimuth: 106 ton-m

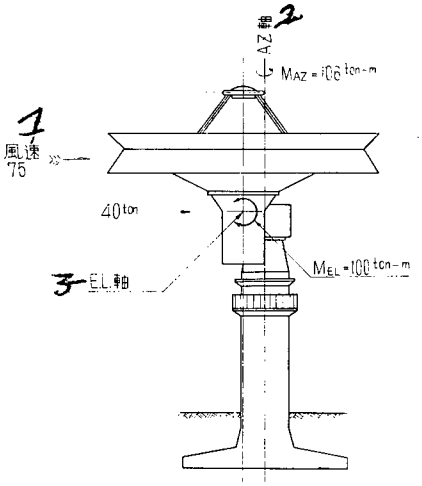

Fig. 2. Load condition at typhoon

1 - Wind velocity, 75 mph; 2 - Azimuth axis;
3 - Elevation axis

(3) Seismic load

Horizontal vibration: 0.3

Vertical vibration: 0

Snow load was not counted.

4. Materials

The specified concrete mix was $\sigma_{28} = 220$ kg cm^2 with DACON 35 reinforcing steel bar. SS41 was used for the other steel structures.

Photo. 2. Antenna anchor bolts and sheet-steel collar

5. Outline of the Design

(1) Antenna system anchor bolts and their base

The antenna system is secured against lifting force and horizontal force by 24 anchor bolts with diameter of 50 mm. Since the tower rim is not thick enough to hold the anchor bolts strongly, a ring of steel L-bar bearing the anchor bolts is welded to the reinforcing steel rods, and buried in the concrete. This ring helps hold the anchor bolts in the concrete, distributes the load to the reinforcing rods and aligns the anchor bolts with the required accuracy. Sheet steel collars inside and outside the rim of the tower prevent the edge cracking.

(2) Main body of supporting tower

The stresses on the main body of the supporting tower were calculated on the NEAC electronic computer with the axial force and bending moment of Fig. 3 applied to the tower.

Next the dimensions and number of reinforcing steel bars were checked. With a slot of 2β in central angle as shown in Fig. 3 and with axially directed force W acting over horizontal distance ϵ, the angle α between the neutral axis

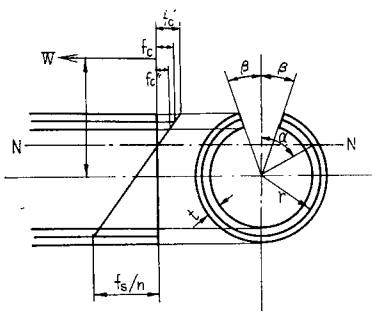

Fig. 3

and center of the slot is determined from the following equation:

$$\frac{e}{r}=\frac{(1-p)(\alpha-\sin\alpha\cos\alpha)-(1-p+np)}{2[(1-p)(\sin\alpha-\alpha\cos\alpha)-(1-p+np)}*$$
$$*\frac{(\beta+\sin\beta\cos\beta-2\sin\beta\cos\alpha)+np\pi}{(\sin\beta-\beta\cos\alpha)-np\pi\cos\alpha]}$$

When we apply the above equation to the doorway area, we obtain

$$r=134\text{ cm}$$
$$e=M/W=611/184=332\text{ cm}$$
$$p=0.00691$$
$$\beta=16°20'$$

and

$$\alpha=67°50'$$

From the above values, we get the stress of the concrete

$$f_c=\frac{W(\cos\beta-\cos\alpha)}{2rt[(1-p)(\sin\alpha-\alpha\cos\alpha)-(1-p+np)}*$$
$$*\overline{(\sin\beta-\beta\cos\alpha)-np\pi\cos\alpha]}$$
$$=36.1\text{ kg/cm}^2$$

at the center of the thickness of the concrete wall,

$$f_c'=f_c\left[1+\frac{t}{2r\cos\beta(\cos\beta-\cos\alpha)}\right]$$
$$=61.2\text{ kg/cm}^2$$

at the outside edge of the concrete wall, and

$$f_c''=f_c\left[1-\frac{t}{2r\cos\beta(\cos\beta-\cos\alpha)}\right]$$
$$=11.1\text{ kg/cm}^2$$

at the inside edge of the concrete wall.

The tensile stress of the reinforcing steel rod is

$$f_s=nf_c\left[\frac{1+\cos\alpha}{\cos\beta-\cos\alpha}\right]$$
$$=1273\text{ kg/cm}^2$$

The above calculations show that the tower will sustain the calculated stress. But since the doorway was the weakest area of the structure, we strengthened it with additional reinforcing rods. We also improved the stiffness of the tower by designing the landing as low as possible. Fig. 4 shows the distribution of reinforcing rods in the tower.

(3) Foundation and footing bars

The surface layer of sandy clay of weathered granite at the site is 7 to 8

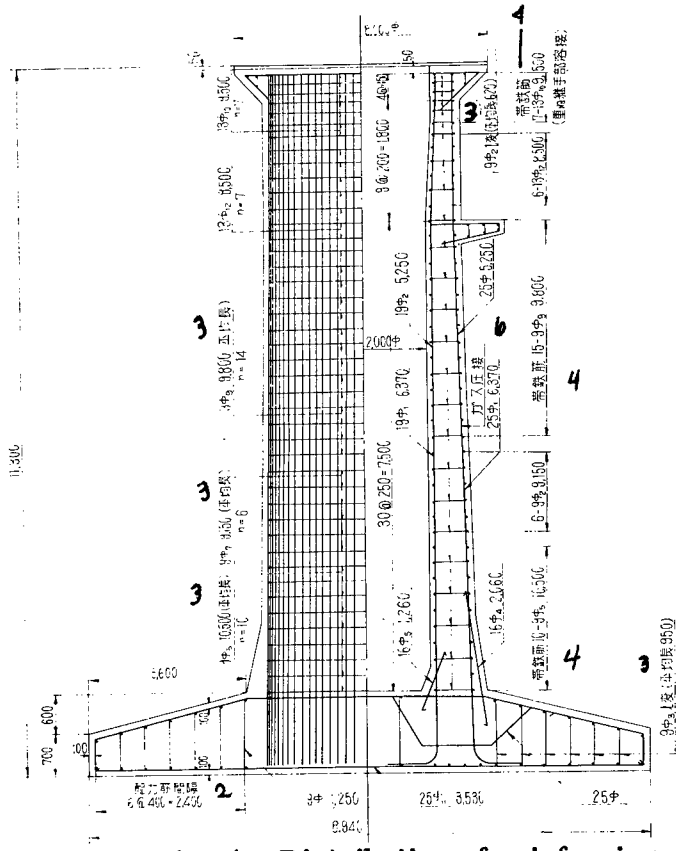

Fig. 4. Distribution of reinforcing rod in tower

1 - Rod spacing; 2 - Average length; 3 - Reinforcing bar; 4 - Welded armature; 5 - Pressure-weld area

Photo. 3. Tower concrete work near completion

meters deep and contains some pumice. This is not the kind of foundation which will support such a heavy structure as the tower, hence we consulted Assistant Professor Mitsugi regarding the results of the soil survey. According to his recommendation, the area was dug out about 4 meters to make a large foundation consisting of comparably hard sands. Then footing bars 300 mm in diameter and 4 m in length were driven into the earth at intervals of 1 to 1.5 m.

6. Conclusion

This type of supporting tower for a large parabolic antenna was the first to be designed in this country. Due to such unproved problems as load conditions and stress distribution we had to adopt a wide margin of safety in the design.

The antenna tower is being constructed by the Zenitaka Construction Company.

(Received on April 9, 1963)

IONOSPHERE DIRECT-OBSERVATION DEVICES AND THE OBSERVATION RESULTS

By Kunio Teshiri

1. Introduction

I had reported on the ionosphere direct-observation device for the K-8 type space rocket in the previous special issue of the Production Research (Vol. 13, No. 10). In this paper we will report on the later models of the ionosphere direct-observation device which were put on the K-9 type space rocket. Since the observation devices are similar in design to the previous one, we will not describe the details of the design of the observation devices. Instead, we will mainly explain the changes in the ionosphere direct-observation devices, the observation results we obtained thus far, and prospects for the future.

2. Changes in the Ionosphere Direct-Observation Devices.

(1) I A type ionosphere direct-observation device (for K-8-7 type space rocket).

The ionosphere observation device for K-8-5 and -6 type space rockets had resonance probes; and by the resonance probes, it could measure the density of the positive ions, electron density, and the temperature of the electrons, as we reported previously. This means that we could measure the quantities of of the positively and negatively ionized particles which are the fundamental values in the plasma observation (and it is known that there are no negative ions in the ionosphere except in the E layer and below). Therefore, we adopted the name, the ionosphere direct-observation device for the observation device and assigned the type number I to it. And the ionosphere direct-observation device will be equipped with additional measuring elements to determine other properties of the ionosphere.

The ionosphere direct-observation device for the K-8-7 type space rocket is made so that we can find the approximate number of photoelectrons in order to know the property of the positive ion probe, that is, we supplied the same voltage which is applied on the ion probe to the Langmuir probe circuit by adding the time division circuit to the Langmuir probe. By this, we can compare the solid sphere probe and reticular sphere probe. Roughly, it can be said that

the ion-trapping surface areas of the two probes are the same but the reticular sphere probe has a much smaller trapping surface area for ultraviolet rays which is the cause of the photoelectron radiation. Therefore, we can find the effect of the photoelectron radiation from the current difference between the two probes. The IA type ionosphere direct-observation device is exactly the same in physical appearance as the I type which was placed on the K-8-5 and -6 type space rockets.

(2) II type ionosphere direct-observation device (for K-8-8 and -9 type space rockets).

K-8-8 and -9 type space rockets were launched at Michigawa Test Center, Akita Province in October 1961. One of the two rockets was launched in the daytime and the other was launched at night. And we placed both the solid-sphere probe and the reticular sphere probe on both rockets to learn more about the reticular sphere probe. In the daytime launching, we sent both probes with the space rocket and received continuous records from both probes in our work to examine the effects of photoelectron radiation and the effect of altitude on photoelectron radiation. In the night launching, we tried to find the following two things: since it was a night test, there was no radiation from the sun and we would find the positive ion's penetration ratio of the reticular sphere probe by comparing it with that of the solid sphere probe. The difference between the positive ion's penetration ratios of the two probes would be clear at the altitude of 110 km which is called the orbital motion region and is where ions have some tens of centimeters as their mean free path. To solve the above two problems meant that we completely understood the properties of the reticular sphere probe except the effect of the velocity of the rocket on the probe.

We also adopted a temperature measuring probe which was developed from the resonance type probe on the rockets. Therefore, the ionosphere direct-observation device had to have five probes to be extended. And, since we knew that the probe extension mechanism of I and IA type ionosphere direct-observation devices would not work, we adopted a new probe extension mechanism. Figure 1 is the photograph of the entire II type ionosphere direct-observation device and Fig. 2 shows the device when the probes are extended.

In designing the probe, it is important that the probe should not vibrate when it is extended and that the extension motion should be smooth. For the former requirement, we made some experiments and reached the conclusion that we should use a teflon tube of 2-mm inside diameter which has, in the tube, three piano-wire lines of 1-mm diameter; in this way, the tube can diminish the vibration rapidly by the friction between the piano-wire lines, and thus the energy consumption of the piano-wire lines. For instance, when we compare the performance of a teflon tube in which a brass wire line, a nickel wire line, or a piano-wire line is inserted, we find that the tube which has the three piano-wire lines in it stops the vibration several times as rapidly as the other tubes; and the reason is that there is almost negligible friction between the teflon tube and a single piano-wire line because the surface of the teflon tube is very smooth.

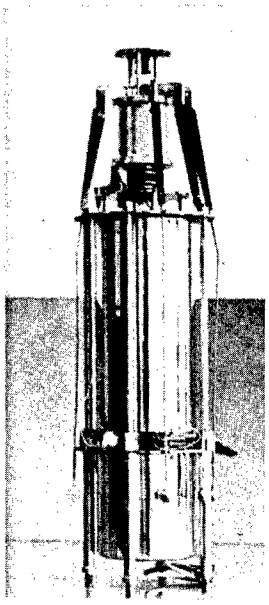

Fig. 1. II type ionosphere direct-observation device.

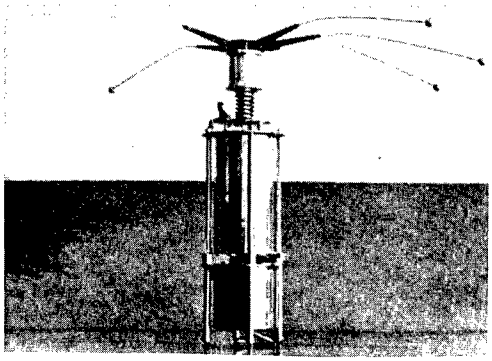

Fig. 2. Same observation device when its probes are extended.

For the latter requirement, we examined the curve of the upper edge of the cylinder which will extend the probes, and the curve of the probe holder which will be in contact with the cylinder edge when it is extended. Then we adopted such curves for the edge and holder so they would give nearly the same angular velocity of the probes when the probes are extended. Without this, the probe holder would bend by the shock of the extension force, and the probe might hit the body of the observation device. We also examined the force of the extension spring and so selected the probe that it could be stretched out in 0.2 second; then the probe would function 2 seconds after vibrations had been damped.

The electron-temperature measuring probe used (type II) is based on the property of a resonance probe: the lag of the characteristic curve of the resonance probe at a frequency region which is far below the plasma frequency is constant regardless of its frequency but is a function of the temperature of the electrons. In actual operation, we detect the difference of the DC voltages of the probe when the voltage of 30 kc frequency is applied to the probe and when the voltage is not applied.

In this observation device, a change is also made in the sweep oscillator. We use a beat frequency oscillator as the sweep oscillator, and our previous method to get sweep frequency was to use a variable oscillator with a variable air condenser which is rotated by a micro motor. However, we adopted the method which uses a variable capacity diode because the previous method is not adequate for a space rocket which has a long flight time. But we had to depend on the resistance which is rotated by a micro motor to generate the DC variable voltage to the diode, and for this we were dependent on the micro motor. However, the problem may be solved if we have a highly insulated and reliable relay, and we have a plan to have an all-electronic system for the test in 1964. We will discuss this problem later.

II type ionosphere direct observation device had the designs which are explained above, and its block diagram is shown in Fig. 3.

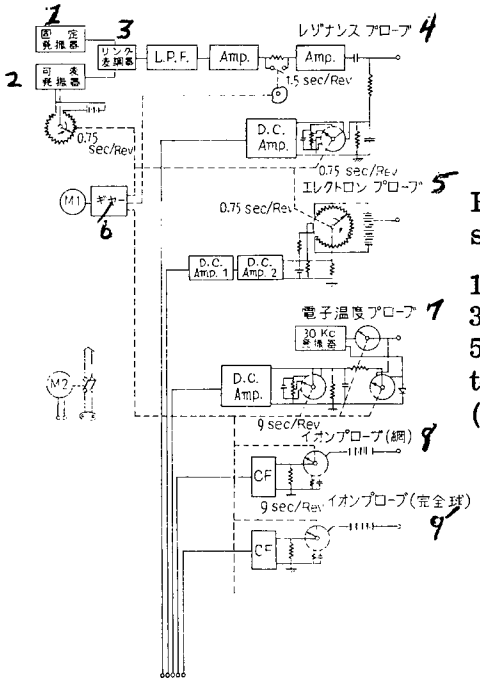

Fig. 3. Block diagram of Type II ionosphere direct-observation device.

1) Fixed oscillator; 2) Variable oscillator; 3) Ring modulator; 4) Resonance probe; 5) Electron probe; 6) Gear; 7) Electron-temperature measuring probe; 8) Ion probe (reticular sphere); 9) Ion probe (solid sphere)

(3) III type ionosphere direct-observation device (for K-9L type space rocket).

Following the K-8-9 type space rocket launching, K-9L type space rocket was launched at Michigawa Test Center on December 26, 1961. With this first three-stage space rocket, it was expected that the space rocket could reach the altitude of 350 km, which is beyond the maximum electron density region in the ionosphere.

This rocket's main rocket had 165 mm diameter and a small payload weight; therefore, we loaded only a resonance probe in the rocket to measure the density and temperature of the electrons.

Ionosphere observation from the ground has been performed by sending an impulse wave to the ionosphere. However, it cannot probe the inside of the ionosphere. But the electron distribution by altitude in the ionosphere is essential data in the research of the equilibrium condition of the ionosphere and thus the dynamics of the ionosphere. The electron temperature distribution in the ionosphere is also important data in research on the energy balance of the ionosphere. We put the resonance probe in the space rocket not only because of the importance of ionosphere measurements but also because the resonance probe was invented in this country. It positively helped in the K-9 type space rocket test that we had developed the observation device which has a 140-mm diameter. And the size of the observation device will also have the advantage that it can be put in future K-6 type space rockets. By the way, the II-B type ionosphere direct-observation device, which is the modification of type II, was put in the Nike-Cajun space rocket as the first U.S.-Japan joint test.

Thus, the type III ionosphere direct-observation device is the resonance probe itself. It consists of a drum with a power source and circuit in it and a probe set in the center of the drum. Its total weight is 3.5 kg, and it can send information through its two channels. The main rocket of the K-9L type space rocket was a spin stabilized type at 7 cps. Therefore, the type III ionosphere direct-observation device could be used to test the spin effect, and we found that the spin had no effect on the probe or on the observation device itself. In the test, we could also examine the heat effect on the observation device because the gap between the observation device and the rocket wall was only 10 mm, and it was also found that there was no heat effect during the rocket flight. Figure 4 shows the type III ionosphere direct-observation device.

(4) Type II-A ionosphere direct-observation device (for K-8-10 type space rocket).

Because the K-8-9 type space rocket failed to open its nosecone as we stated previously, the K-8-10 type space rocket was launched at Michigawa on May 24, 1962, at 7:15 p.m., to compensate for the failure of the K-8-9. However, this launching also failed because of booster trouble. Figure 5 shows the type II-A ionosphere direct-observation device which was put on the K-8-10 type space rocket.

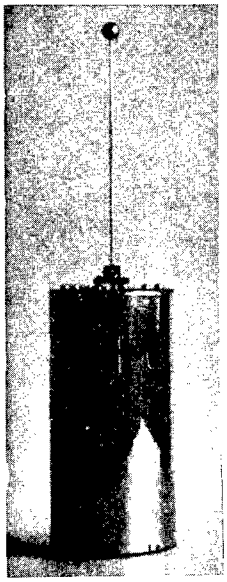

Fig. 4. Type III ionosphere direct-observation device

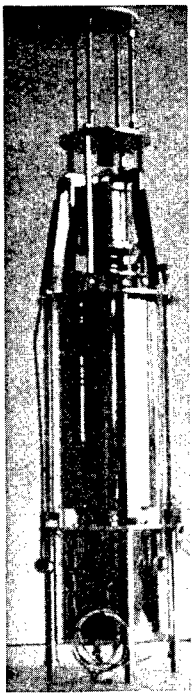

Fig. 5. Type II-A ionosphere direct-observation device

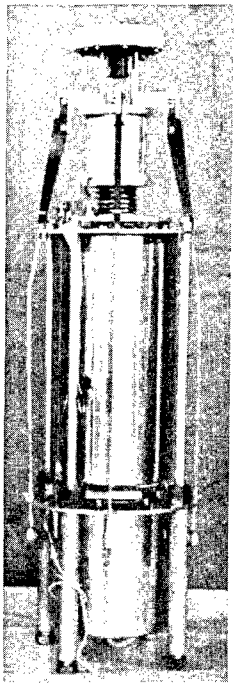

Fig. 6. Type II-C ionosphere direct-observation device

The space rocket, K-8-10 type, had a geomagnetic aspectometer which operates based on the earth magnetism and it could show its axial direction constantly, and therefore we put a plane probe which has a guard ring in front of it on top of the observation device. Then we can find the quantity of the positive ions by applying negative charge to the plane probe. It was a good change to examine the property of the spherical probe for it was a night test and there was no photoelectron radiation; and the mechanism of the trapping surface of the plane probe is very simple when the plane probe faces the direction of rocket flight. It is particularly easy to find the effect of the rocket velocity on the ion probe because the rear face of the plane probe is insulated by a teflon coating. Other probes were the same as those of the type II ionosphere direct-observation device.

(5) Type II-C ionosphere direct-observation device (for K-9M-1 type space rocket).

The first ionosphere observation rocket K-9M-1 type was launched at Kagoshima test ground on November 25, 1962, at 11:01 a.m. It was the test flight of the K-9M type space rocket itself. But the space rocket had superior properties, that is, its estimated maximum altitude was about 400 km and it could carry 50 kg. We put aboard the II-C type ionosphere direct-observation device to observe the ionosphere up to above the maximum electron density region of the F layer; this was done to make up for the recent failure in ionosphere observations. As shown in Fig. 6, the observation device — anion and electron trap on top of it and three probes, two of them being the resonance probes — are located diagonally from each other, and the remaining one, which is the ion trapping reticular sphere probe, is located at a normal direction to the other two probes.

In previous observations, we found that there are periodic changes even in the resonance probe as well as in the ion probe corresponding to the spin of the rocket. According to data, we thought that it was reasonable to take the upper limit value as the true electron density among the periodic changes of the electron densities which were obtained by the resonance probe. The first step to check the phenomenon is to put a resonance probe on each side of the rocket and compare the measurements from the two probes. If the change is due to only the phase of the rocket, the two measurements will have opposite phases of one to the other; and if the change comes from the different position of the rocket, the two measurements will show no difference in phase.

The ion and electron trap is shown in Fig. 7. The trap has (looking down) two grids and a circular collector. The gap between the grids is 5 mm. The grid has a circle 80-mm diameter for the effective surface area. The separators and case are made from teflon. When we apply DC variable voltage between -2.6 v and +6.5 v to the first grid, the ions and electrons in the plasma will be accelerated by the voltage and a part of the particles will flow to the first grid to show current change. This change will be sent by a transmitter. The particles which passed the first grid will be separated and accelerated further by the second grid to which -37.5 v for ion measurement and +10.5 v for electron measurement is

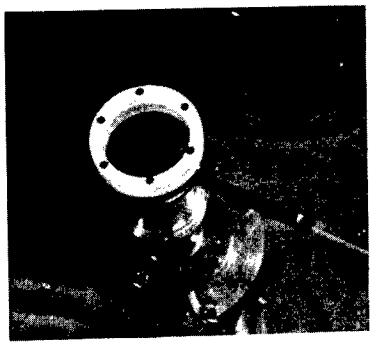

Fig. 7. Ion and electron trap

applied. In case of the ion measurement, positive ions reach the ion collector when -10.5 v is applied. This ion current change will be sent by another channel of the transmitter. In this case, the current is pure ion current and therefore we can find the density and temperature of the ions from the relationship between the ion current and the voltage applied to the first grid. Since the second grid voltage has 27 v relative voltage, smaller than that of the ion collector, the collector emitting photoelectrons will be forced back to the collector by the second grid voltage and, therefore, the effect of the photoelectron radiation will be removed. And this method is based on the assumption that the photoelectron emitted at the height of ionosphere has energy less than 20 electron volts. For the case of electron measurement, 37.5 v voltage is applied to the collector. By this voltage, the collector traps only electrons, and we find the density and temperature of the electrons from the current-voltage characteristics. The above ion and electron measurements are performed alternately with a certain time interval. The time interval in type II-C is 1/2 sec.

In this time, we tried to find the properties of the ion probe with the trap as explained above, but we failed again.

(6) Other ionosphere direct-observation devices.

Type II-B ionosphere direct-observation device (Nike-Cajun space rocket).

Type II-D ionosphere direct-observation device (Aerobee space rocket).

These ionosphere direct-observation devices do not deserve to be reported in this paper. But we will explain the observation devices briefly for they are the modifications of the ionosphere direct-observation device of the Kappa type space rocket. Type II-B, 170 mm in diameter, is the modification of the type II for the Nike-Cajun space rocket and is shown in Fig. 8. It can measure the density and temperature of the electrons and so needs two probes. Therefore, we adopted type II extension mechanism because the type I extension mechanism could not hold the two probes. The K-8 type space rocket had no

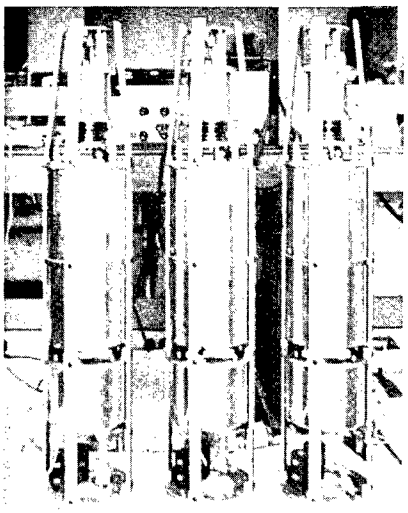

Fig. 8. Type II-B ionosphere direct-observation device

spin motion. Therefore, we could use a string which was connected between the nosecone and the trigger pin of the extension mechanism to give the necessary time delay (in order not to hit the nosecone), and we could adjust the delay time by adjusting the length of the string. But the Nike-Cajun space rocket had 7 cps of spin, and we could not use the same string for it would be wound on the observation device and lose its usefulness. Therefore, we adopted an electronic timer to give the time delay and a powder actuated piston to pull out the trigger pin.

Type II-D was carried by an Aerobee 150 rocket. It had four probes including an ion density measuring probe and NASA's Langmuir probe. It is shown in Fig. 9.

3. Measured Results

(1) The density distribution of the positive ions.

For positive ion density observations, we applied a variable voltage on the probes for K-8-3 and -4 type space rockets. Since then, we have observed the density with the same fixed voltage, -22.7 v. As a result, we could find out the ion density change with altitude and, similarly, the density distribution of ions with respect to that of electrons. But there were almost always some discrepancies in the electron density distribution below the E layer. The observation results of the K-8-6 type space rocket were the only successful observations to match the observations of the K-8-4 type space rocket that the ion density distribution at the sporadic E layer had a triple layer structure, even though it was not clear. From daytime observation, we could not find the layer at which the

ion density decreased because the K-8-3 type space rocket found the layer above the E layer.

(2) The density distribution of the electrons.

The resonance probe begins to function from an altitude of about 95 km, as was shown by the K-8-5 type space rocket. The reason is that at altitudes below 95 km the collision frequency of an electron is greater than the plasma frequency and the motion of the electron decreases. Therefore, the electrons cannot show the resonance probe characteristic. The electron density distribution by altitude observed by the space rocket can be compared with the same kind of distribution data obtained from the ground at the same time and using the vertical probe method of pulse wave. In this comparison, altitudes for the latter method must be converted to true altitudes for the altitudes are so-called bulk altitudes. A comparison of rocket data and ground data in which altitudes are converted to true altitudes by a creditable method are shown in Fig. 10. The rocket data of the figure are taken from the measurements of the K-9L-2 type space rocket. The K-9L-2 itself flew up to 350 km, but the data were transmitted only until 250 km because of failure in a part of the telemetry. Because this was the best available data, we used the data for comparisons, and they agreed well. Above 200 km, the relative densities from rocket data decreases and this trend was also found in the U.S. tests. We think the reason stems from the incomplete altitude data conversion process. In other tests, the electron density measurements were very satisfactory.

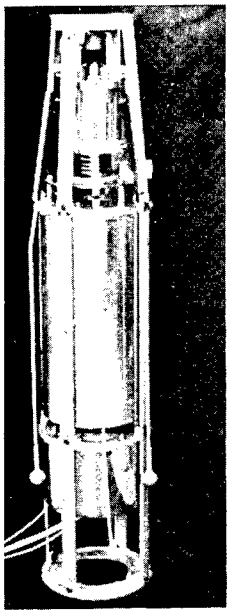

Fig. 9. Type II-D ionosphere direct-observation device.

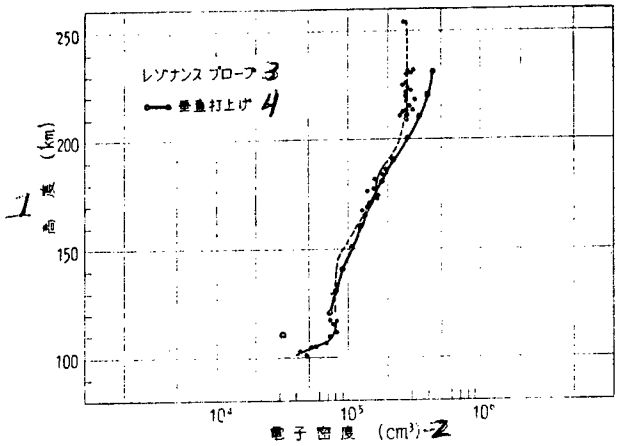

Fig. 10. Comparison of the K-9L-2 type space rocket's data and the data from the ground

1) Altitude; 2) Electron density; 3) By resonance probe; 4) Ground measurement

(3) The temperature distribution of the electrons.

We are approaching high success in electron temperature measuring by the resonance probe method. The main motive behind the U.S.-Japan joint test also came from the successful temperature-measuring method. As a result of the test at Wallops Island, we could compare the temperature measuring methods of the two countries. And it was possible to examine the electron temperature distributions by altitude along the geomagnetic latitudes from the three points, Ft. Churchill, Wallops Island and Michigawa, Akita. The result is very interesting. Figures 11 and 12 show the isothermal lines on the quiet day and active day of the ionosphere condition, respectively. The figures show that the temperature of the electrons is very high at the high latitude region compared with the middle latitude region on a quiet day, and it falls sharply at Wallops Island on an active day. As the figures show, the electron temperature changes widely with the geomagnetic latitude and the geomagnetic activity. The geomagnetic latitude of our country's new Kagoshima Space Center is 20° and the launch site has the lowest geomagnetic latitude in the world, except India's rocket launching site which is under construction. In this connection, we expect Kagoshima Space Center will make great contribution in this field. And, at the same time, we wish to reopen Akita Test Center or a new northside launching site for future geophysics work.

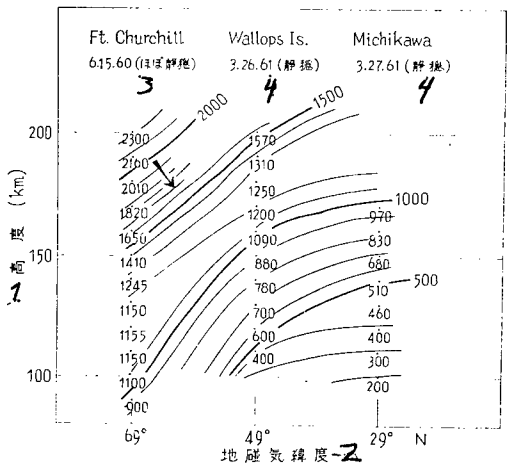

Fig. 11. Relationship between the temperature distribution of the electrons and the geomagnetic latitude (on a quiet day)

1) Altitude; 2) Geomagnetic latitude;
3) Almost quiet; 4) Quiet

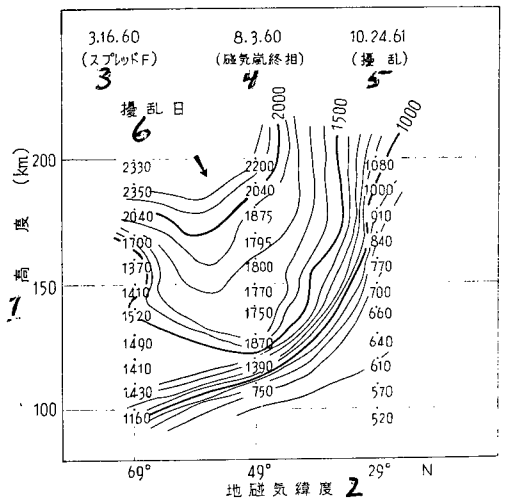

Fig. 12. Relationship between the temperature distribution of the electrons and the geomagnetic latitude (on an active day)

1) Altitude; 2) Geomagnetic latitude; 3) Sporadic F; 4) End phase of the geomagnetic storm; 5) Geomagnetic disturbance; 6) Time of disturbance

4. Conclusion

We discussed mainly the changes of the ionosphere direct-observation devices in this paper for we wish to have an ideal observation device by improving present ones and by adding new elements. As the new observation elements which are under development, we have the electron energy distribution measuring device, mass analysis device, and electrical field measuring device in the ionosphere, and each of them passed its basic experiment stage. And along with the improvement in space rockets in this country, we can expect longer flight and an earth satellite, with which we will be able to observe the activity of the ionosphere. Therefore, we are now performing research to make an observation device which is much lighter and can be used much longer than present ones.

Finally, we wish to express our thanks to the members of the Institute of Production Research, Yokogawa Electric Machinery Co., and other organizations which have contributed in the research and observation. We also extend our appreciation to Mr. Aoyama, the Ionosphere Gas Lab., the Institute of Radio Wave Research and other members of Akita Radio Wave Observation Station and Yamagawa Radio Wave Observation Station who offered us their facilities and much helpful advice.

(Received on April 30, 1963)

MEASUREMENT OF COSMIC RADIATION BY KAPPA 8, NO. 11 ROCKET

By Yukio Miyazaki, Kazu Takeuchi, Imai Takashi, Tadayoshi Yoshizawa, Kozo Otsuka and Koji Oya

1. Introduction

It is of interest to ascertain by experimental observations the existence of a region below the inner radiation belt in which high energy particles are trapped (see for example the K-8-3, 4 report*). The data obtained by Geiger counters carried by artificial satellites suggest that in the altitude region between 200 and 500 km the radiation intensity variation with altitude is far greater than that expected from the strength of primary cosmic rays. A comparison of data from Explorer 1 and Explorer 7 indicates that the intensity and the timing of this radiation is strongly dependent on the strength of solar activities; the stronger the solar activities, the stronger the variation of radiation activity with time. However, these data were obtained while the satellites were travelling over the vicinity of Japan, and may not represent the world-wide trend. Furthermore, the earth's magnetic field is relatively stronger at low altitudes than at high latitudes around 140° E longitude or less and it is even possible to have a region with a higher magnetic field even at the same altitude and with the same air density. This last surmise might explain the observations of the Explorers.

Thus, the main problems are: 1) to investigate whether such radiation exists, or is it a secondary effect caused by the materials which surround the detectors, and 2) if it does exist, what is its origin? The most direct method of solving these problems will be to measure the radiation intensity at various altitudes by a detector with very little material surrounding it. A more indirect method is to compare data from satellites at altitudes higher than 300 km, and

---

* No references were found in the original, even though they are cited by numbers.

from low altitude rocket flights. In the latter case one must be aware of various environmental effects such as the rocket body on the measurement. In the K-8-4 rocket flight in September, 1960 we made simultaneous measurements of radiation intensity by detectors with aluminum and lead shields and concluded that the lead shield increased the counting rate by 20%. This increase was attributed to an increase in the gamma-ray detection efficiency due to the presence of lead, and the production of secondary gamma-rays in lead. The average radiation intensity obtained in this experiment agreed with single counter data from other experiments within 20 to 30%.

The present experiment was planned in order to obtain the effects of various surrounding materials on the radiation counting rate up to the altitude of 200 km. The results from the present experiment may be able to explain the radiation intensity above the altitude of 350 km as due to a secondary effect of cosmic rays.

2. Instrumentation and Experimental Procedures

The detectors for the K-8-11 are Geiger counters of the same physical dimensions surrounded by different materials of different thicknesses. The counting rates from these counters are then the measures of the effects of the surrounding materials. Fig. 1 (a) and Fig. 1 (b) are the schematic diagrams of the counters, and their locations inside the rocket.

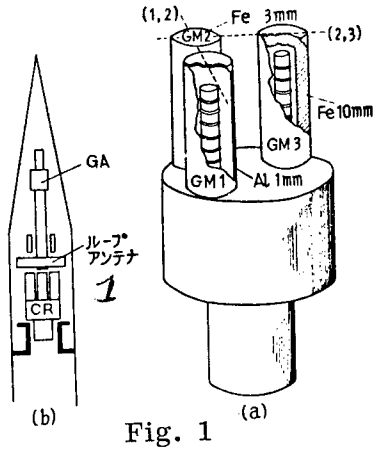

Fig. 1

(a) Sketch of the detector system for the K-8-11 rocket. The dotted lines (1, 2) and (2, 3) indicate the axes of the counter telescopes.
(b) The head section of the K-8-11 rocket showing the relative positions of several instruments.

1 - Loop antenna

Single counts as well as double and triple counts from the counter telescopes were taken in the present experiment. Also a shower detector was installed to detect high energy particles. High coincidence counts can only be obtained with increased mutual interferences among the counters, and the present arrangement of the counters sacrificed the high coincidence counting rates in favor of purer single rates. Therefore the telescopes yielded data with a small statistical significance.

(1) The detector unit consisted of three Anton 112 Geiger counters with stainless steel walls of 81% 30 mg/cm^2 (sic) and 19% 232 mg/cm^2 (sic). They were the same as those used in the K-8-3, 4, Σ-4-2, Explorer 7 and other rockets. Each external shield was a cylinder with a 45 mm OD. The three shields were made of 1 mm (.27 g/cm^2) of aluminum, 3 mm (2.37 g/cm^2) and 10 mm (7.9 g/cm^2) of iron, respectively. These shields were designed primarily as a source of secondary radiation for high energy cosmic rays rather than an absorbing medium. Since the secondary radiation is emitted with an angular spread, these shields serve to increase the detection volume of the counters. The shield also affects low energy radiation, and the total effect should be the algebraic sum of the two. The detection unit was placed in the rocket as shown in Fig. 1 (b) so that very little material surrounded it.

All three counters had the same effective volume and the counting efficiency was within 1% of each other. This greatly eased the analysis of the singles counting rates by eliminating a necessity for normalization. The effective volume and the counting efficiency were measured by means of a standard radiation source at a fixed distance from the counter. Counters (1, 2), (2, 3) and (1, 2, 3) formed the counter telescopes as shown in Fig. 1 (a).

(2) Fig. 2 is the block diagram of the electric circuit for the detection unit. The circuits employed NPN silicon transistors, which made it possible to obtain output signals from the walls of the counters [3]. The outputs from the coincidence circuits were taken in binary, mixed with the single signals, and were sent to a telemeter. The coincidence circuits utilized a parallel diode design, and had a resolving time of 50 microseconds.

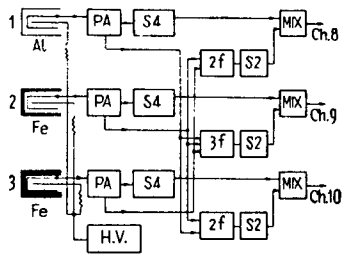

Fig. 2. Block diagram of the circuit

Fig. 3 is an example of the output signal sent to a telemeter. This and two other similar signals carried six pieces of information, and were sent in three channels from rocket No. 8-10 (sic). Eight type-3 manganese batteries in conjunction with Zenar diodes were used to obtain a stable power of approximately 6 volts. A transistorized SW was used as a remote control unit. All of the electronic instruments operated reliably for about four hours with the above power supply.

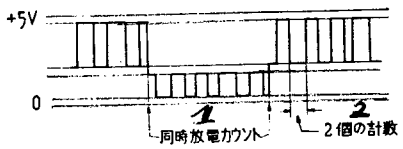

Fig. 3. Output waveform from the detector.

Narrow pulses are from the single counts, which change at every two pulses. Transfer to lower portion indicates coincidence counts.

1 - Coincidence counts; 2 - Counts from two counters

(3) In order to avoid high voltage discharges, O-rings were used to make the instruments airtight. The high voltage sections were covered by silicon rubber, which was also used in other parts of the circuit to absorb vibration and shock. The total weight of the instruments was 3.66 kg.

(4) Vibration and shock tests were performed in a predetermined manner at Mori's laboratory. During the vibration test, a few transistors were found to be partially damaged, and had to be replaced. This was the only trouble during the preparation for the present experiment. Instead of the standard temperature test of the Seiken (Production Institute), the coincidence resolving time and other circuit characteristics were measured at temperatures between -23°C and 70°C. These tests also served as a test of the circuit design.

(5) The K-8-11 was launched at 2:03 p.m. on December 18, 1962 from the Space Observatory of the University of Tokyo in Kagoshima located at 131°4'43" E and 37°15'0" N. The launching angle was 79° with an azimuth angle 150° NE. 796 seconds after the launch, corresponding to the altitude of about 95 km, the payload was ejected. According to a radar measurement, it then reached the maximum altitude of 202 km (corresponding to a lateral displacement of 120 km on the earth surface), and 443 seconds later it landed in the ocean (248 km lateral traverse on the earth surface). The counters performed well until they were damaged when the payload re-entered the earth's atmosphere at the altitude of 53 km, 415 seconds after the launch. All the expected data were obtained.

3. Results of Measurements

(1) The single counts as a function of time from all three counters showed nearly the same shape as those obtained by the K-8-3 and K-8-4 rockets. Fig. 4 shows a curve taken from the aluminum counter (GM-1). Hardly any time variation can be seen from 50 seconds (about 50 km high) through 231 seconds (202 km high) to 415 seconds (53 km high). Table 1 lists the average counts in the period 80 - 390 seconds, corresponding to altitudes greater than 95 km.

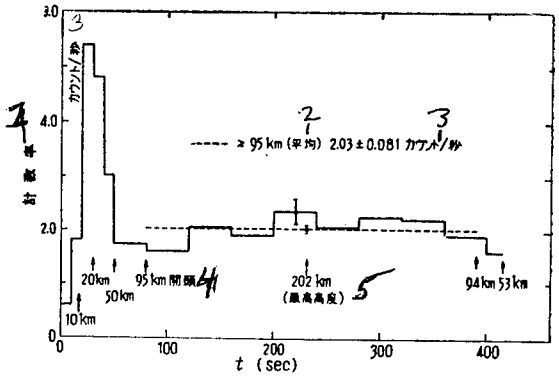

Fig. 4. The time variation of the single counts from the counter with 1 mm thick aluminum shield

Pfotzer mix at about 20 km and the plateau above 50 km are nearly equal to those from the K-8-4 rocket. Error at center is the statistical error based on the 40-second counting period. The other error is the statistical error on the average counting rate above 95 km.

1 - Counting rate; 2 - Average; 3 - Counts/sec; 4 - Ejection; 5 - Max. altitude

Table 1

Average Counting Rate at Altitudes Above 95 km

GM-1 (Al 1)	2.03 ± 0.081	counts/sec	(total counts 639)
GM-2 (Fe 3)	1.83 ± 0.077	"	(" 568)
GM-3 (Fe 10)	1.94 ± 0.079	"	(" 600)

(2) The coincidence counts showed random distributions for altitudes greater than 50 km. The total counts in the 80-415 seconds period are:

(1, 2) = 17 coinc., (2, 3) = 28 coinc., (1, 2, 3) = 4 coinc.

The double coincidence rates are:

$$c_{1,2} = 17/335 \text{ sec} = 0.0507 \pm 0.0123 \text{ coinc/sec}$$
$$c_{2,3} = 28/335 \text{ sec} = 0.0836 \pm 0.0158 \text{ coinc/sec}$$

The errors are statistical. The effect of the triple coincidence counts on the double coincidence counts was taken into consideration in the above rates.

(3) Assuming the angular distributions of radiation to be isotropic at high altitudes, the intensity per solid angle $\bar{j}$ can be obtained from the results obtained in sections (1) and (2). In the following notations S and C_t refer to single and coincidence counting rates, ϵ is the counter efficiency, and G and G_t are the geometric corrections needed for the single and the telescope counters. The errors are statistical.

(a) Singles counts

$$S = \epsilon \bar{j} G, \quad \epsilon = 0.81, \quad G = 52.4 \text{ cm}^2\text{sr}.$$

GM-1 (Al 1)
$\bar{j} = 0.048 \pm 0.0019$ particles $\cdot$ cm^{-2}sec^{-1}sr^{-1}
GM-2 (Fe 3) 0.043 ± 0.0019 "
GM-3 (Fe 10) 0.046 ± 0.0019 "

(b) Coincidence counts

$$C_t = \epsilon^2 \bar{j} G t, \quad \epsilon = 0.81, \quad G_t = 1.98 \text{ cm}^2\text{sr}.$$

(plane approximation and corrections for the cylindrical shape of the counters) (sic)

(1, 2) $\bar{j} = 0.039 \pm 0.010$ particles $\cdot$ cm^{-2}sec^{-1}sr^{-1}
(2, 3) 0.064 ± 0.012 "

4. Effects of Surrounding Materials on the Counting Rates

(1) As seen in Table 1 and in (3)(a), the results from the present experiment gave no clear information on the effects of the shielding materials used. The statistical error involved in comparing the various data is about 5%. In the case of the 10-mm iron shield, a calculation based on the effects of nuclear collisions and knock-on secondary electrons indicates the shielding effect to be less than 5% of the single counts. Even though the counters were arranged in this experiment to minimize the mutual interference, no doubt appreciable effects still remained. For example, the secondary radiation originating from shield 3 could enter the thin walls of counters 1 and 2, and cause an effect larger than those due to shields 1 and 2 alone. Knowing the solid angle subtended by shield 3 at counter 2, and the difference in the counting rates between telescopes (2, 3) and (1, 2), this mutual interference

effect may amount to 2 - 5% of the single counts. If this percentage is correct, we conclude that the effect of the 10-mm thick iron shield is not different from the single rate by more than 10%, since the single counting rate from each counter does not differ by more than 5% from the rest.

(2) Only four triple coincidence counts were recorded in approximately 300 seconds. The frequency of random triple coincidence can be considered to be negligible. Thus we believe that secondary particles were created.

A (1, 2, 3) triple coincidence can be initiated by a particle traversing through counters 2 and 3, knocking an electron from shield 3, which in turn triggers counter 1. This rate, however, is calculated to be negligible compared to the actual 4/300 seconds rate.

Perhaps a multiple emission by a nuclear collision is responsible for this 4/300 sec rate. If a multiple emission took place, this would not necessarily result in a triple coincidence, but perhaps in a (1, 2) or (2, 3) coincidence, or a single count. When we originally computed the double coincidence counts 3.(2), we subtracted the contribution of the triple coincidence counts. Still, the computed values of coincidence counts include the double coincidences resulting from multiple emissions. Therefore, the average intensity of cosmic rays computed from double coincidences will be considered to be the upper limit. The effect of multiple emissions on the single count is small since the probability of having a multiple emission is low.

(3) The single and the coincidence rates do not seem to differ very much from one another on the whole. The (2, 3) coincidence rate, however, seems a little higher due, perhaps, to shield 3. The contribution of gamma rays to the counting rate seems negligible as evidenced by the fact that the (1, 2) coincidence rate is nearly equal to the single rate. One must note again that some contributions from the secondary emissions are included in the coincidence rates.

(4) Fig. 5 shows a summary of data on the intensity of cosmic rays up to the altitude of 200 km. It has been shown in (4)(1) that the counting rate with the 10-mm iron shield is within 10% of the rate with the 1-mm aluminum shield. In the K-8-4 flight, on the other hand, a 20% increase in the counting rate was observed with a 1-mm aluminum shield. The average intensity observed in this flight is 20% greater than that observed in the present experiment. The power supplies and the effective detection volumes employed in both of these flights are not different by more than 5%. Thus we must look elsewhere for a possible explanation of the above mentioned discrepancies.

Table 2 lists various interaction characteristics of the shield materials. Note that 1) $\times$ $(N/A)\sigma$ for 10-mm thick iron is a factor of 10 greater than that for 1-mm thick lead; 2) the quantity t (a measure of the cascade process caused by electrons and photons with energies greater than the critical energies

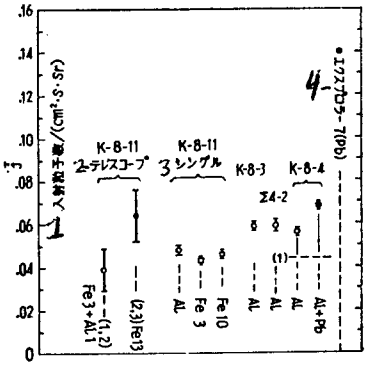

Fig. 5. Average intensities per solid angle obtained from K-8-3, 4, 11 and Σ -4 rockets

Errors are $\sqrt{N}$. A point from Explorer 7 is shown as a reference. Most points have errors about 6.3%, and show little time variation. Altitude ranged from 560 km to 1000 km. In this region the counting rates showed a plateau. April - May 1960).

1 - Particles; 2 -Telescope; 3 - Single; 4 - Explorer

Table 2. Radiation Interaction Constants for Various Substances

物質 (mm)	厚さ x (gcm^{-2})	核衝突			電磁的相互作用			γ-ray efficiency (calc) at 500 KeV
		原子核あたりの幾何学的断面積 σ (cm^2)	$N\sigma/A$	$x\cdot\frac{N}{A}\cdot\sigma$	X_0 (gcm^{-2})	ϵ_0 (MeV)	t	
Al 1	0.27	450×10^{-27}	10.02×10^{-3}	2.71×10^{-3}	24.4	48.8	0.011	0.00089
Fe 3	2.38	680×10^{-27}	7.30×10^{-3}	17.3×10^{-3}	13.8	23.9	0.17	0.0011
Fe 10	7.9			57.6×10^{-3}			0.57	0.0007
Pb 1	1.13	1590×10^{-27}	4.63×10^{-3}	5.23×10^{-3}	5.83	6.9	0.19	0.0052

Nuclear radius of 1.2×10^{-13} cm was used to calculate geometrical cross sections. X_0 is radiation length, ϵ_0 is critical energy, and t is radiation mean free-path; that is, x/X_0. Gamma-ray efficiency was calculated with this particular experimental arrangement taken into consideration.

1 - Material; 2 - Thickness; 3 - Nuclear collisions; 4 - Geometrical cross-section σ; 5 - Electromagnetic interaction

of iron and lead) is three times greater for 10-mm thick iron than for 1-mm thick lead; 3) at lower energies t for lead becomes greater because its critical energy is lower than that of iron; and 4) at much lower energies, lead has the highest efficiency for gamma rays.

These facts indicate that the contribution from low energy gamma rays must be taken into consideration in comparing the two sets of data. Fig. 6 shows the gamma-ray efficiencies for various materials for the gamma-ray energies between 0.1 and 3 mevs. These curves were obtained by extending the method described by Price [3]. The dashed curve for lead plus aluminum is theoretical. This curve must be corrected due to the fact that the secondary electrons scatter more in these substances, thus decreasing the amount which can enter the detection volume. The theoretical curve was normalized to a point experimentally measured with a Co^{60} source. The other curves are theoretical. Using these curves the average counting efficiencies for lead and aluminum were calculated to be 0.00785 and 0.0041, respectively.

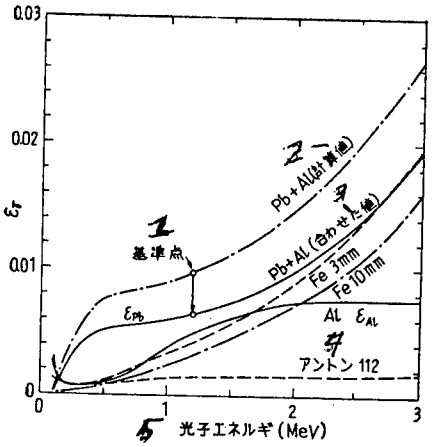

Fig. 6. Calculated gamma-ray efficiencies of the shield materials.

The efficiency of Pb + Al was obtained by first obtaining ϵ_{Pb} experimentally with Co^{60}, then from this value $\epsilon_{Al}/\epsilon_{Pb}$ was obtained, which was then normalized to a point with the efficiency for aluminum alone.

1 - Normalization point; 2 - Calculated; 3 - Normalized; 4 - Anton 112; 5 - Photon energy (mev)

The ratio of the counting rates with and without a lead shield in the K-8-4 flight was 1.2, which made the gamma-ray intensity to be 1.2 photons/cm^2secstr. The dotted horizontal line labeled (1) in Fig. 5 is the particle density corrected for the gamma-ray contributions. By using the gamma-ray intensities obtained by K.A. Anderson [5] at latitudes near 70°, and by Vette [6] at the latitude of 41°, we get a value of $0.1 \sim 0.5$ photons/cm^2secstr for gamma rays with energies greater than 100 kev. Therefore we assume that the major gamma-ray

contributions to the results of the K-8-4 flight must have come from those gamma rays other than albedo gamma rays, even though no usable data exist on albedo gamma rays to substantiate this argument.

Since the detectors were surrounded by an iron wall of considerable thickness in the K-8-4 rocket, the gamma rays must have originated from this wall. The Σ-4-2 rocket, on the other hand, had only one counter with an aluminum shield inside a plastic head. The lower part of this rocket was made of light material, and presented little surrounding substance to the counter. In spite of this arrangement, the counting rate from this rocket was higher than the others. We might be able to explain this contradictory result by considering the effect of the absorption of low energy particles, the difference in the latitude of this flight from the others, and a possible time variation in the gamma-ray intensity.

5. Conclusions

A shield which covers an entire detector affects its single counting rate by no more than 10%, if the shield is made of a material with an atomic number around that of iron, and its density is about 10 gm/cm^2. If, however, the gamma-ray production becomes prominent, the counting rate goes up by 20 - 30% as shown in the K-8-4 flight. A shield with a large atomic number, such as lead, increases the counting rate by 20% over the rate obtained with aluminum or iron shields. Compared with the rate when there is very little gamma-ray production, this increase is as much as 50 - 60%. With a suitable location of a shield, the gamma-ray efficiency can exceed that of the counters in the K-8-4 rocket; and under such a condition, it may be possible to obtain an increase of 100% over that obtainable under good conditions with no surrounding material.

An examination of several experimental data indicates that unless a high gamma-ray efficiency counter, or a high gamma-ray production is involved, all experimental data cluster as shown in Fig. 5. The only exception is a point obtained by Explorer 7. This may be attributed to high energy particles which are trapped, or particles (probably electrons) which produce high energy gamma rays, rather than to a secondary effect of cosmic rays.

Acknowledgements

We would like to express our sincere thanks to Prof. Saito, who as Chief of Operations, made these measurements possible, and to Prof. Tamaki, Deputy Chief of Operations. Thanks are also due to the members of the experimental team.

(Received on April 23, 1963)

MEASUREMENT OF ORIENTATION WITH K-8-11 TYPE SPACE ROCKET

By Ai-o Kato, Iwaho Aoyama,
Yoshio Simizu and Tadashi I-zuka

1. Introduction

Various observations may be performed from space rockets in the upper regions of the atmosphere. Correct processing of the data of these observations requires that the attitude of the rocket be known at every moment of flight. Such information is also of value in rocket engineering. There are many methods of ascertaining the rocket attitude. In every case, however, the the rocket must at least contain a device which can sense a fixed coordinate system with respect to the earth. We developed a geomagnetic attitude sensor the operating principle of which is based on the earth's magnetic field and was first used with the K-8-11 space rocket. It is our desire to improve the magnetometer to permit its use in measuring magnetic fields in the upper atmosphere and space.

2. Theory of Measurement

The geomagnetic field has long been used as the basis of a fixed coordinate system (e.g., the compasses in an airplane or ship). It is also the basis of an effective method of measuring rocket orientation relative to the almost constant geomagnetic field. But this involves a process of magnetic field detection, thus necessitating measurement of a vector quantity. A frequency-modulation type magnetometer is used for this purpose. It detects the direction and intensity of the magnetic field and is thus suitable for measuring a vector quantity. The detecting element is a cylindrical tape-wound magnetic core surrounded by a coil. Three such cores are arranged in a rectangular coordinate system, one on each of the mutually perpendicular axes. The magnetic field vector is measured with respect to the fixed coordinate system. With the three cores correctly installed in the rocket we can detect the angle between the body of the rocket and the geomagnetic field (that is, the orientation of the rocket).

However, the accuracy of this method is limited due to variations in field along the rocket's trajectory. Geomagnetic anomalies and increased rocket altitude also contribute to errors. In Fig. 1, X, Y and Z are the mutually perpendicular axes of the detecting cores. D is the angle between the X axis and the projection H' in the X-Y plane; the Z axis is the longitudinal axis of the rocket; θ is the angle between the Z axis and the geomagnetic field F. If we apply a compensating

magnetic field consisting of X_0, Y_0 and Z_0, then the outputs ΔX, ΔY and ΔZ have the following relationships:

$$X_0 - \Delta X = F \sin\theta \cdot \cos D \tag{1}$$

$$Y_0 - \Delta Y = F \sin\theta \cdot \sin D \tag{2}$$

$$Z_0 - \Delta Z = F \cos\theta \tag{3}$$

From (1), (2) and (3), θ is found as follows:

$$\cos 2\theta = 2\{(X_0 - \Delta X)^2 + (Y_0 - \Delta Y)^2\}/F^2 - 1 \tag{4}$$

where

$$F^2 = (X_0 - \Delta X)^2 + (Y_0 - \Delta Y)^2 + (Z_0 - \Delta Z)^2 \tag{5}$$

$$H'^2 = (X_0 - \Delta X)^2 + (Y_0 - \Delta Y)^2 \tag{6}$$

Space limitations prevented the use of a phase detector which could identify the polarity of the magnetic field. Therefore, instead of such a circuit, we applied the compensating magnetic field X_0, Y_0 and Z_0, which can also be used for regulation of sensitivity and drift detection.

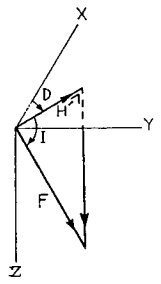

Fig. 1

3. Orientation Measuring System

(1) The Magnetometer. The orientation measuring system, as stated above, is a frequency-modulation type magnetometer. The magnetometer is based on the principle of a magnetic modulator. Instead of the toroidal core of an ordinary modulator, our magnetometer employs a high-permeability (permalloy) device with the following construction. A tape-wound permalloy cylinder is inserted into a silicon tube, thermalloy treated and then wound with an excitation coil, output coil and compensating coil. Figure 2 shows the block diagram of the circuit.

The output of the 1-kc oscillator passes through a 1-kc filter and excites the magnetic core. In the presence of an external steady magnetic field along the axis of the core a high-frequency current is generated in the output

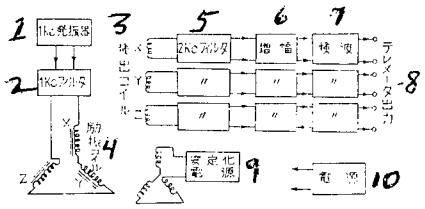

Fig. 2. Block diagram of magnetometer

1) 1-kc osc; 2) 1-kc filter; 3) Detecting coil; 4) Excitation coil; 5) 2-kc filter; 6) Amplifier; 7) Wave detector; 8) Telemetry output; 9) Stabilized power source; 10) Power source

winding. Only the frequency-modulated current is passed by the output filter and then amplified and detected. A phase detector is normally used to maintain polarity (positive or negative). Our method permits detection of a S/N magnetic field with intensity of approximately 1γ (10^{-5} oersted). Orientation measurement in detection of a magnetic field of the order of 100 γ is accurate to less than 1°.

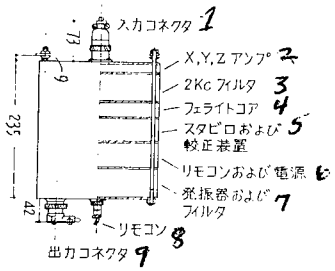

Fig. 3. Sketch of amplifier

1) Input connector; 2) X, Y, Z amplifiers; 3) 2-kc filter; 4) Core; 5) Stabilizer, corrector; 6) Remote control, power source; 7) Oscillator, filter; 8) Remote control; 9) Output connector

Figure 3 is a sketch of the amplifier. Figure 4 is a photograph of the extension system and Fig. 5 is a photograph of the entire magnetometer. The extension system protrudes about 15 cm beyond the rocket head when the cone is opened in order to avoid the effect of other devices and the rocket body. The RN antenna of the rocket was the nearest obstacle and the detecting element of the

extension system was 50 cm away from the rocket body. This extension system is of significance as a preliminary effort to increase the sensitivity for future measurement of extremely weak magnetic fields.

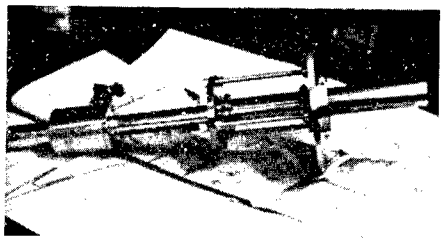

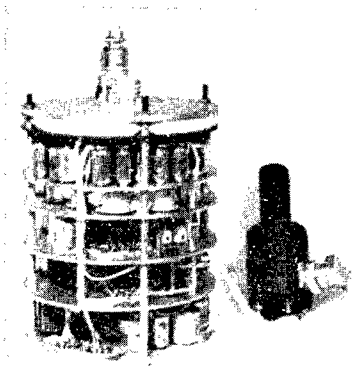

Fig. 5

(2) Characteristics. Figure 6 shows the output characteristic of the magnetometer. Drift due to variations in supply voltage and temperature was anticipated. Supply voltage variation can be minimized for at least an hour by pre-aging the mercury cell. The effect of temperature changes was minimized by placing the core in a bakelite shell and covering the detector with tinfoil to avoid radiant heating. We placed the detector in a vacuum oven (10^{-2} mm Hg) at 200°C and found that the temperature within the detector was below 50°. Core sensitivity does not change even at 70°C. But heat can distort the core sufficiently to create a stress contributing to drift. By employing amplifier and oscillator feedback and temperature compensation output drift can be held to $\pm 2.5\%$ at 10-50°C. Expressed in magnetic field intensity at an output voltage of 3.5 v, the error is $\pm 500\ \gamma$. The error in θ near the maximum point of H' change in Eq. (6) with total magnetic force of 45,000 γ is $|\Delta\theta| \fallingdotseq |\Delta H|/|F|$, and, therefore, the error is $\pm 1°$ for $\Delta\theta \fallingdotseq 50'$ or $\pm 500\ \gamma$ by $|\Delta H|_{max} = 500\sqrt{2} \fallingdotseq 700\ \gamma$.

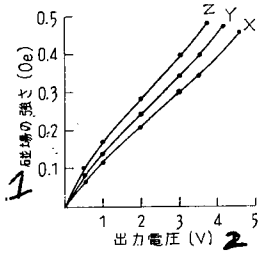

Fig. 6. Output characteristics of magnetometer

1) Magnetic field intensity; 2) Output voltage

Error can arise from inaccurate alignment of the detector and from the magnetic properties of surrounding materials. In the latter case, when the nosecone is not open magnetic field sensitivity of the magnetometer is decreased by 7,000 γ and angular error is 8°. Therefore data obtained before the cone is opened are not reliable. But this effect may be small if the magnetic field is generated by induction. The error between the calculated angle of 35° and the recorded angle of 28° was 8° in the early stage of the flight when the rocket obviously kept the initial attitude of 79° in angle of elevation and 55° E to S in direction with respect to the magnetic coordinates. Therefore error correction is required.

4. Ground Test

The magnetometer for the K-8-11 space rocket was subjected to temperature, permeability, shock, acceleration, and vibration tests according to the environmental test standard at the Institute of Production Research, Tokyo University. The vibration test revealed two resonance points at 200 c/s and 1200 c/s, but the magnetometer functioned normally.

Temperature tests were also performed at the Sok-Kisha Measurement Equipment Co. In the test, the detector and amplifier were separately heated in a vacuum oven and functioned properly. Magnetic tests were performed before and after the cone was opened in order to evaluate environmental effects. As the result of the test, we found that the magnetic sensitivity increased by 7,100 γ after the cone was opened.

Only the Z component of the force did not increase. The Z component in the test was the vertical component of the earth's magnetism, the value of which as measured by the magnetometer was 32,000 γ. Even though we did not measure its absolute value, our estimated value was also 32,000 γ.

5. Launching Test Results

Some of the data for the K-8-11 space rocket are shown in Figs. 7, 8, 9 and 10. From these and the composite plot in Fig. 11 we can see clearly the spin change.

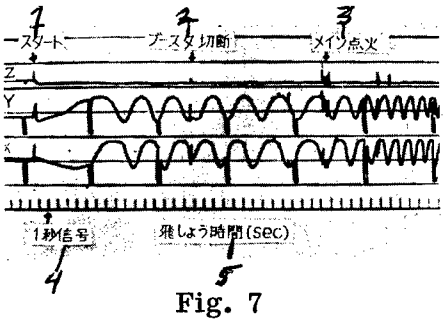

Fig. 7

1) Start; 2) booster cutoff; 3) main rocket ignition; 4) 1-sec marker; 5) elapsed time (sec)

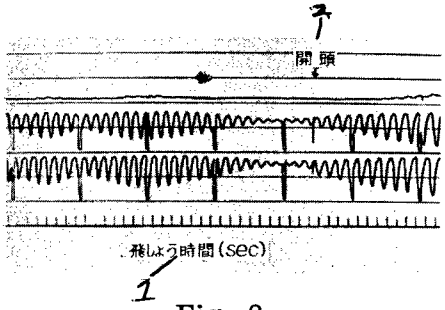

Fig. 8

1) Elapsed time (sec); 2) cone opening

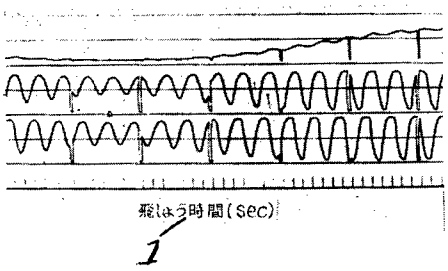

Fig. 9

1) Elapsed time (sec)

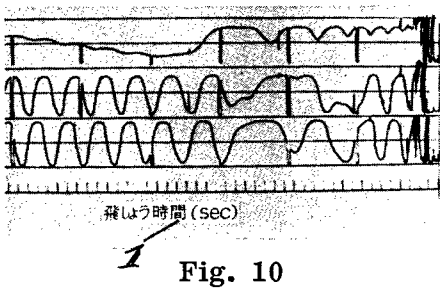

Fig. 10

1) Elapsed time (sec)

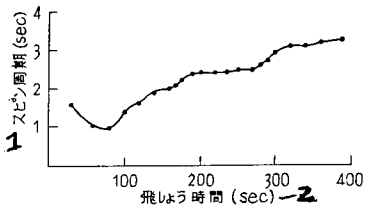

Fig. 11. Spin change

1) Spin frequency; 2) elapsed time (sec)

Noise spikes are observed at booster cutoff, main rocket ignition, and cone opening. Other noise is apparently an indication of detuning. We obtained recorded data for 422 seconds. In the analysis, the data were converted to magnetic field intensity according to Fig. 6 after calibration of the output power of the teletransmitter. The values of θ were then obtained from Eq. (4). The results are shown in Fig. 12. The curve is not extended byond 390 seconds because the motion of the rocket during the remaining period was very complicated and the values of θ in that period were of no importance. Analysis of the data permits the following observations. The rocket maintained the same attitude from booster ignition to main rocket ignition. Thirty seconds after lift-off the rocket began spiraling. This motion became quite severe upon opening of the cone, after which the rocket acquired a smooth precessional motion with period of 80 seconds.

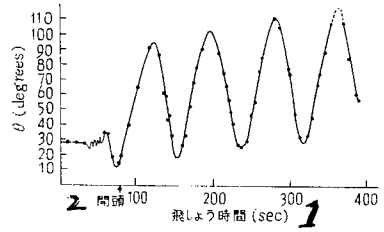

Fig. 12. Angles between the geomagnetic field and the axis of the rocket

1) Elapsed time (sec); 2) Cone opening

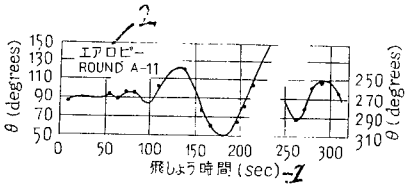

Fig. 13. Aerobee attitudes (J. Geophys. 56, 270, 1951)

1) Elapsed time (sec); 2) U.S. Aerobee Round A-11

For the purpose of comparison, Fig. 13 shows the θ variations of the Aerobee rocket (United States). It is to be noted that the amplitude of sprial motion of this rocket increased gradually. It is believed that the described motion of the K-8-11 rocket is due to the shock created by the cone-opening motion, which must be given further study.

Finally, in Fig. 14 we show the variation in magnetic force with altitude. This is not an adequation evaluation of the variation in magnetic force since the measuring accuracy was $\pm 500\ \gamma$, but it should be noted that there were marked changes at about 100 km and 180 km. However, these changes are inconclusive and require further tests.

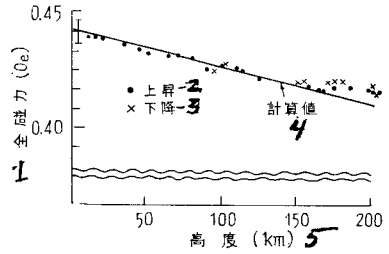

Fig. 14. Variation in magnetic force with altitude

1) Total magnetic force; 2) Ascent; 3) Descent; 4) Calculated value; 5) Altitude

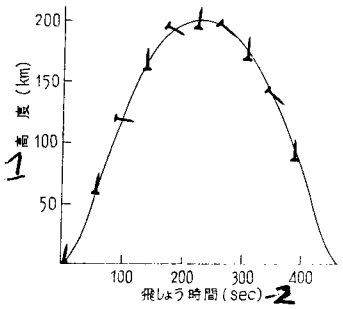

Fig. 15. Attitudes of K-8-11 space rocket

1) Altitude; 2) Elapsed time (sec)

6. Conclusion

We were able to measure rocket orientation. The test results indicate that there are unexpectedly wide variations (precessional) in the rocket attitudes. This will affect future observations, which require high accuracy; thereon rests the importance of rocket orientation measurement. Subsequent research will be directed toward reducing the size and weight of the measuring device and to analyzing the data more rapidly and accurately by using an electronic computer.

(Received on April 3, 1963)

MEASUREMENT OF THE ATMOSPHERIC LIGHT LAYER BY MEANS OF A ROCKET

By M. Furuhata, M. Nakamura, T. Nakamura and J. Nakamura

1. Introduction

What is atmospheric light?. How can one measure the height of the light layer, the main objective of this research?

This has already been mentioned in previous papers (this journal Vol. 13, No. 10).

The instrument, which was installed in the K-8-9 rocket, is slightly improved over the one used in K-8-5 and K-8-6, but is essentially the same.

The following describes the improvement in the instrument, with details of the instrument itself being omitted.

2. Instrument

The K-8-5 and the K-8-9 rockets are almost the same. They each include two light-collecting cylinders and their own photon tubes and amplifiers. They are as follows:

Measurement, line band	Phototube	Filter
Oxygen green line & Sodium D line	Mazuda PM 50	3 interference filters
Near infra-red OH line band	RCA 7102	Interference filter (7620 Å) and red filter

The voltage for the phototube was produced from a battery through a transistorized electric circuit and transformer. This method had some disadvantages, such as lack of lifetime and instability of the battery.

In this experiment, a barrier-layer battery was used. This battery was connected with a fine Toshiba 0180 type 270-volt battery in series. It was installed in a large box (see center of Fig. 1) and each battery supplied the phototube cylinder through a wire on the inside of a glass tube. The box and phototube cylinder were both sealed tightly to prevent any discharge from the upper part. A filter was set in a case with a movable disc, the position of which is changeable by the continuous rotation of a micrometer. The disc has a metal plate which is coated with a photo luminous material, besides having its own filter, and this works as a standard light source. If it comes out, it shows as a standard light and is recorded for its intensity. There is a chopper between the filter and phototube that is rotated by a micro motor. The photo current is multiplied by an alternating current and supplied to the telemetry by the chopper.

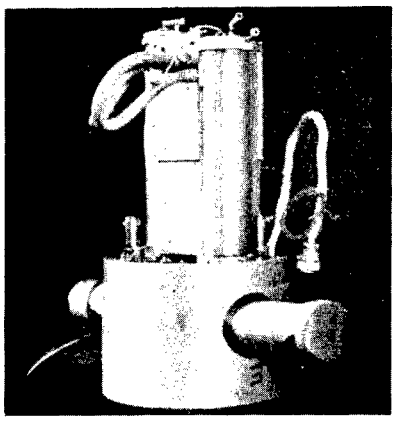

Fig. 1

3. Outline of Experiment

The experiment was performed at Akita, Japan, using a K-8-9 rocket. Launch was scheduled for October 29, 1961, but it was delayed one day due to bad weather. The experiment actually took place on October 30, 1961. The rocket was launched at 8:13 P.M. The altitude was 175 km.

The condition of the instrument was as follows: The light-collecting cylinder for infra-red was not working right. It opened eight seconds earlier than the expected time, which had been set for 62 seconds after launch, thereby injuring the phototube and the cylinder. The cylinder for the visible light opened exactly 65 seconds after take-off and worked quite well recording up to 175 seconds after the launch. Then, the noise level of the phototube got bigger and the readings were in error. We assumed the reason that it did not work was because the sealing of both the high-voltage battery and the cylinder of the phototube was not enough, resulting in discharge and low pressure.

The trouble with the infra-red cylinder was caused by parts that were misaligned, the vibration of which prevented the actuating spring from working.

The projection mechanism of the light-collecting cylinder was quite difficult. However, with the K-8-6 rocket this has not been successful because of trouble with the igniter. In the near future, it will be necessary to improve this mechanism. Figure 2 shows the standard light and atmospheric collected light recorded by the telemetry. Up to injection, the telemetry recorded only the standard light created by the fluorescent paint. However, right after injection, the atmospheric light was recorded also. It showed the intensity of starlight, excluding the atmospheric light band intensity. 5577 Å and 5893 Å should be calculated by subtracting these values. These values are the average of the intensity reached after passing the layer of atmospheric light and at the rocket altitude of more than 120 km. The value of 5300 Å is used as a check value. The recording of the standard light source showed that it looked like a mechanical noise. It was assumed that this noise was caused by the instability of the light source itself rather than by some mechanical noise of the phototube and/or amplifier. However, from these facts, it was confirmed that the sensitivity of both phototubes and amplifiers was not changed during the flight of this rocket. The lower chart of Fig. 2, as mentioned before, was caused by trouble with the phototube. The infra-red band could not yield any reasonable values at all, resulting from the trouble with the phototube, as shown in the lower chart of Fig. 2.

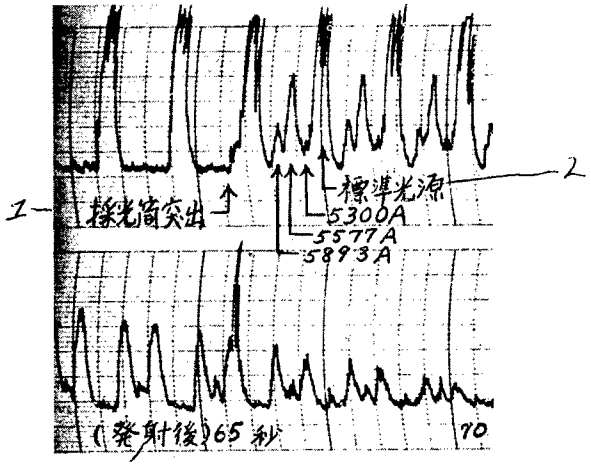

Fig. 2. Colorimetry record of light after and before projection of phototube (above-graph is for visual range of light; below-for infra-red light)
1) Projection of phototube; 2) Standard light source; 3) 65 sec after launching

4. Results

Figure 3 plots the atmospheric light intensity found during the experiment, the values being arrived at by subtracting the starlight intensity from the value of the recorder, as mentioned before. These points are scattered quite a bit due to the following:

First of all, there was the mechanical noise of the phototube and amplifier.

Second, the situation of the rocket itself.

The latter, as it happened, caused the following phenomena:

(1) The different traversed lengths of the layers of atmospheric light caused by the difference in angles of inclination between the rocket and the radiation layer of atmospheric light. If the angle is increased, the intensity is increased.

(2) The rocket faced different intensities of starlight at each moment, making the observation of the light intensity of starlight always a variable.

This phenomenon could only be avoided if the atmospheric light and starlight could be exposed to the rocket at the same time.

In Fig. 2, the intensity of the line value was negative after 90 seconds.

This meant that the exact value of starlight had not been subtracted from the atmospheric light intensity. If the position and attitude of the rocket could be observed simultaneously, this error could be resolved. This fact suggested that it would be practical to use an aspectometer.

However, according to the result of this experiment, the head of the rocket never faced downward, up to the point of highest altitude. If it faced downward, the atmospheric light would enter the rocket and the degree of intensity would be increased. If it is assumed that the rocket had passed through the layer of atmospheric light, keeping its head upward, the relation between the height of the atmospheric light line and the intensity analyzed from Fig. 3, would result in the drawing of Fig. 4. In this regard, the height of the layer of radiation is as follows:

Oxygen green line (5577 Å), 89-113 km; highest intensity, 98 km
Sodium D line (5893 Å), 88-110 km; " " , 93.5 km

This result is identical to the result of American observations.

The American experiment has been done in an area more than 10 degrees higher in latitude than in Akita. It was also the American purpose to discover the difference in the heights of the layer of radiation, but this difference should be included in the experimental error.

Summary:

The experiments regarding atmospheric light using rockets have just started.

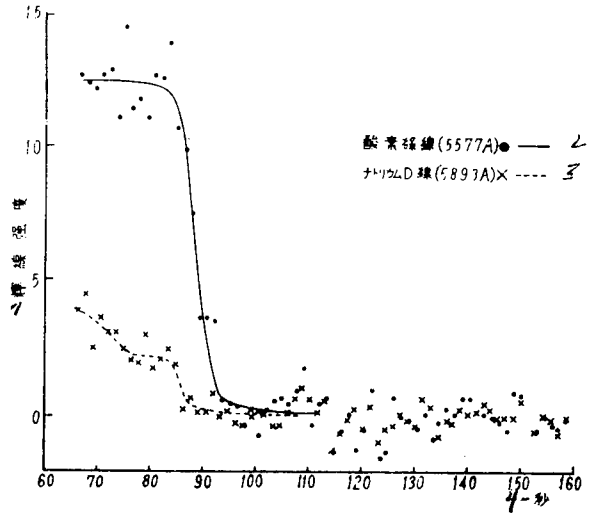

Fig. 3. Atmospheric light intensity shown from telemetry record of the visible spectrum (each value is obtained by subtracting 5300 Å, the star-light intensity)
1) Intensity of spectral band; 2) Oxygen green band (5577 Å); 3) Sodium D band (5893 Å) ; 4) sec

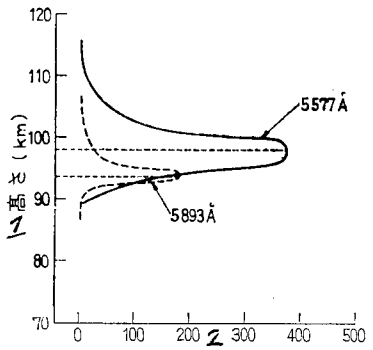

Fig. 4. Atmospheric light intensity vs altitude curves obtained by observation
1) Altitude; 2) Atmospheric light intensity

It is hoped to try to repeat the experiments to get more data, especially of the oxygen line red band (6300 Å), which has not yet been observed by rocket. This kind of experiment is expected from workers all over the world. It should be tried as soon as possible.

The authors are pleased to acknowledge the stimulating discussions of their collaborators of the Research Institute of Seisa Gijutsu and Kubota Observatory Instrumental Co. and gratefully acknowledge the assistance of Mr. S. Saito, Tokyo Observatory, Mr. S. Takezawa, Tokyo University of Education, Optical Institute.

(Received on March 29, 1963)

RESULTS OF THE OBSERVATION OF TEMPERATURE AND WIND IN THE UPPER ATMOSPHERE

Report No. 2 — By K. Maeda, Y. Takeya, H. Matsumoto, T. Okumoto, H. Ohya and W. Tatebe

1. Introduction

In regard to observations of temperature and wind in the upper atmosphere, the detailed accounts of the progress of our research and the outcome obtained by rocket No. TW-8 were reported in our previous report No. 1. Furthermore, we also attained results from rockets Nos. TW-9 and TW-10, which are described in this report.

The test results obtained by Nos. TW-9 and TW-10 are shown in Table No. 1. It is remarkable that the very first observational data, which were obtained in the summer, were satisfactory. In both tests, the observations were carried out up to approximately 70 km, which consequently proved for 70 km, the thrust capacity of the missile was sufficient.

Table 1

Observation Records Made at Michigawa (39°34' N, 140°03' E)

ロケット番号	ロケット発射時刻	レーダによる放出時刻	P_0の受音時間	設置マイクロフォン数	受音マイクロフォン数	フラッシュデテクタ	備考
TW—9 G_1	1960年9月29日11時46分	27.2秒	94.13秒	10 (P_0 2個 P_1～P_8)	10	27.72秒	
TW—9 G_2		40.3〃	151.33〃			40.74〃	
TW—9 G_3		55.4〃	207.55〃			55.75〃	
TW—9 G_4		72.9〃	262.45〃			72.99〃	
TW—9 G_5			322.72〃			95.12〃	
TW—9 G_6			416.73〃			148.08〃	
TW—10 G_1	1961年7月21日11時42分	41.88〃	151.75〃	10 (同上)	5	42.26〃	
TW—10 G_2		46.19〃	180.31〃			46.78〃	
TW—10 G_3		50.50〃	208.00〃			51.08〃	
TW—10 G_4		54.88〃	236.79〃			55.71〃	1号機 1部記録欠損
TW—10 G_5		59.11〃	260.46〃			59.50〃	
TW—10 G_6		63.60〃	290.35〃			64.19〃	
TW—10 G_7		68.39〃	321.78〃			68.96〃	
TW—10 G_8		73.21〃	354.64〃			73.91〃	

1) Rocket type and no.
2) Launching time
3) September 29, 1960, 11:46 a.m.
4) July 21, 1961, 11:42 a.m.
5) Ejection time detected by radar
6) Sec
7) Time at which microphone P_0 received soundings
8) No. of microphones installed
9) ($2P_0$ from P_1 to P_8)
10) Same as above
11) Microphone for receiving sound
12) Flash detector
13) Remarks
14) Partial lack of records for Rocket No. 1

2. Test Results

The results attained by TW-9 and TW-10 are shown in Fig. 1 (re: temperature distribution) and Fig. 2 (re: wind).

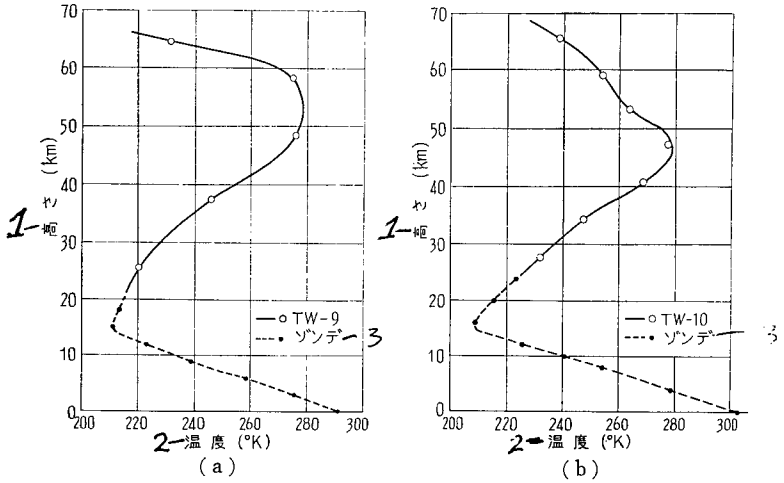

Fig. 1. Temperature distribution observed by rocket TW-9, 10
1) Altitude; 2) Temperature; 3) Radiosonde

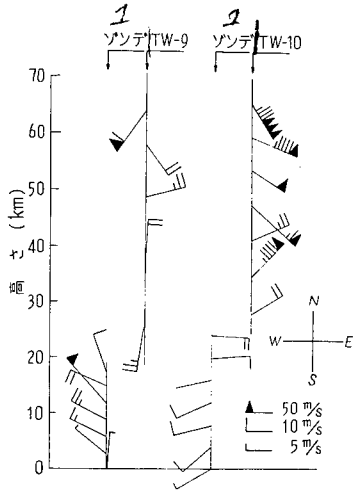

Fig. 2. Wind observed by rocket TW-9, 10
1) Radiosonde

In Fig. 1, small circles indicate the average values at several altitudes, and a solid line connects the circles. Dots show results obtained by radiosonde at Akita Observatory figured for the time of the rocket flight. The results attained by radiosonde went up to 21 km by TW-9 and 25 km by TW-10.

Figure 2 shows the results obtained by radiosonde up to the height of 6 km for TW-9 and 13 km for TW-10. The results were obtained by radiosondes sent aloft from neighborhood of the Akita Experimental Station, and those in higher range are adopted from the report by Akita Observatory.

3. Discussion

As mentioned above, the results obtained by TW-10 are the first summer data.

The temperature distribution in the range up to 45 km, recorded by TW-10, is almost the same as that by TW-8, and had the appearance of the so-called "summer type" which we described in our previous report. When the altitude is limited to between 20 km and 40 km, i.e., the middle layer of the atmosphere, the distributions recorded by TW-6, 7, 8 and 10 are identical. But below 20 km, the distribution differs from that of the so-called "summer time" at Ft. Churchill (59°N), and rather presents a similar aspect to that at Guam (13.5°N). Furthermore, in the range above 50 km, it is quite similar to the summer-fall type distribution at Guam and White Sands (33°N). It is very difficult to classify and model the spring-fall type distribution, although it is comparatively easy to segregate the data and assort them in two types of winter and summer. So far it might be said that the type of distribution at Michigawa in midsummer is more similar to that at Guam and White Sands than at Ft. Churchill.

Next, as to the temperature distribution attained by TW-9,in the range below 20 km, it presents quite the same appearance as that observed by the Michigawa experimental station through their tests carried out in spring and fall; but in the range between 20 to 50 km altitude, the temperature is lower by about 10°K. On this point, compared with the distribution obtained by TW-5 in winter, the distribution in question might be said to reveal the neutral phenomena between spring-fall type, summer type and winter type, or rather presents the winter type. But the meso-peak revealed at the height of 50 km is higher than that recorded by TW-5 by 10°K and is almost equal to that obtained by TW-10.

In regard to wind, the results obtained by TW-10 naturally prove to be of the summer type because of the strong east wind in the middle layer of the air. On the other hand, in the results by TW-9, the component of east wind is also found; yet it is of less value than the one in the direction of south-to-north and of smaller scale than ones shown in other test reports. To study the above phenomena, we gathered all test results on wind and arranged them under four seasons; this is shown in Figure 3 [1-7]. In the diagram, white circles indicate easterly winds, black dots westerly winds, and very short lines attached thereto point the respective directions of winds. The dotted lines are dividing borders between two groups of winds, i.e., of summer type and winter type. Based on this diagram, it is shown that the phenomenon of a larger component in the direction of south-to-north to that of east wind is consistent with the results attained by TW-9 which just fall on the dividing border, i.e., shifting period, in the diagram.

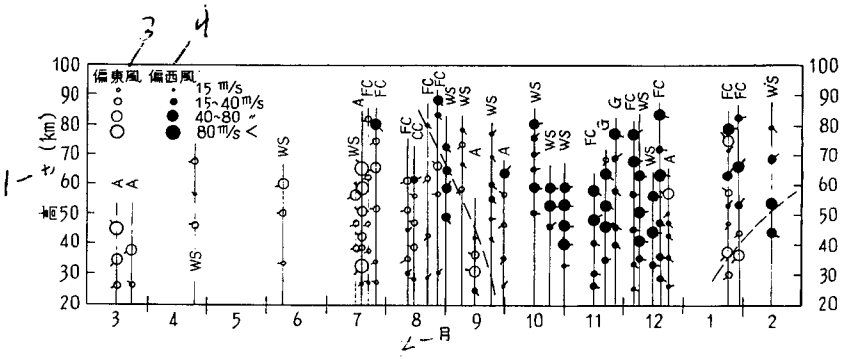

Fig. 3. Seasonal change in wind direction found by wind observations at various parts of the world where: A—Michigawa; WS—White Sands; FC—Fort Churchill; CC—Cape Canaveral; G—Guam
1) Altitude; 2) Month; 3) Easterly winds; 4) Westerly winds

4. Conclusion

With the test results and our study of them, we have come to conclude that the test results obtained by TW-9 reveal phenomena at the period of shifting winds from summer type to winter type, and the results attained by TW-10 prove to be of summer type. There is one thing we want to bring to your special attention, namely, the dividing border in Fig. 3 forms itself in a curved line. That means the shifting (period) at every altitude involves a certain time lag according to the respective altitude. This phenomenon should be taken into consideration in looking not only at the test results obtained by TW-9 but also at other temperature distributions. For instance, it could be supposed that in the case the altitude is divided into three ranges, 0-20 km, 20-50 km, above 50 km, the transition is made independently at intervals caused by the time lags. This idea must be available for research consideration when viewing the variation of the phenomena resulting from latitudinal differences. Keegan [8] and Wexler [9] reported valuable findings in their research of a great circulation of wind of a certain period of February to September. And also several scientists, beginning withFaust [10], on the basis of the idea of variation of atmospheric phenomena resulting from latitudinal differences, adopted the null-layer concept and concluded that, in the range of 30°Longitude to 60°Longitude, the wind circulation is generated in relation to the height of the air; and further, by generalizing Rossby's Three-Cell theory [11] (re: a great wind circulation generated up to about 20 km altitude) to wider ranges which involve a middle air layer or higher. We have come to the stage to study the yearly variation of atmospheric phenomena classified under summer type and winter type, referring to the data above mentioned. So far, we have too many complicated problems and unknowns to set up a definite theory.

In conclusion, we would like to express our sincere appreciation to the gentlemen of Akita Observatory and other parties concerned for their favorable cooperation extended during our tests.

(Received on April 1, 1963)

REFERENCES

1. Maeda, Takeya, Matsumoto, and Okumoto: Prod. Res. 13, No. 10, October 1961.

2. Maeda, K., H. Matsumoto, Y. Takeya, and T. Okumoto: Report of Ionosphere and Space Research in Japan, 14, 4, 1960.

3. Maeda, Ohie, Matsumoto, Takeya, Okumoto, and Tatebe: Report No. 13-3 Prepared for Joint Conference of Japanese Electrical Engineering Societies, Kansai District. November, 1963.

4. Stroud, W.G., W. Nordberg, and J.R. Walsh: J.G.R. 61, 1, 1956.

5. Stroud, W.G., W. Nordberg, W.R. Bandeen, F.L. Bartman, and P. Titus: Space Res. I, Proc. 1st Int. Sp. Sci. Symp. Nice, pp. 117-143, January 1960.

6. Jones, L.M.: Space Res. II, Proc. 2nd Int. Sp. Sci. Symp. Florence, pp. 1037-1048, April 1961.

7. Lowenthal, M.: Ibid., pp. 1049-1060.

8. Keegan, T.J.: Ibid., pp. 1061-1079.

9. Wexler, H.: Ibid., pp. 1083-1093.

10. Faust, H. and W. Attmannspacher: Ibid., pp. 1094-1106.

11. Rossby, C.G.: The Bulletin of the Am. Met. Soc. 28, 2, pp. 53-68, 1947.

OBSERVATION OF THE PROPAGATION MODE OF LOW FREQUENCY RADIO WAVE AND NOISE IN THE IONOSPHERE BY K-8-11 TYPE SPACE ROCKET

By Kenichi Maeda, Iwane Kimura and Tatsuo Takagura

1. Introduction

It was thought that the low frequency radio wave noise in the ionosphere and the layer above the ionosphere would differ from that which was observed on the ground because of the shielding effect of the lower part of the ionosphere. For this reason, we made a plan to measure the noise in the ionosphere by means of a space rocket. As the first test, a K-8-11 type space rocket which carried a receiver was launched on December 18, 1962.

The propagation mode of low frequency radio waves in the plasma in a magnetic field became clear to a certain extent by the research of Heusler and others. But there are still uncertain areas in the penetration factor of the lower part of the ionosphere, antenna impedance and effective length of an antenna in the ionosphere. There have been some low frequency radio wave observations through space rockets and earth satellites in the United States. But we have not enough data to determine the receiver gain and optimum antenna for the test conditions. Therefore, we aimed in this test to get reference data for the following tests; and the following are our objectives:

(1) Comparison of loop and dipole antennas.

(2) To measure the performance of the loop antenna in the plasma.

(3) To measure the propagation direction and loss by receiving the radio wave of a ground station.

(4) To measure the spectrum of the noise in the ionosphere.

For the objective (1), 100 kc/s radio wave will be received by a loop antenna and a dipole antenna, and the noises will be compared. For (2), the radio waves of 100 kc/s and 105 kc/s will be received by a synchronized loop antenna. For (3), 17.44 kc/s radio wave of Isami transmitting station, Aichi Province, will be received. For (4), we will analyze the intensities of the noises in the two radio waves of 17.44 kc/s and 100 kc/s.

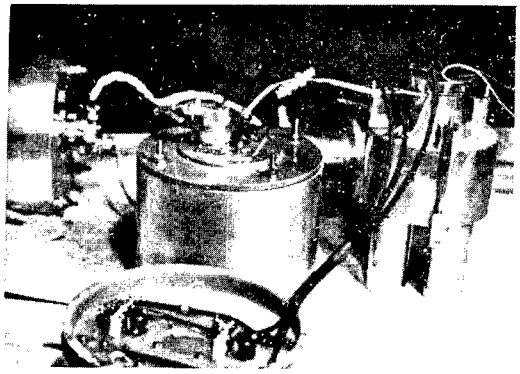

Table 1

	ch 1	ch 2	ch 3	ch 4
1 周波数	100 kc/s	105 kc/s	100 kc/s	17.44kc/s
2 帯域幅	1 kc/s			
3 アンテナ	4 ループアンテナ 直径 21 cm, 120 回巻		5 ダブレットアンテナ 巻尺式 2 本各 4.6 m	
6 アンテナ実効長	7 約 0.01 m		8 約 4.6 m	
dynamic range	9 70 db (対数的)		10 120 db (対数的)	
11 検波時定数	12 0.25 秒			13 0.025 秒
14 検出可能最低レベル	8×10^{-9} AT/m		4×10^{-2} μV/m	

1) Frequency; 2) Bandwidth; 3) Antenna; 4) Loop antenna — 21 cm in diameter, 120 windings; 5) Dipole antenna; two, tape measure type, 4.6 m each; 6) Effective length of antenna; 7) About 0.01 m; 8) About 4.6 m; 9) 70 db (logarithmic); 10) 120 db (logarithmic); 11) Detecting time constant; 12) 0.25 sec; 13) 0.025 sec; 14) Minimum detectable level

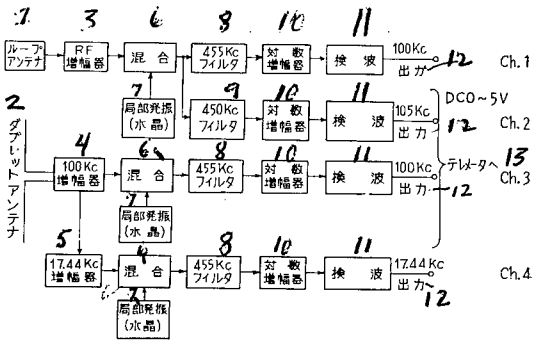

Fig. 1 . Block diagram of the receiver.

1) Loop antenna; 2) Dipole antenna; 3) RF amplifier; 4) 100 kc amplifier; 5) 17.44 kc amplifier; 6) Mixer; 7) Local oscillator (crystal); 8) 455 kc filter; 9) 450 kc filter; 10) Logarithmic amplifier; 11) Detector 12) Output; 13) To teletransmitter

2. The Receiver

The receiver carried in the rocket consists of four channels and its block diagram is shown in Fig. 1 . The characteristics of each channel are listed in Table 1. Circuits of the receiver are transistorized and crystals are used as the local oscillator and the bandpass filter of the intermediate frequency amplifier. Such use of a crystal in this test was the first such employment in this country; and we found that a crystal could safely overcome the shock of the launching.

Two types of antenna, loop and dipole antennas are used, and they receive the same 100 kc/s radio wave for comparison purposes. And the dipole antenna also receives 17.44 kc/s and the loop antenna receives 105 kc/s, too. The antennas are placed at the top of the main rocket, open cone area. The spool of the loop antenna is placed concentrically with the axis of the rocket body, and it is exposed to the outside by the nosecone opening. Two of the tape-measure type steel dipole antennas are wound and kept at the inside of the cone. The antennas stretch out 4.6 m to both sides and form a pair which are perpendicular to the axis of the rocket body, and the surfaces of the dipole are painted with silicon enamel for surface insulation in order to reduce the ionizing effect which occurs in the ionosphere.

The dipole antenna has 9.2 m in total length and therefore has almost no radiation impedance for the antenna is almost full capacity. But, the impedance of the antenna will be reduced in the ionosphere because the dielectric constant E and the capacity will increase in the ionosphere. Therefore, the input citcuit of the receiver is adjusted to match the antenna at low impedance. Because of this, the gain at the ground receiver is reduced 40 db due to mismatching.

The loop antenna is tuned; its Q is 30; peak frequency is 102.5 kc/s; and 100 kc/s and 105 kc/s are received. If the tuning disappears, it will be detected.

Among the time constants of the channels in the receiver, channel 4 has one-tenth of the value of the time constant of the other channels because it receives the signal which is transmitted from a ground station and because we want to have a more detailed record of the signal. For the ground station, we used the Isami transmitting station which is located at Karidani City, Aichi Province (137°01'11" E, 34°35'40" N) (call sign, NDT), 700 km away from the rocket launching point (131°04'45" E, 31°15'0" N). It has 260 kw output and frequency 17.44 kc/s. At the launching point, the radiowave from the ground station is received by a field intensity meter and recorded by a pen recorder along with the record of the teletransmitter output of channel 4. The signal of NDT was 1 mv/m (60 db) at ground.

3. Observed Results

The K-8-11 type space rocket was launched at 14:03 JST on December 18, 1962. It flew about 440 sec and all devices functioned without trouble.

The nosecone of the rocket was opened 79.6 sec after the launching at the altitude 95 km, and each channel started to receive through the exposed loop antenna and stretched out dipole antenna. The rocket reached the maximum altitude 202 km about 230 sec after the launching. In the descending period of the rocket, the teletransmitter had burnt away at about 40 km altitude, 421 sec after the launching, and the signal faded out then. During the flight, all channels received comparably intense pulse type noises, and channel 4 also received the signals from NDT. We will discuss them below.

(1) Pulse type noise

(i) It was unique that all four channels received the same pulse type noises at 95 km to 202 km above the ground as shown in Fig. 2. The pulses of channel 4 (17.44 kc/s), which have the smallest time constant, had the largest amplitude. Wave front of pulses was 1.8×10^4 μv/m (where band width was 1 kc/s), minimum width of the pulse was less than 0.025 sec, and we think that the wide pulse was the combined pulse of narrow pulses.

On the other hand, most of the pulses of channel 3 were seemingly wider than those of channel 4 even though the amplitudes of the pulses of channel 3 (100 kc/s) were smaller than those of channel 4 because channel 3 had a larger time constant. When we compare the width of the pulses of the two channels only, we get that the field intensity of channel 4 (17.44 kc/s) was 8 db higher than that of channel 3 (100 kc/s). And when we also consider the difference in the indexes of refraction by frequencies, the difference of the field intensities was 11.5 db by power flux. This is the frequency characteristic (spectrum) of the noise.

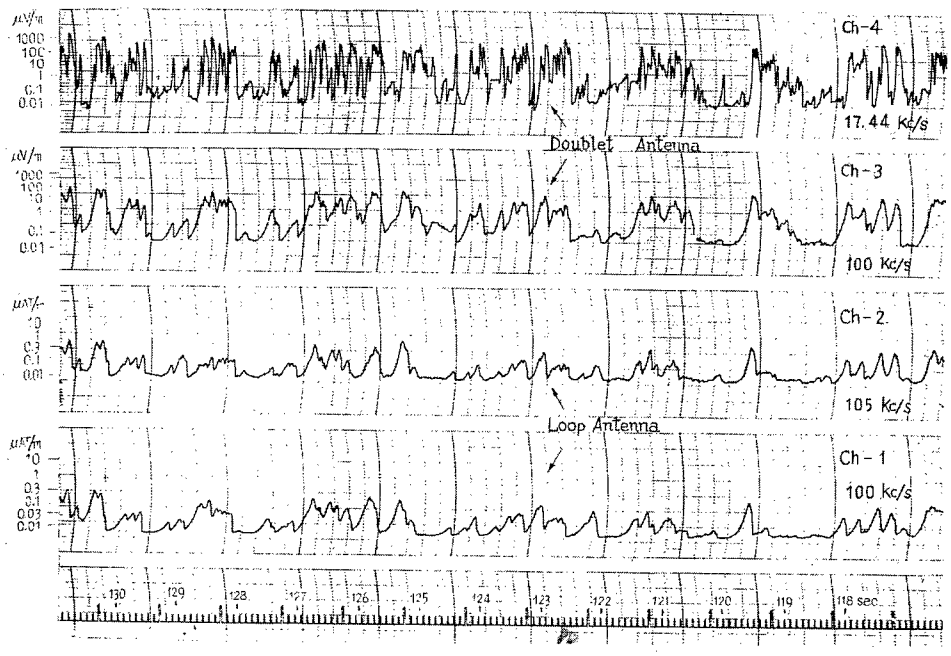

Fig. 2. Pulse type noise (refer to Table 1)

(ii) The levels of the pulse type noises were not necessarily random but they changed within 50 sec of period, and sometimes, the levels fell below the noise level of the receiver itself for 3 to 5 sec. This periodical level change did neither necessarily agree with the precession of the rocket (the period of the precession of the rocket was 50 to 60 sec) [1] nor had any relationship with the spin of the rocket (the period of the spin of the rocket was 1.5 to 5 sec).

(iii) Ground field intensity showed the noises of 3 mv/m to 0.1 mv/m were logarithmically compressed and the band width of the noises was 300 c/s. But 17.44 kc/s output of the receiver did not show the pulse type noises which correspond to those of channel 4.

(iv) In the descending period, the mode of the noises seemed to be changed completely from 92 km above the ground (391 sec after the launching). The noise levels fell suddenly then rose gradually (see Fig. 3).

(v) There should have been no difference in noise levels between 100 kc/s and 105 kc/s. But the noise level of channel 1 (100 kc/s) was always higher than that of channel 2 (105 kc/s), and it was possibly due to the shock of the ground test which deviated the synchronization and it was not due to the synchronization deviation of the loop antenna in the ionosphere.

(vi) In comparing the loop antenna and dipole antenna, the dipole antenna

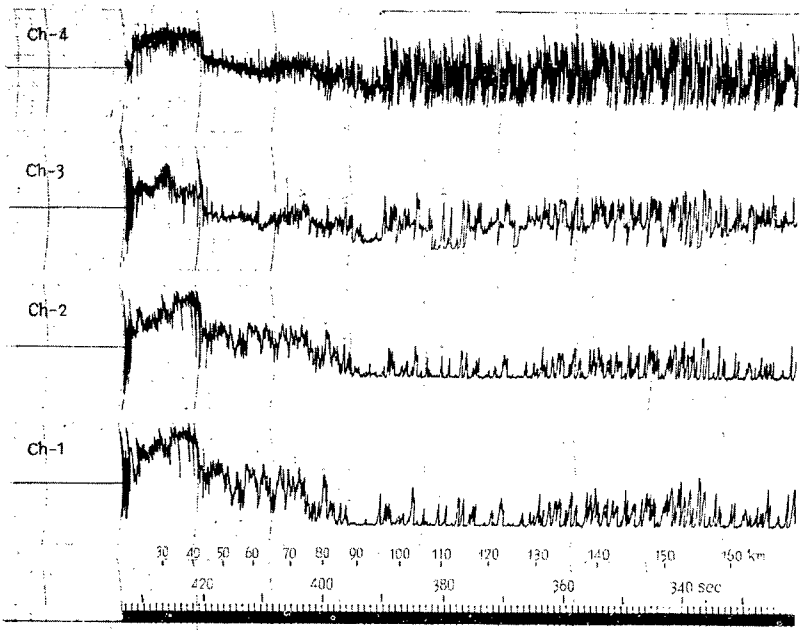

Fig. 3. Noise changes at about 90 km in altitude (refer to Fig. 2 and Table 1)

is better for its effective length is definitely long provided that the matching is maintained in the ionosphere. But it should be considered with the dipole antenna that the total gain of a dipole antenna will change with the altitude in the lower part of the ionosphere.

(2) Cause of the pulse type noise.

We can first assume the noises come from such as lightning in the Southern Hemisphere or as Heusler's atmospheric electricity discharge. But this assumption must be discarded for the following reason. The spectrum of 17 kc/s radiowave in the lightning is 14 db higher than that of 100 kc/s radiowave [2]. And, according to our calculation [3], 18 kc/s and 100 kc/s radiowaves decrease 55 db and 160 db, respectively, when they pass through the ionosphere in the Southern Hemisphere. The difference is 105 db, and the difference must be 120 db with 17.44 kc/s and 100 kc/s. But the measured difference was only 12 db, as we stated previously.

Thus, we think the causes of the noises are as follows:

(1) Intermittent breakdown of the ionozed particles creates the noise.

(2) Meteors radiate noise waves.

But there are also problems in these assumptions and the mechanisms of the

assumed solutions are not known. Mechtly and Bowhill reported that they received strong noise waves, which had large variations, with 512 kc/s at above 400 km [4]. It may also be possible that the noises in our test have the same cause as the noises of the above report.

(3) Electric field intensity of the radiowave of Isami transmitting station (NDT).

The radiowave of Isami transmitting station began to be received from the point at 112.5 m above the ground, and the receiving continued until the rocket reached the point 82.5 km above the ground in its descent. Even in the period when the signals were being received, the signals being very weak were not able to be identified for they were masked by pulse type noises when there were noises. Generally, the signals were very clear when the noise levels were low, as shown in Fig. 4a. But in some case the signals were not received even when the noise levels were low, as shown in Fig. 4b. The levels of the NDT signals had generally deep fading. The level change reached 25 db/sec at most. We are not sure that the fading is due to the interference fading of several waves which have different propagation directions or due to the instability of the dipole antenna. We think there was no relationship between the fading and the spin of the rocket.

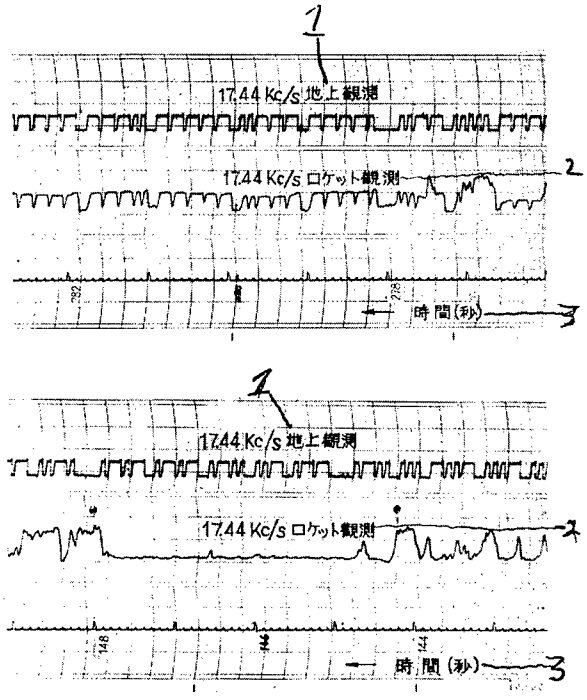

Fig. 4

Fig. 4a. An example of the signals of Isami transmitting station.

Fig. 4b. An example of the case where the signals of Isami station were not received even though the noise levels were low.

1) 17.44 kc/s, received at the ground; 2) 17.44 kc/s, received at the rocket; 3) Time (sec)

We took the maximum value of the intensities of NDT signals for each second and plotted the values with respective altitudes in Fig. 5.

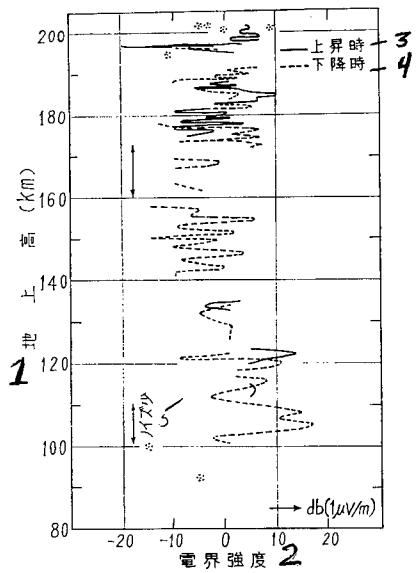

Fig. 5. Levels of the Isami (NDT) signals.

1) Altitude; 2) Electric field intensity; 3) Ascending period; 4) Descending period; 5) Low noises

The electric field intensity at the ground was 1 mv/m (60 db) as stated previously. But the electric field intensity decreases near the surface of the earth. Therefore, we calculated the electric field intensity at the ground exactly below the ionosphere from the following equation, where P(w) is transmitting power and d(m) is the distance between the transmitting and receiving points:

$$E = 3\sqrt{5}\sqrt{P}/d \ \text{[V/m]}$$

and E was about 5 mv/m or 74 db. On the other hand, we obtained the observed value of the electric field intensities during the descent period from Fig. 5 by m making intensity envelop line. Then we subtracted 74 db, the ground intensity, from the observed intensities. The solid line in Fig. 6 is the plot of the remainders. In order to analyze the characteristic of the solid line in Fig. 6, we adapted the method of Leiphart and others; that is, we calculated accumulating values of the intensity decreases of 18 kc/s radiowave by the receiving altitude changes in the model ionosphere. The dotted line in Fig. 6 is the plot of the accumulating values [3]. In this case, we took 45° as θ, the angle between the

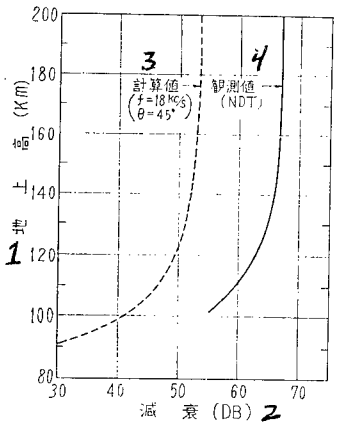

Fig. 6. Accumulating values of the wave decrease.

1) Altitude; 2) Decrease (db); 3) Calculated value (f = 18 kc/s, $\theta = 45°$); 4) Observed value (NDT)

normal line of the radiowave and the direction of the geomagnetic field. $\theta = 45°$ is an appropriate value at Kagoshima launching ground. In comparing the two curves in Fig. 6, we find that the two curves agree well when we move a curve 12 to 13 db to the other curve. And we think the deviation between the two curves indicates the part of the radiowave which was lost when the radiowave moved into the ionosphere from the free space. According to the calculation by Maeta and Oya [6], the radiowave loss is about 25 to 30 db when the bottom of the ionosphere is assumed to have a sharp boundary.

4. Conclusion

Since it was our first radiowave observation by a rocket, we tried as far as we could to get any new facts even though we had no initial confidence for the success of the experiment. Fortunately, every system functioned perfectly and we were able to obtain the entire records. We also admit that there were some approaches which were not perfect and some results which could not be treated quantitatively due to our lack of experience. However, we could get valuable experience on the experiment in this field which will be important in future tests.

This test was completed with the help of Professors Takagi and Itogawa and other members of the rocket group, the Institute of Production Research, Tokyo University, and we express our appreication to them. We also express our thanks to the members of Denki Kogyo Co. and Yokosuka U.S. Navy Communication Unit who helped in connection with the radiowave of the Isami transmitting station.

We wish to thank the members of Akebashi Electric Co. and particularly Messrs. Urimoto and Tanabe who made the receiver.

We also wish to express our gratitude to Professor Tanaka, Tokyo University, Professor Obayashi, Kyoto University, Mr. Hiroshi Oya, Professor Kanehara, the Atmospheric Discharge Lab., Nagoya University, Professor Takayama, Plasma Lab., and Professor Onakakami, Kobe University, who have contributed many helpful comments and suggestions in the analysis of the observed results.

(Received on April 2, 1963)

REFERENCES

1. Kato and Aoyama, Prod. Res., Vol. 15, No. 7, 127, 1963.

2. D.J. Malan, Recent Adv. Atmos. Elec., 557, Pergamon Press, 1958.

3. Maeda, Kimura and Takakura, J. Soc. Radio Communication, Radio Wave Propagation Special Committee Reference Material, March 20, 1963.

4. E.A. Mechtly and S.A. Bowhill, J.G. R. 65, 3501, 1960.

5. J.P. Leiphart et al., NRL Report 5721, 1961.

6. Maeda and Oya, J. Soc. Radio Communication, Radio Wave Propagation Special Committee Reference Material, March 20, 1963.

WIND-TUNNEL EXPERIMENT OF IONOSPHERE PROBE

--PROBE MEASUREMENT IN DRIFTING PLASMA--

By Toshihiko Tsuchide, Torao Ichimiya and Fusao Kamaki

1. Introduction

As it is known, the proof developed by Langmuir was adapted to observe the ion density of the ionosphere in this country and we succeeded in obtaining some data on the ion density of the ionosphere in advance of other countries. In case ion density is measured by a probe, the relative velocity of the probe mounted on a rocket entering the ionosphere plasma should not be ignored for the rocket flies with relatively high speed. Previously, we reported the method of calculation of positive ion density from the positive ion current which is trapped at a probe ignoring the relative velocity of the probe in the ionosphere plasma [1]. In the analytical method, some assumptions were involved and their validity needed to be proved by an experiment. This paper is the report of the experiment. We placed a probe in the plasma created in the supersonic, low density wind-tunnel of the Institute of Production Research, Tokyo University, and measured the probe characteristics. Then we evaluated the validity of the previous method of analysis. We report the outline of the experiment because the details of the experiment were reported separately [2].

2. Outline of the Theory [1]

In order to calculate the positive ion density from a probe current, we assume that a reasonable positive ion case will surround the probe. Then we apply the analysis of the characteristic of a flat probe in the drift plasma to a spherical probe. The positive ion current I_+ trapped at the probe is given by the following equation, where we denote the current density, which is perpendicular to the drift, and diameter of the case as j_0 and r_0, respectively:

$$I_+ = 4\pi r_0^2 j_0 \varphi_0(\eta_0) \tag{1}$$

where φ_0 is the correction factor when the probe has a relative velocity to the plasma and the function of η_0, the ratio of the drift energy of the positive ion to its thermal kinetic energy. Figure 1 is the graph of η_0 vs $\varphi_0(\eta_0)$ curve when the positive ions frequently collide with neutral gas particles where the gas pressure

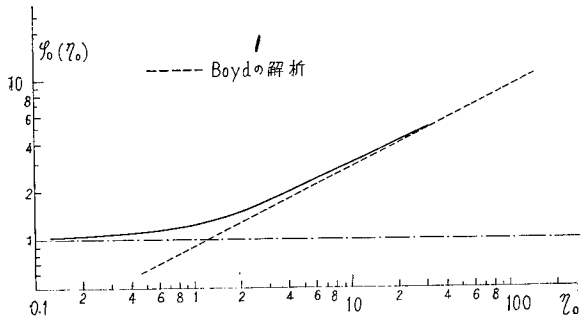

Fig. 1. Graph of the correction factor φ_0 as the function of η_0. Dotted line is the result of Boyd's analysis [3]

1) Boyd's analysis

is relatively low. When $\eta_0 = 0$, of course $\varphi_0 = 1$. The dotted line, as the result of Boyd's analysis, is the curve which was obtained from $\varphi_0 = \frac{\sqrt{\pi}}{2}\sqrt{\eta_0}$ with the assumption that the positive ions are trapped only at the circular cross sectional area which is perpendicular to the drift. One may find that the above equation is approximately true when the value of η_0 is large.

3. Experiment

The wind tunnel which is used for the experiment is a shielded circulation type wind tunnel and can create a current of Mach number 3 under static pressure 100 to 10 μHg. Photo 1 shows the wind tunnel.

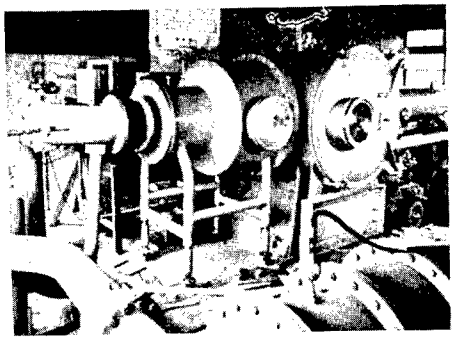

Photo 1. Entire view of the low-density wind tunnel

In order to create a plasma in the wind tuhnel, we placed a copper ring, 20 mm in width and 86 mm in diameter, in front of the Laval nozzle (the distance between the ring and Laval nozzle is 67 mm) and applied high voltage to them using the Laval nozzle as the negative pole and the ring as the positive pole. The probe, a sphere of 5 mm in diameter made from stainless steel, is placed in between the poles. The distance from a pole is adjustable. We moved the probe in five steps 20 mm per step, from the point 47 mm forward of the negative pole during the experiment. Photo 2 is the entire view of the discharge space and Photo 3 is its close-up.

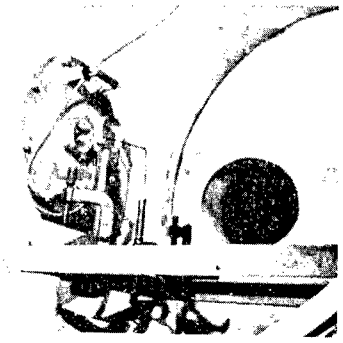

Photo 2. Entire view of the discharge space in the wind tunnel

Photo 3. Close-up of the discharge space

We maintained the static pressure in the wind-tunnel at 86 μHg constant and kept the drift velocity to Mach number 3. Initiating discharge voltage at the discharge space was about 470 v and the voltage maintained was between 310 v and 320 v which depends on the discharge current. Photo 4 shows the discharge in the drift. In the photograph, we see the probe in the light portion between the right Laval nozzle and left ring. Figure 2 is the block diagram of the measuring

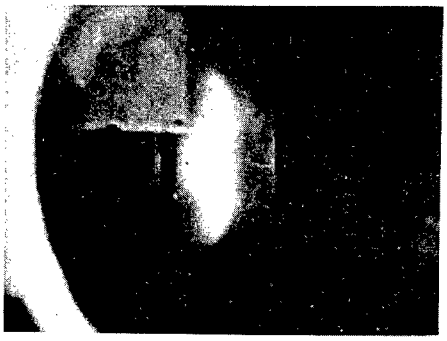

Photo 4. Pole is discharging (bright portion is the glow)

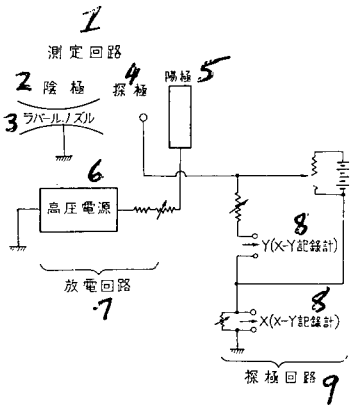

Fig. 2. Block diagram of the measuring circuit

1) Measuring circuit; 2) Negative pole; 3) Laval nozzle; 4) Probe; 5) Positive pole; 6) High voltage power source; 7) Discharge circuit; 8) (X-Y recorder); 9) Probe circuit

circuit. Probe measurements were plotted by an X-Y recorder. Discharge current was from 2 ma to 10 ma with 2 ma per step. The noise voltage below 10 ma was less than 0.1 v.

With the above experimental conditions, we obtained probe measurements and calculated the positive ion density N_+ by the analytical method of the probe characteristics in a drift plasma, and the electron density Ne from the characteristics of the electron current. Figure 3 shows the result of the comparison. It showed agreement between N_+ and Ne in contrast with our rough experiment. At the upper part of the figure we showed another comparison of N_+ to Ne in which

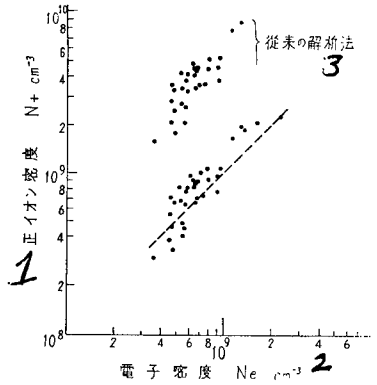

Fig. 3. Comparison of the positive ion density N_+ to electron density Ne. Former value is calculated by the analytical method of the probe characteristic in a drift plasma and latter value is calculated from electron current characteristics. The result of the analysis which used $\varphi_0 = 1$ is shown at the upper part.

1) Positive ion density; 2) Electron density; 3) Previous analysis method

N_+ was calculated without the effect of the drift, that is, we put $\varphi_0 = 1$.

4. Conclusion

So far, we reported the outline of the experiment which was performed to evaluate the calculation method of positive ion density from the positive ion current trapped at the rocket probe and the experiment result.

We used air as the gas in this experiment, and we know that the experimental conditions depend largely on the environmental conditions. But we think we obtained a satisfactory result within the conditions we set. In this experiment, the discharge region belongs to the high-pressure region and only Mach number 3 was adopted as the drift velocity of the plasma.

We can say that the previous analysis method is quite valid and proved that the ionosphere probe can be used to measure the positive ion density at least in the ionosphere because the ionosphere falls in the D layer or the lower part of E layer.

(Received on April 2, 1963)

REFERENCES

1. T. Dote, K. Takayama and T. Ichimiya: Analysis of probe characteristics in drifting plasma, J. Phys. Soc., Japan 17, 1, 174/183, 1962. 01

2. T. Dote, T. Ichimiya and F. Tamaki: Some experiments on probe characteristics in drifting plasma, J. Phys. Soc., Japan, 18, 2, 260/265, 1963. 02

3. R. L. F. Boyd: Plasma probes on space vehicles, Proceedings on the fifth international conference on ionization phenomena in gases, (North-Holland, Amsterdam), pp. 1387/1396, 1962.

THE "COMMENCEMENT" CEREMONY OF KSC AND THE ESTABLISHMENT OF KSC COOPERATIVE SOCIETIES OF KAGOSHIMA PREFECTURE AND UCHINOURA TOWN

1. The "Commencement" Ceremony of KSC

The commencement ceremony, marking the beginning of building of KSC of Tokyo University, was held on 2 February 1962 with about 200 attendees at the observatory, located at Nagatsubo, Minamikata-aza, Uchinouracho, Kimotsuki-gun, Kagoshima Prefecture, the second rocket station in our country. Since the first serious thought was given to the project on October 1960, the day of the ceremony fell on the 16th month from that time. The construction work was started in October 1961, with two plans for cutting open a highway of 230 meter width and leveling by bulldozers in the Second Area; and, by the courtesy of Kagoshima Prefecture, the latter was completed within the year. The place where the ceremony was held is in this Second Area.

The ceremony was held under the auspices of the President of Tokyo University, from 13:00 to 16:00, scheduled as follows:

The Program of the Ceremony

1. An Opening Address
1. "Shubatsuno-gi," a Shinto ritual. Prayer for purification.
1. "Koshinno-gi," a Shinto ritual. Prayer for presence of God.
1. "Kensenno-gi," a Shinto ritual. Making an offering to God.
1. "Norito," a Shinto ritual. Prayer for blessings.
1. "Setsuma no-gi," a Shinto ritual.
1. "Kuwaireno-gi," a Shinto ritual. Hoeing on the ground.
1. "Tamagushi Hoten," a Shinto ritual. Offering a branch of sacred tree.

1. "Tessenno-gi," a Shinto ritual. Taking away offerings.

1. "Shoshinno-gi," a Shinto ritual. Prayer for ascension of God.

1. Speech by the President of Tokyo University.

1. Report on the progress of the project made by the Chief of the Production Technique Laboratory.

1. Report on the development of the construction made by the Chief of the Institution Dept., Tokyo University.

1. Greetings:

    by Minister of Education
    by the Chairman of the Science Council of Japan
    by the President of Kagoshima University
    by Governor of Kagoshima Prefecture
    by the Chairman of Kagoshima Prefecture Council
    by the Headman of Uchinoura Town

1. Closing Address:

    - Planting the tree in commemoration of the ceremony by the President of Tokyo University

    - The first trial of launching a rocket

    - Dinner party

In the above programs, all the religious ceremonies were done by a Shinto priest of Takaya Shrine, and the ceremony of hoeing by several persons beginning with the President of Tokyo University, and the ceremony of offering the branch of a sacred tree by many persons concerned as listed below:

(Tokyo Area)

Prof. Kaya, the President of Tokyo University
Mr. Yoshisato, proxy for Ministry of Education
Mr. Fukui, proxy for the Chairman of the Science Council of Japan
Mr. Fujitaka, the Chief of the Production Technique Laboratory of Tokyo University
Mr. Takagi, Professor of Tokyo University
Mr. Itokawa, Professor of Tokyo University
Mr. Tsuruta, the Secretary-General of Tokyo University

Mr. Tsuge, the Chief of Institution Department, Tokyo University
Mr. Iwata, the Chief of Paymasters' Dept., Tokyo University
Mr. Komaki, the President of "Komaki-Gumi" construction Company
Mr. Shimoonoda, the President of Kunimoto Kensetsu

(Kagoshima Area)

Mr. Terazono, Governor of Kagoshima Prefecture
Mr. Otsubo, the Chairman of Kagoshima Prefecture Council
Prof. Fukuda, the President of Kagoshima University
Mr. Nikaido, a member of Parliament
Mr. Kukimoto, Headman of Uchinoura Town
Mr. Kanbayashibo, Councilor of Uchinoura Town
Mr. Hirasa, the President of Kagoshima Prefecture Mayors' Council
Mr. Kitada, proxy for the Chief of Towns and Village Council
Mr. Nagata, proxy for the President of the Chairman's Congress of Kagoshima City Council
Mr. Jurogi, proxy for the President of the Chairman's Congress of Kagoshima Towns and Villages Councils
Mr. Takano, Representative of Kagoshima Keizai Doyukai

Then, beginning with the opening address given by the President of Tokyo University, reports on the project were presented by the Chief of the Production Technique Laboratory of Tokyo University and the Chief of the Institution Department. Then, congratulatory greetings were given by the guests mentioned above. After closing the ceremony, memorial plantings of a tree by the President of Tokyo University and then the first trial launch of a rocket, small sized, were performed. The tree planted was a Phoenix, which symbolizes the Southern country; and the rocket "launch" button was pushed by the President. The rocket was of a small type, 75 mm in diameter. The ceremony was followed by a dinner party, with Mr. Kaya as chairman. The party was so cheerfully carried on that many guests made speeches expressing their cordial congratulations.

KSC is sometimes called "Florida of Japan," because of its southern country-like atmosphere and beautiful landscape. But once you go through the Osumi Peninsula far from the coastline, you will surely feel as if you are standing at a remote border of the country. The town is occupied in 70 percent of its area by a national forest. It has a population of a little more than 10,000 people, and has no history of flourishing days since far back to the reign of Emperor Keiko. When I think of the fact that now the newest scientific laboratory is established at such a remote place, I feel the oddness of the contrast between the new and the very old.

For maintenance of the observatory and for rocket experiments, transportation of long, bulky and heavy goods is naturally expected. Also, establishing the observatory will render some acceleration to development of a tourist industry in Osumi Peninsula. Because of this, the Kagoshima Prefecture did, keeping pace with the public works done by KSC, repair the prefectural highway for the 20 km between Takayama and Uchinoura, and rebuilt some bridges.

Such positive aid given by the authorities concerned meant much for the party of Tokyo University as well as for the travelers. Returning to the subject, the weather of the day was very fine, and the whole town gave congratulations on the commencement of the project, decking all streets with drapery, flags and arches, students lining up to form the word "ROCKET," and arranging fully decked fishing boats in the sea. Besides, the information media of newspaper and TV treated the event as worthy of special mention and joined the ceremony by overflights and throwing down many bouquets. It was indeed unprecedented that Nagatsubo was crowded with so many spectators, about 3,000.

The latitude on which KSC is located is lower than that of Akita Laboratory by more than 8 degrees, but does not reach the latitude of 20 degrees in the terrestrial magnetism distribution chart. That of the latter exists on the nearest latitude from the equator among the existing observatories in the Northern Hemisphere, and further is regarded as the important spot advantageous for attaining the data of cosmic physical research. As the result of the fact that Osumi Peninsula is of a typical dislocation of strata, KSC faces the sea at a height of 230 to 320 meters above sea level. KSC consists of five areas in No. 1 District in Nagatsubo, one area each in Miyahara and Tosaki, i.e., seven areas in total and approximately 18 ha in entirety. Total length of principal roads between areas and/or area and prefectural highway is about 1.7 km; and the arrangement of areas thus made at random is also not distinguished. At the first stage of setting up the plan, we adopted a priority policy on the following four points: ground leveling, road, water and electricity; building and accommodations with equipment therefor were next. Water was pumped to the upper region from the valley; and for a supply of electricity, the capacity of Takayamagawa Power Plant was expanded and a transmission line was laid from Kirshira to KSC, a distance of 8 km. There is scheduled to be built: rocket center, control center, telemetry center, radio center, gauge center, rocket shed, radar center and four optical observation spots in seven area. These facilities, started in 1961, are expected to be completed for the use of Lambda rockets on a three years' program. This ceremony is the first step of this massive project.

2. Collaboration Society

After the commencement ceremony, the opening ceremony of Uchinoura Town KSC Cooperative Society was held at Uchinoura Town Assembly Hall, and on the following day, February 3, that of the Kagoshima Prefecture KSC Cooperative Society at Nomurashoken Building.

Uchinoura Town Society, with Mr. Kukimoto, the head of Uchinoura Town Council, and Mr. Kanbayashibo, the chairman of the promotors, decided on the regulations mentioned below; inaugurated Mr. Kukimoto and the chairman and Mr. Kanbayashibo as vice chairman, respectively. In response, the president of the University presented his congratulations, and Prof. Mr. Itogawa made an address to express thanks for their cooperation.

Kagoshima Society, with Mr. Terazono, the governor of the prefecture, Mr. Otusubo, the chairman of Kagoshima Prefectural Council, Prof. Mr. Fukuda, President of Kagoshima University and Mr. Kukimoto, Uchinoura Town Headman as the promoters, decided on the regulations mentioned below, and appointed Mr. Terazono to the post of Chairman, Mr. Kanamaru, Deputy Governor, to the post of Vice Chairman, respectively. Then, addresses of thanks and congratulations were made by the President of the University and Prof. Takagi. In both meetings, the congratulations delivered by Mr. Araki, Minister of Education, were read by Mr. Yoshisato, the chief of the Science Section. One thing that we shall never forget is the valuable information on the project given to us by Mr. Tashiro, chief of Planning and Research.

Once the society was organized at Akita Prefecture, its function was indispensable for conducting tests and also for promoting mutual understanding between the university and the authorities at the site and the various parties concerned. In order to perform the tests successfully, the University must ask various technical organizations for their cooperation in their respective special functions by informing them of the test plan and necessary data thereof. For instance, for the preservation of public peace, the test cannot be carried out without dispatch of guards and other necessary preparations arranged by the authorities of Prefecture and/or the Ministry concerned; in respect to fishery, the cooperation of fishermen's union is indispensable; the land leased is partly owned by the government and partly by private ownership, which brings up many problems that cannot be solved without mutual understanding among the agencies involved. Furthermore, beginning with the transportation of material and equipment for the test, employment of the workers required at the field, and arrangement of the lodgings of the resident staffs, the University has to handle many problems. Hence, with the society functioning, fundamental understanding on many problems can be realized, which promises to lead us halfway to the successful attainment of the tests. Meanwhile, we do hope and believe that the society will carry on their positive public relations as well.

The membership lists of both societies are attached hereto.

(Received on April 24, 1963)

Ground breaking by Dr. Shiba, President of Tokyo University

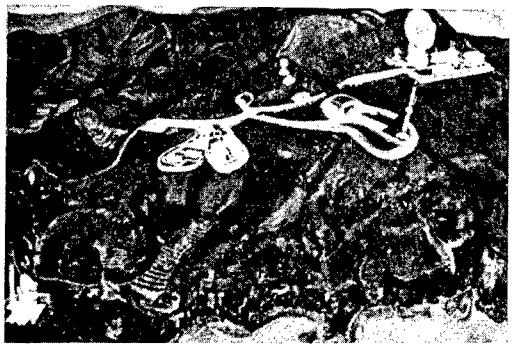

Proposed layout of Kagoshima Space Center

II

The Opening Address by the President of Tokyo University at the Commencement Ceremony

It is my greatest joy that we have come to hold the commencement ceremony of Tokyo University KSC in the presence of the many gentlemen concerned.

It has not been so long that the words "Space Science" were created. But space, so vast, mysterious and indestructible from the very beginning of the world to eternal future, has come to show itself as an object of science by direct observations. The first shooting of rockets in our country was that of pencil-thin rockets and was carried out at Michigawa, Akita Prefecture, on August 6, 1955. Then, in succession, the Third International Geophysical Year of 1957 to 1958 came, and we, Japan, also joined in this international research, making observations of the upper regions of the atmosphere through the medium of the rocket. Consequently, this inquiry meant much as the stepping-stone to the remarkable advance in learning the techniques of the rocket. Especially, the medium of the rocket enabled us to attain data of the upper atmosphere which had been beyond our reach; thus it rendered great help to the field of astronomy, meteorology, geophysics. Taking advantage of the successful work in the International Geophysical Year, every country has continued its observations by means of the rocket, and the committee commonly called COSPAR was set up. Our country, being enlisted in the committee, has been carrying on research in cooperation with international activities.

The history of the development of the rocket in our country begins with the pencil-like rocket, a very small type, the test of which has been mainly performed by our University, Production Technique Laboratory. Currently, the utilization of stabilized rockets, Kappa No. 6, No. 8 and No. 9 is realized. Now the reaches of the rockets are in the range of 60 km to 350 km and, according to the purpose intended, the proper rocket can be provided. This academic achievement receives much recognition in considering that these attainments were obtained in a shorter period of our study and at smaller expense than that of other countries. The fact that our rockets and accessories are nowadays in demand abroad might be said to testify to our recognition abroad.

Surrounded by the sea, though, our country could hardly afford the missile bases for the large type rockets without causing troubles on air lanes, sea routes or operation of fishermen. With the need, though, to flight test rockets unable to be flight-tested at Akita because of its unfavorahle location of looking out upon the Sea of Japan, members of our SE research group explored the areas along the coast of the Pacific Ocean from Hokkaido, Honshu to Kyushu. Finally, in April last year, the location here was decided upon with the approval and cooperation of Kagoshima Prefecture and Uchinoura Town. Osumi Peninsula has many historical evidences and legends, and now is going

to be surveyed and outfitted with the latest scientific facilities such as a launching pad, telemetry, radar, and so forth. Therefore, I hope to see a unique and world-famous rocket station upon its completion.

Again, I would like to express my greatest joy for holding the commencement ceremony on this day in the presence of these gentlemen. The initial hoe for breaking ground has been driven into the earth. Here, I sincerely with that Osumi Peninsula may appear before the footlights of the times taking advantage of the establishment of the observatory, and further, may go on successfully to the goal of its sound development.

In conclusion, I would like to express my sincere thanks to you, and all, beginning with the officials at the Ministry of Education, respective liaison offices of each ministry, the authorities of Kagoshima Prefecture and also of Uchinoura Town, and others concerned, for your valuable guidance and cooperation extended to us on the project.

February 2, 1962

Seiji Kaya
The President of Tokyo University

Congratulations by Uchinoura Town Headman
at the Commencement Ceremony

I would like to offer my congratulations to you for your successful commencement ceremony, as the representative of town people who have been eagerly looking forward to realization of the project of KSC, which has been planned by Tokyo University.

At the end of 1960, the authorities of the university made a field investigation here at the site proposed, and yet we could hardly believe that our town, so remote that it might be called "solitary island of land," should meet the requirements.

But, later, we were informed of your decision that our town had been approved because it is located in the most proper environment for the intended tests. And we did our best to cooperate with you, under the leadership of authorities of the prefecture. Since we received the formal notice April last year, the whole town realized the significance of the project, and finally we have come to greet the day of your commencement ceremony with our applause.

Nowadays the development in culture, especially science, has reached the stage of cosmic research, yet it goes on progressing day by day. Ranking among the best of other advanced countries, Tokyo University has been and is taking part in the science field, for which we pay sincere respects to the University. Meanwhile we, all of the town people, are very proud of our contribution to the scientific research, which we hereafter will be privileged to make in spite of our remote location.

Pondering over our present status, I find the people of the town, accustomed to carrying on their isolated lives far from all society, know little of the times; and though we have been enlightened and have made a little progress in industrial culture, yet we do not leave the state of the "less advanced." Hence, establishment of "a sanctuary of the latest science" will surely stimulate and awaken us in every respect, and at the same time, will have no small effect upon our economy. Furthermore, I presume to plan and hope for development of our tourist industry by taking advantage of the project, which will also be of help to all of the Osumi Peninsula.

Anyway, all of the town people heartily welcome the establishment of the KSC here, and it shall be recorded in the history of our town administration as a memorable event and we express our sincerity by hoisting national flags. We shall appreciate it very much if you would accept our hearty congratulations.

As the laboratory shall be of international significance and use, difficulties are presupposed to occur in the course of construction. We, all town people, will do our utmost to eliminate hindrances anticipated by means of the cooperation offered by all parties concerned in neighboring towns and villages as well as by the government and the prefecture. As the first step thereof, we organized the town society, the opening ceremony of which is going to be held later today.

In conclusion, I wish I could appropriately deliver the heartfelt joy and congratulations of all town people, also I hope the construction will successfully be completed in the earliest possible time.

February 2, 1962

Shun Kukimoto
Uchinoura Town Headman

Congratulations by Ministry of Education at the
Commencement Ceremony of Kagoshima
KSC Cooperative Society

I would like to offer my congratulations to you at this commencement ceremony.

In our country, the origin of cosmic space observations by means of rockets came in the Third International Geophysical Year when we procured remarkably successful data during observations of the ultrahigh atmosphere. Later, under the international science league, called COSPAR, we have performed an important part of their research. The research in our country has been made mainly by Tokyo University, Production Technique Laboratory, which is taking a leading part, with the cooperation of respective laboratories of other universities and government offices. National expenditures laid out for the research have not been small; thus the nation herself did her best to promote steady progress.

The application for establishment of Tokyo University KSC was made because of the remarkable progress in rocket research, and was accepted by us. Now, through the cooperation and support of Kagoshima Prefecture authorities, the commencement ceremony for the project was held yesterday, for which I would like to express my sincere congratulations.

When making observations through a rocket facility, there are delicate concerns for preservation of public peace on land, sea and in the air; atmospheric phenomena, electric rates, communications, fishery and so forth. Besides, the project involves many other problems such as transportation, lodgings, a relief station, etc. Hence, without a good understanding with and positive cooperation of all inhabitants in the Prefecture as well as from all organizations and parties concerned, the aim to promote and achieve the project successfully cannot be realized.

For this point, the foundation of Kagoshima KSC Cooperative Society, the opening ceremony of which is held today, means much for us, and I, as a person concerned with the project, would hereby like to express my respects and appreciation to all who help us for their earnestness and endeavor.

My hearty congratulations; I sincerely hope your society will go on successfully, functioning as a promoter of the project, and consequently will render great services to the propagation of the general idea of science and the development of the Prefectural administrations.

February 3, 1962

Masuo Araki
Ministry of Education

Congratulations by Governor of Kagoshima Prefecture at the Commencement Ceremony of Kagoshima KSC Cooperative Society

As I am privileged to make a speech at this opportunity of your commencement ceremony, firstly, I would like to express my deep appreciation to the President of Tokyo University and officials of the Ministry of Education.

Yesterday, Tokyo University held the commencement for KSC. KSC is planned to provide facilities to gather cosmic science data and it has taken its first step to the realization of this goal.

As you all know well, Tokyo University started their tests on rockets at Michikawa coast, Akita Prefecture in 1955; since then, it joined with international science as a member of the World Observation Organization and later achieved research of the ultrahigh atmosphere, etc. The remarkable development of the techniques in the field of rockets has required new laboratories

of such larger scale that geographical conditions at the coast of the Sea of Japan could not meet the needs. For this reason, the new project has been set up and is to be located at the spot on the coast of the Pacific Ocean, Nagatsubo, Uchinoura Town of our prefecture.

In spite of the younger history of cosmic science research in our country, the extraordinary abilities of Japanese scientists have been recognized with world-wide applause and is ranked as No. 3 in rocket technique next to the USA and USSR. I, all Japanese as well, am very proud of this achievement, and earnestly ask for further cosmic studies and wish for even greater results.

I think that before the final stage of launching rockets, there are not only necessary procedures to be taken in installing equipment, transporting rockets, bringing in visiting scientists but also some other arrangements to be made: for instance, maritime guarding at the time of rocket impact on the water, shore guarding, information of meteorological phenomena, notification of the tests to air bases, precise system of telegraphic and telephonic communication, preservation of propellants, negotiation with fishermen and so forth. Thus, there are many problems of very wide scope. Upon completion of the orderly arrangement of this complicated mass of detail in a way that each organization functions under the control of the laboratory with smoothness then the world-famous work and techniques of our country will display their real worth.

Some of you now sitting before me may be involved in a large part of the project or some very small part. But regardless of its size, every part is of the same importance in contributing to the greatest achievement of our scientist group, which is participating in an inquiry into the cosmic science; in other words, it is our duty to try to be of help with our united efforts in the course of development which will make its way through the clouds of mystery in the universe. Meanwhile, I do wish and expect that Kagoshima Prefecture now listed under "less-advanced" would be stimulated by this opportunity and devote itself to scientific education and give the children endless dreams of universe.

In conclusion, I, as the chairman of the society, cordially solicit your special consideration for the project and your cooperation.

February 3, 1962

Kagoshima KSC Cooperative Society

K. Terazono
Governor, Kagoshima Prefecture

The Regulations of the Society

(Kagoshima KSC Cooperative Society)

NAME:

Item No. 1 — The society shall be called Kagoshima KSC Cooperative Society.

OFFICE:

Item No. 2 — The office shall be set up in the Kagoshima Pref. Government, No. 68, Yamashita-cho, Kagoshima City

AIM:

Item No. 3 — The society shall aim at cooperative functioning of various organizations concerned with carrying out tests of rockets and others accompanied therewith smoothly, for research of cosmic physics.

ORGANIZATION:

Item No. 4 — The society shall be organized with officials, parties, representatives of the companies and staffs concerned with rocket observations and other tests related thereto.

The society shall have a chairman and vice chairman in its administration; the society shall inaugurate the Governor of the Kagoshima Pref. to the post of chairman, and the chairman shall appoint the vice chairman.

The chairman shall represent the society, and carry out its general administration. The vice chairman shall act for the chairman when he is unable to function.

CONFERENCE:

Item No. 5 — To attain the aim described under Item No. 3, the society shall institute a liaison conference, and the chairman shall convene it when necessary.

COMMITTEE:

Item No. 6. — For smooth management, the society shall organize a steering committee formed with several managers, and the chairman shall convene it in case it is necessary. Managers shall be appointed by the chairman from among the members of the society.

MISCELLANEOUS:

Item No. 7 Besides the above items, any necessary items in regard to the administration of the society shall be decided on by the chairman as the case may be.

Membership list of Kagoshima KSC Cooperative Society

As of February 1962

Chairman	Governor of Kagoshima Pref.	TERAZONO Katsushi
Vice-Chairman	Deputy Governor of the same	KANAMARU Saburo
Members:	The Chief of General Adm. Department of Kagoshima Pref. Government	FUKUMOTO Kiyotetsu
	The Chief of Agricultural Adm. Dept. of the same	TOKUDA Masaaki
	The Chief of Fisheries, Commerce & Industry Dept. of the same	YAMAGUCHI Hideharu
	The Chief of Forest Adm. Dept. of the same	ARATAKE Toshinori
	The Chief of Public Works Dept. of the same	ISHII Okinaga
	The Chief of Planning & Research Room	TASHIRO Hiromitsu
	Head of Education Bureau of the same	KURIKAWA Hisao
	The Chairman of Kagoshima Pref. Council	OTSUBO Shizuo
	The Vice Chairman of the same	HIDAKA Hirotame
	The Chief of General Adm. Police Dept. of Kagoshima Pref. Council	UEZONO Tatsuo
	Ditto, but of Agriculture & Forestry Dept.	KAWAHARA Shinjiro
	Ditto, but of Public Works Dept.	HAMURO Osuka

Members:	Ditto, but of Education & Sanitation Dept.	HIRAHARA Tetsuo
	Ditto, but of Fishery, Commerce & Industry, and Public Welfare Dept.	SATA Shuji
	The President of Kagoshima Towns and Villages Council	NAGAI Masao
	The President of Kagoshima Mayors' Congress	HIRASE Sanetake
	Mayor of Kanaya City	NAGATA Ryokichi
	The Headman of Uchinoura Town	KUKIMOTO Shun
	The Chairman of Town Council	KANGAYASHIBO Masanobu
	The President of Kagoshima University	FUKUDA Tokushi
	The Chief of Kagoshima Adm. Bureau of J.N.R.	ERIGUCHI Masao
	Kagoshima Elec. Communication Dept.	NISHI Tsunehachi
	The Chief of Kagoshima Weather Bureau	MASHIMA Yoshio
	The Chief of Uchinoura Forestry Bureau	TOYODA Isaku
	The Chief of Guard & Rescue Sec., The Maritime Safety Headquarters of No. 10 District	YANAGIDA Osamu
	The Chief of Kagoshima Maritime Safety Agency	INOUYE Hideya
	The Chief of Kagoshima Police Headquarters	KANABORI Kazuo
	The Chief of Guard Sect. of the same	IWAKI Yasutsuna
	The Chief of Aviation Security Office	YUBARA Tomoharu
	The Chief of Yamakawa Electromagnetic Observatory	ISHIKAWA Saburo
	The Chief of Kagoshima Branch Office of Kyushu Electric Power Co.	KUWAHATA Yoshiji

Members:	The Chief of Kagoshima Branch Office of Japan Express Co.	FUKUO Yoshio
	The Chief of Kagoshima Branch Office of Japan Tourist Bureau	FUJISAWA Hiroyuki
	The Director of Kagoshima Pref. Kanaya Hospital	ISHII Taizo
	The Chairman of Kagoshima Fishermen's Union	MATSUMOTO Akito
	The South Japan Press	TANEDA Kageo
	Kagoshima Shinpo-sha	MITSUI Umio
	Kagoshima Branch Office of Kyodo Press	KOBAYASHI Kenji
	Ditto, but of News Agency	FUKUTOME Yukinori
	Ditto, but of Asahi Press	MATSUOKA Takashi
	Ditto, but of Mainichi Press	OJIMA Harumi
	The West Japan Press	MARUDA Kenkichi
	Kagoshima Branch Office of Yomiuri Press	KAWANO Junji
	Ditto, but of Japan Economy Press	TACHIKAWA Yoshi-mine
	Ditto, but of Kumamoto Nichinichi Press	KOGA Masashi
	N.H.K. Kagoshima Station	HONDA Takeyuki
	Minami-Nihon Broadcasting Station	HATANAKA Suetaka

The Regulations of the Society

(Uchinoura Town KSC Cooperative Society)

NAME:

Item No. 1 — The society shall be called Uchinoura KSC Cooperative Society.

OFFICE:

Item No. 2 — The office shall be set up in the Uchinoura Town Office.

AIM:

Item No. 3 — The society shall aim at cooperative functioning of various organizations concerned with carrying out rocket tests and others accompanied therewith smoothly for the research of cosmic physics.

ORGANIZATION:

Item No. 4 — The society shall be organized with officials, parties, representatives of the companies and staffs concerned with rocket observations and other tests related thereto.

The society shall have a chairman and vice chairman in its administration; the society shall inaugurate Uchinoura Town Headman to the post of chairman, and the chairman shall appoint a vice chairman.

The chairman shall represent the society, and carry out its general administration. The vice chairman shall act for the chairman when he is unable to function.

CONFERENCE:

Item No. 5 — To attain the aim described under Item 3, the society shall institute a liaison conference, and the chairman shall convene it in case it is necessary.

COMMITTEE:

Item No. 6 — For smooth management, the society shall organize a steering committee formed with several managers, and the chairman shall convene it in case it is necessary. Managers shall be appointed by the chairman from among the members of the society.

MISCELLANEOUS:

Item No. 7 Besides the above, any other items necessary in regard to the administration of the society shall be decided on by the chairman as the case may be.

Membership List of Uchinoura Town KSC Cooperative Society

As of February 1962

Chairman	The Headman of Uchinoura Town	KUKIMOTO Shun
Members:	The Assistant of Town Office	KAWAHARA Seizo
	Treasurer of the same	MATSUYMA Katsumi
	The Chief of Education Section of the area	SAEDA Hanshiro
	The Chief of General Affairs Sect. of the same	MATAKI Hiroshi
	The Chief of Public Works Sect. of the same	NIDAYAMA Tstuyoshi
	The Chairman of Uchinoura Town Council	KANBAYASHIBO Masanobu
	The Vice Chairman of the same	OTODA Yoshio
	The Chairman of General Affairs Committee	YANO Yoshihiro
	Ditto, but of Public Works Committee	YAMANOGUCHI Masashi
	Ditto, but of Economy Committee	KURA Yoshio
	The Chief of Uchinoura Forestry Bureau	TOYODA Isaku
	The Superintendent of the Field Station of Kagoshima Public Works	MAEDA Masanori

Members:	The Chief of Uchinoura Post Office	
	The Chief of Kishira Post Office	NAKAHARA Noboru
	A Police Sergeant, Takayama Police Station	ARATA Torao
	The Chairman of Uchinoura Schoolmasters' Committee	TSURUNO Yoshitoku
	The Chairman of Uchinoura Agricultural Cooperative Association	KANBAYASHIBO Masanobu
	Ditto, but of Uchinoura Fishermen's Union	NAGANO Kesayoshi
	The Chairman of Uchinoura Commerce & Industry Association	HINOMOTO Tsunetaro
	Ditto, but of Uchinoura Tourist Association	
	The Chief of Uchinoura Fire Company	CHOSA Hiroyuki
	Uchinoura Women Liaison Office	TANAKA Kimi
	Head of Uchinoura Young Men's Association	MINAGUCHI Takashi
	The Representative of Miyahara Shinko-Kai	NAGATSUBO Kiyoshi
	The Chairman of Uchinouracho Promotion Association's Liaison Office	UCHINOKURA Michiyoshi
	The Superintendent of Elec. Works, Kyushu Elec. Power Co.	NAKAMURA Shigetoshi
	Ditto, but of Branch office of Japan Express Co.	NAGATA Teikichi
	The Uchinoura Wire Communication Station	MAKI Michio

OUTLINE OF THE KT PROJECT

By Akio Tamoki and Tatsuhiko Watari

1. KT Project

On the night of May 24, 1962, a K-8-10 space rocket (name of a Kappa series space rocket) was launched from an Akita test site. Soon after it was launched, it accidentally exploeded and the flame and fragments of the rocket body damaged nearby residences. Because of this accident, we had to re-examine more thoroughly the safety involved in a space rocket launching including unexpected accidents. As a result of many discussions, we concluded that it would be very difficult to secure even minimum safety at the Akita test site because there was not enough surrounding area. Therefore, there was no alternative but to move all the rocket launching program to the Kagoshima Space Center, which had enough space to secure launch safety. Originally, we had decided not to use the Kagoshima Space Center for actual operations before it was completed — around May 1963. Therefore, when we did decide to move to Kagoshima, the place was still under construction. But two sites were in readiness there, so we decided to set up a temporary launch site and use it before the original scheduled time for Kagoshima's completion. This temporary test-site project of Kagoshima was called the KT Project (which stands for Kagoshima Transfer or Temporary). This project consisted of two subprojects: one to transfer all test equipment from the Akita test site, and two, to establish a temporary test site at Kagoshima using the old equipment. The KT Project was proposed for Akita on May 27, 1962, and Mr. Tamoki took charge of the over-all project. Mr. Watari became executive secretary, and Professor Nomura took charge of the safety security problem. At the same time, it was essential to maintain safety at the temporary test site at Kagoshima. For this purpose, we obtained the cooperation of everybody involved. Having actual surveys of the sites, we were able to finish the blueprint phase of the work on the KT Project by June 25.

2. Site Survey

Professor Nomura and Messrs. Itogawa, Moruysu, Tamoki, and Watari left for Kagoshima Space Center to find out how the construction work was coming along, to look into the possibility of establishing a temporary test site there, and to obtain permission from the Province Government for

launching space rockets in advance of the date the Kagoshima Space Center was scheduled to be operational.

Arriving there, we found out that the construction work was delayed far behind schedule by the long rainy days. The two sites and the connecting roads were completely covered with mud. We had to wait to start the KT Project until the weather was better. One of the main objects of our discussion was to agree on an operational date for the KT Project. Some of us insisted on an August deadline while others, considering possible difficulties called for September. Finally, we decided on a mid-August date. Fortunately, we were able to get wholehearted cooperation for our project from the Province Government. So we laid out our plans in detail for the actual construction work.

3. Decision for a mid-August Space Rocket Experiment

On June 27, 1962, at the Inter-Ministry Committee meeting on space rocket research held at the Ministry of Education, we told of our plan to establish a temporary test site at the Kagoshima Space Center and to launch K-8L-1, AT-150-1, and OT-75-2 rockets from August 20 to 30.

4. Temporary Construction

Bids for the construction work were opened in the conference room of the Uchinoura town office. The construction contact for the observation building was awarded to the Gomoku Construction Company, Inc.; and the electric-power-installation contract was awarded to the Kyushu Electronics Company, Inc. According to the contract, construction was to start on July 10 and be completed by August 19. The following were the construction items:

Item	Structure	Quantity	Location
Telemetry observation room	Wood	10 Hyo*	Computing and measuring center in 2nd site
Computer	"	"	"
Main office room	"	"	"
Main office conference room	"	"	"
Radar observation room	"	4	"
2nd Optical observation room	"	1.5	"
1st Optical observation room	"	2	Rear of 1st site

(Table Continued)

Room	Structure	Quantity	Location
Rocket assembly room	Wood	10	Launching area in 1st site
Lavoratory (1st)	"	0.5	Computing and measuring center in 2nd site
Lavoratory (2nd)	"	0.5	Launching area in 1st site
Safety communications station	Steel-concrete	2 Ea.**	Nagahiro town
Protection -- concrete wall	"	4 Ea.	Computing and measuring center in 2nd site
Launcher base	Concrete	225 m^2	Launching area in 1st site
Base for a telemetry antenna	"	1 Ea.	Computing and measuring center in 2nd site
Base for a GMDI radar	"	1 Ea.	Same as above

* Hyo is unit of area which corresponds to approximately 36 ft^2.
** Number of units.

By the hard work of these two companies, the construction progressed very smoothly and all buildings were finished by early August. The only thing left for completion of the temporary test site was to bring the old facilities from the Akita test site. Using seven trucks we were able to transfer all the old facilities to Kagoshima by August 14.

5. Conclusion

The accident of the K-8-10 space rocket at the Akita test site made it impossible to use Akita anymore as a launching site. Thus, space rocket research for 1962 would be blocked unless we could find another launching site. At this time, though, a new test ground was being established at Kagoshima; construction work there was already far enough along so that a temporary launching site could be set up merely by adding minor temporary changes. Thus, our space rocket research had to undergo a momentary pause.

Finally, we are very grateful to many people without whose understanding and cooperation the KT Project could not have been successfully worked out in such a short time. And we express our thanks to the two companies named for their wholehearted understanding of our difficulties.

(Received on May 1, 1963)

BLUEPRINTS (KSC)

By Yo Ikebe

Overall Construction

Siting plan	Ikebe Research Institute
Structural design	Hiroi Research Institute
Facility design	Katchda Research Institute

Buildings

Telemetry Center (T.C.)	$221.2m^2$
Control Center (C.C.)	$122.9m^2$
Instrument Center (I.C.)	$49.2m^2$
Rocket Center (R.C.)	$474.6m^2$

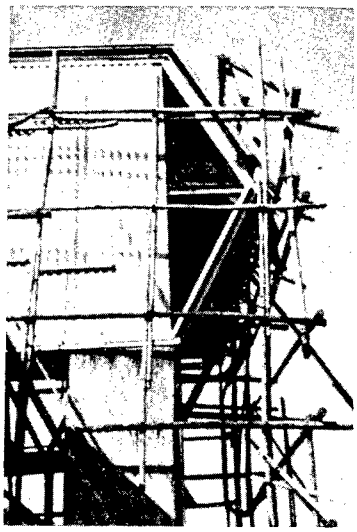

Entrance to rocket center
View showing installation of electric door

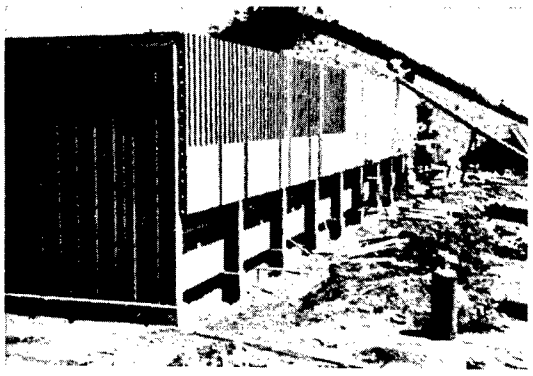

Outside of telemetry center

Sandwich structures are used: foam plastics are put on the deck plate and asbestos-concrete boards cover the foam plastics. The window frame is made of aluminum and the window itself is reinforced glass. Below the window, the area is covered by an iron slat.

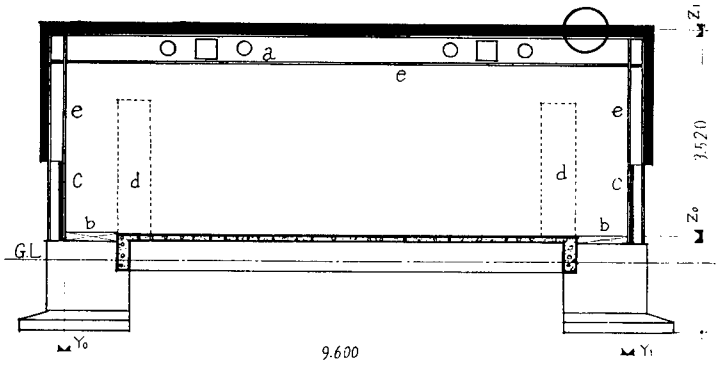

Fig. 1. Side view of basic layout

a - Air-conditioning duct; b - Power-line duct; c - Opening to bring in light; d - Computing device; e - H-type steel frame

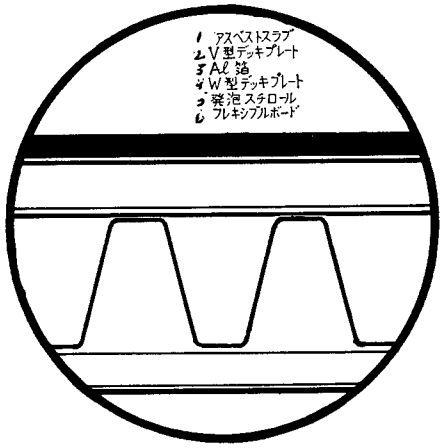

Fig. 2. Fundamental structure

1 - Asbestos slab; 2 - V-type deck plate;
3 - Aluminum foil; 4 - W-type deck plate;
5 - Foam styrol; 6 - Flexible board

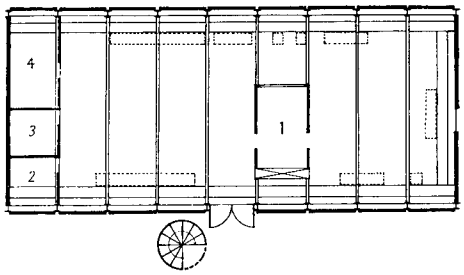

Fig. 3. T.C.*

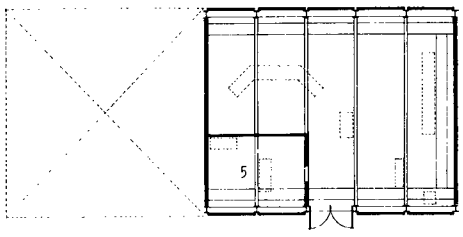

Fig. 4. C.C.*

*See next page for legend.

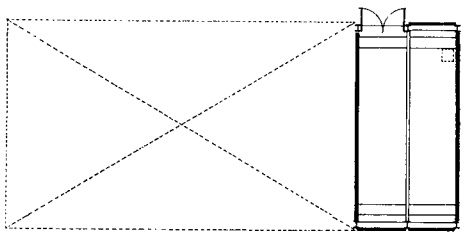

Fig. 5. I.C.

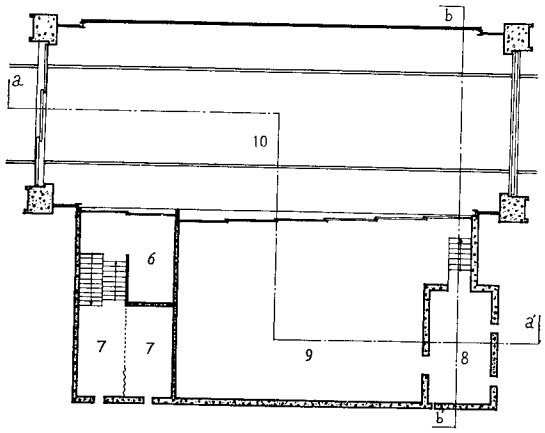

Fig. 6. First floor of R.C.

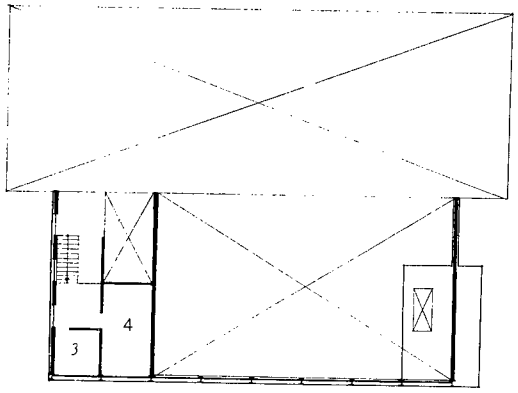

Fig. 7. Second floor of R.C.

1. Conference room
2. Data processing room
3. Lavoratory
4. Workshop
5. Automatic telephone switchboard room
6. Instrument assembly room
7. Preparation room
8. Control room
9. Operation room
10. Assembly room

2.560 10.240

0 5.120

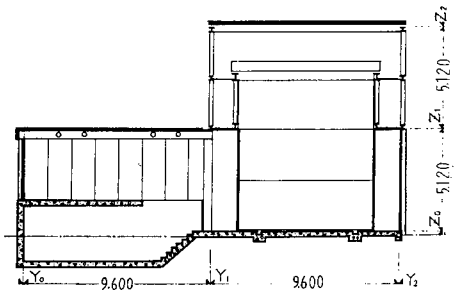

Fig. 8. Side view of R.C. (b-b')

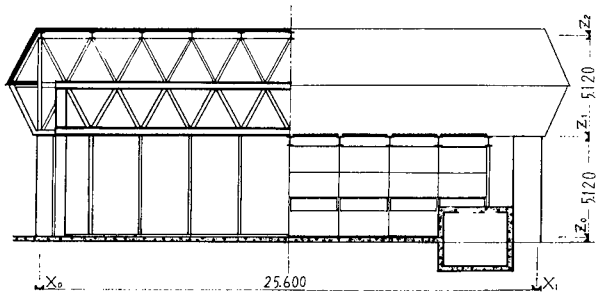

Fig. 9. Side view of R.C. (Rocket Center) (a'-a)

As of this writing, the rocket center, the telemetry center, the control center, and part of the computing center have been completed. In the design of this temporary test facility, the condition of the land, plans for future expansion and safety had to be considered. And it was desirable to use the same basic structure for all the buildings. This idea was carried out for all buildings except the rocket center (refer to Fig. 1).

A frame having a 9.6 m span and 2.56 m width is the structural module for these buildings. This frame is made of steel and the roof and wall use multi-layer boards in which steel plate and asbestos-concrete plate are sandwiched (refer to Fig. 2). The floor was also originally designed to have the same structure; however, because of a limited construction budget, a concrete floor was used. The circular holes shown in the ceiling are the air-conditioning ducts. Using the structural module as a building block, all buildings were constructed as shown in Figs. 3, 4 and 5. The dashed line portions are planned for the future.

As shown in Figs. 6, 7, 8 and 9, the rocket center consists of two parts: one is the rocket assembly room, and the other is the rocket-engine control room. In view of future expansion and some other factors, the rocket assembly room was designed to have very few pillars. The structure of the control room was partly concrete but followed closely the fundamental structure.

The construction companies involved in the KT project are as follows:

Construction:	Detchko Construction Co., Fukuoka Branch
Air Conditioning:	Koken Industry Co., Inc.
Electric Power:	Asoumi Electronics Co., Inc.
Asbestos:	Asana Slate Co., Inc.
Deck Plate:	Hochiban Econ.Co., Inc.
Panel:	Ohohoda Gum, Inc.
Chassis:	Fuji Chassis, Inc.

(Received on April 24, 1963)

BRIEF OUTLINE OF KAGOSHIMA SPACE CENTER CONSTRUCTION

By Takakazu Maruyasu, Yoshio Nakamura and
Shamei Tsuda

1. Introduction

The Tokyo University Kagoshima Space Center was planned to be constructed in the town of Uchinoura, in the country of Kansoku, in Kagoshima Province. As members of Tokyo University Production Research Institute, we were in charge of planning and designing the Space Center. We shall report in the current paper on our work.

The construction was to be completed in three years. While the construction work was under way, the province government took over a part of the road construction which would connect a second launch site to the province highways. Therefore, our construction work consisted of preparing the land, construction of a network of roads, and installation of the necessary facilities, buildings and other construction.

2. Aerial-Photography and Mapping

On March 1961, before making the construction plans, we took aerial photographs of the location for the new space center site and of neighboring areas (Fig. 1); and from these pictures, using our Autograph A-7, we made two kinds of maps: 1/5,000 scale and 1/2,500 scale topographical maps. With these maps, we carefully examined possible access roads over which materials could be carried; and we analyzed the neighboring areas and determined the total amount of available soil for our construction work. Based on these data, we planned the exact locations of new roads.

3. Plans

We planned the primary project (first construction project) for 1961. In this project, land preparation for a rocket launching site and adjoining area, road construction work for access to this land, and construction of a water-supply system were included. For 1962, we planned a second construction project in which the construction of bases for ground-test facilities, land preparation for a radar center site, and a road connecting the radar center with the main site were included. In making these plans, we based our designs

on aerial photography, the topo maps, actual land surveys, and other factors necessary to consider in building a space-rocket launching site. Our original plan was discussed extensively by a KC committee before the final plan was approved. The final construction plans were based on actual measurements of the land.

Fig. 1

1 - Water tank; 2 - 2nd access road; 3 - tracking station; 4 - access road; 5 - 18-m radar; 6 - telemetry; 7 - control center; 8 - center; 9 - reservoir
10 - Province highway; 11 - To Uchinoura area

4. Design

The land preparation was designed in such a way that the final surface would be formed without bringing soil in or carrying it away; in other words, in such a way that the cutting down of land would be balanced by filling other land. All roads were designed to meet the specifications for second-class national highways. The most important aspect for the road design was draining the water and protecting the edges of the roads during heavy rains. There

was no stone available to make stone walls for drainage purposes so we substituted cement walls (refer to Fig. 3). The roads were planned to be paved in the future. However, because of a limited budget, for the time being they were designed as pebble roads (refer to Fig. 2). Since this area's soil easily turns to mud on a rainy day, the higher areas were protected from erosion by extensive cement block walls, and many drains were planned for rapid draining of the water (see figures).

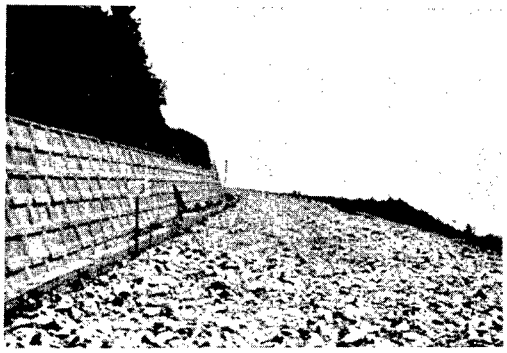

Fig. 2. First access road

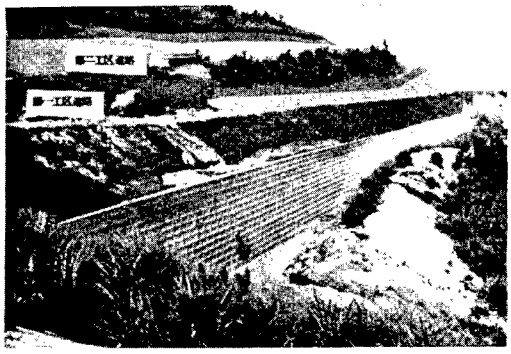

Fig. 3. Block layer wall

5. Construction Work

(1) The first construction project

The start of the first step in the construction project took place in January 1961; and in February of the same year, in the presence of Dr. Tsukime, President of Tokyo University, the land-breaking ceremony was held. The construction items were as follows:

(a) Land preparation for the first site. This land was to be used for the launching area, rocket assembly room, and rocket-transport tracks. The area and elevation are about 5,000 m^2 and 277 m, respectively. The surface of the roads was covered by pebbles at that time (refer to the frontispiece).

(b) Land preparation for the second site. This land was to be used for the computing center, rocket storage, research, and optical observations. The area and elevation are about 1,500 m^2 and 260.3 m, respectively.

(c) The first access road. This road runs from the province road mentioned at the beginning of this paper to the first site and has a length of about 195 m. In order to have enough room for the L-type rocket, this road was planned to have a 4.5-m width.

(d) The second access road. This road runs from the proposed province road to the third site and has about a 400-m length and a 4-m width. Its maximum slope of 13% was dictated by the lay of the land.

(e) The third access road. Actually, this road was the extension of the second access road. When the second access road was under construction, the exact plan for the third site (we shall see later) was not fixed and so the road to the third site was constructed separately later.

(f) Water supply. Finding a fountain at the east side of the first site at an elevation of about 250 m, we constructed a reservoir with a dam 10 m wide and 1.5 m high about 10 m downstream from the source. Pumping the water into a water tank of 10 m^3 capacity located at the highest point (elevation 322 m) in the north side of the first site, and then treating it, we used a total length of 2 km of pipe for our water supply.

These construction works were divided into two parts. The first part included land preparations for the first and second sites, and construction of the first access road; this work was done under contract by Komoku Construction Co., Inc. of Kagoshima. The second part included construction of the second access road, third access road, and water supply system; and this work was done under contact by the Kokugi Construction Company, Inc. of Kagoshima.

During the construction works, hit by several heavy rains and a long rainy season, several high areas were swept away and some other damage was inevitable and the work was very much delayed. Finally, the first step of the project was successfully completed in November 1962.

(2) The second construction project

The construction items for this project were as follows:

Fig. 4. The third access road

(a) The third access road. This road was designed to connect the third optical-observation room with the radar center in which the 4 mφ parabolic tracking radar of the Akita test ground would be installed. The total road length is 900 m and the maximum difference in elevation is about 100 m. This road runs through many steep areas and it has a maximum slope as high as 15%.

(b) The water-supply system. In order to supply water to the radar center as cooling water for the 4 mφ radar antenna (4t/h), and drinking water, we planned to dig a 7-10 m deep well near the province highway and pump the water up to a water tank of 5 m^3 capacity located at the highest point of the radar center. From this water tank, water would be supplied through water pipe to all points in the radar center.

(c) The rocket-transport tracks. To launch an L-type space rocket, a rocket-transport track running from the rocket assembly room to the launch pad was designed. The base of the track was made of a steel-concrete slab able to support a total weight of 50 tons comprising rocket and the launcher. For the track, 37-kg rails (track width 5.00 m) were used. At the launching point, a 3.5-m deep, 17-m long, and 3-m wide flame channel was dug.

(d) The third site. This land will be used for the telemetry center, radio center, and control center. Together with the land used for the 18-mφ parabolic antenna, this area is 3,000 m^2 at about 319-m elevation.

(e) Water reservoir for cooling water for the 18-mφ parabolic antenna. To operate the 18-mφ parabolic antenna, we have to supply 16 m^3/hr of water. To precool the circulated water intended for the oil pressure pump, a 50-ton capacity octagonal steel-concrete water tank was built. From the parabolic antenna's oil-pressure pump, the water is then directed to flow through a sloped waterway back to the reservoir. From here, it is re-circulated through the oil-pressure pump for a closed cycle.

These constructions were called for in the third project. The third access road and the water supply system were contracted by the Komoku Construction Company, Inc. The water tank for the cooling water and rocket-transport track were contracted by the Kanetaka Construction Company, Inc., as an extension of the first and second projects in the second-step project. These works were started in December 1962 (see Figs. 7-10).

(f) Repair of the damages. As mentioned before, this area's soil is hard as long as it is dry; but once it absorbs moisture, it becomes soft and easy to crumble. During the first-step project, a long rainy season started in March and there were unusually heavy rains. Perhaps as the result of these rains, the southern slope of the first site eroded, destroying the stone wall and flooding about 400 m^2 of land (see Fig. 11). Immediately, repair work followed to replace the stone wall by a double layer of wall comprised of a steel-concrete wall and a stone wall; and the low part of the slope was protected by a wider wall.

(3) The third-step project

This project will start after 1963 and includes construction of a rocket storage room, the first optical observation room, fourth observation site which is planned to be established at Tozoki, sewerage systems for all facilities, and road pavement.

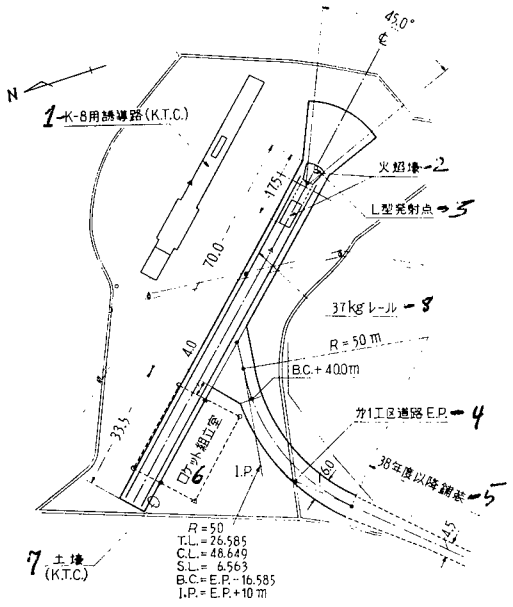

Fig. 5. The rocket-transport track (L-type)
The access road to the track (paved)

1 - K-8 rocket carrying track (K. T. C.); 2 - Flame channel; 3 - L-type rocket launching point; 4 - First access road; 5 - Paved after 1963; 6 - Rocket assembly room; 7 - Channel; 8 - Rail

Fig. 6. Work to dig flame channel for rocket-transport track

Fig. 7. Bulldozer lent by province government

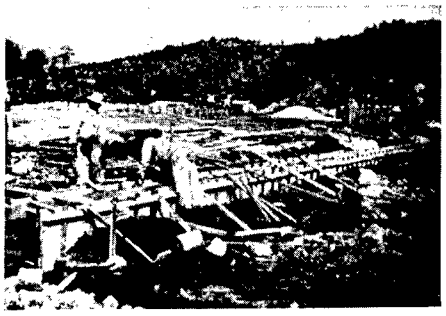

Fig. 8. Making drain for the second site

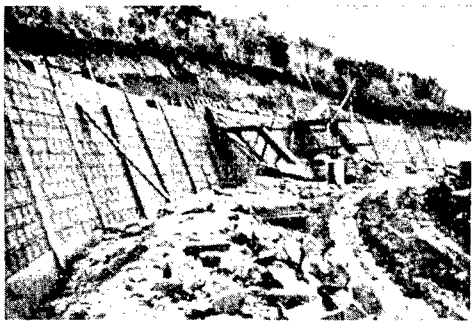

Fig. 9. Laying blocks

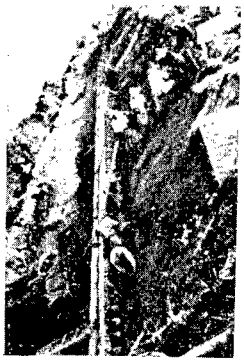

Fig. 10. Laying blocks

Fig. 11. Demolished part

(Received on May 3, 1963)

THE GROUND FACILITIES OF KAGOSHIMA SPACE CENTER

By Norihumi Saido, Iwaho Yoshida and
Hirosumi Takanaka

1. Introduction

After seven years of operation as a center for space rocket research, the Michgawa test site in Akita Province became unsuitable for large space-rocket launching. Finally, a new location at Nagahiro, south of Uchinomura on Ohosumi Peninsula in Kagoshima Province, was selected in April 1961 as a new test site. Two new groups were organized in the SE research committee. One was named KC group (Kagoshima Construction) and took charge of planning for the construction works, for instance, land preparations, road construction, and buildings. And the other one was named KE (Kagoshima Equipment) and took charge of planning for the ground equipment. To do effective work developing the new test site, close cooperation between these two groups was demanded. According to the original plan, this project was supposed to be completed within two years — from 1961 to 1963. Thus, the ground equipment was not completely installed as of this writing. Since only part of the ground equipment is in operation, it does not seem worthwhile to describe the ground facilities in the limited space of this paper. We will report on this subject after having more of the facilities completed. We shall report in the current paper on the planning of the KE group with respect to the ground facilities at Tokyo University Kagoshima Space Center. It is our hope that this will help as a reference to the ground facility of Kagoshima Space Center.

2. Equipment Plan of the KE Group

Soon after the decision was made for establishing a new space research center at Kagoshima, many useful ideas were proposed in several SE discussion sessions about the location, area, and structure of each building, total land area, roads, water reservoirs, positions of devices, arrangements of interior of buildings, rent, etc. In a SE conference, Professor Maruyasu led the discussion of land preparations, road construction, and water reservoir construction. We led the discussion regarding construction of all necessary instruments for rocket launches. Thus, KC and KE as two research groups were organized in October 1961. Since the first KE meeting was held in January 1962, we have had more than ten meetings and several joint discussion sessions with the KC group. Finally, we drafted our plan and obtained approval of the SE committee. The essential part of the plan consisted of launching control and

command devices, telephone communication systems, radio communication systems, weather-map receiving equipment, public address system, ITV and electric power-supply system. The project was divided into two parts, the first project (for 1962) and the second project (for 1963).

3. The First Project

The first project consisted of setting up launch control and command equipment for control center and the rocket center, installation of a telephone system, and installation of a power-supply and distribution system. As the first project, the following instruments were planned for the various centers:

(1) Launch control device.

Control Center. A launch control panel, payload control panel, launch command desk, electric-power-supply panel, and relay terminal box.

Telemetry Center. A standard-time generating device and relay terminal box.

Rocket Center. A relay desk for the payload signal, relay terminal box, igniter control panel, launch control panel, clock, and terminal box in the launching area.

Computing Center. A clock and relay terminal box.

(2) Telephone system.

Control Center. A 60-channel crossbar PBX automatic switchboard (installing 5 exchange lines, it is possible to connect directly to Control, Telemetry, Computing and Radar Centers, and reception desk at night), three telephones.

Telemetry Center. Five telephones.

Rocket Center. Four telephones.

Computing Center. Two telephones.

(3) Radio communications system.

A control station (1711.5 kc/350 w), and 1-3 stations (mobile stations, same frequency as above, 10 w).

(4) Public address system.

Control Center. A transmitter, two loudspeakers, and an amplifier.

Telemetry Center. Five loudspeakers and an amplifier.

Rocket Center. Five loudspeakers and an amplifier.

Computing Center. Two loudspeakers and an amplifier.

(5) ITV

Installing a remote control ITV camera and a receiver in Control Center, it was planned to watch the exact situation on the launching area and also the attitude of a rocket after it is launched.

(6) Weather-map receiving equipment.

This was planned to be installed in Control Center. It consists of a facsimile machine and high sensitivity all-wave receiver. It would be used to find out weather conditions for a flight experiment by accumulating weather information for several days before the experiment.

(7) Power distribution system.

Using the ducts made by the KC group, electric wires were laid all through the buildings for all the equipment including that planned for the second project. And all equipment in the first project was properly connected. And those wires laid in uncompleted buildings were gathered in shanks for use after the building is completed.

(8) Electric-power supply system.

To supply electric power, we installed two 50 kva and two 20 kva transformers at the first site, and two 15 kva, and four 30 kva transformers at the second, and third sites, respectively; and will supply three-phase 200 v, and single-phase 200 v and 100 v.

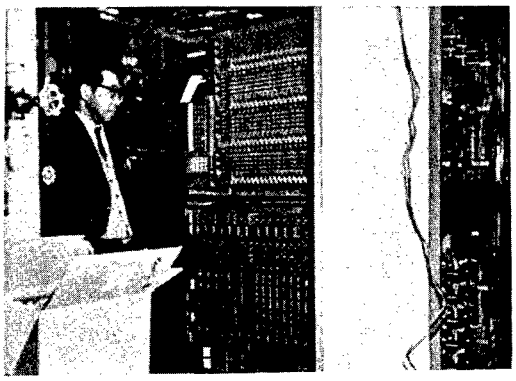

Fig. 1. 60-channel crossbar PBX automatic switchboard

4. The Second Project

The second project was scheduled to be worked on in 1963 and the following instruments were planned to be installed in the various centers:

(1) Launch control devices.

Control Center. A program command panel, program display panel, program control panel, large time display, sea safety-guard display panel, and rocket trajectory display panel.

Telemetry Center. First and second telemetry control panel, first radar-control panel, and radar antenna-direction control device.

Rocket Center. An assembly room display panel, launcher, time indication device for launch control, outdoor large time-indicating panel, and wind direction and velocity meter.

Radar Center. The second radar-control panel, transmitter for rocket trajectory display, and a telemetry antenna-direction control device.

(2) Telephone system.

a. General purpose telephone and loudspeaker for uncompleted buildings.

b. Single purpose telephone for launch command (four channels, four connections).

c. Intercom system.

(3) Power distribution system.

Wire laying for the Radio Center, first and second Optical Observation Rooms, observation tower, rocket hangar, and computing center, which were planned to be completed in 1963, and wire laying to Radar Center.

5. Conclusion

We described briefly the project of the KE research group for the ground facility of Tokyo University Kagoshima Space Center. The main purpose of this project is to get effective communications, for space rocket-flight experiments, between the Control Center and other local centers (Rocket, Telemetry, Radar, Radio and Computing Centers). In other words, our project is designed in such a way that when a rocket is launched, all the information necessary for the flight can be obtained precisely and quickly through the agencies of push buttons, relays, and pilot lamps. When our plan is completed, the ground facility will look like the organization diagram reported on in a separate paper.

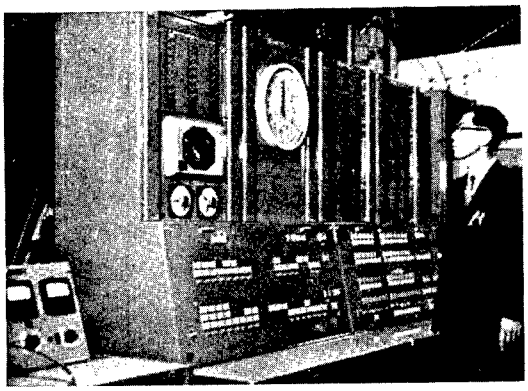

Fig. 2. Launch control panel

Unfortunately, we could not describe the particular purpose of each instrument, their correlations, and their operation. However, we hope this paper will be able to serve as a reference. Finally, we are very grateful to Professor Nomura for his kind help and also to members of KC research group for their useful discussion. And we express our thanks to engineer Michisi for his consulting and Nipong Denki Co., Inc., Michibichi Denki Co., Inc., Tamoru Co., Uraga Chuko Co., Inc., Oki Denki Co., Inc., and Tokyo Chiboura Denki Co., Inc., for their construction work. And mention should also be made of Mr. Hideko Kawano for his drafting work and other help.

(Received on April 6, 1963)

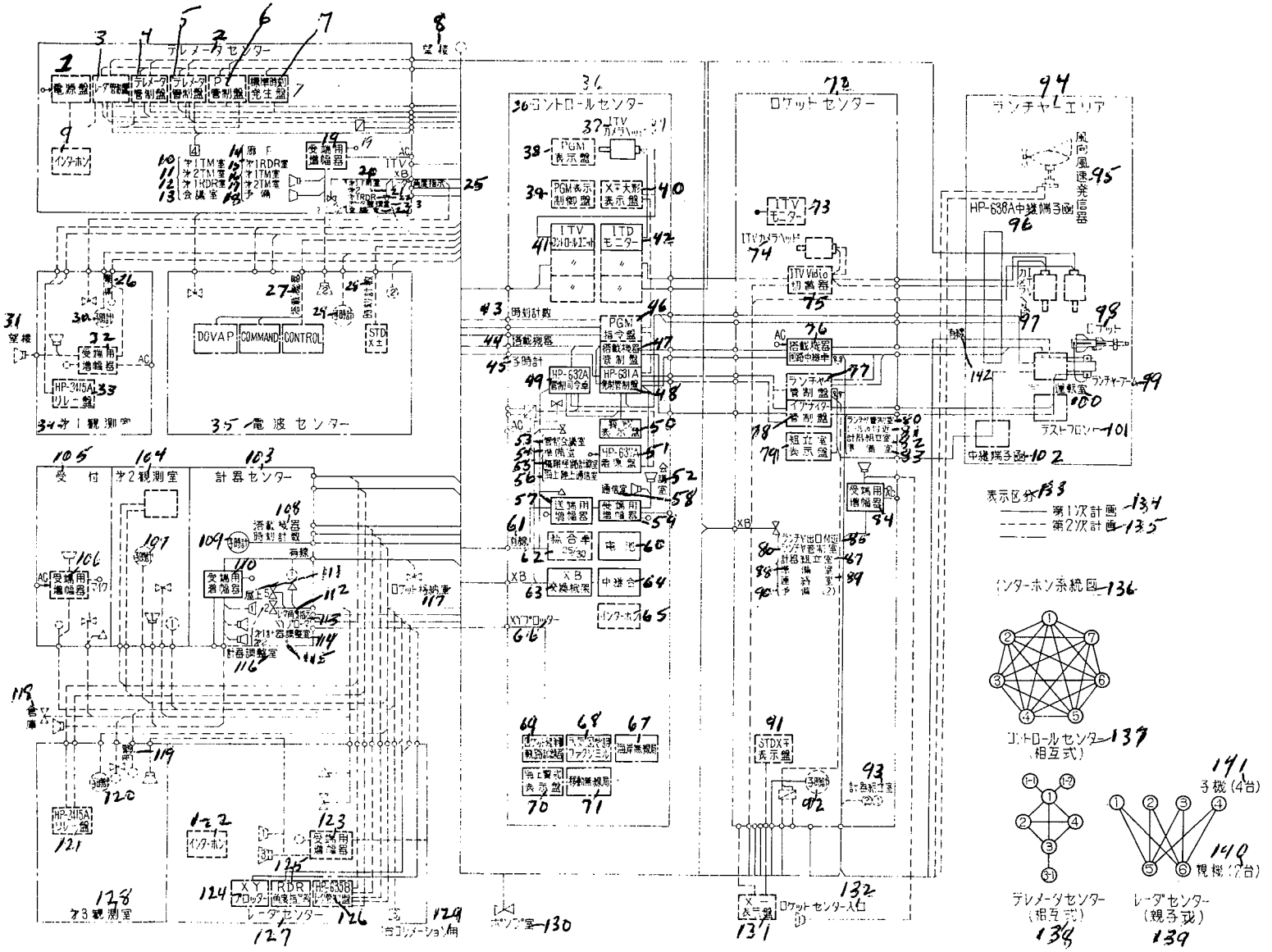

Organization diagram of the ground facility

1. Electric power-supply panel
2. Telemetry Center
3. Radar control panel
4. Telemetry control panel
5. Telemetry control panel
6. PI control panel
7. Standard-time generating panel
8. Observation tower
9. Intercom
10. First TM room
11. Second TM room
12. First RDR room
13. Conference room
14. Corridor
15. First RDR room
16. First TM room
17. Second TM room
18. Reserved room
19. Amplifier for receiver
20. First TM room
21. Second TM room
22. First RDR room
23. Data processing room
24. Conference room
25. Radar direction indicator
26. Telegraph
27. Payload, classified
28. Timer
29. Clock
30. Clock
31. Observation tower
32. Amplifier for receiver
33. HP-2415A relay panel
34. First observation room
35. Radiowave radar
36. Control Center
37. ITV camera head
38. PGM display panel
39. PGM display control panel
40. XK giant display panel
41. ITV control unit
42. ITD monitor
43. Timer
44. Payload
45. Clock
46. PGM control panel
47. Payload control panel
48. HP-631A launch control panel
49. HP-632A command desk
50. Safety-guard display panel
51. HP-637A electric-power supply panel
52. Conference room
53. Conference room of control section
54. Preparation room
55. Rocket trajectory computing room
56. Communications room for ground and sea stations
57. Amplifier for transmitter
58. Communications room
59. Amplifier for receiver
60. Battery
61. Telegraph
62. Data reduction
63. XB switchboard
64. Relay terminal
65. Intercom
66. XY plotter
67. Radio communications stations on the beach
68. Weather map receiver focusing mirror
69. Rocket trajectory recoding machine
70. Safeguard-indicator for sea
71. Mobile radio communications station
72. Rocket Center
73. ITV monitor
74. ITV camera head
75. ITV video switch
76. Payload's signal relay desk
77. Launch control panel
78. Igniter control panel
79. Assembly room indicator
80. Launch control room
81. Near the rails of rocket-carrying track
82. Computer assembly room
83. Preparation room
84. Amplifier for received signal
85. Near launch exit
86. Launch control room

87. Computer assembly room
88. Preparation room
89. Liaison room
90. Second preparation room
91. Display panel
92. Clock
93. Computer assembly room
94. Launch area
95. Wind direction and speed dispatcher
96. HP-638A relay terminal box
97. ITV camera head
98. Rocket
99. Launch boom
100. Operations room
101. Test observation point
102. Relay terminal box
103. Computer center
104. Second observation room
105. Reception desk
106. Amplifier for receiver
107. Clock
108. Payload timer
109. Clock
110. Amplifier for receiver
111. Roof
112. Radar direction indicator
113. XY plotter
114. First computer control room
115. Second computer control room
116. Computer control room
117. Rocket hangar
118. Storage
119. Telegraph
120. Clock
121. HP-2415A relay panel
122. Intercom
123. Amplifier for receiver
124. XY plotter
125. RDR direction indicator
126. HP-635B radar control panel
127. Radar Center
128. Third observation room
129. For one collimation
130. Pump room
131. X display panel
132. Rocket center entrance
133. Classification of these organizations
134. First project
135. Second project
136. Intercom system diagram
137. Control center
138. Telemetry center
139. Radar center (master-substation typ
140. Master station (two)
141. Substation (four)
142. Cable

TRANSPORTATION OF ROCKET

By Iwaho Yoshiyama

1. Introduction

The research rocket-launch facility at the Michigawa test site in Akita Province moved to a new location at Nagahiro of Uchinoura Town, Kagoshima Province. Transportation of a rocket to the Michigawa test site was relatively easy and we did not worry about packing and handling. It took three days from Tokyo to the Michigawa railway station by train, and the test site was located only 2 km away from the railway station. However, for the new launch site at Kagoshima, the situation is quite different. It is far from Tokyo and also it is located far from the railway station. We should be more circumspect in handling large rockets in the future. We examined the transportation problem by ship as well as by train. However, the facility of Uchinoura harbor was not large enough to handle rocket cargoes. So we finally decided we would depend entirely on the train for a while.

2. Ground Transportation Route

For the time being, a rocket is packed at Deikoku Kakohing Industry, Inc., at Kawagae city. It is carried by truck to Ogikubo railway station and then transferred to a train to be taken to Tokayama station of Ohasumi, Kagoshima. And here it is transferred to a truck belonging to Nipong Toung Company. It travels through Namimi and Uchinoura, and finally it reaches the new test site. Figure 1 shows the truck road from Namimi to the test site. As we can see, the road zigzags very much.

3. Packaging the Rocket

When we worked at Akita, rocket transportation did not take long and so we did not use any special method of protecting the rocket from moisture. However, in transporting a rocket to the new launch site, we carefully examined the moisture problem and determined the following protective measures:

Rocket type	K-150	K-240	K-420	K-730	K-1420
Silica gel (gr)	100	150	250	600	4000

Fig. 1

1 - Namimi; 2 - Uchinoura town; 3 - Test site; 4 - Uchinoura Bay

We inserted amounts of silica gel into each rocket in accordance with the above table, and every nozzle was sealed by tape. Because of the rough road condition, the packing box was made to protect the rocket against a 2-g load. And to protect the rocket from any bending in the direction perpendicular to the body axis, an elastic packing material was used. To protect the rocket from the 2-g shock load, felt or synthetic rubber was put at every contacting part as a shock absorber.

4. On the Actual Transportation

Arriving at the Takayama railway station, the rocket was transferred to a truck. Figure 2 shows the scene of transferring the cargo from train to truck. Led by a jeep of Takayama police, the trucks were driven at about 10 km/hr to the test site. Figure 3 shows a truck convoy heading to the test site, and also shows one of the sharp curves of the road. With the kind help of the Kagoshima

Province government, the road condition will be much improved in 1963. Thereafter, there will not be much transportation trouble even for a large rocket. For this we are very grateful to the province government for its wholehearted help. And finally, we express our thanks to the Nipon Toung Transportation Company Takayama branch for their careful handling and untiring work for us.

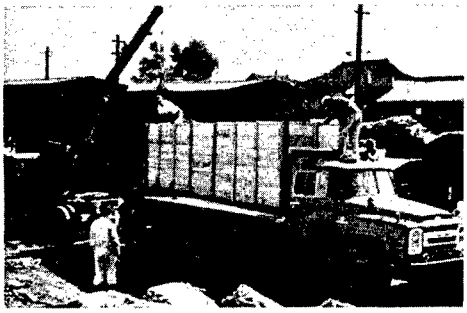

Fig. 3

1 - Propellant (explosive)

(Received on April 9, 1963)

THE LM TEST STAND

By Ryaziro Akiba and Iwaho Yoshida

The LM test stand was established for the ground test of L and M series rockets. When the L-735-2/3 space rocket ground test was planned, the LM test stand was built at Michigawa, Akita. Later on the Akita test facility turned out to be unsuitable for the space-rocket test. Therefore, this test stand was moved to the Noshiro test facility established at Hamaasa Beach of Noshiro City, Akita Province. Using this new test facility a L-735-3/3 space rocket was successfully tested.

1. Test Stand Base

As far as the shape of test stand base is concerned, there is not much difference between that of Noshiro and of Michigawa. However, the underground structures are very different. Since the test stand at the Michigawa test site was good enough for actual use, there was no particular reason to change its design at the Noshiro test site. However, the soil of the latter area is much softer than that of the former. Therefore, at Noshiro, it is more difficult to support the test stand. We designed the base in such a way that its upper surface would be kept horizontal even if the base were to sink. This was accomplished by properly selecting the center of mass point and the shape of the base. The actual thrust of the rocket engine is about 100 tons and the weight of base is 270 tons. In designing a rocket launcher base on soft land, we found that the structure's static weight over and above the impulsive thrust force is certainly significant. Based upon these two factors, the Noshiro-type launcher base was designed to be able to test rockets having up to 150 tons of thrust. The safety factor of the structure itself is 7. And without external load, it can keep its surface horizontal even if the base weight reached up to 400 tons. However, the load limit depends very much on the method of supporting the base.

2. TS34-type Test Stand

The K-735-2/3 space rocket was too big to be tested on the Michigawa test stand. So a new big test stand was urgently needed. A new test stand

should have the capacity for testing a rocket with dimensions up to a diameter of 1100 (sic), length 11 m, and thrust 80 tons.

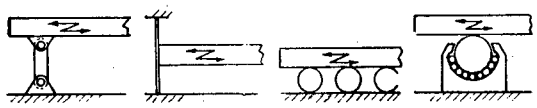

Fig. 1. Various type of stands

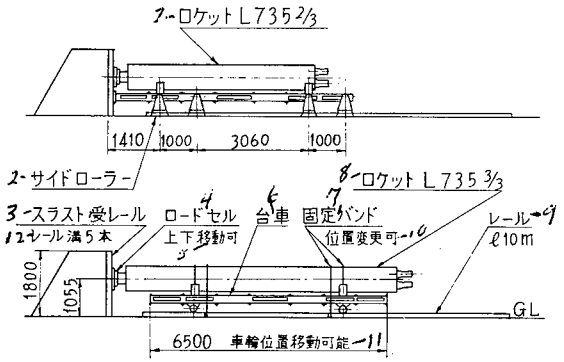

Fig. 2. TS 34 test stand

1. Rocket L-735-2/3
2. Side roller
3. Thrust directing rail
4. Load cell
5. Movable up and down
6. Vehicle mount
7. Band
8. Rocket L-735-3/3
9. Rail
10. Position movable
11. Vehicle mounts can be changed
12. Five rails

As seen in Fig. 1, many horizontal-type test stands were proposed. Among those test stands, the TS34 was adopted because its operation was very accurate and it had the added advantages of easy handling, high reliability and low cost.

Generally, a roller-type was used for a small rocket because such a test stand had the least frictional effect. In a large rocket, however, the situation is quite different. Generally, for a mounting-vehicle-type test stand, the anti-rolling friction force is relatively big and this is the main difficulty for this type of test stand. However, it was possible to reduce the friction so much that the stand was able to start rolling just with the natural wind of the Michigawa area.

The mounting vehicle was not restrained against vibrating in the transverse direction; therefore, a rocket mounted on this stand had unavoidable tail vibrations during combustion and hardly obtained the thrust zero-point recovery. To overcome this difficulty, we mounted side buffers having a small friction but being able to withstand 1/10 of the rocket thrust. Since the mounting vehicle is pinned at four supporting points, bending or torsional force could act on the rocket unless all four supporting points are aligned with the base line at any point along the rail. Thus, we designed the mounting vehicle to allow a tolerance of the four supporting points within 0.3 mm.

In determining the number of rocket mounting points and wheels for the L-735 type rocket, we found it would be enough to have two supporting points with four wheels for the L-735-3/3 as indicated in Fig. 2. Precautions were taken not to generate any low-frequency vibration.

3. Load Cell and Checking Devices

In measuring the thrust, the following conditions should be satisfied at least within a good approximation: 1) the direction of the thrust force must coincide with the center of the cell, 2) any unnecessary oscillations should not be generated except the ones generated by combustion, and 3) zero-point recovery should be accurate.

To meet all three of these requirements, a conventional stand was designed in such a way that the rocket and load cell were contacted by an oil-pressure-point contacting method (contacting surface being spherical), and the thrust was checked after the rocket was mounted. This stand was constructed as a trial one, and safety and cost were the main factors in the design. Since a short load cell is attached very tightly to a rocket, as shown in Fig. 2, the load cell looks simply like a part of the rocket.

With this stand, we were not able to obtain satisfactory results for the L-735-2/3 rocket combustion test; later on, we improved the method of

attaching a load cell to the rocket. And finally, we obtained very satisfactory results for the L-735-3/3 combustion test with an improved test stand. (Refer to the article on the thrust meter and development of the L-735 rocket engine.) We built a portable, single load cell checking device which was the minimum device for our research.

(Received on April 5, 1963)

PRESENT SPACE RESEARCH OF WESTERN COUNTRIES (PART 2)

By Noboru Takagi

(2) Goddard Space Flight Center

Goddard Space Flight Center is located in Greenbelt, Md., about 10 miles northeast of Washington, D.C. It was built in a wooded area, and the following buildings are almost completed: Space Project Building, Research Project Laboratory, Central Flight and Range Operations Building, and Fabrication and Environmental Test Laboratory. The Instrument Construction and Installation Laboratory and the Space Science Laboratory are presently under construction. It is a very big organization with about 1600 employees. Unfortunately, the author was able to spend only several hours visiting the place. He met the following people:

Dr. Harry J. Gaett, Director

Dr. John C. Lindsay, Associate Chief, Space Science Division

Mr. Harold J. Peake, Head, Flight RF Systems

Mr. John W. Townsend, Assistant Director, Space Science and Satellite Applications

Mr. Friedlich O. Vonbum, Consultant, Tracking Systems Division

The overall interest of this research center covers the spectrum from the design of space rockets and satellites to the final step of data analysis. In other words, it covers: (1) the determination of the purpose and design of a space experiment, (2) construction of the necessary equipment for the experiment, (3) construction of a rocket or satellite for the experiment, (4) launching the rocket or satellite, (5) tracking the rocket or satellite and taking data, and (6) analyzing the data and putting the information into a form that scientists and technicians can use. Sometimes all of the steps (1) through (6) are carried out by this center; frequently, however, other research organizations cooperate on certain experiments and in some instances, only the data reduction is done at Goddard.

This Flight Center consists of the following divisions and groups:

(1) Theoretical Division

(2) Space Science Division

(a) Solar, (b) Astronomy, (c) Ionosphere, (d) Atmosphere, (e) Instrumentation of Sounding Rocket, (f) Particle and Fields - - 6 groups

(3) Payload Division

(a) Flight Data, (b) Radio Frequency, (c) Mechanical and Thermal Integration

(4) Satellite Applications Division

(5) Tracking and Data Systems Division

(a) Minitrack, (b) Mercury Network, (c) Orbital Computation, (d) Data Processing

(6) Environmental Test Division

The Space Science Division consists of six specialized research groups (total of about 100-150 people work in this division) and it has close contact with the Theoretical Division. Behind the many rockets and satellites launched by NASA, not only those research members of NASA were involved but also many universities and other research organizations. In many cases, many research instruments made by organizations other than NASA were loaded into a rocket or satellite with or without modification. Many people of the Space Science Division belonged to a military research laboratory before NASA was founded.

The Payload Division constructs the actual instrument which is loaded into a rocket or satellite. It does this by combining what is designed by the Space Science Division and what is submitted by outside research organization. The Satellite Application Division works by keeping in close contact with the Payload Division. For example, the payload of Vanguard, the payload P-14 which contained a new kind of magnetometer, and the payload S-51 which was constructed jointly with Great Britain for ionosphere research were all finally completed in the Payload Division. (In the U.S., the sphere part of the head of a satellite is called the payload. All the instruments such as the telemetry, power sounce, etc., form the group called payload, while in Japan, the group of instruments loaded in a nosecone of a space rocket is called the payload.)

For a large satellite project, sometimes, the work is done under contract with private industry. For instance, in constructing some of the instruments for the weather satellites Tiros and Nimbus, RCA had the contract for this project. And one other company contracted for building the observation instruments.

After a space rocket or a satellite is launched, the tracking and data collection and processing are worked out by the Tracking and Data Systems Division. The Minitrack of this division is a tracking system having two antenna networks: one is the east-west direction and the other in the north-south direction. One can compute the orbit of a satellite by the radio signal transmitted from the rocket by the interference detecting method. For this purpose, the U.S. established 12 tracking stations all over North and South America, and these tracking stations were and will be used to trace a satellite traveling in the east-west direction and to compute its orbit. Since many polar orbit satellites are planned for the future, the U.S. is planning to establish Minitrack stations along the equator. The data obtained by the Minitrack stations all over the world are transmitted to the Tracking and Data Systems Division through a radio communications system or any other communications method considered best; and the orbit of the satellite is calculated by the Orbital Computation Section and the data are analyzed and put into forms useful for scientists by the Data Processing Section.

For an unmanned satellite, the time taken for orbital determination is not such a critical problem; however, for a manned satellite such as in the Mercury project, all data should be analyzed instantaneously to eliminate all possible troubles. For this particular purpose, the Mercury Network was established consisting of 14 radar and telemetry stations along the orbit of the project Mercury manned satellite. All data collected by any of these stations would be sent immediately to the computing center of NASA (it has 3 IBM 7090 computers) and then the calculated orbit of the satellite would be dispatched to the very next tracking station and all flight information also would be sent to the Cape Kennedy flight control room. More information on the Mercury project will be seen in detail in other report papers of this series . The author was very much impressed by the scale of the communications system network and by the computing center of Goddard Space Flight Center.

Beside the abovementioned places and instruments, in the Payload Division we had a chance to look at three British payloads which were planned to be loaded to a U.S. Scout. These three payloads were identical and were made for experimental, testing and prototype uses. And we found also many British space scientists and engineers who had come to the U.S. to discuss their joint research program. To have an international joint research project, some travel expense should be included in the budget in order to have joint discussions all through the preparation period.

In the space-rocket section, we saw people studying the attitude control of the Aerobee rocket. It is clear that in space rocket research as well as in satellite research, attitude control is one very important factor and we have already tried many methods of attitude control in Japan, too. So we were very fortunate to have the chance of looking into their work on attitude control.

(3) Jet Propulsion Laboratory (JPL)

JPL is located at Pasadena, a suburb of Los Angeles, and had been operated for more than 20 years as a branch research institute of California Institute of Technology (private school and abbreviated Caltech). It is a very big organization having more than 2500 employees; about one-third of the employees are scientists. We spent one day to visiting this organization. The following were the important people we met during our visit:

Dr. W. H. Pickering, Director

Dr. E. Rechtin, Director, Deep Space Instrumentation Facility

Mr. J. D. Burke, Director Ranger Project

Dr. A. R. Hibbs, Chief, Division of Space Science

Dr. Mercia Neugebauer, Deep Space Instrumentation Facility

Mr. W. H. Bayley, Deputy Chief, Telecommunication Division

For the past 20 years, JPL has been working mainly for the U.S. Army research; for example, they constructed the supplemental rocket JATO to aid aircraft taking off, and the first guided missiles, Corporal and Sergeant. In the space research field, they successfully launched the first satellite Explorer I and the moon rockets Pioneer III and IV. When JPL went over to NASA, it terminated its contract with the U.S. Army. Ever since, its main research has been in the lunar and planetary programs.

Among the JPL organizations, except administration and management offices, the following eight science and technology divisions were of interest to us.

(1) Systems Division
   (a) Program Support, (b) Systems Analysis
   (c) Systems Design, (d) Systems Test and Operation
(2) Space Sciences Division
   (a) Research Analysis, (b) Space Instruments,
   (c) Experimental Space Science
(3) Telecommunications Division
   (a) Communications Systems Research
   (b) Communications Engineering and Operations,
   (c) Communications Elements Research

(d) Communications Systems Development

(4) Guidance and Control Division

(a) Flight Computers and Sequences ,

(b) Spacecraft Secondary Power

(c) Guidance and Control Analysis and Integration

(d) Spacecraft Control,

(e) Guidance and Control Research

(5) Engineering Mechanics Division

(a) Material Research, (b) Spacecraft Development,

(c) Professional Services, (d) Engineering Research,

(e) Spacecraft Design, (f) Design

(6) Physical Sciences Division

(a) Chemistry, (b) Gas Dynamics, (c) Physics

(7) Engineering Facilities Division

(a) Instrumentation, (b) Applied Mathematics,

(c) Wind Tunnels and Environmental Facilities

(8) Propulsion Division

(a) Solid Propellant Engineering, (b) Polymer Research,

(c) Propulsion Research, (d) Liquid Propulsion,

(e) Advanced Propulsion Engineering

Along with these eight divisions, JPL has the lunar program (under which the Ranger and Surveyor Projects belong) and the planetary program, and JPL also has the Deep Space Instrumentation Facility. We find that the operational function of those eight divisions and two programs are analagous to the streets and avenues of a town. In other words, those two programs work with the help of all eight divisions.

The remarks of Director, Dr. W. H. Pickering and Ranger Project Director, Mr. J. D. Burke can be summarized as follows:

Since JPL belongs to Caltech, all contracts with NASA have to be signed between Caltech and NASA. However, actual problems are worked out between JPL and NASA. The personnel administration belongs completely to JPL and there are not many scientists exchanged between Caltech and JPL. After JPL became affiliated with NASA, the JPL foreign scientist training program was relieved of many of its previous difficult restrictions. Research

projects are set up in JPL and the organization drafts detail plans for the work and finally obtains approvals from NASA. We can find an example of the working process in the Ranger project of the lunar program. Under Mr. Burke as overall manager, the project is organized as shown in the following chart:

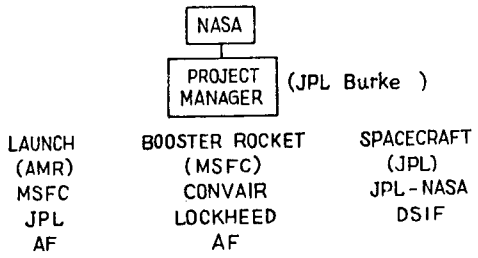

The launching assignment belonged to AMR (Cape Kennedy) and MSFC (Huntsville); JPL and the U.S. Air Force cooperated in the launching. The rocket construction was worked out by MSFC with the help of private industries. The spacecraft was built by JPL and the payload instruments were built with close cooperation with NASA. The tracking and communications belonged to DSIF (an organization of JPL).

In order to carry out the project, scientists in many fields and with varied connections cooperated through the following organizations:

(1) Headquarters; (2) Various divisions; (3) Universities; (4) Industries

All the project work done by these organizations was centered in JPL. In other words, the system was as follows: JPL drafted the spacecraft specifications giving the basic design, timetable up to launching, and necessary budget, and sent the information to NASA headquarters for approval. At NASA headquarters the budget was allowed after the project was studied and found to be valuable research. In the meantime, scientists of SSB (Space Science Board) of the NAS (National Academy of Science) proposed that the most important aspect of moon research was not to study the geology of the moon, but to study the seismic characteristics of the moon. At the same time, space scientists at universities, engaged in independent research, voluntarily suggested some ideas about particular subjects. And several divisions of NASA proposed their own favorite research subjects. Having interest in the Ranger project, the AEC also proposed some ideas for the project. Some of these suggestions were received by NASA and some others were received by JPL, and all suggestions were carefully studied at JPL before the final spacecraft and observation instrument list was fixed. This final plan was sent to NASA to obtain approval of the NASA Space Science Steering Committee for the budget allocation and technical aspects of the project.

After this planning stage was over, all the necessary instruments were built. Those instruments proposed by universities were built in their own laboratories, or sometimes ordered from private industries under a subcontract. Some instruments were made in JPL laboratories while others were made by private industries under contracts between JPL and the industries. Finally, all the instruments were shipped to JPL to be checked out and installed according to the original design.

To achieve effective research work and valuable results from the work, the wholehearted cooperation of scientists as well as a well-organized system were more essential than anything else. To have such cooperation between scientists, they had to meet each other to discuss their ideas and difficulties as frequently as possible. This could not be done unless the scientists were financially supported for their travel expenses as well as research expenses. For example, for the scientists of universities, their travel expenses were paid by the U.S. Government up to 90% of actual expenses; and in NASA research contracts, the travel expenses were included and NASA paid travel expenses for those attending the Space Science Steering Committee of NASA. When JPL or NASA invited scientists of universities to a certain conference, they paid for the travel expenses of the scientists in the names of the members of the universities or consultants.

As a branch research institute of Caltech, JPL was operating as described. Such an operational system is a unique method of the U.S. and we can find some other examples of such research institutes in addition to JPL. For example, there are some well-known research institutes such as Argonne Laboratory of Chicago University and Livermore Laboratory of University of California, both of which are well-known nuclear physics research laboratories; and Lincoln Laboratory of MIT which is well-known in the electronics engineering field.

(5) Summary of Lunar and Planetary Programs

Table 1, Lunar Program

	61	62	63	64	65	66	67	68	69	70
SPACECRAFT DEVELOPMENT	2									
RANGER ROUGH LANDING		3								
CENTAUR SOFT LANDING			2	2	3					
CENTAUR LUNAR ORBITERS				1	1					
SATURN SOFT LANDINGS							2	2	2	3

Table 1 shows the lunar projects scheduled for the 10 years from 1961 to 1970. In 1961, two spaceships were launched using the Atlas-Agena B rocket. These satellites were called Ranger 1 and 2, and designed to pass near the moon. In 1962, 3 spaceships, Ranger 3, 4, and 5, were launched to be landed on the moon (unfortunately all five Ranger spaceships failed). From 1963 to 1965, Centaur will be used to put a satellite into moon orbit. During this time, some observing instruments will be landed on the moon on a hard-landing; some spaceships will take pictures of the moon within a short distance from the moon; and some other spaceships will orbit the moon to take pictures and observe the moon. All these spaceships will be called Surveyor.

In 1966, Saturn will be used as the booster rocket. With Saturn, it is planned to land small moving observation stations on the moon.

Table 2, Planet Availability
Quarterly Launch and Encounter Dates

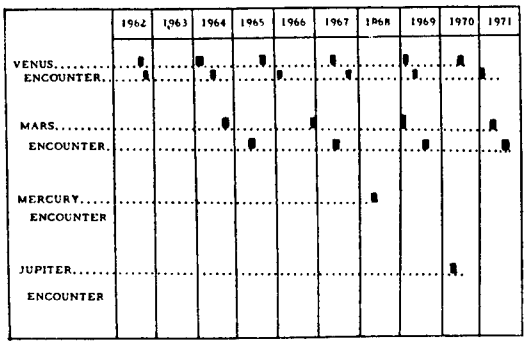

Table 2 shows the Planetary program for 10 years. For the Venus project, two spaceships were launched in 1962 and further work was planned for 1964 and 1965. To study a certain planet, it is desirable to launch the spaceship at the time the particular planet comes near the earth. There is one such chance every two years for Mars. The Mars project is scheduled to finish its experimental tests in 1963, and the actual spaceship will be launched toward Mars in 1964; it was discussed to land a spaceship on Mars using the Saturn booster rocket. Jupiter and Mercury projects will start after 1968 (fortunately the Venus project worked out successfully).

1) Ranger 1 and 2 Spaceships

Ranger 1 was launched toward the moon in such a way that it would have an elliptical orbit with about a one million km major axis. However, the spaceship had a velocity much less than escape. Ranger 2 was launched with a much larger velocity than escape and so it never came back to earth. Both of

these spaceships were launched in 1961 and were designed to be in useful operation for a few months.

The experiments and instruments of Rangers 1 and 2 and cognizant scientists are listed in Table 3.

Table 3, Ranger Project
Scientific Experiment Plan

SPACE-CRAFT	EXPERIMENT	INSTRUMENTS AND MEASUREMENTS	COGNIZANT AGENCY AND SCIENTIST
RA-1 RA-2	FIELDS, CHARGED PARTICLES, AND SOLAR X-RAYS	1. ELECTROSTATIC ANALYZER FOR SOLAR PLASMA	JPL, M. NEUGEBAUR, C. SNYDER
		2. SEMICONDUCTOR DETECTORS AND THIN-WALLED GEIGER COUNTER A. CDS PHOTOCONDUCTOR B. THIN-WALLED GEIGER C. MEDIUM-WALLED GEIGER D. AU-Si COUNTER	ST. U. OF IOWA/U. OF CHICAGO J. A. VAN ALLEN/ J. A. SIMPSON
		3. IONIZATION CHAMBER	CALTECH/JPL H. V. NEHER/ H. R. ANDERSON
		4. TRIPLE-COINCIDENCE TELESCOPES	U. OF CHICAGO J. A. SIMPSON
		5. RUBIDIUM VAPOR MAGNETOMETER	GODDARD SPACE FLIGHT CENTER J. P. HEPPNER
		6. X-RAY SCINTILLATION DETECTORS	LASL/SANDIA CORP. J. A. NORTHROP
RA-1 RA-2	HYDROGEN GEOCORONA	1. LYMAN ALPHA TELESCOPE	NAVAL RESEARCH LAB/JPL T. A. CHUBB
	INTERPLANETARY DUST	1. MICROMETEORITE COMPOSITE DETECTORS	GODDARD SPACE FLIGHT CENTER W. M. ALEXANDER

Conventional counters were used to measure particles in space over a wide energy range. To measure low energy particles, an electrostatic analyzer was used which might be able to detect protons having 0-5, 000 ev and electrons having several hundred ev and to measure the solar plasma. A CdS photoconductor and Geiger counter were used to detect electrons and protons having higher than the above energies. Besides these counters, a Au-Si semiconductor detector was used to detect positively ionized particles; these detectors do not work on negatively charged particles, for instance, electrons.

An ionization chamber and a triple-coincidence telescope were used in Pioneer V to measure protons having 10-100 Mev and the results were quite satisfactory. With all these instruments, it was possible to measure particles over all energy regions.

For measuring magnetic flux, either a fluxgate type or a proton precision type magnetometer was conventionally used. Adding to these, a new magnetometer using rubidium gas was used. This new rubidium magnetometer is based on the principle that the fine structure of the rubidium spectrum depended on the applied magnetic field and so, conversely, by measuring the fine

structure of the rubidium spectrum, one can determine the magnetic field intensity. This instrument is the most sensitive magnetometer among those available today. In measuring solar soft X-ray and cosmic dust, several conventional methods were adopted. To detect the existence of an electron-cloud in the outer atmosphere, a telescope using the Lyman-α line was planned. According to this method, the telescope would take pictures of the surface of the earth as the spaceship is departing from the surface.

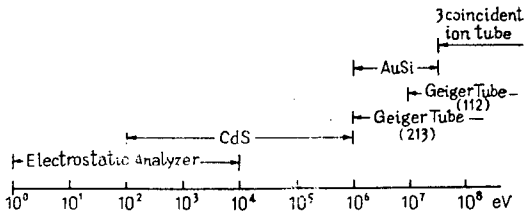

Figure 1

Fig. 2 shows the mockup with full equipment and we can easily notice a solar-cell, a parabolic antenna used for communicating with the ground stations, and an attitude control device. From the viewpoint of flight technique, the success of launching and flight depends largely on how accurately one can control the attitude of a spaceship. When we visited JPL (toward the end of February), scientists were just working on attitude control instrument to orient it with respect to the sun (Fig. 3). And we heard that Ranger 1 was launched unsuccessfully in August of 1961.

2) Ranger 3, 4, and 5 Spaceships

These were scheduled to be launched for trips to the moon in 1962. The experiments, mockup and attitudes during flight are shown in Table 4 and Figs. 4 and 5, respectively.

The main body consists of two parts: the capsule and the bus. A seismometer and a capsule temperature meter would be loaded in the capsule, and a vidicon-television camera and gamma ray spectrometer would be loaded the bus. With the attitudes shown in Fig. 5 the spaceship would approach the moon and at a fixed distance from the moon (30 km), which would be measured by the altimeter (which is not shown in Fig. 4), the bus would separate from the capsule and descend to the moon by free falling; on the other hand, the capsule would be decelerated by the retro-rocket and land on the moon with the seismometer.

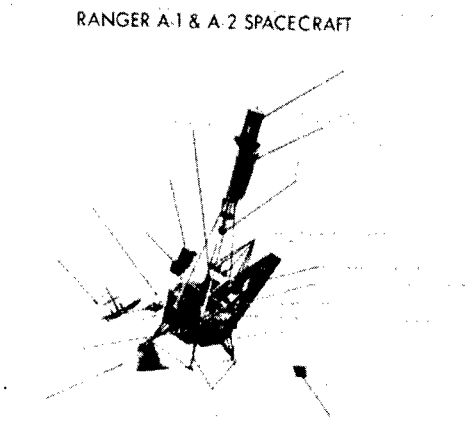

Fig. 2

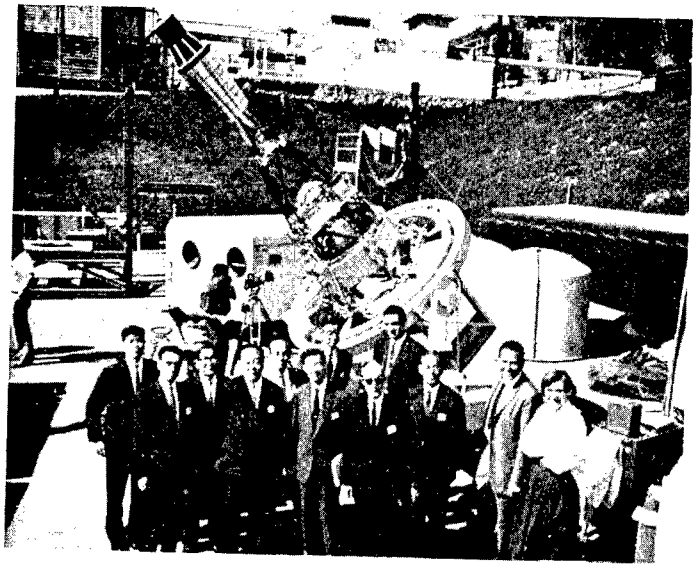

Fig. 3

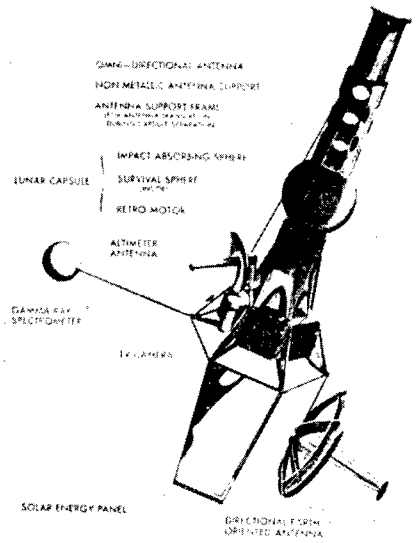

Fig. 4

Table 4

RANGER PROJECT, SCIENTIFIC EXPERIMENT PLAN

SPACE-CRAFT	EXPERIMENT	INSTRUMENTS AND MEASUREMENTS	COGNIZANT AGENCY AND SCIENTIST
	CAPSULE: SEISMOLOGY	1. SEISMOMETER	CALTECH/COLUMBIA UNIV. F. PRESS/M. EWING
		2. CAPSULE TEMPERATURE MEASUREMENT	
RA-3 RA-4 RA-5	BUS: PHOTOGRAPHY OF SMALL LUNAR AREA AND γ-RAY SPECTROSCOPY	1. VIDICON TELEVISION	JPL E. F. DOBIES
		2. GAMMA RAY SPECTROMETER	UNIV. OF CALIF/LASL/JPL J. R. ARNOLD/M. A. VAN DILLA E. C. ANDERSON/A. METZGER

As the spaceship approaches to the moon, the TV camera would take pictures of the surface of the moon and send them to the ground stations on earth. The gamma-ray spectrometer would detect the existence of radioactive materials on the moon.

The capsule was designed to stand up to 4 G. It was, moreover, designed to impact the moon at a speed of about 30 m/s to ensure maximum safety. In the capsule, an automatic control device would be installed to arrange the seismometer, transmitter, antenna, and power source in exactly the right position and to control the operations of all these instruments. These instruments were designed to be in operation for a few months on the moon.

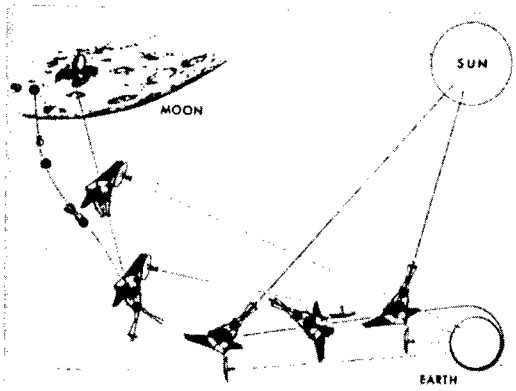

Fig. 5

3) Surveyor Spaceship

This project calls for sending instruments to a soft-landing on the moon through the use of a Centaur rocket. Its main purpose is to study the geology of the moon.

The experiments and instruments for this project are shown in Table 5. The main experiments are as follows: chemical and physical analysis of the lunar surface, taking pictures of the nearby area by a TV camera, and measuring the temperature distribution and composition of the subsurface of the moon by drilling down 4-5 feet. Besides the instruments needed for the above research, a seismometer and a gravimeter will be loaded into the space-

ship to study the structure of the moon and to provide part of all available data sent to earth ground stations. The spaceship will also carry communications gear. In this way, employing many new techniques, it seems that this project will yield very promising research on the moon.

Table 5

EXPERIMENT	INSTRUMENT AND MEASUREMENTS
SURFACE CHEMICAL ANALYSIS	1. X-RAY FLUORESCENCE SPECTROMETER
	2. NEUTRON ACTIVATION TECHNIQUES
	3. MASS SPECTROMETER
	4. GAS CHROMATOGRAPHY (DETECTION OF ORGANIC MOLECULES)
SURFACE PHYSICAL ANALYSIS	1. DENSITOMETER (γ-RAY SCATTERING)
	2. THERMAL AND ELECTRICAL CONDUCTIVITY MEASUREMENTS
	3. SOUND SPEED MEASUREMENTS
	4. VIDICON WITH VARIETY OF MAGNIFICATIONS
LOCAL SUB-SURFACE PROPERTIES (DRILL TO 4 OR 5 FEET)	1. X-RAY SPECTROMETER AND NEUTRON ACTIVATION INSTRUMENT IN CAVEHOLE
	2. VERTICAL TEMPERATURE GRADIENT MEASUREMENT
	3. THERMAL AND ELECTRICAL CONDUCTIVITY MEASUREMENTS
	4. DENSITOMETER
STRUCTURE	1. THREE-AXIS SEISMOMETER
	2. GRAVIMETER

JPL Surveyor Project typical scientific experiments

JPL Surveyor Project typical scientific experiments

Many geologists were more interested in terrestrial geology than in lunar geology and so did not pay much attention to the lunar research projects. However, stimulated by the lunar programs of JPL and NASA, some of these geologists have just started to become interested and to cooperate.

4) Mariner Spacecraft

All planetary spaceships are called Mariners. Mariner A is a Venus research spaceship and Mariner B is a Mars research spaceship.

The experiments for Mariner A are as follows:

1. Venus Temperature (Surface, Atmosphere, Ionosphere)
2. Venus Atmospheric Composition
3. Venus and Interplanetary Magnetic Field
4. Near Venus and Interplanetary Dust and Charged Particle Spectrum

The detailed technical specifications were made after many discussions among specialists in many fields. They include the following: the

spaceship should be designed not to hit Venus but to pass as near as possible to the planet and all observations should be done during that time. Experiments and instruments:

a) Measure four kinds of microwaves having wavelengths 4, 8.5, 13.5, and 19 mm, emitted from Venus; for this purpose, a radiowave receiver would be carried.

b) Measure the ultraviolet emitted from Venus over the wavelength band 1100-4200 Å; for this purpose a 10 Å resolving power spectrometer would be carried.

c) Measure the magnetic field in interplanetary space and near Venus; for this purpose, a wide-range magnetometer would be carried. Besides these observations, some instruments would be carried for measuring particles as in the Ranger project.

In reaching these specifications, scientists from various divisions in NASA, from universities, and from industry carefully studied the project in order to include enough research items and to select (sic) chiefs of all sections.

Mariner B was designed to probe Mars and is planned to be launched in 1964. A preparatory experiment was planned in 1963. There were long discussions over whether the spaceship should hit Mars or orbit Mars. Finally, the experimenters decided that the spaceship should consist of two parts: a capsule and a bus; separating at about 5 million miles from Mars, the capsule would fall on Mars and the bus would orbit Mars.

The final decision regarding instruments was not delayed until results from the Ranger program would be forthcoming. The most important instruments were designated as follows: various particle detectors (plasma, cosmic-ray), magnetometer, cosmic dust detector should be carried in the bus. A similar ultraviclet spectrometer as in the Mariner A case, and an infrared spectrometer used for detecting the existence of any organic material on Mars should be carried in the capsule. Adopting several suggestions, the detection of water vapor, carbon dioxide, carbon monoxide, and methane and the measurement of the vertical temperature gradient were already decided upon as research items. Pictures of Mars would be taken by the capsule and the bus with resolutions of 10 cm and 1 km, respectively. Analyzing the infrared CO_2 absorption spectrum, the temperature distribution of the Martian atmosphere could be determined.

There were several suggestions that a device for analyzing possible bacteria on Mars by means of a microscope, and other device for analyzing

the Martian dust should be carried in the capsule.

It was generally believed that we could use a parachute to land the capsule on Mars since it is surrounded by an atmosphere.

(Received on May 1, 1963)

S. E. DATA CENTER REPORT

By Hanao Hirozawa, Kikuo Yamawaki, and Nobuo Sashiro

1. Records on the Ground and Flight Tests

(a) Tests in October 1961

Test Period: October 18 to October 31

Test Place: Tokyo University, Akita Test Center

Test Rockets: K-8-8 (ID-7), FN-150 and K-8-9 (ID-9, AG-3)

Composition of Test Teams:

(1) K-8-8 space rocket team

Chief, Saito; Assistant Chief, Tamaki; 45 personnel from the center (from the Production Research, Communication Research, and Radio Wave Research groups); 21 nonmember personnel (from Prince Automobile, Nippon Electronics, Akehosi Electronics, Yokogawa Denki, Matsusida Tsusin, and Yusiya Machinery Companies); and 25 students.

(2) FN-150 space rocket test team

Chief, Tamaki; 33 center personnel (from the Production Research group); 18 nonmember personnel (from Prince Automobile, and Akehosi Electronics Companies); and 25 students.

(3) K-8-8 space rocket test team

Chief, Tamaki; Assistant Chief, Saito; 51 personnel from the center (from the Production Research and Radio Wave Research groups and Tokyo Observatory); 18 nonmember personnel (from Prince Automobile, Nippon Electronics, Akehosi Electronics, Yokogawa Denki, and Kuboda Weather Observation Instruments Companies); and 25 students.

October 18:

Unpacking and inspection of the test instruments.

October 19:

Preliminary preparation at the test site. At 10 a.m., a meeting regarding the safety guard at Akita. At 1 p.m., news conference at Akita. At 3 p.m., Michigawa county committee meeting. Arrival of space rockets K-8-8 and FN-150 at the test center.

October 20:

Unpacking and inspection of K-8-8 space rocket. At 1:30 p.m., meeting of center members of K-8-8 test team. At the meeting, the team chief explained the outline of the test plan; each section reported the status of its preparation, and arrangements for a rehearsal of the test were made.

October 21:

Rehearsal and demonstration to reporters and guests from 10 a.m. to 1:40 p.m. After the rehearsal, chiefs' meeting to review the time schedule. Radar antenna test. Shock test on computers and instruments. Window, which is at the head of the rocket, opening test.

October 22:

Interaction test of all devices in the morning. Chiefs met in the afternoon to check preparations and to reach agreement on launching time. Telemetry antenna test. Vacuum test on radar transponder.

October 23:

Chiefs met immediately after their arrival at the test center, and discussed launching question because of bad weather. The meeting was suspended until 11 a.m., when a new weather forecast could be obtained. At 11 a.m., chiefs met again and decided to postpone the space rocket launching until the next day because of the bad weather and upon the request of the ionosphere observation team. Arrival of K-8-9 space rocket at the test center.

October 24:

At 12:59 p.m., K-8-8 space rocket launching with launching angle 81°, surface wind 4 m/sec North, temperature 10.5°C, atmospheric pressure 1032 mb, and cloudy weather.

October 25:

Meeting of center members of FN-150 test team in the morning. At the meeting, each section reported the status of its preparation; arrangements for

the rehearsal of the test were made. From 1:00 to 2:00 p.m., the rehearsal. After the rehearsal, chiefs' meeting to fix time schedule.

October 26:

At 11:43 a.m., FN-150 space-rocket launching with launching angle of 45°, surface wind 9 m/sec Southeast, temperature 13°C, atmospheric pressure 1025 mb, and clear weather conditions.

October 27:

K-8-9 space rocket window-opening test in the morning. At 1:00 p.m., meeting of center members of K-8-9 test team. At the meeting, each section reported the status of its preparations; arrangements for rehearsal of the test were made. Shock test in the afternoon. Some center members remained in the evening to prepare the illumination for the night test.

October 28:

Afternoon duty for the evening rehearsal. Interaction test between instruments and telemetry. From 4 p.m. on, the rehearsal. After the rehearsal, chiefs' meeting to fix time schedule.

October 29:

Afternoon duty. Chiefs met and decided to postpone the launching until the next day because the wind speed was too high, and there was no immediate possibility that it would slacken.

October 30:

At 8:13 p.m., K-8-9 space rocket launching with launching angle of 80°, surface wind 4 m/sec Northeast, temperature 9° C, atmospheric pressure 1030 mb, and clear weather conditions.

October 31:

Withdraw the test instruments.

(b) Test in December 1961

Test Period: December 16 to December 26

Test Place: Tokyo University Akita Test Center

Test Space Rockets: RT-150 and K-9L-2 (ID-9)

Composition of Test Teams:

(1) RT-150 space rocket test team

Chief, Mori; Assistant Chief, Nomura; 41 personnel from the center (from the Production Research group); 27 nonmember personnel (from Prince Automobile, Akehosi Electronics and Mitsubisi Denki Companies); and 31 students.

(2) K-9L-2 space rocket test team

Chief, Mori; Assistant Chief, Nomura; 52 personnel from the center (from the Production Research and Radio Wave Research groups); 27 nonmember personnel (from Prince Automobile, Nippon Electronics, Akehosi Electronics, Mitsubisi Denki, Yokogawa Denki, Matsusida Tsusin and Yusiya Machinery Companies).

December 16:

At 11 a.m., a meeting regarding the safety guard at Akita. At 1 p.m., news conference at Akita. At 3 p.m., Michigawa county committee meeting.

December 17:

Meeting of center members of the RT-150-1 test team. At the meeting, the team chief explained the outline of the test plan and each section reported the status of its preparations and schedule.

December 18:

Chiefs met early in the morning for the RT-75 flight (RT-75 is a small rocket for the radar test) and determined the launching directions and angles of the RT-75s. At 10:52 a.m., 12:27 p.m. and 1:28 p.m., the RT-75s were launched. After the launchings, the chiefs met to fix the time schedule of the RT-150 space rocket launching.

December 19:

The launching of the RT-150-1 was suspended because of heavy rain. In the afternoon, the chiefs met to review the schedule.

December 20:

At 3:05 p.m., RT-150-1 space rocket launching with the launching angle of 48°, surface wind 10 m/sec Northwest, temperature 4° C, atmospheric pressure 1009 mb, and cloudy weather conditions. After the launching, chiefs meeting to check the preparation for K-9L-2 space rocket launching.

December 21:

Meeting of the members of the K-9L-2 test team in the morning. At the meeting, each section reported the status of its preparations and arrangements for the rehearsal of the launching were made. Window-opening test and no trouble found. The rehearsal of the K-9L-2 space rocket launching test was performed.

December 22:

Shock test on radar and antenna test in the morning. Chiefs met to check time schedule and weather forecast.

December 23:

Prepared K-9L-2 space rocket launching. At 11:45 a.m., the launching was suspended because of bad weather. In the afternoon, the chiefs met and decided to take off the following day and postpone the launching to December 25.

December 24:

Off.

December 25:

K-9L-2 space rocket launching was postponed to the next day because of gusty winds.

December 26:

At 2:05 p.m., K-9L-2 space rocket launching with the launching angle 81°, surface wind 5 m/sec North-Northwest, temperature 4°C, atmospheric pressure 1010 mb, and cloudy weather.

(c) Tests in March 1962

Test Period: March 22 to April 1

Test Place: Tokyo University Akita Test Center

Test Space Rocket: HT-150 and L-735-2/3 engine (ground test)

Composition of Test Teams:

(1) HT-150 space rocket test team

Chief, Tamaki; Assistant Chief, Nomura; 34 personnel from the center (from the Production Research group); 16 nonmember personnel

(from Prince Automobile, Akehosi Electronics, Mitsubisi Denki, and Matsusida Tsusin Companies); and a student.

(2) L-735-2/3 engine test team

Chief, Itogawa; Assistant Chief, Akita; 34 personnel from the center (from the Production Research group); 14 nonmember personnel (from Prince Automobile, Matsusida Tsusin, and Yusiya Machinery Companies).

March 22:

Unpacking and inspection of the test instruments.

March 23:

Adjustment of the computers and instruments for the L-735-2/3 engine test.

March 24:

At 11 a.m., moved the L-735-2/3 engine into the engine test site. Unpacking, inspection, and setting the engine on the test stand. Temporary setting of the thrust meter. At 11 a.m., a meeting regarding the safety guard at Akita. At 1 p.m., news conference at Akita. At 3 p.m., Michigawa county committee meeting. Demonstrated L-735-2/3 engine to reporters.

March 25:

Brought in the rocket launcher for the HT-150 space rocket. Worked the launching-angle adjustment of the launcher. Locations of gauge attachment points on the L-735-2/3 engine were fixed. Moved the L-735-2/3 engine into the constant temperature room. Adjusted LM test stand and made preparations for dedication ceremony.

March 26:

Dedication ceremony of LM test stand in the morning. At 1 p.m., meeting of the center members of the HT-150 test team. At the meeting, each section reported on the status of its preparations, and arrangements were made for the rehearsal of the launching test. At 1:30 p.m., meeting of the members of the L-735-2/3 test team. At the meeting, arrangements regarding the safety guard, the rehearsal, and the press were made.

March 27:

At 9 a.m., chiefs met to check preparations for the HT-150 space rocket and to make arrangements for the rehearsal. Shock test on the computers and instruments of the HT-150 space rocket in the morning. From 12:30 to 2:15 p.m., the rehearsal. After the rehearsal, chiefs met to discuss the time schedule.

March 28:

Launching preparations had been carried out in the morning. Because of strong wind, the chiefs met and decided to postpone the launching until the next day for there was no possibility of the wind calming down.

March 29:

At 11:34 a.m., the HT-150 space rocket launching with the launching angle 60°, surface wind 7 m/sec Northwest, temperature 6° C, atmospheric pressure 1021 mb, and clear weather. At 12:30 p.m., chiefs met and made arrangements for L-735-2/3 engine test. Moving the engine out, putting it on the test stand, attaching gauges on the engine in the afternoon.

March 30:

Preparation for the rehearsal of the L-735-2/3 engine test. From 1:00 to 4:30 p.m., the rehearsal. After the rehearsal, chiefs met and set up the time schedule.

March 31:

At 4:05 p.m., L-735-2/3 engine was ignited; ambient temperature 11° C, atmospheric pressure 1022 mb, and clear weather.

(d) Tests on May 1962

Test Period: May 19 to May 25

Test Place: Tokyo University Akita Test Center

Test Space Rocket: K-8-10 (ID-10, AG-1)

Composition of the Test Team:

Chief, Nomura; Assistant Chief, Mori; 54 personnel from the center (from the Production Research, Communication Research and Radio Wave Research groups and Tohoku University); 24 nonmember personnel (from Prince Automobile, Nippon Electronics, Akehosi Electronics, Mitsubisi Denki, Yokogawa Denki, Sokutei Kikai Shia, and Yusiya Machinery Companies).

May 19:

Unpacking and inspection of the test instruments.

May 20:

Facilitating night illumination and other preparations.

May 21:

Moving K-8-10 space rocket into the test site in the morning. At 11 a.m., a meeting regarding the safety guard at Akita. At 1 p.m., news conference at Akita. At 3 p.m., Michigawa county committee meeting. Selection of observation points. Unpacking the space rocket.

May 22:

Assembling the upper body of the space rocket for window-opening test in the morning. At 1 p.m. meeting of the center members of the test team. At the meeting, discussions on preparations and schedules. At 4 p.m., window-opening test and shock test on the upper body of the space rocket. From 7 p.m., trial illumination to check the lighting conditions.

May 23:

In the morning, chiefs met to make arrangements for the rehearsal of the launching test and to review the weather forecast. Interaction test between the computers and instruments and telemetry in the afternoon. From 5 to 8 p.m., the rehearsal. After the rehearsal, chiefs met to fix the time schedule.

May 24:

At 7:50 p.m., K-8-10 space rocket launching with the launching angle 81°.

May 25:

Review the test results of K-8-10 space rocket. Removing the test instruments.

(e) Tests in August 1962

Test Period: August 14 to August 23

Test Place: Tokyo University Kagoshima Space Center

Test Space Rockets: AT-150 and K-8L-1

Composition of the Test Team:

Chief, Mori; Assistant Chief, Nomura; 43 personnel from the center (from the Production Research group), and 18 nonmember personnel (from Prince Automobile, Toikoku Kayaku, Nippon Electronics, Akehosi Electronics and Matsusida Tsusin Companies).

August 14:

At 10:30 a.m., Kagoshima Province Cooperation Committee meeting. At noon, news conference. At midnight, test team arrived at Uchinoura.

August 15:

At 10 a.m., Uchinoura Town Cooperation Committee meeting. Arrival of the test instruments from Akita Test Center. Unpacking the instruments.

August 16:

Moving the launcher and a crane from Takayama railroad station to the test ground.

August 17:

Chiefs met and discussed preparations and other important test matters. A good-will party was held by Uchinoura Town authority and the Fishery Union from 6 to 9 p.m.

August 18:

Moving the space rockets. Left Takayama station at 10:15 a.m., arrived at the test site at 3 p.m. Between 6 to 9 p.m., a good-will baseball tournament with Uchinoura Town Office members.

August 19:

Meeting of center members of the test team. At the meeting, each section reported the status of its preparations, and an explanation regarding the safety guard was made.

August 20:

The rehearsals for the OT-75 and AT-150 space rockets.

August 21:

At 10 a.m., OT-75 launching with the launching angle 60°, AT-150 space rocket launching in the afternoon was postponed until the next day because of bad weather.

August 22:

At 1 p.m., AT-150 space rocket launching with the launching angle 60°, surface wind 4 m/sec Southwest, temperature 29° C, clear weather. After the launching, the rehearsal for the K-8L-1 space rocket.

August 23:

At 4:15 p.m., K-8L-1 space rocket launching with the launching angle 80°, surface wind 0, temperature 30° C, and clear weather.

(f) Test in October 1962

Test Period: October 22 to October 29

Test Place: Tokyo University, the Production Research Institute Noshiro Test Center

Test Space Rocket: L-735-3/3 engine (ground test)

Composition of the Test Team:

Chief, Akiba; Assistant Chief, Mori; 36 personnel from the center (from the Production Research group); 20 nonmember personnel (from Prince Automobile, Matsusida Tsusin, and Siuko Tsusin Companies).

October 22:

At 10 a.m., news conference at Akita Province Office. At 3 p.m., news conference at Noshiro Town Office. One of the two sections of the test team arrived at Noshiro Test Center at noon. The other section went to the Akita Test Center and moved the test instruments to Noshira Test Center by jeeps.

October 23:

Unpacking and inspection of the test instruments. Position of each section in the computing and observation room was fixed. At 6 p.m., arrival of L-735-3/3 engine at the test site. Unloaded the engine from the moving van by 8-ton crane. Under illumination, unpacked and inspected the engine and no trouble was found.

October 24:

Setting up the rocket-engine test stand in the morning. Attaching the thermostat to the engine test stand in the afternoon.

October 25:

Adjustment of the computers and instruments in the morning. At 3 p.m., meeting of the center members of the test team. At the meeting, each section reported on the status of its preparations, and arrangements were made for the rehearsal and for the safety guard.

October 26:

Laid phone lines in the morning. Chiefs met to make arrangements for the rehearsal in the afternoon. Reporters visited.

October 27:

The rehearsal was performed until 1 p.m. After the rehearsal, the chiefs met to fix the time schedule.

October 28:

Chiefs met in the morning to check each section's preparations and the safety guard. Final adjustments of the computers and instruments in the afternoon.

October 29:

L-735-3/3 engine ground test; ignited at 2:15 p.m., surface wind 0.4 m/sec North-Northwest, temperature 12.5°C, atmospheric pressure 1012 mb, and cloudy weather.

(g) Tests in November 1962

Test Period: November 15 to November 25

Test Place: Tokyo University Kagoshima Space Center

Test Space Rockets: LT-150-1, SP-150-3, SP-150-4, and K-9M-1 (ID-11).

Composition of the Test Teams:

(1) LT-150-1, SP-150-3, and -4 test team

Chief, Tamaki; Assistant Chief, Saito; 40 personnel from the center (from the Production Research group); 11 nonmember personnel (from Prince Automobile and Akehosi Electronics Companies); and 6 students.

(2) K-9M-1 test team

Chief, Tamaki; Assistant Chief, Saito; 51 personnel from the center (from the Production Research and Radio Wave Research groups); 24 nonmember personnel (from Prince Automobile, Nippon Electronics, Akehosi Electronics, Yokogawa Denki, Matsusida Tsusin, and Yusiya Machinery Companies); and 6 students.

November 15:

At 10 a.m., Kagoshima Province Cooperation Committee meeting. At 11:20 a.m., a meeting regarding the safety guard. At noon, news conference. All of meetings were held in the Province office building because of rain.

November 16:

Rainy, all outdoor works were suspended. At 3 p.m., Uchinoura Town Cooperation Committee meeting.

November 17:

Unpacking and inspection of the test instruments. Laying out communication lines. Setting wind direction and wind speed meter. Laying out igniter lead line.

November 18:

At 2 p.m., meeting of the center members of the LT-150-1, SP-150-3 and -4 test team. At the meeting, the team chief discussed the launching time and direction, each section reported the status of its preparations and arrangements were made for the rehearsal. After the meeting, a demonstration of fire extinguishers. At 5 p.m., arrival of space rockets at the test site.

November 19:

In the morning, preparation for the rehearsal of the launch of the LT-150 and SP-150 space rockets. The rehearsals in the afternoon.

November 20:

Chiefs met and decided to postpone the launching of the rockets.

November 21:

At 11.09 a.m., LT-150-1 space rocket launching with the launching angle 60°, surface wind 3.5 m/sec North-Northeast, temperature 18.5°C, atmospheric pressure 989 mb, and cloudy weather. At 3:12 p.m., SP-150-3 space rocket launching with the launching angle 60°, surface wind 2 m/sec Northeast, temperature 18.5°, atmospheric pressure 988 mb, and light rainy weather. At 4:20 p.m., the meeting of the center members of the K-9M-1 test team. At the meeting, the team chief explained the results of the LT-150-1 and SP-150-3 space rocket launchings; each section reported its preparations and schedule.

November 22:

In the morning, assembled the upper body of the K-9M-1 space rocket for the launch rehearsal and started to warm the body-assembling room. At 11 a.m., the rehearsal was started, but it was shortly suspended because of rain. Later, the rehearsal was postponed because there was no possibility that the weather would calm down. In the afternoon, the chiefs met to review the time schedule. At 4:30 p.m., window-opening test — window opened in 46.8 seconds. At 5 p.m., interaction test between the computers and instruments and telemetry.

November 23:

The rehearsal was performed in the morning. By 12:30 p.m., the rehearsal was completed. In the afternoon, the chiefs met to check each section's preparations and to review the launching time. Had many visitors for it was a holiday.

November 24:

In the morning, assembled the upper body of the space rocket for the launching. Chiefs met to make necessary arrangements for the launching schedule. From 3:50 p.m., a good-will baseball tournament with Uchinoura Town Office members.

November 25:

At 11:05 a.m., K-9M-1 space rocket launching with the launching angle 78°, surface wind 2 m/sec North-Northwest, temperature 15.5°C, atmospheric pressure 995 mb, and cloudy weather. At 3:11 p.m., SP-150-4 space rocket launching with the launching angle 65°, surface wind 0, temperature 18.5°C, atmospheric pressure 991.5 mb, and cloudy weather.

(h) Tests in December 1962

Test Period: December 13 to December 20

Test Place: Tokyo University Kagoshima Space Center

Test Space Rockets: K-8-11 (CR-6, GA-2, and RN-1) and SO-150-1

Composition of the Test Teams:

(1) K-8-11 space rocket test team

Chief, Saito; Assistant Chief, Tamaki; 52 personnel from the center (from the Production Research and Physics and Chemistry Research groups, Kyoto University, Tokyo Observatory, and Tohoku University); 22 nonmember personnel (from Prince Automobile, Nippon Electronics, Akehosi Electronics, Kubota Weather Observation Instruments Companies); and 17 students.

(2) SO-150-1 space rocket test team

Chief, Saito; Assistant Chief, Tamaki; 40 personnel from the center (from the Production Research group); 16 nonmember personnel (from Prince Automobile, Nippon Electronics, Akehosi Electronics, Matsusita Tsusin Companies); and 7 students.

December 13:

At 10 a.m., Kagoshima Province Cooperation Committee meeting at the province office. At 11 a.m., a meeting at the province office regarding the safety guard. In the morning, unpacking the test instruments. In the afternoon, the rocket launcher was cleaned. At 4:15 p.m., K-8-11 and SO-150-1 space rockets were moved into the assembly room. Unpacking and inspection of the rockets and found no trouble.

December 14:

Rainy; outdoor works were suspended. Indoor adjustment of the test instruments. In the afternoon, rocket was mounted on the rocket carrier. At 3 p.m., Uchinoura Town Cooperation Committee meeting.

December 15:

In the morning, setting K-8-11 space rocket on the launcher, inspection of the rocket tail. At 2 p.m., meeting of the center members of the K-8-11 test team. At the meeting, the team chief explained the time schedule,

Each section reported on its preparations, and a review of the window-opening test was made. At 4 p.m., interaction test between the computers and instruments and telemetry.

December 16:

From 11:15 a.m. to 3:10 p.m., the rehearsal. At 4 p.m., shock test on the upper body of the space rocket. At 5 p.m., test of the timer and igniter.

Table 1

1 型号	2 観測 No.	3 飛しょう日	4 発射時間	5 重量(Kg)	6 全長(mm)	7 発射角度	8 高度(Km)	9 搭載計器
K-8-8	ID—7	36.10.24	12.59	1513	10485	81°	198	T, Y_2, T_i, TM, RT, ID
FN-150-1		36.10.26	11.45	66	3398	45°	4.1	RT
K-8-9	ID—8, AG—3	36.10.30	20.13	1540	10928	80°	175	AG, ID, T_i, TM, RT
RT-150-1		36.12.20	15.05	70	3036	48°	5.4	RT
K-9 L-2	ID—9	36.12.26	14.05	1591	12774	81°	348	T, Y, ID, T_i, TM, RT
HT-150-1		37. 3.29	11.34	115	5176	60°	20	X_1, X_2, Y, T, TM
K-8-10	ID—10, GA—1	37. 5.24	19.50	1545	10937	81°	0	ID, GA, T_i, TM, RT
AT-150-1		37. 8.22	13.00	71	3018	60°	13	TM, RT
K-8 L-1		37. 8.23	16.15	348	7300	80°	172	X_1, X_2, Y, T, σ, TM, RT
LT-150-1		37.11.21	11.09	70	3473	60°	5	
SP-150-3		37.11.21	15.12	68	3472	60°	6	RT
K-9 M-1	ID—11	37.11.25	11.01	1439	11177	78°	56	X_1, X_2, Y_1, Y_2, T, σ, T_i, ID, TM, RT
SP-150-4		37.11.25	15.11	70	3473	65°	10	RT
K-8-11	CR—6 GA—2, RN—1	37.12.18	14.03	1499	10930	79°	202	GA, RN, CR, T_i, TM, RT
SO-150-1		37.12.20	12.11	88	3541	70°	12	ED, ET, TM

記号説明 X_1: 加速度計, X_2: 減速度計, Y_1, Y_2: 横加速度計, T: 温度計, σ: 歪計, T_i: タイマ, ID: 電離層観測器, AG: 夜光高層観測器, GA: 地磁気によるロケット姿勢計, RN: 電波雑音観測器, CR: 宇宙線観測器, ED: 異常検出装置, ET: 電子式タイマ, TM: テレメータ送信機, RT: レーダトランスポンダ

1) Type of space rocket
2) Observation number
3) Date of flight
4) Launching time
5) Weight of the space rocket (kg)
6) Total length of the space rocket (mm)
7) Launch angle
8) Altitude (km)

9) Counters and instruments on board

10) Explanation of the symbols:

X_1:	Accelerometer
X_2:	Deceleration meter
Y_1Y_2:	Normal components accelerometer
T:	Thermometer
σ:	Strain gauge
Ti:	Timer
ID	Ionosphere probe
AG:	High-altitude airglow observation probe
GA:	Rocket attitude detector using geomagnetic field
RN:	Radiowave noise probe
CR:	Cosmic-ray probe
ED:	Trouble detector
ET:	Electronic timer
TM:	Telemetry
RT:	Radar transponder

December 17:

Assembled the upper body of the K-8-11 space rocket in the morning. In the afternoon, a good-will baseball tournament with Uchinoura Town Office members.

December 18:

At 2:03 p.m., K-8-11 space rocket launching with the launch angle 79°, surface wind 1 m/sec West, temperature 13°C, atmospheric pressure 988.5 mb, and clear weather. At 3:45 p.m., meeting of the center members of the SO-150-1 test team. At the meeting each section reported its preparations and schedule, and arrangements for the rehearsal were made. At 4:00 p.m., the chiefs met to check the preparations.

December 19:

During the rehearsal of the SO-150-1 space rocket launching, the telemetry went out of order. At 5:30 p.m., the rehearsal was discontinued without completion because of the sunset.

December 20:

At 12:11 p.m., the SO-150-1 space rocket launching with the launch angle 70°, surface wind 4 m/sec Northeast, temperature 13°C, atmospheric pressure 99 mb, and cloudy weather.

The above data are the records of the ground and flight tests we have made so far. And we do not intend to include the launch results because the test team chiefs have reported on these separately. Table 1 summarizes the data of the launched rockets.

Detailed records about the launchings are filed and kept at the SE data center, Itogawa Laboratory. We also have 80 rolls of 16mm film dealing with the ground and flight tests.

(Received on April 16, 1962)

A RECORD OF EXPERIMENTS

--From July 1961 Experiment to December 1962 Experiment--

By Tatsuhiko Watari

1. Experiments at the Akita Test Site

As one of the series of experiments for international joint observations, the Kappa 8-7 space rocket experiments were done in 10 days starting from July 20, 1961.

The purpose of these experiments was to measure the ion and electron densities, the temperature of electrons in the ionosphere, and the atmospheric wind and temperature using the sound bomb method. In these experiments, we have just finished our sixth observation of the ionosphere, and our tenth of the atmospheric wind and temperature; and it was the first time that the Kappa-8 type space rocket was used in such research. We estimated that the space rocket would fall in the sea either within 23 km of the launch point or within the region 230-330 km; and we decided that these areas were the most dangerous regions because of the possibility of the rocket falling there. With suitable precautions, we launched the space rocket at 11:42 a.m., July 21, 1961.

The sea at Michigawa Beach flows over a 200-m deep continental shelf up to 25-30 km from the coastline. Many Kappa 6 and 8 type booster rockets and other small rockets sank on the continental shelf during previous experiments. We wanted to recover the rockets on the continental shelf because we could find some useful data from them and, in addition, because they caused problems for some of the fishing boats. The recovery work was impossible for a coastguard boat because of the depth of the continental shelf; so we discussed the problem with the Fisheries Section of the Akita Province government. With the help of the Fisheries Section, we decided to do the recovery work using troll boats in July and August when the troll boats had some spare time. The Marine Association arranged for the recovery work to be done by one of its member companies and it was done in July.

Space observations using K-8-8, K-8-9, and FN-150-1 space rockets were successfully carried out on the 24, 26, and 30 of July, res-

pectively. The K-8-8 experiment, together with the observations using the K-8-7 space rocket, were a part of the international joint observation project which had been scheduled from 16 to 25 of July. The K-8-9 space rocket was designed to observe simultaneously the ionosphere and airglow and five probes were used for observing the ionosphere. Many scientists from NASA and Taiwang University attended this experiment as guests. In November 1961, a new 4-m-diameter radar antenna was built at a location about 700 m south of the Akita test site in a province-owned forest. The operation of this antenna was checked in December by tracing a small space rocket. In December, the L9-2 and RT-150 space rocket were launched for space observations. In spite of our previous experiences on these type of experiments, the weather conditions were so bad that we had to revise the schedule several times and finally the experiments were carried out on the 26th of the month.

On March 26, the L-type engine stand was completed. After adding the necessary fire equipment such as a fire line and hydrant, the ground test of L-735-2/3 type rocket engine was performed in March 1962.

The K-8-10 space rocket was ignited at 7:50 p.m., May 24, 1962. However, because of some trouble in the booster rocket, the space rocket failed in flight. As a result of this accident, a special committee was formed to study the safety measures needed during further experiments. Examining all aspects relating to the accident, the committee decided to establish a new space-rocket launching site.

2. Experiment in Noshiro Test Site

The ground-combustion test site at Ashahamouchi of Noshiro City was newly established. All details of this test site and the reasons for establishing it in the face of the accident at the Akita test site were reported on in another paper, and so these aspects are omitted here. This test site had not yet been completed. It was planned that all necessary instruments would be built starting in 1963. Even though there were many difficulties in the ground-combustion test of L-735-3/3 with the temporary facilities, the test not only was performed on schedule, October 29, 1962, but also successfully finished. The Noshiro test site would be used to test all M-type rocket engines as well as other types of rocket engines.

3. Experiment in the Kagoshima Test Facility

Kagoshima Space Center construction was scheduled in 1961 and with the help of Kagoshima province government and Uchinoura town office, the

land breaking ceremony was held by Tokyo University Production Research Institute in February 1962. In the meantime, the OT-75 space rocket was experimentally launched. However, this is not important to mention. In August 1962, K-8L-1 and two other small space rockets were launched using the temporary facilities in the first and second sites at Kagoshima. This was the first full-scale experiment replacing the Akita test facility. In November 1962, the K-9M-1 and three other small space rockets were in a launching stand ready to be fired. The three small space rockets gave satisfactory results, but the main rocket of 9M-1 was not ignited. There was such a heavy rain just before the 9M-1 was to be ignited, that it was difficult just to prepare for the launch: for instance, the window (in the head of the space rocket) opening test was prepared in the heavy rain and, with the help of the town office, sandbags were carried in at night to reinforce the road leading to the launching stand.

K-8-11 and SO-150-1 space rockets were in the experimental schedule of December 1962. The K-8-11 space rocket experiment gave not only quite satisfactory results but also reached 202-km altitude. All members of this research program were very happy about the results.

The research records for one and a half years were summarized. The author hopes to have another chance to report on subjects not covered here.

(Received on April 23, 1963)